

AUTHOR:**TITLE:****YEAR:****OpenAIR citation:**

This work was submitted to- and approved by Robert Gordon University in partial fulfilment of the following degree:

OpenAIR takedown statement:

Section 6 of the "Repository policy for OpenAIR @ RGU" (available from <http://www.rgu.ac.uk/staff-and-current-students/library/library-policies/repository-policies>) provides guidance on the criteria under which RGU will consider withdrawing material from OpenAIR. If you believe that this item is subject to any of these criteria, or for any other reason should not be held on OpenAIR, then please contact openair-help@rgu.ac.uk with the details of the item and the nature of your complaint.

This is distributed under a CC _____ license.

INFLUENCE OF ENVIRONMENTAL CONDITIONS AND
ARCHITECTURAL FORM ON THE DESIGN AND THERMAL
PERFORMANCE OF THE FLAT-PLATE SOLAR
COLLECTOR SYSTEM

by

Peter Robertson

A thesis presented in partial fulfilment of the
requirements for the Degree of Doctor of
Philosophy of the Council for National
Academic Awards

Scott Sutherland School of Architecture
Robert Gordon's Institute of Technology
Aberdeen

May, 1981



IMAGING SERVICES NORTH

Boston Spa, Wetherby

West Yorkshire, LS23 7BQ

www.bl.uk

BEST COPY AVAILABLE.

VARIABLE PRINT QUALITY

Acknowledgements

I wish to express my sincere gratitude to my Director of Studies, Professor S. Wilkinson and my Supervisor, Dr. G.S. Saluja for guidance and constant encouragement throughout the period that led to the preparation of this thesis.

Acknowledgements are due to the technical staff at the Scott Sutherland School of Architecture for the construction of the experimental collector test facilities. The computer and technical staff at Robert Gordon's Institute of Technology are also thanked for services.

The author thanks the Science Research Council and Robert Gordon's Institute of Technology for the opportunity and financial support to carry out this research.

Finally, I thank Mrs Hilda Young for her patience and expertise in typing this thesis.

TABLE OF CONTENTS

	<u>Page</u>
ACKNOWLEDGEMENTS	i
ABSTRACT	ii
NOMENCLATURE	iii
<u>SECTION</u>	
1. INTRODUCTION	1.
1.1. General Introduction	2.
1.2. Brief Review of Previous Investigations	3.
1.3. Objectives of Present Work	4.
2. THERMAL PERFORMANCE OF THE FLAT-PLATE SOLAR COLLECTOR	7.
2.1. Review of Previous Work	8.
2.2. Theoretical Analysis - Dynamic Behaviour of Collector Unit	11.
2.3. Computer Simulation	17.
2.4. Experimental Investigation	21.
2.5. Presentation and Discussion of Results	27.
3. SIMULATION OF CLIMATIC CONDITIONS AND THEIR EFFECT ON COLLECTOR PERFORMANCE	38.
3.1. Review of Previous Work	39.
3.2. Theoretical Analysis - Derivation of Solar Radiation Model	42.
3.3. Computer Simulation	48.
3.4. Experimental Investigation	50.
3.5. Presentation and Discussion of Results	50.

<u>SECTION</u>	<u>Page</u>
4. THERMAL PERFORMANCE OF SOLAR WATER HEATING SYSTEMS UNDER INTERMITTENT SOLAR RADIATION AND ENERGY USAGE CONDITIONS	58.
4.1. Review of Previous Work	59.
4.2. Theoretical Analysis - Dynamic Behaviour of Solar Water Heating System	63.
4.3. Computer Simulation	64.
4.4. Experimental Investigation	66.
4.5. Presentation and Discussion of Results	67.
4.6. Monitoring of Solar Water Heating Installation in a 15 Person Hostel	73.
5. DESIGN AND THERMAL PERFORMANCE OF INTEGRATED SOLAR COLLECTOR INSTALLATIONS IN BUILDINGS	90.
5.1. The Influence of Restricted Built Environmental Conditions on the Performance of Solar Water Heating Installations	91.
5.2. Theoretical Analysis - Dynamic Behaviour of Integrated Solar Installations in Restricted Built Environmental Conditions	91.
5.3. Computer Simulation	98.
5.4. Experimental Investigation	103.
5.5. Presentation and Discussion of Results	111.
6. CONCLUSIONS AND SUGGESTIONS FOR FURTHER WORK	123.
6.1. Conclusions	124.
6.2. Suggestions for Further Work	126.

APPENDICES

1.	DERIVATION OF SOLAR COLLECTOR SYSTEM MODEL	127.
1.1.	Derivation of Heat Transfer and Energy Storage Processes within the Solar Collector	128.
1.2.	Derivation of Solar Radiation Prediction Model	132.
1.3.	Derivation of Heat Transfer and Energy Storage Processes within the Solar Water Storage Tank	138.
1.4.	Derivation of Shadow Prediction Model	142.
2.	DESCRIPTION OF COMPUTER PROGRAMS	144.
2.1.	SOLAR 7 - Solar Collector System Model	145.
2.2.	STAPEL - Analysis of Experim- ental Results	182.
2.3.	MONITR - Analysis of Monitored Installation Results	194.

BIBLIOGRAPHY

Details of postgraduate courses of study

211.

214.

ABSTRACT

PETER ROBERTSON

INFLUENCE OF ENVIRONMENTAL CONDITIONS AND ARCHITECTURAL FORM ON THE DESIGN AND THERMAL PERFORMANCE OF THE FLAT-PLATE SOLAR COLLECTOR SYSTEM.

Solar heating systems, by the nature of their design and inherent thermal mass, are sensitive to the changes in the prevailing climatic conditions.

A computer program has been developed to predict and display the dynamic performance of solar water heating systems and their installation designs under transient climatic and restricted site conditions. A multi-node capacitance model describes the dynamic heat transfer and energy storage processes within the solar collector unit, storage tank and the connecting pipework. This simulation model predicts the dynamic system performance under intermittent solar radiation, system operation and energy usage conditions.

Validation studies have been carried out on the computer simulation results against the performance of a purpose-built solar collector test facility and a commercial solar water heating system in actual operation in Aberdeen. A good correlation has been obtained in both cases. The accuracy of the prediction was found to be dependant upon the time interval of the available climatic data and the complexity of the thermal simulation network chosen.

The experimental facilities and the computer simulation program have been developed to investigate the effect of integrating the solar collector installation as part of the roof fabric, as a possible technique to improve the system performance in exposed locations.

The application of this computer program lies in the development of innovative solar collector system and installation designs to achieve optimum system performance under transient climatic and restricted urban site conditions.

NOMENCLATURE

A_s	area of elemental collector unit section. (m^2)
A_{sp}	surface area of system pipework. (m^2)
A_{st}	surface area of elemental storage tank section. (m^2)
A_p	perimeter edge surface area of collector unit. (m^2)
C_1	thermal capacitance of collector cover elemental section. ($J/^\circ C$)
C_2	thermal capacitance of collector plate unit elemental section.
C_3	thermal capacitance of storage tank top section.
C_4	thermal capacitance of storage tank middle section.
C_5	thermal capacitance of storage tank bottom section.
C_6	thermal capacitance of system pipework section.
C_a	total thermal capacitance of collector unit. ($J/^\circ C$)
C_L	overall rate of heat removal to load. ($W/^\circ C$)
C_{p_c}	specific heat capacity of collector cover material. ($J/kg^\circ C$)
C_{p_i}	specific heat capacity of collector insulation material.
$C_{p_{si}}$	specific heat capacity of storage tank insulation material.
$C_{p_{st}}$	specific heat capacity of storage tank material.
C_{p_p}	specific heat capacity of collector plate material.
C_{p_t}	specific heat capacity of collector tube material.
C_{p_u}	specific heat capacity of frame unit material.
C_{p_w}	specific heat capacity of circulating fluid.
C_s	total thermal capacitance of storage tank. ($J/^\circ C$)
C_w	mass flow rate of circulating fluid. (kg/s)
D	day number
d_c	thickness of collector cover. (m)
d_i	thickness of rear insulation.
d_p	thickness of collector plate.
d_{pi}	thickness of system pipework insulation.
d_{pw}	thickness of system pipework.
d_r	thickness of rear collector plate unit.

d_{st}	thickness of storage tank material.
d_{ti}	thickness of storage tank insulation.
d_u	thickness of frame unit.
F'	collector plate efficiency factor - dimensionless.
F''	flow rate factor - dimensionless.
F_1	pump control function - dimensionless.
F_2, F_3, F_4	storage tank flow control functions - dimensionless.
F_5	load control function - dimensionless.
F_e	edge heat loss correction factor - dimensionless.
h	hour angle. (degrees)
h_1	overall heat loss coefficient from collector plate. ($W/m^2 \text{ } ^\circ C$)
h_2	overall heat loss coefficient from collector cover.
h_r	the rear convection heat loss coefficient. ($W/m^2 \text{ } ^\circ C$)
h_t	the film heat transfer coefficient of collector fluid. ($W/m^2 \text{ } ^\circ C$)
h_w	the forced convection heat loss coefficient due to wind. ($W/m^2 \text{ } ^\circ C$)
I_c	total incident solar radiation on plane of collector. (W/m^2)
I_D	direct horizontal solar radiation. (W/m^2)
I_d	sky diffuse solar radiation. (W/m^2)
I_H	total horizontal solar radiation. (W/m^2)
k_{pi}	thermal conductivity of system pipework insulation. ($W/m \text{ } ^\circ C$)
k_{pw}	thermal conductivity of system pipework material.
k_{st}	thermal conductivity of storage tank material.
k_{ti}	thermal conductivity of storage tank insulation.
L	longitude of the sun. (degrees)
L'	characteristic size of the collector plate. (m)
mCp_c	thermal capacitance of collector cover. ($J/^\circ C$)
mCp_p	thermal capacitance of collector plate unit. ($J/^\circ C$)
mCp_w	mass flow rate of circulating fluid. (kg/s)
Q_{LOAD}	rate of energy supply to energy demand load. (W)
q_u	net heat collection rate from collector. (W)

q_u/A_s	average useful heat collection rate. (W)
R_p	thermal resistance from collector plate to tube. ($m^{20}C/W$)
r_b	thermal resistance of collector plate-tube bond. ($m^{20}C/W$)
r_p	thermal resistance of collector plate.
r_t	thermal resistance of collector tube.
S	solar insolation rate on the collector plane. (W/m^2)
S_1	solar radiation absorbed by collector cover. (W/m^2)
S_2	solar radiation absorbed by collector plate.
S_a	edge addition coefficient - dimensionless.
t	time
T_1	top storage tank section mean temperature. ($^{\circ}C$)
T_2	middle storage tank section.
T_3	bottom storage tank.
T_a	external air temperature.
T'_a	internal air temperature.
T_c	mean collector cover temperature.
T_i	inlet collector fluid temperature.
T_{mw}	mains water temperature.
T_o	outlet collector fluid temperature.
T_p	mean collector plate temperature.
T_{pw}	mean system pipework section fluid temperature.
T_s	mean storage tank temperature.
T_{sky}	sky temperature.
T_{SL}	supply fluid temperature to load.
T_{st}	elemental storage tank section temperature.
T_w	mean collector fluid temperature.
U_L	overall collector unit heat loss coefficient. ($W/m^{20}C$)
U_p	overall heat loss coefficient from system pipework.
U_R	heat transfer coefficient from the collector plate to the perimeter of the collector unit. ($W/m^{20}C$)
U_s	overall heat loss coefficient from storage tank.

v	wind velocity. (m/s)
V_{pw}	volume of pipework fluid. (m ³)
V_{st}	volume of storage tank elemental section.
V_t	volume of collector tube material.
V_w	volume of collector fluid within tubes.
α_c	absorptivity of collector cover - dimensionless.
α_p	absorptivity of collector plate.
β	collector tilt. (degrees)
ρ_c	density of collector cover material. (kg/m ³)
ρ_i	density of rear insulation material.
ρ_p	density of collector plate material.
ρ_{pi}	density of pipework insulation.
ρ_{pw}	density of pipework material.
ρ_{si}	density of storage tank insulation.
ρ_{st}	density of storage tank material.
ρ_t	density of tube material.
ρ_u	density of frame unit material.
ρ_w	density of circulating fluid.
ϵ_c	emissivity of collector cover - dimensionless.
ϵ_p	emissivity of collector plate.
σ_c	reflectivity of collector cover - dimensionless.
σ_g	reflectivity of ground surface.
σ_p	reflectivity of collector plate.
δ	solar declination. (degrees)
σ	Stefan-Boltzmann constant.
τ_c	transmissivity of collector cover - dimensionless.

SECTION 1

INTRODUCTION

1.1. General Introduction

Solar energy can provide the world with its energy requirements. Its use for the space and hot water heating of buildings is not new. In the past, the low cost of fossil fuels has prevented the widespread use of solar power although several experimental houses incorporating solar heating systems have been built. Rising fuel costs, the exhaustion of fossil fuels and modern technology have initiated a radical re-assessment of this situation.

Basically a solar heating system comprises a collector to absorb solar radiation, the heat from which is then transferred to a storage medium. A flat-plate solar collector is normally chosen in order to maximise the collection of diffuse radiation. Storage of the heat may be achieved by heating water or small pebbles, or by inducing reversible chemical changes. From the storage tank, the collected heat energy is distributed to the space heating appliances of the domestic hot water for use when needed. Both air and water have been used as the heat transfer media to and from the storage.

The present development of solar heating systems is limited by the short term heat storage available, the payback period of the installation cost and the accurate assessment of system performance.

1.2. Brief Review of Previous Investigations

1.2.1. Dynamic Thermal Simulation of Solar Collector Performance

Solar heating systems, are by the nature of their design, sensitive to the changes in the prevailing environmental conditions. In order to simulate the complex thermal behaviour of the flat-plate solar collector, a number of steady-state heat transfer prediction techniques have been developed ^{1,2,3}. These techniques neglect the effect of collector thermal capacitance. As a result, these prediction techniques are limited to the calculation of the average daily useful energy collection under steady-state solar radiation conditions.

Subsequent studies to predict the dynamic collector performance under variable climatic conditions led to the development of a simple collector capacitance model ^{4,5}. This model simulates the collector heat transfer and energy storage processes as a single thermal nodal unit. This technique has been extended to create a two node model in which the dynamic thermal behaviour of the collector plate and the cover are simulated separately ^{6,7}. The prediction results from both models have been analysed under fluctuating solar radiation conditions, revealing significant inaccuracies in the collector temperature and performance. ⁷

For the present investigation, a multi-node model has been postulated as a possible technique to improve the accuracy of short term collector performance under prevalent variable climatic conditions ⁶.

1.2.2. Prediction of Solar Radiation Conditions

The accurate prediction of the incident solar radiation on the inclined collector surface is an essential part of any steady-state and transient collector performance models. In previous studies, it has been assumed that the hourly horizontal solar radiation measurements are available for the particular location to be simulated ^{8,9}.

The prediction of solar radiation on inclined surfaces from the measured horizontal radiation, assuming clear sky conditions, has been extensively studied^{8,9,10}. However, the degree of cloud conditions varies over each day and for the particular location.

As a consequence, Page¹¹ has developed techniques to predict the direct and diffuse solar radiation on vertical surfaces under clear sky and overcast cloud conditions for particular geographical locations in the United Kingdom.

At present, no suitable technique is readily available to predict the incident solar radiation on an inclined collector surface under intermittent cloud conditions. In this investigation, the technique developed by Page¹¹ has been modified to provide a simple, accurate method of predicting the direct and diffuse radiation components under fluctuating cloud conditions.

1.2.3. Dynamic Thermal Simulation of Solar Heating System Performance

The energy collected by the solar collector unit is most commonly stored within a water tank system. In conjunction, with the solar collector prediction model, the accurate simulation of the heat transfer and energy flow processes within the storage tank is essential. This behaviour has been extensively studied to form a dynamic simulation model of a solar water heating system^{12,13,14}. These simulation techniques have been used to analyse the influence of various environmental parameters on system performance^{13,14}. As a result of the previous limitations in the prediction of the dynamic collector performance under intermittent cloud conditions, the accuracy of these studies is restricted.

1.3. Objectives of Present Work

The objectives of the present investigation are:

- (i) the development of a comprehensive thermal network technique and computer program to predict the dynamic thermal behaviour of the flat-plate solar water heating system under transient climatic conditions.
- (ii) the validation of the predicted results of the computer program against experimental results from a solar water heating test facility and the monitored performance of a commercial solar heating system under actual operating conditions.
- (iii) the investigation, by the development of the computer program and the experimental collector facility, of the design and thermal performance of integrated solar collector installations in buildings, to improve the system performance under restricted environmental conditions.

Section 1

References

1. Hottel, H.C. and Woertz, B.B., 'Performance of flat-plate solar heat collectors'. Trans ASME, 1942. pp. 91-100.
2. Whillier, A., 'Design factors in influencing solar collector performance'. Low Temperature Engineering Application of Solar Energy, 1967. pp. 27-38.
3. Bliss, R.W., 'The derivations of several plate efficiency factors useful in the design of flat-plate solar heat collectors'. Solar Energy, 1959. pp. 55-64.
4. Close, D.J., 'A design approach for solar processes'. Solar Energy, 1967. pp. 112-114.
5. Klein, S.A., 'Transient considerations of flat-plate collectors'. Trans ASME, 1974. p. 111.
6. Ibid., p. 112.
7. Wijesundera, N.E., 'Comparison of transient heat transfer models for flat-plate collectors'. Solar Energy, 1978. pp. 517-518.
8. Parmelee, G.V., 'Irradiation of vertical and horizontal surfaces by diffuse solar radiation from cloudless skies'. Heating, Piping and Air Conditioning, 1954. pp. 129-135.
9. Liu, B.Y.H. and Jordan, R.C., 'The inter-relationship and characteristic distribution of direct, diffuse and total solar radiation'. Solar Energy, 1960. pp. 1-15.
10. Liu, B.Y.H. and Jordan, R.C., 'Daily insolation on surfaces tilted toward the equator'. ASHRAE Journal, 1961. pp. 53-59.
11. Page, J.K., 'Geographical variations in the climatic factors influencing solar building design'. Proc. Conf. Solar Building Technology, 1977. pp. 1-15.
12. Close, D.J., 'A design approach for solar processes'. Solar Energy, 1967. pp. 113-115.
13. Gutierrez, G., Hincapie, F., Duffie, J.A. and Beckman, W.A., 'Simulation of forced circulation water heaters; effects of auxiliary energy supply, load type and storage capacity'. Solar Energy, 1974. pp. 288-292.
14. Courtney, R.G., 'A computer study of solar water heating'. Building and Environment, 1977. pp. 74-77.

SECTION 2

THERMAL PERFORMANCE OF THE FLAT-PLATE SOLAR COLLECTOR

2.1. Review of Previous Work

A brief review of the previous work has been outlined in Section 1.2. In this section, a detailed review of the more important aspects of the collector simulation techniques presently available will be given.

2.1.1. Hottel-Whillier-Bliss Steady-State Model

At present, the prediction method developed by Hottel and Woertz ¹, Whillier ², and Bliss ³ is the most common technique utilised to simulate the steady-state performance of the flat-plate solar collector. In the prediction of the steady-state performance, this model neglects the effect of the collector thermal capacitance. As a result, this model can be defined as a Zero Capacitance Model.

The steady-state collector performance, based on the useful energy gain of the fluid circulating through the collector tubeways is expressed by Whillier ⁴ as:

$$\text{Rate of useful energy gain} = \text{Amount of solar energy absorbed by collector plate} - \text{Heat loss from collector plate}$$

$$q_u/A_s = F''F'[S - U_L \cdot (T_i - T_a)] \quad (2.1)$$

where $F''F'$ is the heat removal efficiency factor for the particular collector construction derived by Whillier ⁵ and Bliss ⁶.

The accuracy of the zero capacitance prediction model is limited to the short or long term average collector performance under steady-state climatic and operating conditions as defined by Liu and Jordan ⁷. Klein ⁸ and Wijesundera ⁹ have analysed the prediction accuracy of the zero capacitance model under simulated variable climatic conditions.

The results from these studies have shown that the short term prediction accuracy of this method is sensitive to the fluctuation of the climatic conditions and the effect of the collector thermal capacitance./

Under simulated solar radiation conditions, Klein ⁸ and Wijesundera ⁹, found a significant error in the short term collector performance.

Although, the short term inaccuracies tend to be cancelled out, as indicated by Klein ⁸, over the period of a heating season. These studies have highlighted the need for a prediction method to accurately model the short term collector performance under variable climatic conditions.

2.1.2. One Node Capacitance Model

From the previous steady-state work, Close ¹⁰ developed a dynamic thermal model which incorporated the effect of collector thermal capacitance. This model utilises a simplified thermal node technique, in which one nodal equation models the heat transfer and energy storage processes within the collector unit.

$$\begin{aligned} \text{Energy stored within} &= \text{Amount of solar energy} - \text{Heat loss from} \\ \text{the collector plate} &\quad \text{absorbed by collector} \quad \text{collector plate} \\ &\quad - \text{Energy transferred by circulating fluid} \\ C_a \frac{dT_w}{dt} &= F[S - U_L(T_w - T_a) - C_w dT_w] \end{aligned} \quad (2.2)$$

where T_w is the mean collector fluid temperature. This technique can be defined as a One Node Capacitance Model.

In the above expression, Close ¹¹ assumed that the collector plate temperature was equivalent to the fluid temperature, and that the temperature distribution along the collector was linear. In addition, the net collector unit thermal capacitance was simplified to the product of the total collector thermal mass multiplied by the rise of the mean collector fluid temperature over time. The thermal capacitance effect of the collector cover was neglected.

Klein ¹², described this model, with the application of factors to allow for differential thermal storage effects within the collector unit component materials. However, Klein ¹³ and Wijesundera ¹⁴ still/

still found that the assumptions taken in the model restricted the prediction accuracy under variable solar radiation conditions.

2.1.3. Two Node Capacitance Model

Recognising the need for a more detailed simulation model, Klein ¹⁵ outlined a theoretical technique which divided the collector unit into a series of interconnected thermal nodes. This model can be defined as a Multi-Node Capacitance Model.

The simplest application of this technique is a two-node model in which nodes are positioned at the collector plate and the cover. The heat balance equations for the whole collector plate and cover have been expressed by Klein ¹⁵ as follows:

collector cover:

$$mCp_c \cdot \frac{dT_c}{dt} = S_1 + h_1 \cdot (T_p - T_c) - h_2 \cdot (T_c - T_a) \quad (2.3)$$

collector plate:

$$mCp_p \cdot \frac{dT_p}{dt} = S_2 - h_1 \cdot (T_p - T_c) - 2mCp_p \cdot (T_p - T_1) \quad (2.4)$$

where h_1 and h_2 are the heat loss coefficients from the collector plate and cover respectively.

The prediction accuracy of the two node capacitance technique has been analysed by Wijesundera ¹⁶ against experimental work and the results compared against those predicted by zero and one node capacitance methods. The investigation concluded that the zero capacitance model is limited to the prediction of average daily useful energy collection using hourly averaged meteorological data, given steady-state conditions. A significant improvement in the prediction of the short term dynamic collector behaviour has been found by Wijesundera ¹⁶ for the two node method as compared against the previous one and zero capacitance techniques. However, under fluctuating solar radiation conditions, the two node capacitance model, revealed significant discrepancies in the hourly useful energy collection and/

and the collector fluid temperature. As a consequence, a more refined collector simulation technique is required for the accurate prediction of the dynamic short term thermal performance and the detailed temperature behaviour under fluctuating solar conditions, prevalent in the United Kingdom.

2.2. Theoretical Analysis - Dynamic Behaviour of Collector Units

2.2.1. Method of Analysis

In this section, the two node capacitance model, outlined in Section 2.1.3., has been developed to form a nodal thermal network of elemental sections at the collector plate and cover, illustrated in Figure 2.1. The equations describing the heat balance within each elemental section can be expressed as follows:

Heat balance within collector cover

Energy stored within cover section = Solar radiation absorbed by cover section + Net heat gain from collector plate

$$C_1 \cdot \frac{dT_c}{dt} = S_1 + \left[F \cdot \sigma \cdot \frac{(T_c^4 - T_a^4)}{1/\epsilon_p + 1/\epsilon_c - 1} + F \cdot h_c \cdot (T_w - T_c) \right] - \left[\sigma \cdot \epsilon_c \cdot (T_c^4 - T_a^4) + h_w \cdot (T_c - T_a) \right] \quad (2.5)$$

Heat balance within collector cover

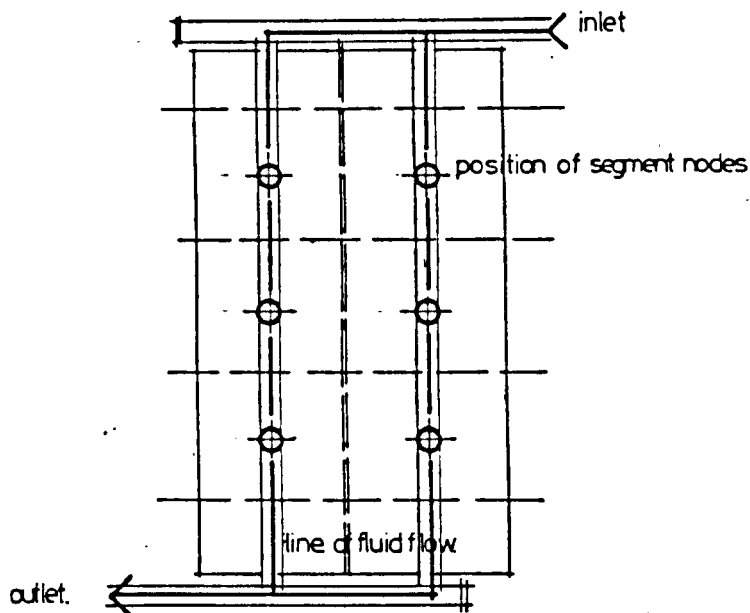
Energy stored within collector plate section = Solar radiation absorbed by collector plate section + Upward heat loss from collector plate to cover

- Rear and edge heat losses from collector plate to external air - Heat transfer from plate to circulating fluid

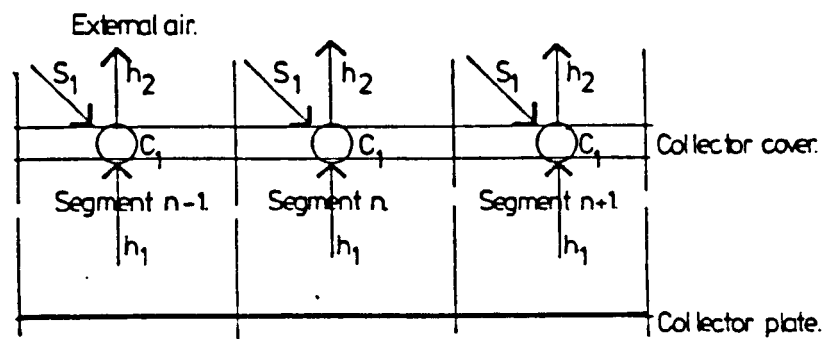
$$C_2 \cdot \frac{dT_w}{dt} = S_2 - \left[F \cdot \sigma \cdot \frac{(T_c^4 - T_a^4)}{1/\epsilon_p + 1/\epsilon_c - 1} + F \cdot h_c \cdot (T_w - T_c) \right] - \left[F \cdot F_e \cdot \frac{(T_w - T_a)}{d_r / k_r + 1/h_r} \right] - m C_{p_w} \cdot dT_w \quad (2.6)$$

The derivation of the heat transfer and energy storage terms within the elemental collector plate and cover sections are fully outlined in Appendix 1.1.

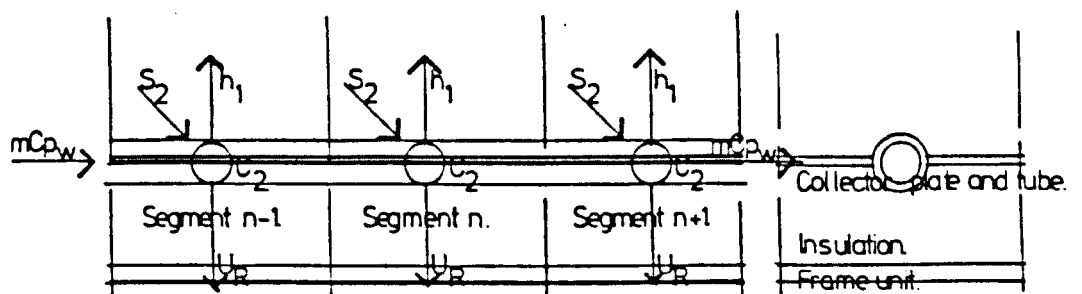
The following assumptions have been taken in the derivation of the terms within the heat balance equations:



Thermal network model of solar collector: 6 Node model.



Elemental collector cover segment.



Elemental collector plate segment.

Figure 2.1 Multi-node thermal capacitance model.

- (i) The convection coefficient h_c , of the heat transfer between the collector plate and the cover has been tabulated by Tabor¹⁷ for a range of collector inclinations and temperature differences between the collector plate and the cover. The tabulated values, derived by Tabor¹⁸ from an experimental study of the natural convection between inclined parallel heated plates give greater accuracy than the normal calculation method to obtain the convection coefficient.
- (ii) The radiation shape factor for the radiation transfer between the elemental section of the collector plate and the cover has been graphically determined to be 1.0 for the possible elemental collector section geometrics to be studied¹⁹. As a result, this factor has been neglected from the radiation transfer term in equations (2.5 and 2.6). This factor is illustrated in Figure 2.2.
- (iii) The rear insulation within the collector unit has been assumed to be a parallel slab of finite thickness and length. As a consequence, the heat flow as derived by Tabor²⁰ is greater at the collector perimeter. To compensate for this increased heat flow, Tabor²¹ has formulated an edge correction factor Fe , which is applied to the rear heat transfer coefficient.

$$Fe = 1.0 + Sa \cdot d_1 / L' \quad (2.7)$$

where Sa is the edge addition coefficient tabulated by Tabor²² and L' is the characteristic size of the collector plate.

- (iv) The following approximate values²³ have been taken for the rear convection loss coefficient h_r , for the various collector constructions:

(a) fixed externally to the roof fabric, with $h_r = 14-23 \text{ W/m}^2\text{ }^\circ\text{C}$ depending on the climatic exposure of the site.

(b) integrated within the roof construction with $h_r = 9.5 \text{ W/m}^2\text{ }^\circ\text{C}$.

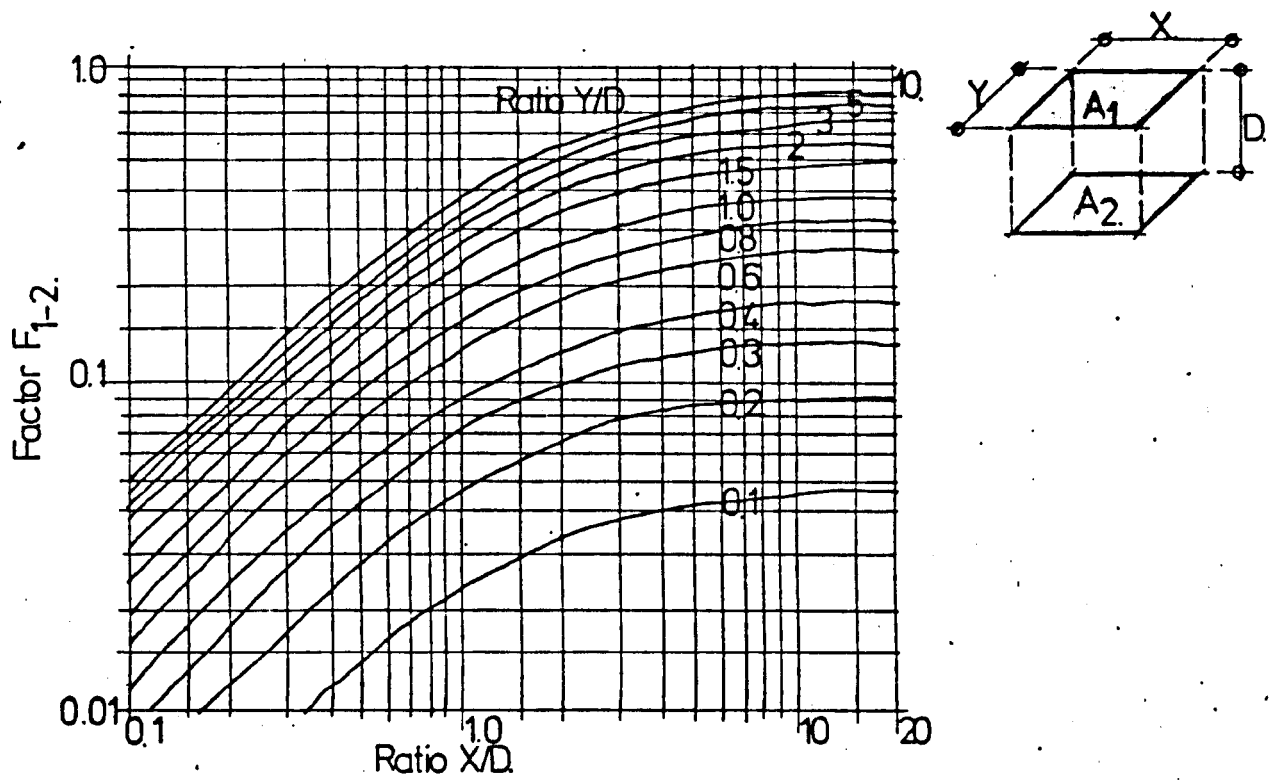


Figure 2.2 Graphical representation of the radiation shape factor F_{1-2} . (from Holman¹⁹).

- (v) The forced convection heat loss coefficient h_w , for the heat transfer from the collector cover due to the wind effects has been obtained from the empirical relationship derived by McAdams²⁴, and expressed as follows:

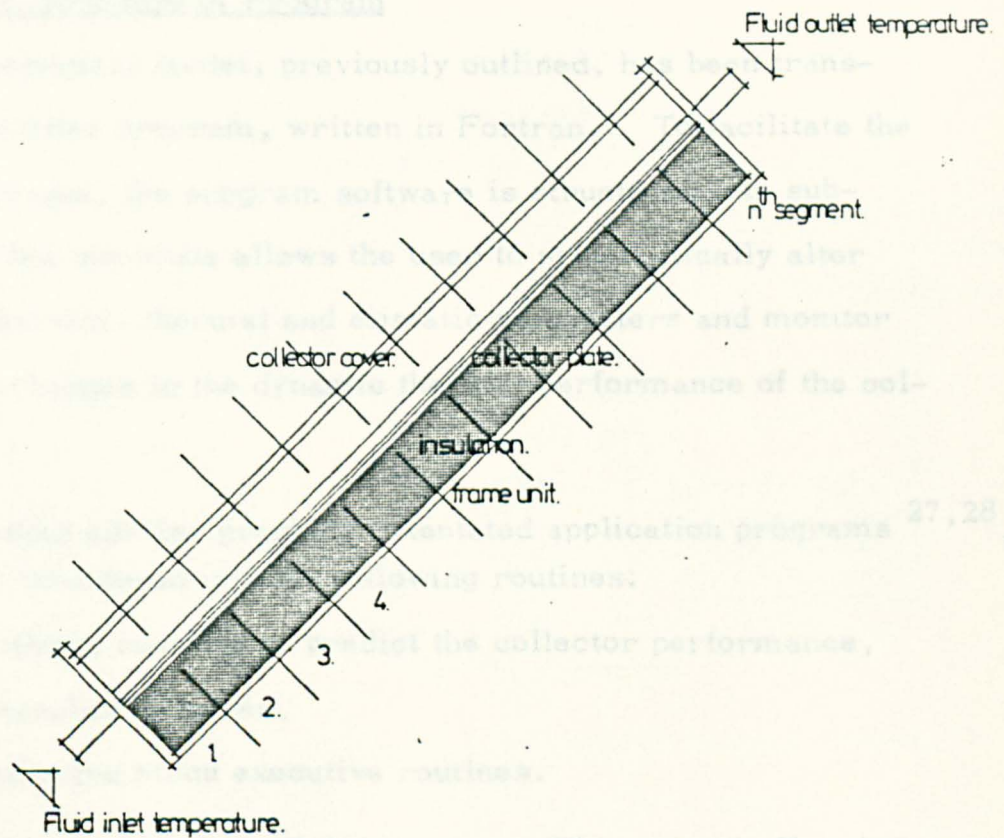
$$h_w = 5.7 + 3.8.v \quad (2.8)$$

- (vi) The fluid temperature gradient along each elemental collector plate section is assumed to be linear as a result of the small collector section lengths involved, as illustrated in Figure. 2.3.

The matrix representation required for the numerical solution of the simultaneous heat balance equations is outlined in Appendix 1.2. This method of matrix solution was chosen because it is relatively easy to execute on the digital computer since only the non-zero terms within the matrix will contribute to the calculation. This explicit numerical method obtains the new values of the cover and fluid section temperatures T'_c and T'_w from the initial temperature values T_c and T_w .

The Modified Euler numerical method was chosen as the easiest predictor-corrector technique to implement on the computer program²⁵. However, it was found that during the program validation studies, outlined in section 2.4.2., that this particular method became strongly unstable at above 8 section nodes, because of the effect of the roundoff error caused by the number of iterations required to attain 2 digit accuracy.

In an attempt to solve this problem, a fourth order Runge-Kutta numerical method was chosen. This numerical method, outlined by Stark²⁶, has the advantage over the Euler method of greater accuracy for the comparable amount of calculations. Four digit accuracy was achieved within five iteration steps. The numerical technique requires that the period from the initial value point X_0 , to the point of the X_0 desired solution of X_n is divided into n subintervals performing an/



Longitudinal section thro. hypothetical solar collector model.

Figure 2.3 Representation of typical multi-node model of a flat-plate solar collector.

an iteration of the following form.

$$y_1^{(n+1)} = y_0 + 1/6.(k_1 + 2k_2 + 2k_3 + k_4) \quad (2.9)$$

This method has been successfully tested in the program validation studies, showing no sign of instability at large collector thermal networks.

2.3. Computer Simulation

2.3.1. Outline Structure of Program

The mathematical model, previously outlined, has been translated into a computer program, written in Fortran. To facilitate the simulation technique, the program software is structured into subprograms. This technique allows the user to systematically alter the collector physical, thermal and climatic parameters and monitor the subsequent changes in the dynamic thermal performance of the collector.

As with other similar graphics orientated application programs^{27,28}, the program is structured into the following routines:

- (i) the algorithmic routines to predict the collector performance,
- (ii) the data handling routines,
- (iii) the graphics and menu executive routines.

The executive component of the program, illustrated in flowchart form in Figure 2.4., outlines the structure and the interactive nature of the program routines.

2.3.2. Description of Computer Program

A brief description of each of the subprogram routines to perform the above algorithmic, data handling and graphics functions is outlined. The computer program is fully listed in Appendix 2.1.

(i) Subroutine MOD 1

The function of the subprogram MOD 1, is to enable the user to visually check the input data submitted to the program storage area.

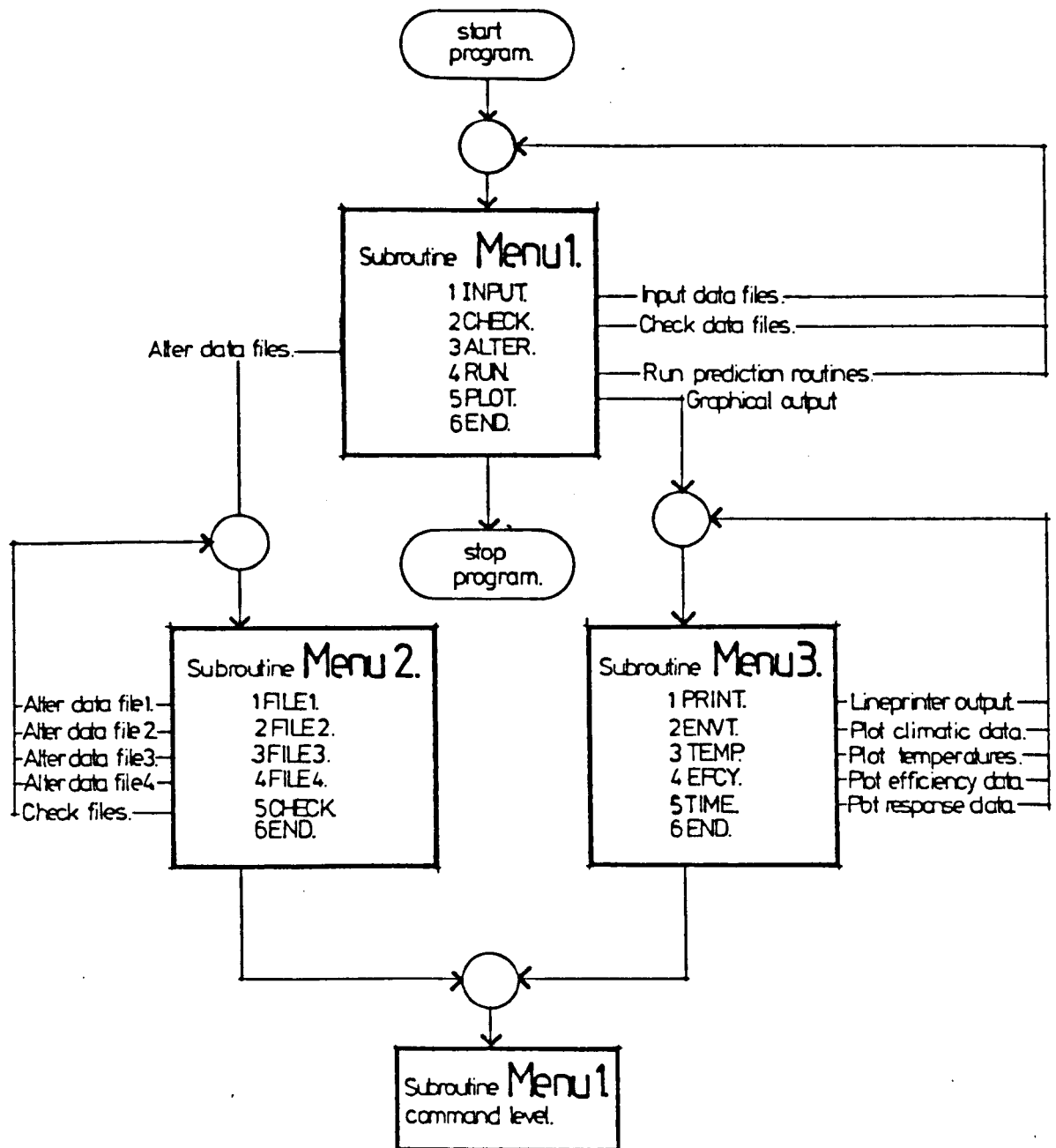


Figure 2.4 Flowchart representation of the collector performance prediction subprogram.

The user specifies the name of a particular external data file, which has been created beforehand with the required collector physical characteristics. This data is subsequently transferred to the program common storage area.

(ii) Subroutine NUSELT

The function of the subroutine NUSELT, is to calculate the thermophysical properties of the heat transfer fluid, which in this case is taken to be water. From the tabulated physical data of the fluid thermal behaviour for various temperatures within the routine, the Prandtl, Reynold's and Nussett numbers, fluid conductivity, viscosity and density are calculated to determine the fluid convective heat transfer coefficient.

(iii) Function CPRO

The purpose of the routine CPRO, is to calculate the thermal capacitance of the heat transfer fluid from the tabulated values of the fluid density and specific heat capacity for temperatures between 0 and 120 deg. C.

(iv) Subroutine MOD 2

The function of the routine MOD 2, is to calculate the components of the heat balance equations. These components consist of the thermal capacitance of the collector plate and cover, the top, rear and edge heat loss coefficients, and the fluid heat transfer.

The first subprogram section initialises the calculation constants within the routine, and calculates the thermal capacitance of the cover section, the fluid mass flow rate and velocity. The second subprogram section MOD 2 BC, calculates the values of the collector material component thermal resistances and capacitance to determine the collector plate section capacitance, and the top, rear and edge heat losses for the particular collector construction. The third subprogram section MOD 2 D, calculates the/

the fin and collector efficiency factors for the particular collector construction, and the solar radiation absorbed by the cover and collector plate sections.

(v) Subroutine MOD 3

The function of the routine MOD 3, is to initialise the numerical method matrix, and iteratively solve by the Quartic Runge-Kutta method, the network section node temperatures after each time increment.

(vi) Subroutine MOD 4

The function of the routine MOD 4, is to control the operation of the other interrelated subprograms, from which to calculate and display the section temperatures at each time increment over the specified simulation period.

(vii) Subroutine MOD 5

The function of the routine MOD 5, is to determine the convection heat transfer coefficient between the collector plate and the cover above. The convection coefficients have been tabulated within the routine for various collector tilts given the temperature difference between the collector plate and the cover.

(viii) Subroutine MOD 6

The function of the routine MOD6, is to print in tabular form, the calculated values of the inlet and outlet collector fluid temperatures, the collector and cover section node temperatures, the level of solar radiation, air temperature, and the collector efficiency for each time increment over the specified simulation period.

(ix) Subroutine MENU 1

The function of the routine MENU 1, illustrated in flowchart form in Figure 2.4., is to control the operation of the program by the selection of a number of options. As a consequence, it is possible/

possible from the MENU 1 program options, to iteratively alter, predict and analyse the dynamic thermal performance of any number of different solar collector designs.

(x) Subroutine MENU 2

The function of the routine MENU 2, illustrated in flowchart form in Figure 2.4, is to control the alteration of the data files, which store the collector parameters and climatic data.

(xi) Subroutine MENU 3

The function of the routine MENU 3, illustrated in flowchart form in Figure 2.4, is to select the particular method of displaying the predicted collector performance over the simulation period.

(xii) Subroutine PLOT 1

The function of the routine PLOT 1 is to display in graph form the range of actual climatic data and predicted collector performance results. In addition, the routine allows the user to overlay any combination of results. The graphics software within the routine has been written from the GINOGRAPH graphics software ²⁹.

2.4. Experimental Investigation

2.4.1. Objectives of Experimental Investigation

The objective of the experimental investigation has been to validate the predicted dynamic collector behaviour under variable climatic conditions against actual performance results. This objective has been achieved by the following experimental studies, utilising a purpose-built solar collector test facility to investigate the heat transfer and energy storage processes within the collector unit. As a consequence of this investigation, the simulation model has been amended to improve the accuracy of prediction.

2.4.2. Error Analysis Against Previous Work

The first part of this investigation has been an error analysis of the/

the computer simulation results against previous work. The aim of this initial analysis is to detect major errors in the computer simulation program.

The analysis involved the detailed study of the heat transfer components against previous steady-state work by Whillier³⁰ and Duffie and Beckman³¹. This investigation was restricted to the collector steady-state performance, due to the lack of previous work on dynamic collector performance.

The majority of errors detected in the program were caused by Fortran language errors, rather than discrepancies in the theoretical heat transfer model. The second major error, revealed by the program analysis, was found within the initial numerical method chosen: the Modified Euler Method. This method was found to be unstable for thermal networks above 8 sections, in which large round-off errors occurred, due to the excessive number of iterations involved to obtain a solution.

With the elimination of the major subprogram errors, the next stage in the program validation studies involves the analysis of the accuracy of the prediction results against actual collector performance experimental data.

2.4.3. Apparatus and Experimental Procedure

A flat plate solar water collector system, illustrated in Figure 2.5, has been designed for the indoor and outdoor performance validation studies. A copper tube in plate solar collector of domestic scale has been chosen as representative of the present commercial collector design available. In addition, this insert type of collector has been selected for further experiments involving the collector unit incorporated within the roof fabric. In the present indoor and outdoor experiments, the collector unit is completely exposed to the external/

Key.

t. position of thermocouples.
s. solarimeters.

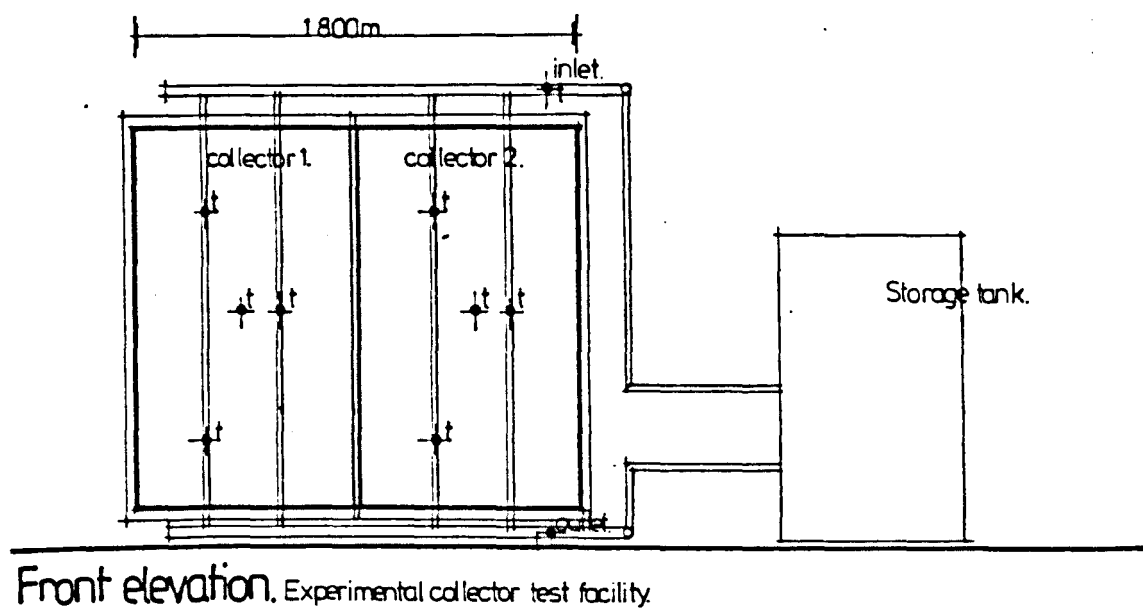
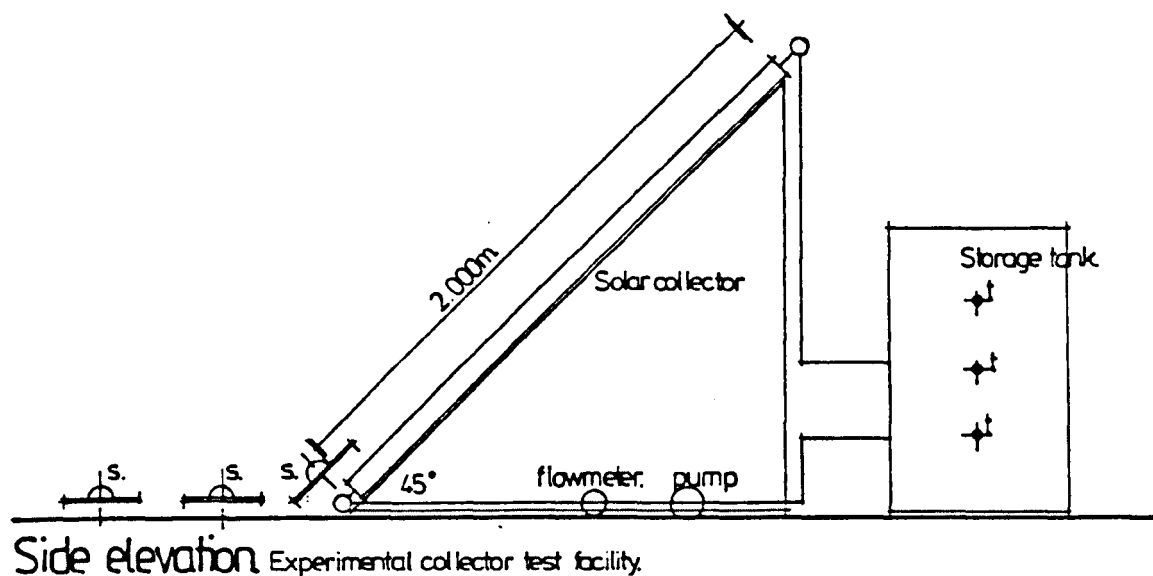


Figure 2.5 Outdoor solar collector experimental test facility.

external air to facilitate heat loss measurements. Alternative collector glazing is supplied, with 4mm glass or 6mm perspex.

Constructed on a 45° mild steel angle frame, the collector array is connected by 15mm copper pipework to a 150 litre insulated hot water storage tank. For this investigation, the temperature measurements from the storage tank have not been taken into account. A commercial pump is used to circulate the fluid through the collector system. The pump operation is continuous for each experiment.

The measurement of the collector thermal behaviour was monitored by a network of premium grade copper constantan thermocouples, positioned as shown in Figure 2.5. This network gave, as far as possible, a complete record of the temperature behaviour within the collector unit, accurate to within $\pm 0.5^{\circ}\text{C}$. The fluid flowrate is measured by an electronic turbine flowmeter manufactured by Litre Meter for a specific flow range, in this case the range between 0.1 - 4.5 litres/minute. The measurements of the turbine rotation are electronically integrated over intervals of 1 minute for the complete experiment. This type of flow measurement is sensitive to small changes in the flow velocity, and gives an accuracy of ± 0.05 litres/minute.

The flowrate was held constant over each experiment. The measurement of the solar radiation was recorded by three solarimeters, manufactured by Kipp and Zonen, measuring the horizontal, incident 45° tilt and the diffuse solar radiation. The solarimeters were calibrated previous to the experiments, at the Meteorological Office in Bracknell, to give an accuracy of $\pm 1.5\%$. The air temperature is measured by an enclosed dry bulb thermocouple probe, the wind velocity is measured by a hand held wind speed recorder, accurate to $\pm 0.5\text{m/s}$.

These measurements were recorded at specified intervals by a Solartron data logger, which electronically processed the analogue experiment readings into digital form, and subsequently transfers these readings onto punched papertape. The inherent error within the transfer of the analogue readings to the digital papertape form is limited to $\pm 1.5\%$ error. The papertape records were subsequently read onto magnetic tape for long term storage and analysis within the Institute main frame computer. A purpose-written computer program STAPEL, outlined in Appendix 2.2, is used to analyse, tabulate and graphically display the results of each experiment. These results were finally analysed against the predicted values from the simulation program.

The procedure used to obtain the above results from the indoor and outdoor experiments is outlined as follows:

(i) Indoor collector experiments

Briefly, the purpose of the indoor experiments is to measure the solar collector, storage tank and pipework heat losses under no radiation input, steady-state conditions.

With the experiment test facility set up as shown in Figure 2.5, and the measurement apparatus calibrated, the indoor collector experiments were carried out for three collector heat loss studies. The experimental method used is to raise the water temperature in the storage tank, by the use of an immersion heater, to an arbitrary temperature between 55° and 65°C . The circulation pump is activated and the subsequent variation in the temperature at the sensor locations in the collector unit and storage tank recorded. All three experiments were monitored for a period of two hours, with a recording interval of 1 minute.

During the experiment period, the internal air temperature within/

within the laboratory space is continuously monitored. The wind velocity within the laboratory is assumed to be negligible after the initial air movement measurements registered no significant air velocity. A selection of the results from the indoor experiments are illustrated and discussed in section 2.5.1.

(ii) Outdoor collector experiments

The purpose of the outdoor experiments is to measure the collector heat gain, heat loss and the thermal efficiency under various types of solar radiation conditions.

As with the indoor experiments, the experimental procedure is initially the recalibration of the thermocouples after the reconstruction of the test facility at the outdoor location within the School of Architecture. With the experiment test facility set up, as shown in Figure 2.5, and the measurement apparatus calibrated, the outdoor collector experiments were carried out for five studies.

The experimental method used is to first run three experiments for a detailed monitoring period of 10 hours, under a range of solar radiation conditions. The second stage in the outdoor experiment procedure is to run two experiments for a long term monitoring period, under, as far as possible, a similar range of solar radiation conditions. In both cases, intermittent measurements and observations were taken of the wind speed and the sky cloud conditions respectively over the experiment period. A continuous pump operation is used. As a consequence, heat loss measurements were taken during the evening of the experiment period under no radiation conditions. A selection of the results from the outdoor experiments are illustrated and discussed in section 2.5.2.

2.5. Presentation and Discussion of Results

The results from the indoor and outdoor collector performance experiments are discussed and illustrated in sections 2.5.1 and 2.5.2. In addition, the prediction results from the computer simulation are compared against the actual thermal behaviour of the collector test facility.

2.5.1. Indoor Experiment Results and Prediction Validation

The results of the indoor experiments carried out in the laboratory to investigate the collector heat loss under no radiation, steady-state conditions are discussed and illustrated. The temperature distribution profile within the collector, for one experiment representative of the heat loss studies, is illustrated in Figure 2.6. The temperature distribution, within the collector unit, over the experiment period, gives an indication of the rate of heat loss dissipated from the collector plate. For the steady-state conditions present in the experiments, this rate of heat loss is a constant, as illustrated in Figure 2.6. To facilitate the analysis of the temperature distribution within the collector, the results are plotted at 10 minute intervals.

The results predicted from the computer simulation studies are overlayed on the actual experiment temperatures, as shown in Figure 2.6. The predicted temperature distribution within the collector unit is graphically compared against the actual distribution. A good correlation has been obtained. As a result, this correlation validates the accuracy of the theoretical heat transfer equations modelling the collector heat loss under steady-state no radiation conditions.

2.5.2. Outdoor Experiment Results and Prediction Validation

From the five experiments carried out on the outdoor collector test facility, the results of two experiments, representative of the complete study are illustrated and discussed in detail. The inlet, outlet/

Inlet and outlet collector fluid temperatures.

Date of experiment : 20 Feb. 1980. 2 hour experiment.

Experiment time interval.

1 minute.

□—□ experimental results.

○—○ predicted results.

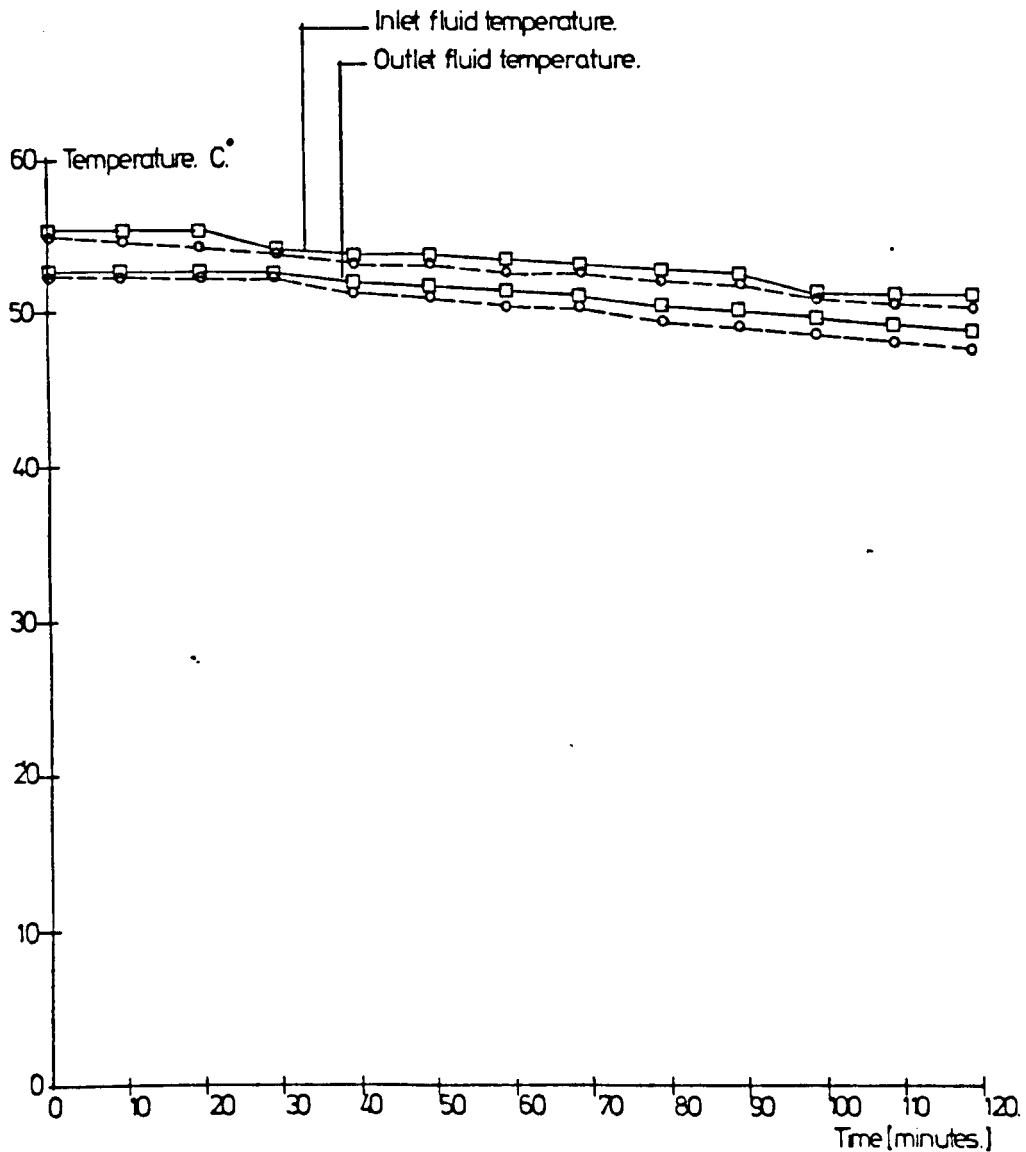


Figure 2.6 Actual vs Predicted collector outlet fluid temperatures - indoor heat loss experiment.

outlet and the collector temperature distribution results for these experiments are illustrated in Figures 2.7 - 2. 10.

(i) Short Term Collector Performance

In the first two experiments, the collector behaviour and climatic conditions were monitored for 10 hours, at 1 minute intervals. The experiments were carried out under clear sky, intermittent and overcast cloud conditions, illustrated and discussed in detail in section 3.5.

The results from the experiment, illustrated in Figure 2.7, clearly indicate the effect of different solar radiation conditions on the solar collector thermal performance. The temperature distribution profile within the collector, for one experiment representative of the short term performance studies is illustrated in Figure 2.7. A significant temperature distribution is present under clear sky conditions in contrast to the negligible distribution present under overcast sky conditions.

The results predicted from the computer simulation studies are overlayed on the experiment results, as shown in Figure 2.7. A good correlation has been obtained against the actual temperature distribution within the collector. The actual and predicted collector efficiency values are plotted in Figure 2.8, in conjunction with the variation of the solar radiation. These results indicate the significant influence of the fluctuation of solar radiation conditions on the prediction of the steady-state collector efficiency. A good correlation has been obtained, however, the results illustrate an error in the prediction of the solar radiation conditions at low solar attitudes. As a result, these correlations validate the general accuracy of the collector thermal simulation under variable solar radiation conditions.

Inlet and outlet collector fluid temperatures.

Date of experiment. 28 April 1980. 10 hour experiment.

Experiment time interval

1 minute.

□—□ experimental results.

○—○ predicted results.

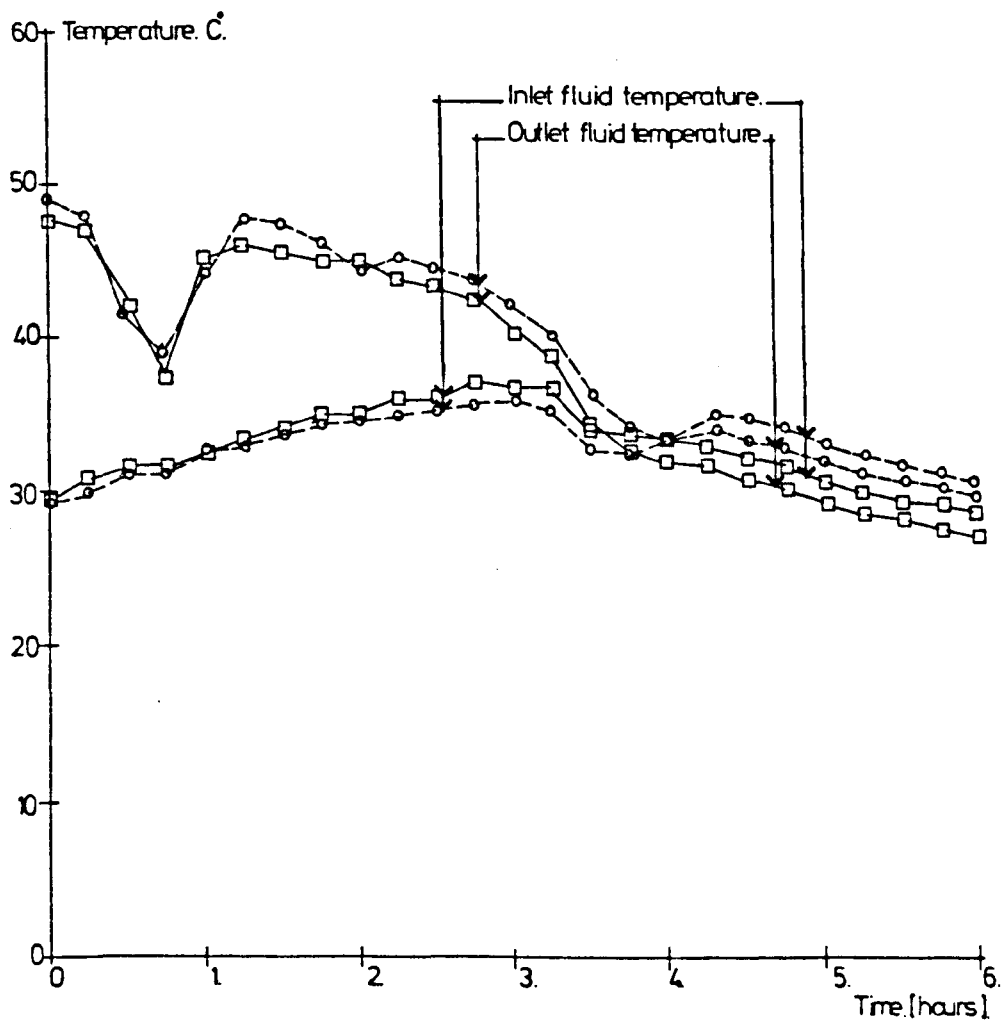


Figure 2.7 Actual vs Predicted collector fluid temperatures
- short term outdoor experiment.

Collector efficiency.

Date of experiment. 28 April 1980. 10 hour experiment.

Experiment time interval.

1 minute.

□ experimental results.

● predicted results.

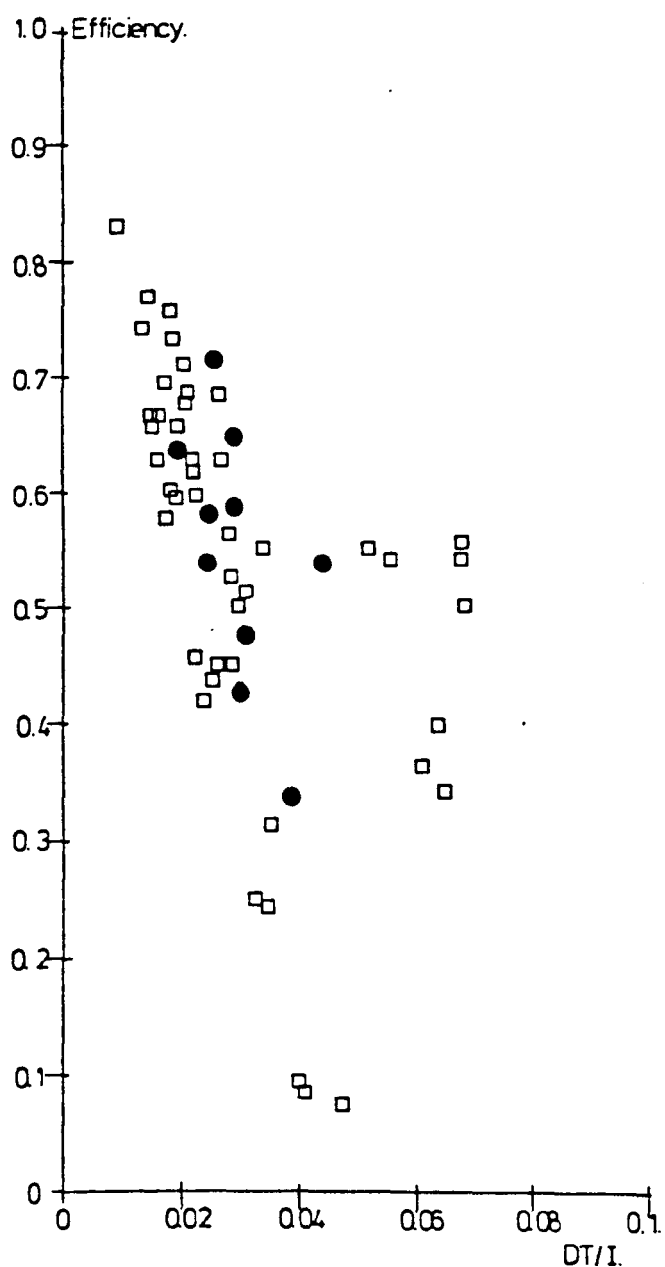


Figure 2.8 Actual vs Predicted collector efficiency
- short term outdoor experiment.

Inlet and outlet collector fluid temperatures.

Date of experiment. 29 April 1980. 1 day experiment.

Experiment time interval.

10 minutes.

□—□ experimental results.

○—○ predicted results.

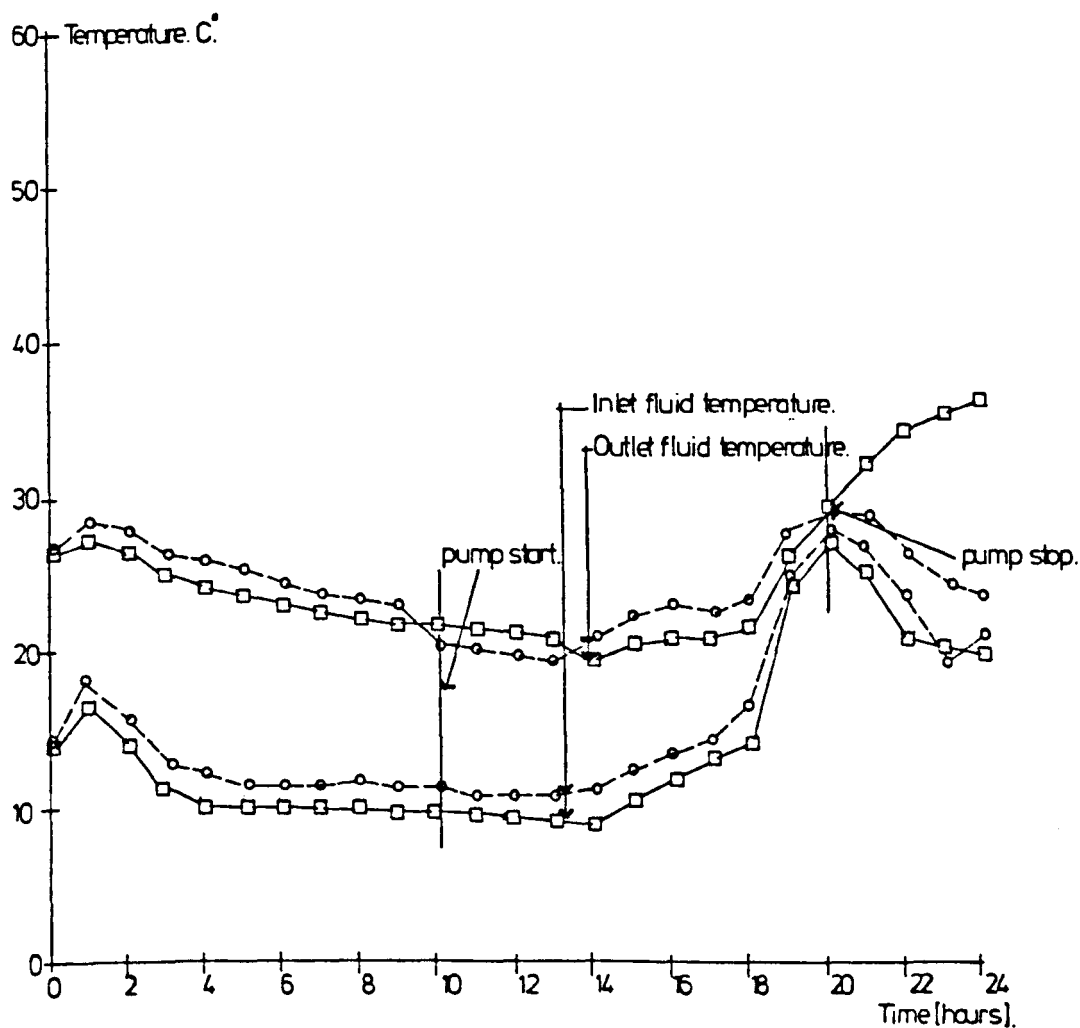


Figure 2.9 Actual vs Predicted collector fluid temperatures
-long term outdoor experiment.

Collector efficiency.

Date of experiment. 29 April 1980. 1 day experiment.

Experiment time interval.

10 minutes.

□ experimental results.

● predicted results.

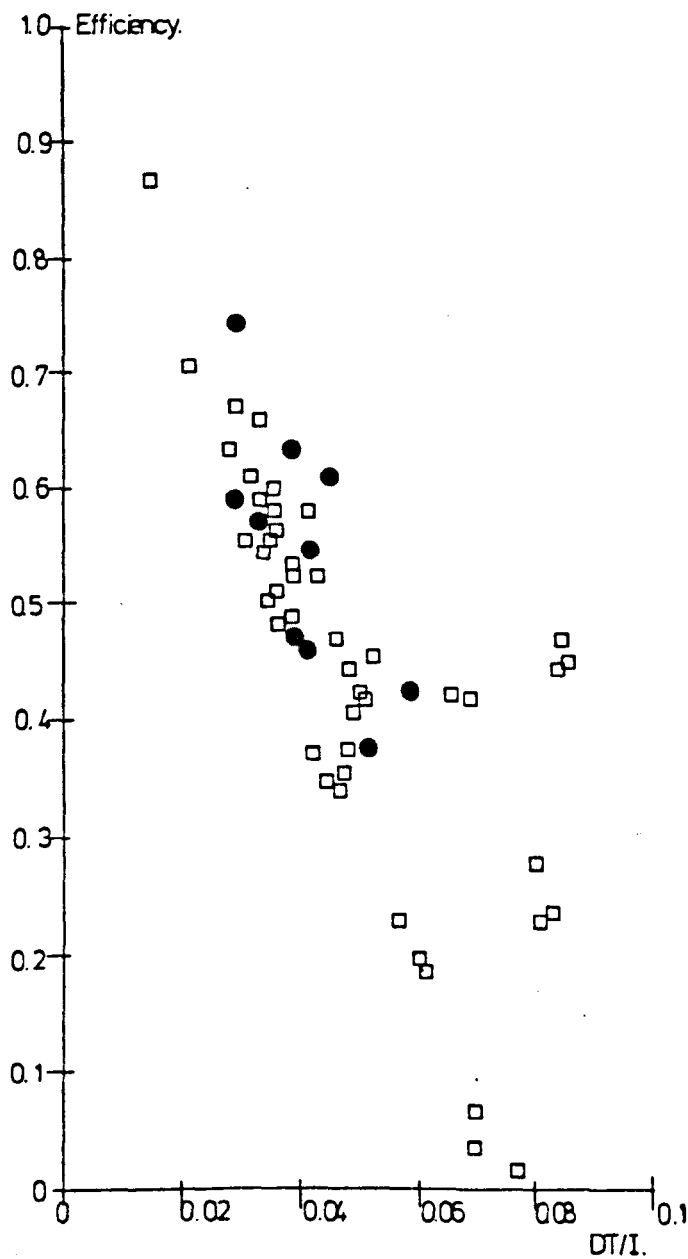


Figure 2.10 Actual vs Predicted collector efficiency
- long term outdoor experiment.

(ii) Long Term Collector Performance

In the second range of experiments, the collector thermal behaviour and climatic conditions were monitored for 2 days, at 10 minute intervals. As with the short term experiments, these studies were carried out under different solar radiation conditions, illustrated and discussed in detail in section 3.5.

The temperature distribution profile within the collector, for one experiment representative of the long term performance studies, is illustrated in Figure 2.9. The collector efficiency over the period is plotted in Figure 2.10. The results emphasise the effect of fluctuating solar radiation conditions, indicated in the short term experiments, on the collector performance and efficiency.

The results predicted from the computer simulation studies are overlayed on the actual experiment collector temperatures and efficiency values, as shown in Figures 2.9 and 2.10. The predicted temperature distribution within the collector unit is graphically compared against the actual distribution. A good correlation has been obtained during solar radiation conditions above $100\text{--}150\text{W/m}^2$, however below this level and during no radiation conditions a significant error is introduced into the temperature distribution. This error can be explained by an increase in the radiation and convection heat loss to the external air, above the level predicted by the simulation model. The second feature from the results is the significant temperature gradient within the collector, along with fluid flow parallel and perpendicular to the collector tubes. A good correlation has been obtained against the actual collector efficiency results over the longer experiment period, significantly better than in the short term experiments.

2.5.3. Summary of Results

The present indoor and outdoor collector test rig experiments and the subsequent computer program validation studies can be summarised as follows. With the correction of the obvious errors within the computer program revealed by the error analysis against previous steady-state collector performance results, the following validation studies were carried out. These studies consisted of the comparison of the predicted collector temperature distribution and efficiency against the experiment results. A good correlation has been obtained between the predicted and indoor heat loss experiment results.

In the short term and long term outdoor experiments, a significant inaccuracy has revealed in the prediction method to calculate the incident solar radiation on the collector surface from the actual measured total horizontal solar radiation. This error occurred at low solar altitudes, and has been corrected in the method outlined in section 3. A second error revealed by the experimental studies is the under estimation of the predicted collector heat loss to the external air during no radiation conditions in the evening. This error is corrected in section 3.1.2. This study has validated the general accuracy of the multi-node prediction method utilised to model the dynamic collector performance under fluctuating radiation conditions.

Section 2

References

1. Hottel, H.C. and Woertz, B.B., 'Performance of flat-plate solar heat collectors'. Solar Energy, 1942. pp. 98-102.
2. Whillier, A. 'Design factors influencing solar collector performance'. Low Temperature Engineering Application of Solar Energy, 1967. pp. 31-37.
3. Bliss, R.W. 'The derivations of several plate efficiency factors useful in the design of flat-plate solar heat collectors'. Solar Energy, 1959. pp. 55-59.
4. Whillier, A., 'Design factors influencing solar collector performance'. Low Temperature Engineering Application of Solar Energy, 1967. p. 32.
5. Ibid., p. 34.
6. Bliss, R.W., 'The derivation of several plate efficiency factors useful in the design of flat-plate solar heat collectors'. Solar Energy, 1959. pp.
7. Liu, B.Y.H. and Jordan, R.C., 'The long term average performance of flat-plate solar energy collectors'. Solar Energy, 1963. pp. 65-70.
8. Klein, S.A., 'Transient considerations of flat-plate collectors'. Trans. ASME, 1974. pp. 109-113.
9. Wijesundera, N.E., 'Comparison of transient heat transfer models for flat-plate collectors'. Solar Energy, 1978. pp. 517-518.
10. Close, D.J., 'A design approach for solar processes'. Solar Energy, 1967. pp. 112-116.
11. Ibid., pp. 112-114.
12. Klein, S.A., 'Transient considerations of flat-plate collectors'. Trans. ASME, 1974. pp. 111-112.
13. Ibid., p. 112.
14. Wijesundera, N.E., 'Comparison of transient heat transfer models for flat-plate collectors'. Solar Energy, 1978. pp. 519-521.
15. Klein, S.A., 'Transient considerations of flat-plate collectors'. Trans ASME, 1974. pp. 112.
16. Wijesundera, N.E., 'Comparison of transient heat transfer models for flat-plate collectors'. Solar Energy, 1978. pp. 519-520.
17. Tabor, H., 'Radiation, convection and conduction coefficients in solar collectors'. B.H. Res. Council Israel, 1958. pp. 157-162.

18. Ibid., p. 162.
19. Holman, J.P., Heat Transfer. 1976. p. 287.
20. Tabor, H., 'Radiation, convection and conduction coefficients in solar collectors'. B.H. Res. Council Israel, 1958. pp. 167-168
21. Ibid., pp. 167-169.
22. Ibid., p. 168.
23. Ibid., pp. 168-169.
24. McAdams, W.H., Heat Transmission, 1954. pp.
25. Stark, P.A., Introduction to Numerical Methods, 1970. pp. 254-256.
26. Ibid., pp. 265-266.
27. Sussock, H., 'Graphics facilities for computer-aided architectural design'. ABACUS Occasional Paper 25, 1973. pp. 2-3.
28. Clarke, J., 'ESP-Package for appraisal of environmental systems performance'. ABACUS Occasional Paper 48, 1976. pp. 1-10.
29. GINOF User Manual, Computer-Aided Design Centre, 1976.
30. Whillier, A., 'Design factors influencing solar collector performance'. Low Temperature Engineering Application of Solar Energy, 1959. pp. 37-38.
31. Duffie, J.A. and Beckman, W.A., Solar Energy Thermal Process, 1974. pp. 149-153.

SECTION 3

SIMULATION OF CLIMATIC CONDITIONS AND THEIR
EFFECT ON COLLECTOR PERFORMANCE

3.1. Review of Previous Work

A brief review of the previous work has been outlined in Section 1.2. In this section, a detailed review of the more important aspects of climate simulation techniques are discussed.

3.1.1. Solar Radiation Prediction

The accurate prediction of the total amount of solar radiation incident on an inclined solar collector plate is essential for the assessment of the actual collector performance. The prediction of the solar radiation on inclined surfaces under clear sky conditions has been extensively studied by Parmelee ¹, Liu and Jordan ^{2,3,4}, Unsworth and Monteith ⁵ and Page ⁶. Although these techniques vary in detail, the general prediction method involves the calculation of the following solar components:

- (i) the solar geometry
- (ii) the direct and diffuse solar radiation on an inclined surface
- (iii) the solar radiation transmission through the collector cover

As a consequence, these components can be outlined as follows:

(i) Solar geometry

The derivation of the fundamental equations to calculate the solar components which describe the position of the sun for a specified time: the solar altitude and azimuth, are fully outlined in the classical works of the astronomical or nautical data such as the Astronomical Ephemeris ⁷ and the Nautical Almanac ⁸. In addition, these components provide the data to calculate the period of sunshine from the times of sunrise and sunset for the particular location.

(ii) Direct and diffuse solar radiation on inclined surfaces

From the fundamental data on the position of the sun for a specified time and location, the amount of solar radiation incident on an inclined surface can be determined. The general method outlined/

outlined by Liu and Jordan ⁹, from previous studies by Moon ¹⁰, is to divide the total incident solar radiation into three components: the direct, the sky diffuse and the ground reflected solar radiation. This general equation can be expressed as follows:

$$\begin{aligned} \text{Total incident solar radiation} &= \text{Direct solar radiation} + \text{Sky diffuse radiation} + \text{Ground reflected diffuse radiation} \\ I_c &= I_D \cdot RD + I_d \cdot Rd + I_H \cdot Rs \quad (3.1) \end{aligned}$$

where RD, Rd and Rs are respectively the conversion factors for the direct, diffuse and ground reflected radiation and are defined by the following ratios:

$$RD = \frac{\text{the direct radiation incident upon the inclined surface}}{\text{the direct radiation incident upon a horizontal surface}}$$

$$RD = \frac{\cos(\phi - \beta) \cdot \cos \delta \cdot \cosh + \sin(\phi - \beta) \cdot \sin \delta}{\cos \phi \cdot \cos \delta \cdot \cosh + \sin \phi \cdot \sin \delta} \quad (3.2)$$

$$Rd = \frac{\text{the diffuse sky radiation incident upon the tilted surface}}{\text{the diffuse sky radiation incident upon a horizontal surface}}$$

$$Rd = (1 + \cos \beta) / 2 \quad (3.3)$$

$$Rs = \frac{\text{sum of the radiation reflected on the inclined surface from the ground}}{\text{total radiation incident upon a horizontal surface}}$$

$$Rs = \rho_g \cdot (1 - \cos \beta) / 2 \quad (3.4)$$

The prediction method outlined by Liu and Jordan ¹¹ is limited to clear sky conditions and the assumption that the sky diffuse radiation is isotropic. Parmelee ¹² and Page ¹³ have observed that an expression of non-isotropic sky diffuse radiation is more relevant to actual clear sky conditions. The sky diffuse radiation is expressed by Page ¹⁴ as an empirical relationship with an angular correction for the position of the sun.

$$I_{dh} = a' + b' \alpha \quad (3.5)$$

where a' and b' are correction factors for the particular location. This relationship has been further developed by Page ¹⁵ to apply to overcast and average cloudy sky conditions.

In the present investigation, these concepts have been further modified for the prediction of total solar radiation incident on an inclined collector plate under actual variable cloud conditions. This method is outlined in section 3.2, and described in Appendix 1.2.

(iii) Solar radiation transmission through collector cover

The fundamental derivation of the transmittance of solar radiation through transparent covers and the behaviour of short wave radiation between parallel planes has been outlined by Duffie and Beckman¹⁶ and Whillier¹⁷. The fraction of the incident direct solar radiation that is absorbed by a single cover S_{1D} , and the collector plate S_{2D} , is expressed by Duffie and Beckman¹⁶ as:

$$S_{1D} = I_D \cdot \alpha_c \cdot (1 + \tau_c \cdot \rho_p / (1 - \rho_c \cdot \rho_p)) \quad (3.6)$$

$$S_{2D} = I_D \cdot (\tau_c \cdot \alpha_p) / (1 - \rho_c \cdot \rho_p) \quad (3.7)$$

where the reflection and absorption losses are dependant upon the angle of incidence of the direct radiation and the transmittance of the cover material as outlined by Whillier¹⁸.

The transmittance of the diffuse radiation through the cover is treated separately and is assumed by Duffie and Beckman¹⁹ to be unidirectional in nature. All radiation components are neglected after two reflections within the collector unit²⁰.

3.1.2. Air temperature and wind effects

The derivation of the equivalent sky temperature from the air temperature is outlined by Duffie and Beckman²¹. The accurate determination of the sky temperature is important in the calculation of the radiation heat transfer between the collector plate and the surrounding sky hemisphere, outlined in equation form in Appendix 1.1. Whillier²² has related the sky temperature to the air temperature under clear sky conditions by the following simple expression.

$$T_{\text{sky}} = T_a - 6^\circ\text{C}. \quad (3.8)$$

The influence of average sky conditions on the sky temperature has been partially taken into account by the expression outlined by Duffie and Beckman ²³.

$$T_{\text{sky}} = 0.0552T_a^{1.5} \quad (3.9)$$

At present, no expression is available which fully models the influence of overcast cloud conditions and the ground reflectance on the sky temperature

The forced convection heat loss coefficient from the collector cover due to wind has been derived by McAdams ²⁴ as the following empirical relationship to the wind speed, expressed as:

$$h_w = 5.7 + 3.8v \quad (3.10)$$

3.2. Theoretical Analysis - Derivation of Solar Radiation Model

In this section, the solar prediction techniques outlined in section 3.1.1, have been amended and incorporated into a hybrid prediction method, to calculate the incident solar radiation on an inclined collector surface under actual conditions given the total horizontal radiation data. The application of the previous work to form the prediction method is described below, for the calculation of the solar geometry, the incident solar radiation and the solar transmission. This method is described in equation form in Appendix 1.2.

3.2.1. Solar geometry

The solar geometry has been predicted from the method outlined by Walraven ²⁵, which simplifies the classical equations ⁸, to obtain a lesser accuracy of 0.01 degree of the position of the sun. The simplifications made by Walraven ²⁶ are to neglect the detailed perturbations of the earth's orbit by the moon, and other minor effects such as the refraction by the atmosphere and parallax. This method is illustrated in Figure 3.1 and outlined in Appendix 1.2.

3.2.2. Solar radiation on inclined surfaced under actual sky conditions

The solar radiation on an inclined surface under actual conditions has /

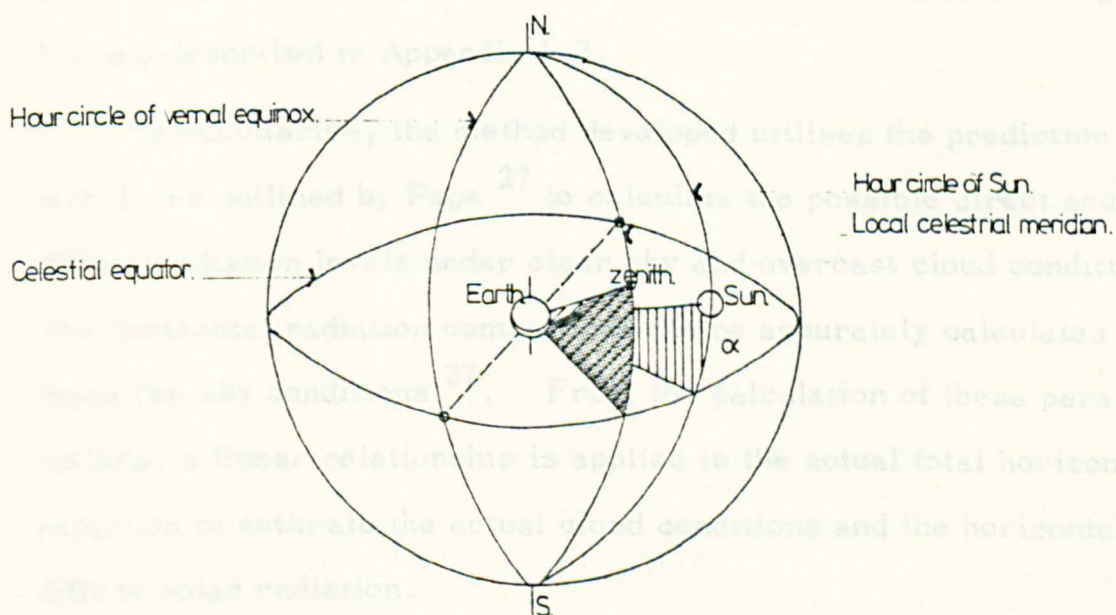
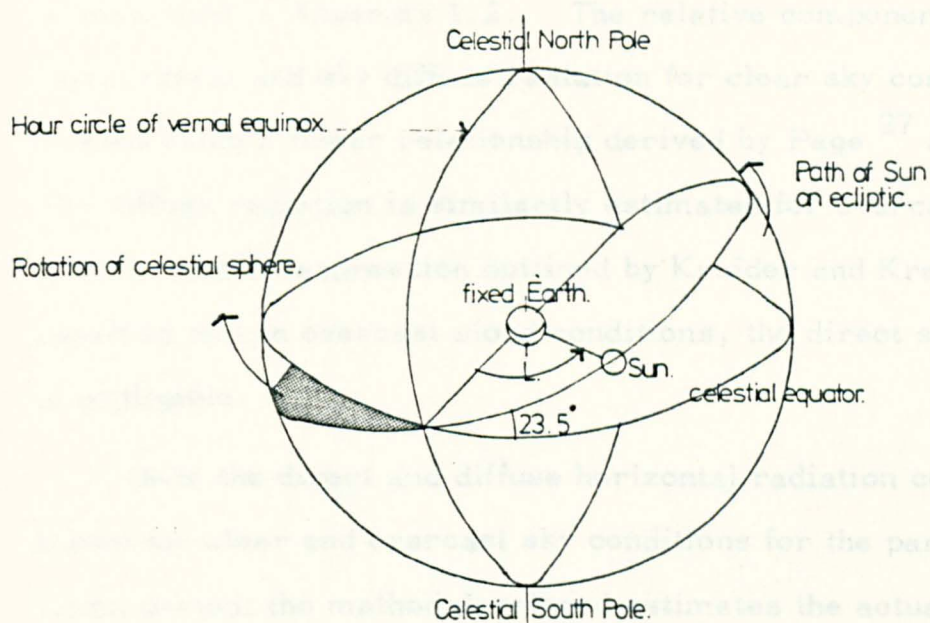


Figure 3.1 The components of the solar geometry within the celestial sphere.

has been predicted given the horizontal radiation data from a method which estimates the horizontal direct and diffuse radiation components and transforms the components to the inclined surface. This method is described in Appendix 1.2. The relative components of the horizontal direct and sky diffuse radiation for clear sky conditions are calculated using a linear relationship derived by Page ²⁷ and Parmelee ²⁸. The diffuse radiation is similarly estimated for overcast cloud conditions, from an expression outlined by Kreider and Kreith ²⁹. It is assumed that in overcast cloud conditions, the direct solar radiation is negligible.

Once the direct and diffuse horizontal radiation components are known for clear and overcast sky conditions for the particular simulation period; the method developed estimates the actual level of cloud cover and the subsequent horizontal diffuse solar radiation. This is determined from the interpolation of the actual horizontal solar radiation level between the possible horizontal radiation under clear sky and overcast cloud conditions. This method is illustrated in Figure 3.2 and described in Appendix 1.2.

To summarise, the method developed utilises the prediction techniques outlined by Page ²⁷ to calculate the possible direct and diffuse radiation levels under clear sky and overcast cloud conditions. The horizontal radiation components can be accurately calculated for these two sky conditions ²⁷. From the calculation of these parameters, a linear relationship is applied to the actual total horizontal radiation to estimate the actual cloud conditions and the horizontal diffuse solar radiation.

As a result of the estimation of the direct and sky diffuse components are transformed to an inclined surface. The method, derived by Liu and Jordan ³⁰ and outlined in section 3.1.1, involves the/

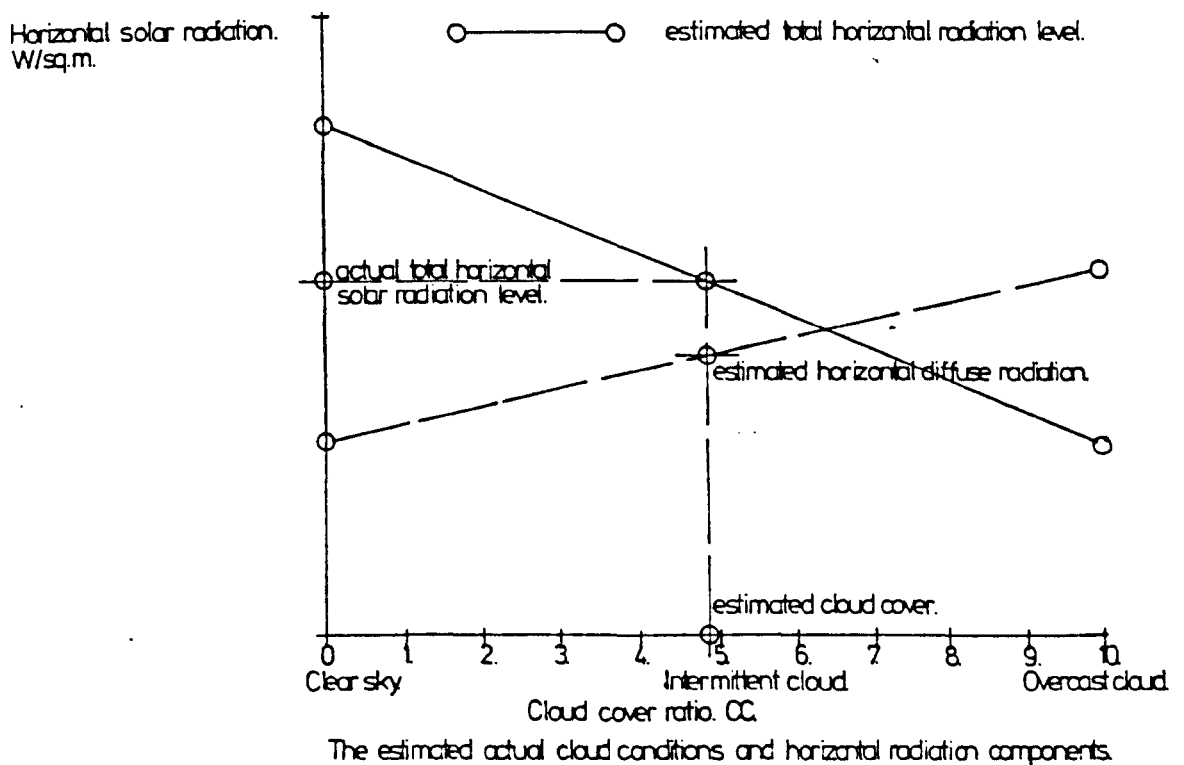
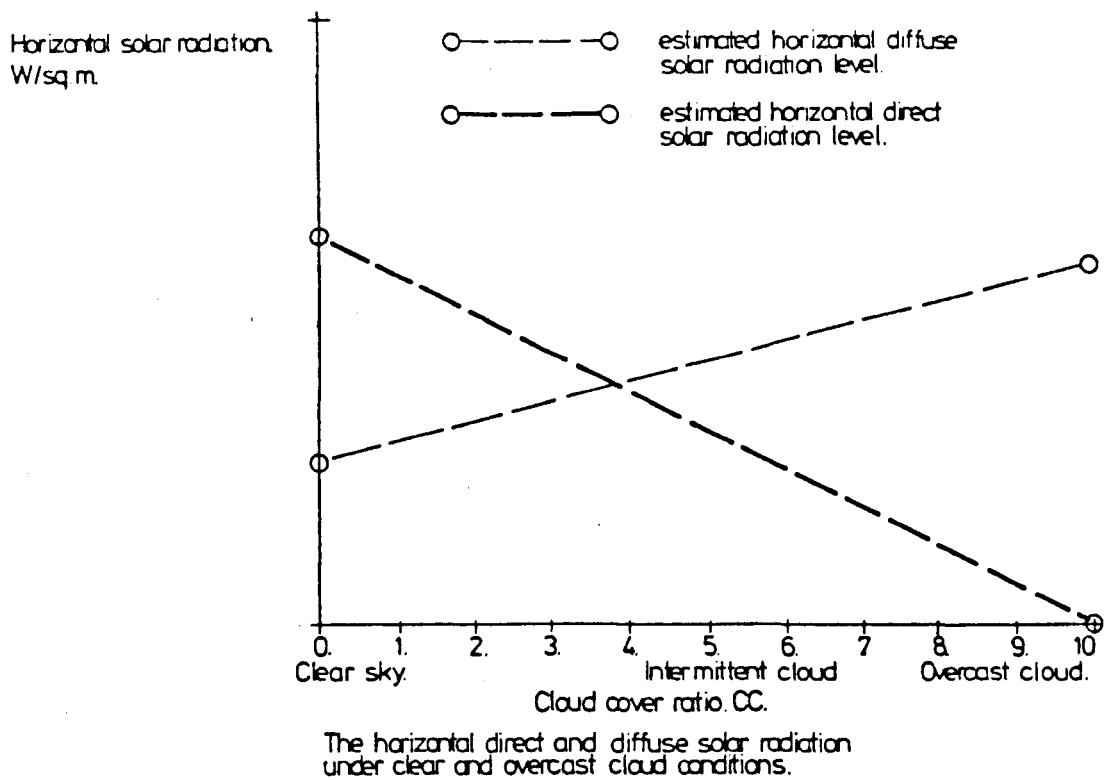


Figure 3.2 The prediction of the cloud cover and the horizontal radiation components under actual sky conditions.

the application of conversion factors to the direct, diffuse and total horizontal radiation to calculate the direct, diffuse and ground reflected diffuse radiation on an inclined surface.

3.2.3. Solar radiation transmission through collector cover

The transmittance and absorption of the incident direct and diffuse solar radiation on an inclined collector cover and plate has been described by Duffie and Beckman³¹. This method assumes that all radiation components that have undergone more than two reflections within the collector unit are disregarded, as illustrated in Figure 3.3. In this study, a single cover collector is taken to be representative of the commercial designs available.

The reflection and absorption losses within the collector cover system are dependant upon the angle of incidence of the direct radiation, and the transmittance of the cover material. The transmittance of direct solar radiation through a glass cover has been outlined by Varma³² as a regression function of the solar angle of incidence. This expression has been amended to incorporate any type of cover material such as Tedlar or Filon plastic covers. The transmission and absorption of diffuse radiation through the transparent cover is treated separately by Varma³³, with the transmittance and absorption coefficients assumed for the particular cover material as constants.

As outlined by Whillier³⁴, the absorption coefficient for the collector plate surface is dependant upon the surface treatment, whether a matt black or selective surface coating has been applied. The absorption and emittance coefficients of the selective coating has been taken by Whillier³⁵ to be constants. The absorptivity and emissivity of the matt black coating have been expressed by Kreider and Kreith³⁶ as a range of coefficients from 0.96 - 0.66 dependant upon the solar angle of incidence of direct radiation. The absorptivity and emissivity/

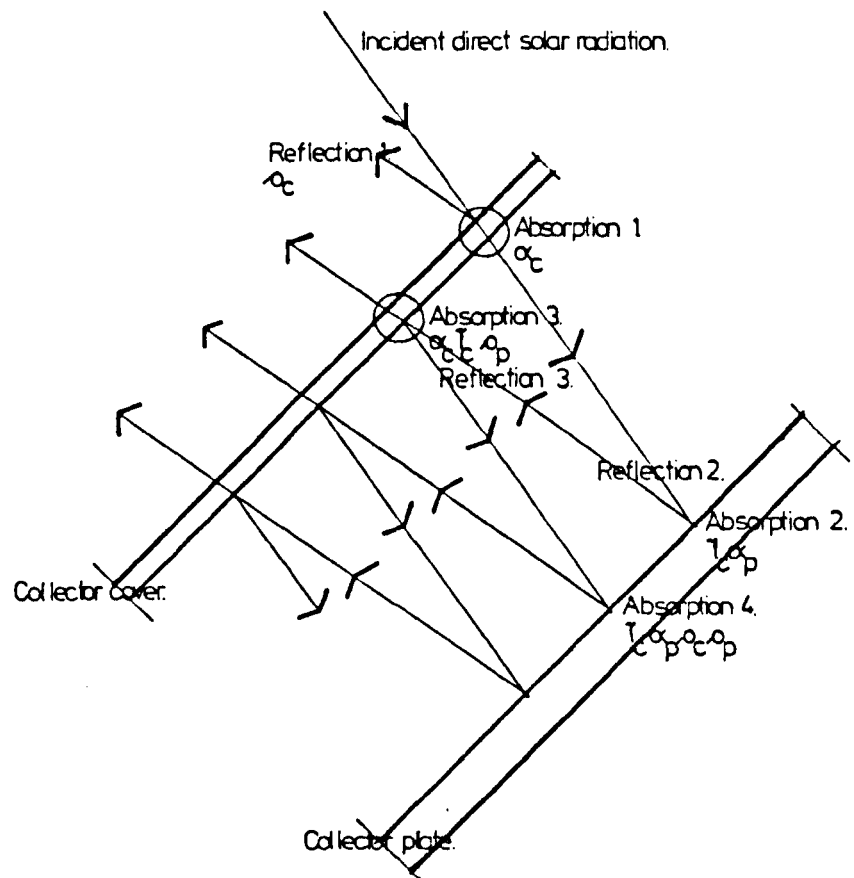


Figure 3.3 The transmission and absorption of the incident direct solar radiation on an inclined collector.

emissivity of a matt black plate are assumed to be equal. This method is described in Appendix 1.2.

3.3. Computer Simulation

3.3.1. Description of computer program

The solar radiation prediction method equations previously outlined have been translated into a series of computer subprograms, written in Fortran. These subprograms have been incorporated into the solar collector performance prediction program. A flowchart representation of the subprogram structure of the solar radiation prediction routines is given in Figure 3.4. A brief description of each of the subprogram routines to perform the algorithmic functions in the prediction of the incident solar radiation is outlined. The computer program is fully listed in Appendix 2.1.

(i) Subroutine HOUR

The function of the subprogram HOUR is to calculate the sidereal time and provide solar data to determine the sunrise and sunset times for the day under study.

(ii) Subroutine SUNRS

The function of the subprogram SUNRS is to calculate, using the solar data supplied by the routine HOUR, the sunrise and sunset times for the particular day under study.

(iii) Subroutine SUNPOS

The function of the subprogram SUNPOS, is to calculate the solar azimuth, declination and altitude angles.

(iv) Subroutine SUNRAD

The function of the subprogram SUNRAD, illustrated in flowchart form in Figure 3.5, is to calculate, utilising the method set out in section 3.2, the solar radiation absorbed by the collector cover and plate.

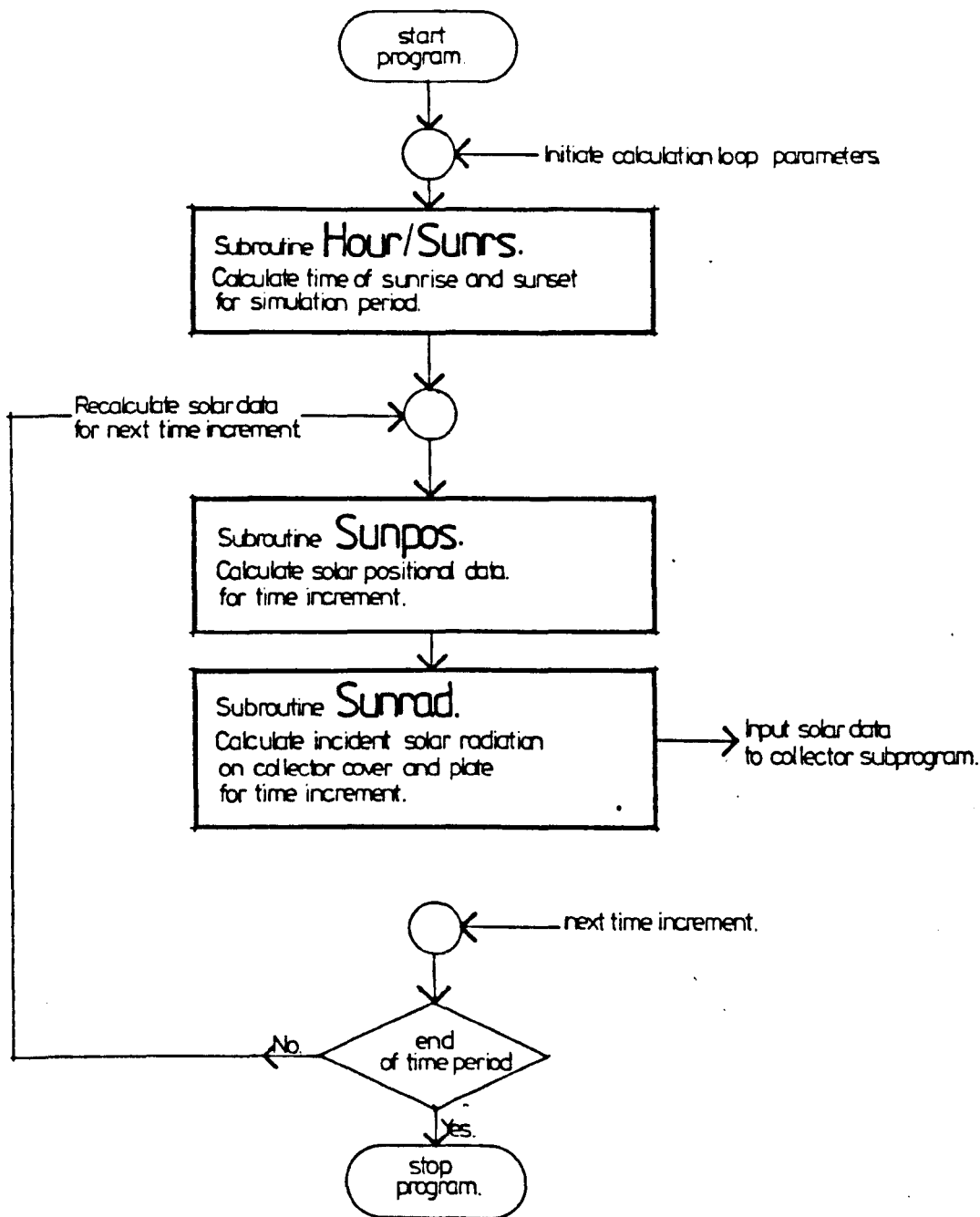


Figure 3.4 Flowchart representation of the solar radiation prediction subprogram.

(v) Subroutine ABSORB

The function of the subprogram ABSORB, is to calculate the angular variation of the absorptivity of a matt black collector plate surface.

3.4. Experimental Investigation

3.4.1. Objective of Experimental Investigation

The objective of the experimental investigation is to validate the predicted results of the solar radiation incident on the inclined collector surface against the actual solar radiation measurements. This objective has been achieved by the following experimental studies, utilising a purpose-built solar collector test rig and associated solar radiation measurement facility, illustrated in Figure 3.5.

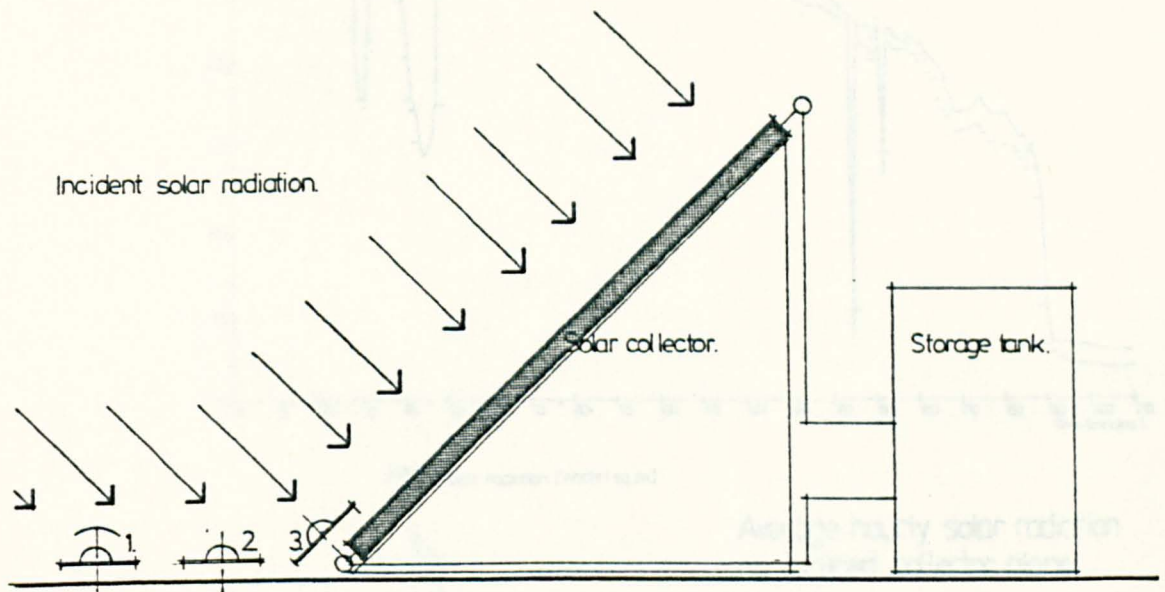
3.4.2. Apparatus and Experimental Procedure

A solar radiation measurement facility has been designed to monitor the components of the solar radiation climate, the direct and sky diffuse radiation, during each outdoor experiment period. The radiation measurement facility consisted of three solarimeters, manufactured by Kipp and Zonen, calibrated to an accuracy of $\pm 1.5\%$. The solarimeters recorded the total horizontal, the direct incident and the horizontal sky diffuse radiation. Previous to the series of outdoor experiments, the absorptivity and transmissivity of the cover material was determined. The experimental procedure for each outdoor experiment has been previously outlined in section 2.4.3.

3.5. Presentation and Discussion of Results

3.5.1. Validation of Solar Radiation Prediction Model

The monitored levels of solar radiation during the outdoor collector experiments are graphically illustrated in Figures 3.6 - 3.8. The experiments were carried out over a period of three weeks and a representative/



Solar radiation measurement apparatus.

1. Horizontal sky diffuse radiation.
2. Horizontal total radiation.
3. Total incident radiation on inclined collector plane.

Figure 3.5 Solar radiation experimental measurement facility.

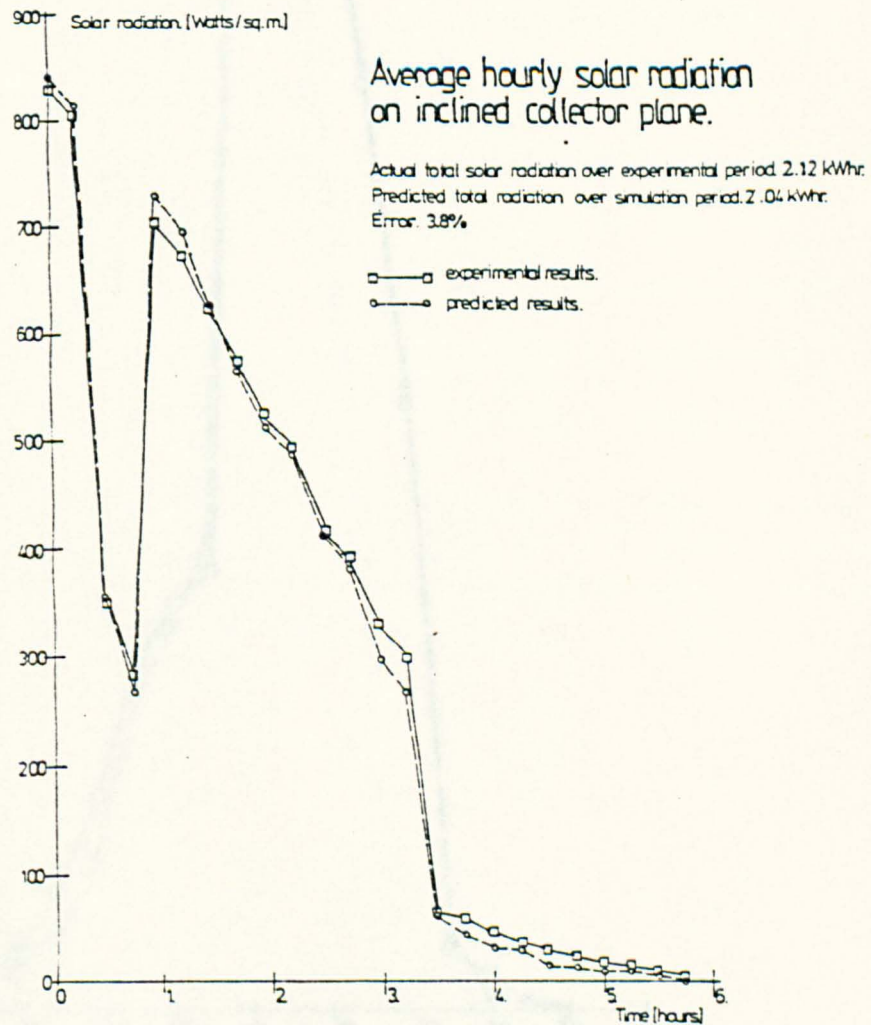
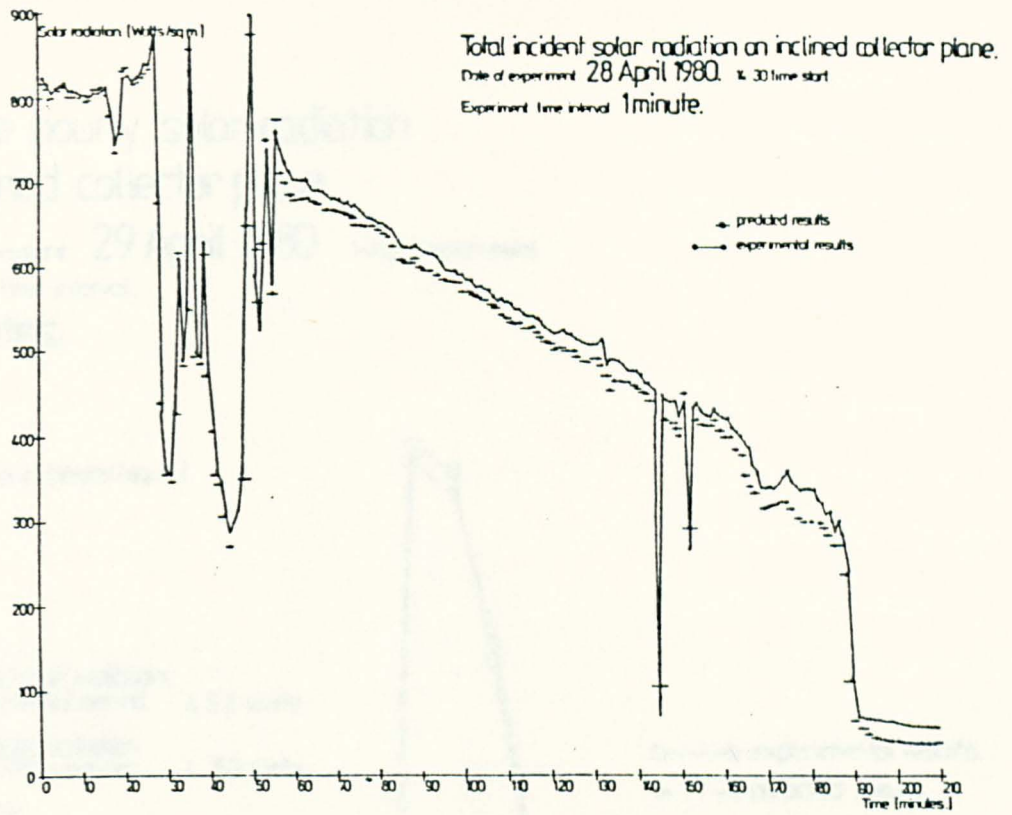


Figure 3.6 Actual vs Predicted incident solar radiation on inclined collector surface.

Average hourly solar radiation on inclined collector plane.

Date of experiment: 29 April 1980. 1 day experiment.

Experiment time interval.

10 minutes.

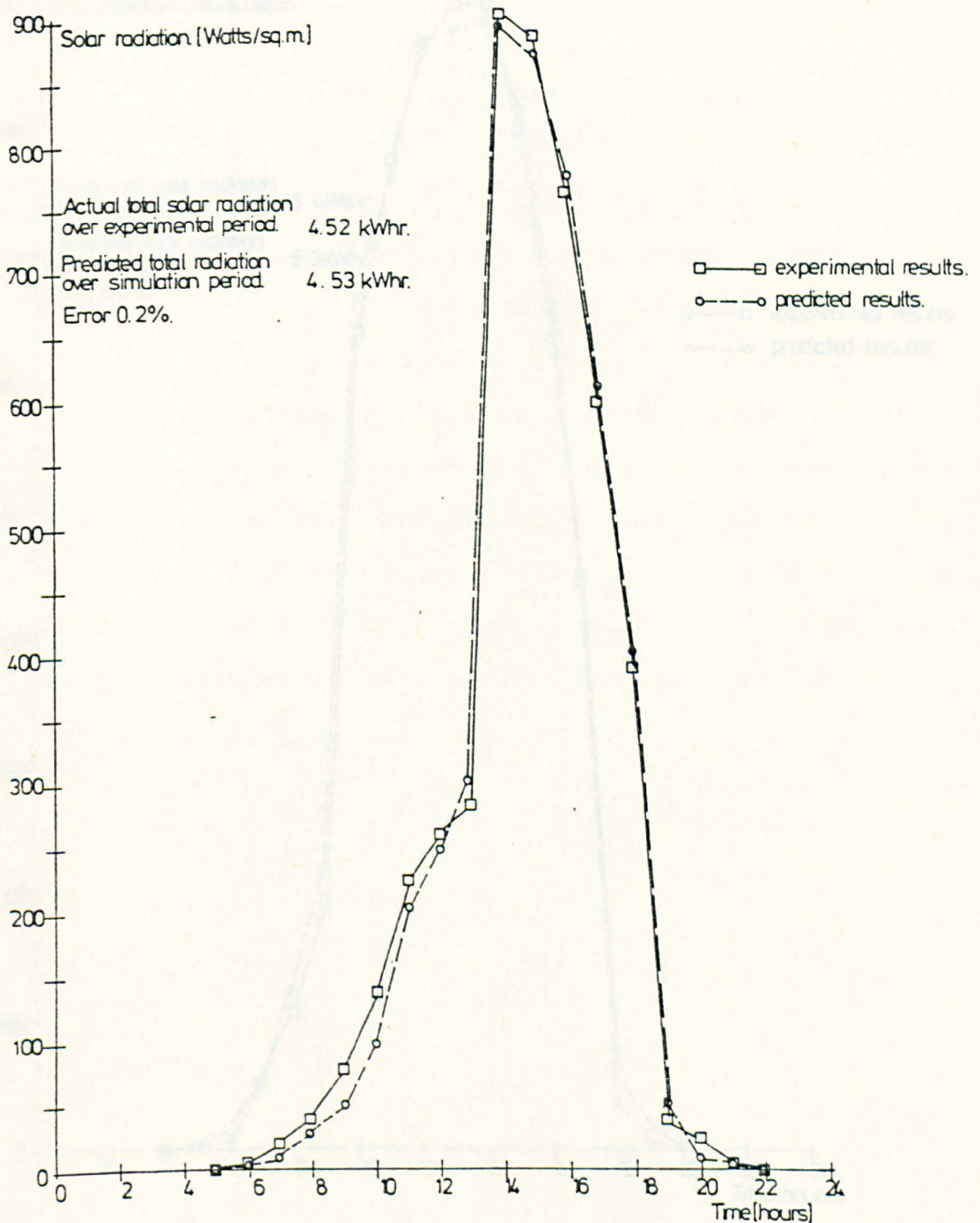


Figure 3.7 Actual vs Predicted incident solar radiation
on inclined collector surface.

Average hourly solar radiation on inclined collector plane.

Date of experiment. 2 May 1980. 1 day experiment

Experiment time interval. 10 minutes.

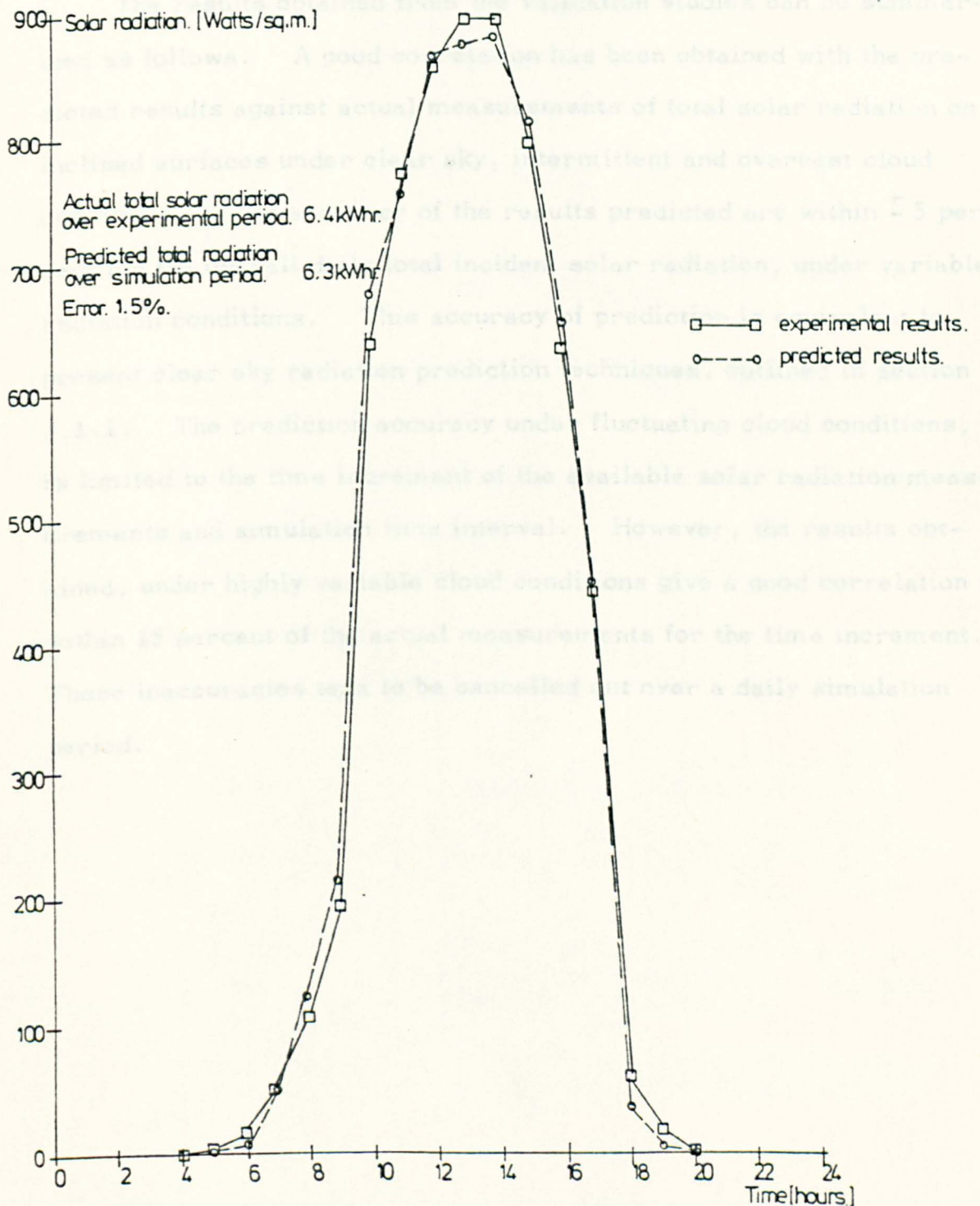


Figure 3.8 Actual vs Predicted incident solar radiation on inclined collector surface.

representative range of solar radiation conditions have been used to validate the prediction model. The predicted results from the computer program are superimposed on the actual radiation conditions in Figures 3.6 - 3.8.

3.5.2. Summary of Results

The results obtained from the validation studies can be summarised as follows. A good correlation has been obtained with the predicted results against actual measurements of total solar radiation on inclined surfaces under clear sky, intermittent and overcast cloud conditions. The accuracy of the results predicted are within ± 5 percent for the overall daily total incident solar radiation, under variable radiation conditions. This accuracy of prediction is equivalent to present clear sky radiation prediction techniques, outlined in section 3.1.1. The prediction accuracy under fluctuating cloud conditions, is limited to the time increment of the available solar radiation measurements and simulation time interval. However, the results obtained, under highly variable cloud conditions give a good correlation to within 15 percent of the actual measurements for the time increment. These inaccuracies tend to be cancelled out over a daily simulation period.

Section 3

References

1. Parmelee, G.V., 'Irradiation of vertical and horizontal surfaces by diffuse solar radiation from cloudless skies'. Heating, Piping and Air Conditioning, 1954. pp. 129-135.
2. Liu, B.Y.H. and Jordan, R.C., 'The inter-relationship and characteristic distribution of direct, diffuse and total solar radiation'. Solar Energy, 1960. pp. 1-19.
3. Liu, B.Y.H. and Jordan, R.C., 'Daily ins lation on surfaces tilted toward the equator'. ASHRAE Journal, 1951. pp. 53-59.
4. Liu, B.Y.H. and Jordan, R.C., 'The long-term average performance of flat-plate solar-energy collectors'. Solar Energy, 1963. pp. 53-70.
5. Unsworth, M.H. and Monteith, J.L., 'Aerosol and solar radiation in Britain'. Quart. J.R. Met. Soc., 1972. pp. 778-797.
6. Page, J.K., 'Geographical variations in the climatic factors influencing solar building design'. Proc. NELP/UNESCO Conf., London. 1977. pp. 1-15.
7. Newcomb, Astronomical Papers prepared for the use of the use American Ephemeris and Nautical Almanac, Vol. 6. 1898.
8. Explanatory Supplement to the Astronomical Ephemeris and the American Ephemeris and Nautical Almanac, H.M.S.O., London. 1961.
9. Liu, B.Y.H. and Jordan, R.C., 'The long-term average performance of flat-plate solar-energy collectors'. Solar Energy, 1963. pp. 55-59.
10. Moon, P., 'Proposed standard solar radiation curves for engineering use'. J. Franklin Inst., 1940. pp. 583-617.
11. Liu, B.Y.H. and Jordon, R.C., 'The long-term average performance of flat-plate solar-energy collectors'. Solar Energy, 1963. p. 57.
12. Parmelee, G.V., 'Irradiation of vertical and horizontal surfaces by diffuse solar radiation from cloudless skies'. Heating, Piping and Air Conditioning, 1954. pp. 130-134.
13. Page, J.K., 'Geographical variations in the climatic factors influencing solar building design'. Proc. NELP/UNESCO Conf., London. 1977. pp. 9-10.
14. Ibid., p. 12.
15. Ibid., pp. 10-13.
16. Duffie, J.A. and Beckman, W.A., Solar Energy Thermal Processes, 1974. pp. 108-119.

17. Whillier, A., 'Plastic covers for solar collectors'. Solar Energy, 1963. pp. 148-151.
18. Ibid., p. 150.
19. Duffie, J.A. and Beckman, W.A., Solar Energy Thermal Processes, 1974. pp. 113-115.
20. Ibid., p. 110.
21. Ibid., pp. 76-77.
22. Whillier, A., 'Design factors influencing solar collector performance'. Low Temperature Engineering Application of Solar Energy, 1967. p. 32.
23. Duffie, J.A. and Beckman, W.A., Solar Energy Thermal Processes, 1974. p. 76.
24. McAdams, W.C., Heat Transmission, 1954. pp. 345-347.
25. Walraven, R., 'Calculating the position of the sun'. Solar Energy, 1978. pp. 393-397.
26. Ibid., pp. 393-394.
27. Page, J.K., 'Geographical variations in the climatic factors influencing solar building design'. Proc. NELP/UNESCO Conf., London. 1977. pp. 7-10.
28. Parmelee, G.V., 'Irradiation of vertical and horizontal surfaces by diffuse solar radiation from cloudless skies'. Heating, Piping and Air Conditioning, 1954. pp.
29. Kreider, J.F. and Kreith, F., Solar Heating and Cooling, 1977. pp. 77-78.
30. Liu, B.Y.H. and Jordan, R.C., 'The long-term average performance of flat-plate solar-energy collectors'. Solar Energy, 1963. p. 57.
31. Duffie, J.A. and Beckman, W.A., Solar Energy Thermal Processes, 1974. pp. 108-119.
32. Varma, H.K., 'A model to calculate solar radiation absorbed by absorber surface of a flat-plate solar collector'. Proc. Conf. Solar Building Technology, 1977. pp. 711-714.
33. Ibid., p. 713.
34. Whillier, A., 'Design factor influencing solar collector performance'. Low Temperature Engineering Application of Solar Energy, 1967. pp. 28-30.
35. Ibid., p. 29.
36. Kreider, J.F. and Kreith, F., Solar Heating and Cooling, 1977. p. 75.

SECTION 4

THERMAL PERFORMANCE OF SOLAR WATER HEATING
SYSTEMS UNDER INTERMITTENT SOLAR RADIATION
AND ENERGY USAGE CONDITIONS

4.1. Review of Previous Work

A brief review of the previous work has been outlined in section 1.2, a detailed review of the more important aspects of solar water heating system performance simulation techniques presently available is given. As a consequence of the previous study of collector simulation techniques given in section 2.1, this section outlines the present methods of modelling water storage tank and collector system usage behaviour.

4.1.1. Solar Water Storage Tank Model

At present, water storage is the most inexpensive and readily available method of harnessing the sensible heat gain from a solar water collector system. The thermal modelling of the internal heat transfer processes within the storage, the interaction with the collector system and the energy usage demand is complex. The simplest method to simulate the dynamic thermal behaviour, outlined by Duffie and Beckman¹, is to assume a fully mixed, non-stratified water storage tank, modelled by the following heat balance expression:

$$\begin{aligned} \text{Heat energy stored} &= \text{Rate of heat} - \text{Rate of heat} - \text{Rate of heat re-} \\ \text{within water mass} & \quad \text{gain from} \quad \quad \text{from storage} \quad \quad \text{moval to load} \\ & \quad \quad \text{collector} \quad \quad \text{tank} \end{aligned}$$
$$C_s \cdot \frac{dT_s}{dt} = q_u - U_s \cdot (T_s - T_a) - C_L \quad (4.1)$$

This simple expression has been developed by Close² to incorporate the effect of temperature stratification within the storage tank. The storage system is simulated as an insulated, stratified water tank. The dynamic thermal behaviour of the water storage tank is modelled as a series of separate isothermal sections. The thermal processes between each elemental section are illustrated in Figure 4.1.

The fluid flow heat gain from the collector unit to the storage tank is modelled by a set of flow control functions which direct the fluid/

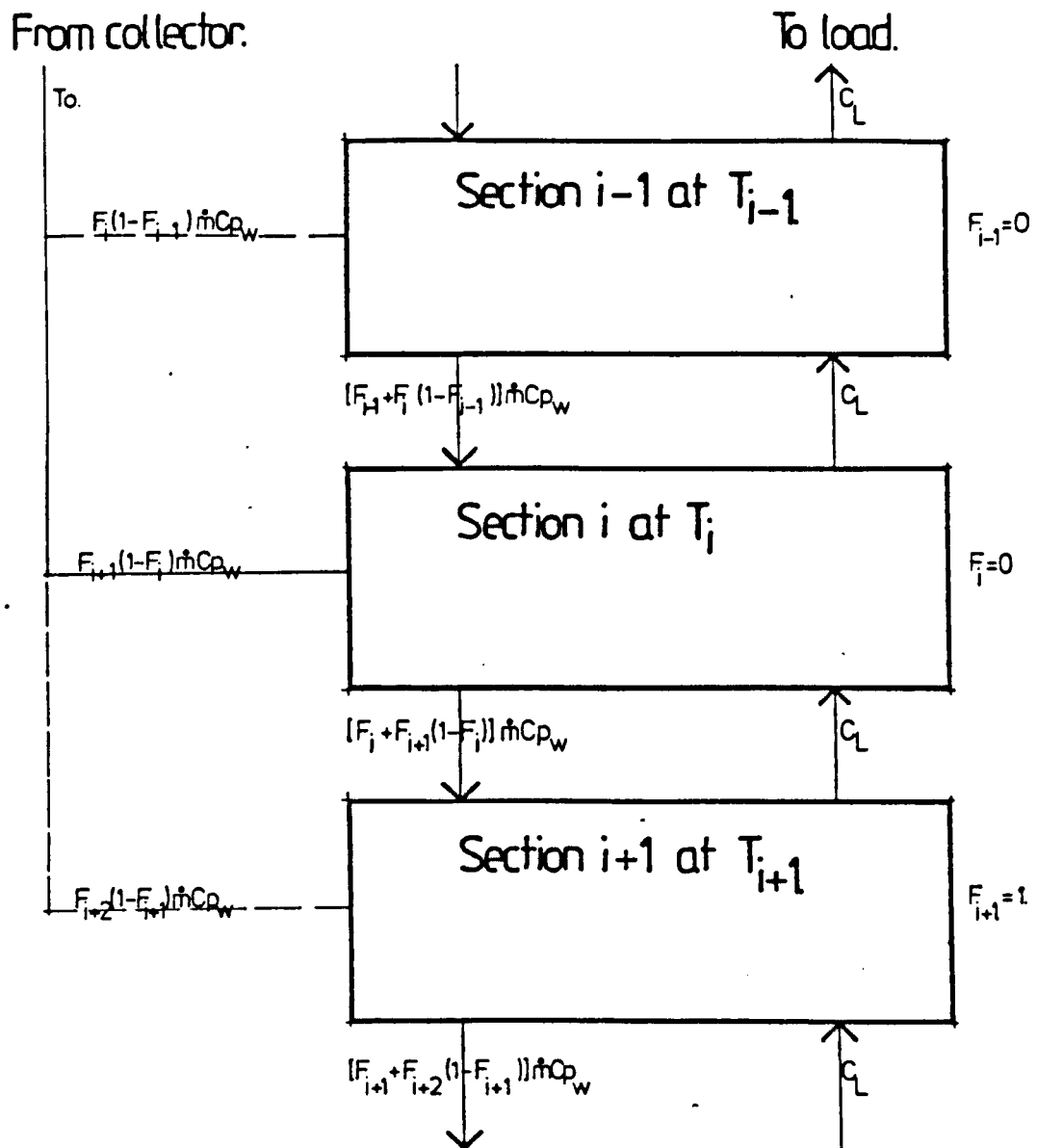


Figure 4.1 The thermal processes within the elemental sections of a water storage tank model.

fluid heat gain to the appropriate tank section. The flow functions operate the fluid mass transfer by the relative fluid density of the collector outlet and the elemental tank section. The internal fluid flow behaviour between the elemental tank sections, illustrated in Figure 4.1, is modelled by a set of control functions. The heat balance expressions for the three section stratified water storage tank are described in equation form in Appendix 1.3.

Close ³ compared the predicted results for a three section and a six-section tank and concluded that a negligible difference existed for the increased simulation accuracy. As a consequence, in this investigation a three section simulation model is used, as described in Appendix 1.3 and illustrated in Figure 4.2

The rate of heat removal to the load is assumed by Close ⁴ to be a fixed quantity of energy supplied by the storage tank as hot water at some preselected minimum temperature. This type of load represents a use in which cold water from the mains is mixed with the hot water from the storage tank to obtain water at some minimum temperature. The relationship between the mass flowrate of the load and the storage tank temperature is expressed as follows:

$$C_L = F_5 \cdot Q_{\text{load}} / (T_{\text{SL}} - T_{\text{mw}}) \quad (4.2)$$

where Q_{load} is the rate at which the solar heating system must supply energy for the specified load period. Close ⁵, Gutierrez et al ⁶, and Courtney ⁷, have all modelled the time dependant load functions of different simulated domestic water usage patterns. In each study, whenever the temperature of the storage tank supply water drops below the preselected minimum water temperature, it is assumed that some form of auxiliary energy is used to supplement the load requirement.

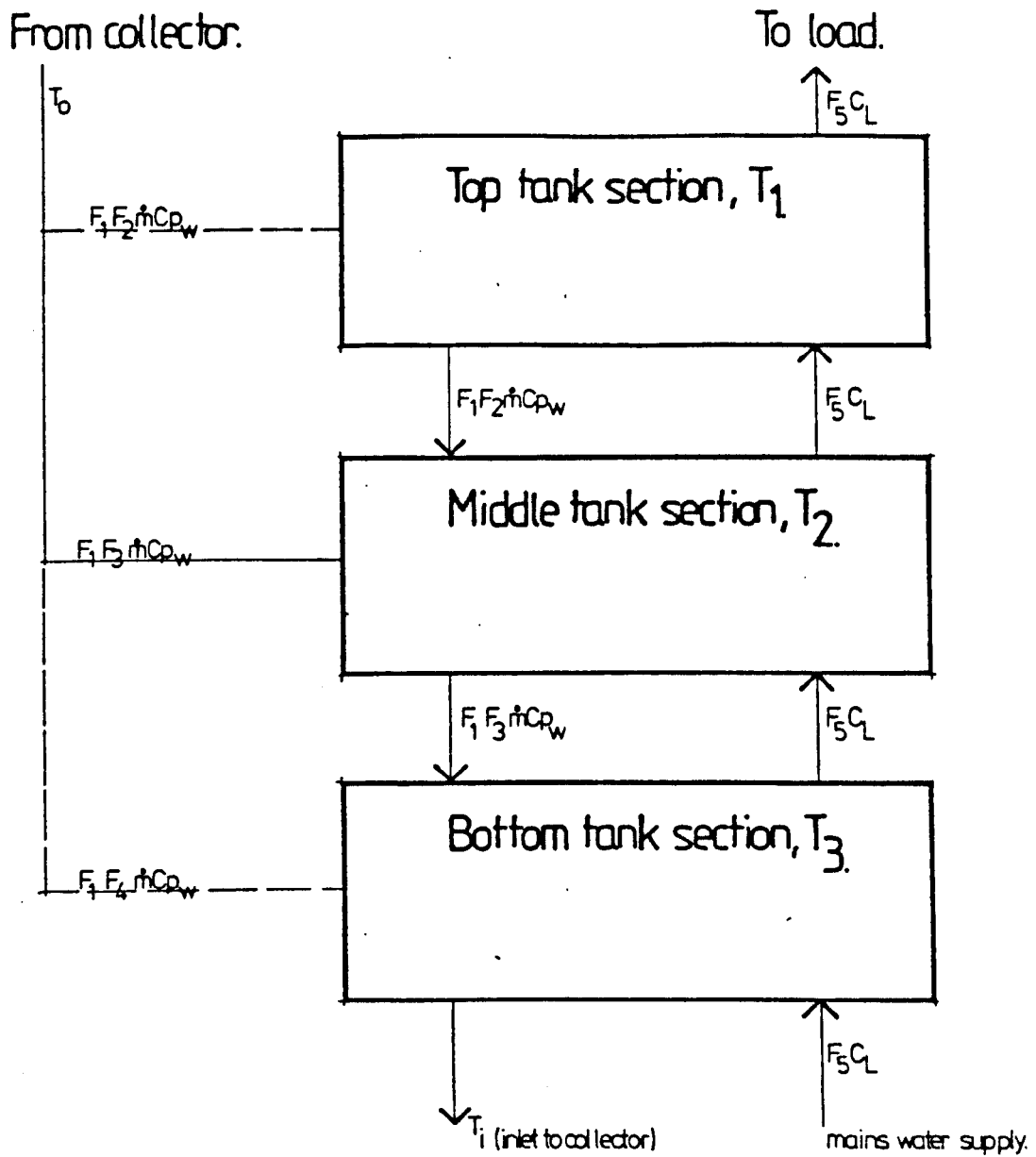


Figure 4.2 The thermal processes within a three section model of a water storage tank.

The heat losses from the connecting pipework between the collector unit and the storage tank have been considered by Beckman⁸ to be significant if the pipework is uninsulated, and can be modelled by the following expression:

$$Q_p = U_p \cdot (T_1 - T'_a) + U_p \cdot (T_o - T'_a) \quad (4.3)$$

where U_p is the heat loss coefficient of the pipe.

The temperature of the daily mains water has been predicted by Brinkworth⁹ for the United Kingdom over a year from the following expression:

$$T_{mw} = 9 - 3 \cos\left(\frac{2\pi}{365} \cdot (D + 11.25)\right) \quad (4.4)$$

where D is the day number.

4.2. Theoretical Analysis - Dynamic Behaviour of Solar Water Heating System

4.2.1. Method of Analysis

In this section, the three node model of a stratified water storage tank, outlined in section 4.1.1, has been used in conjunction with the multi-node model of the collector unit to simulate the dynamic thermal behaviour of a solar water heating system. The equations describing the heat balance within the top, middle and bottom sections of the storage tank are described in Appendix 1.3.

The following modifications have been incorporated into the model of the storage tank and system pipework previously outlined.

- (i) the option of either a direct or indirect solar water heating system simulation is available with the insertion of a heat exchanger within the storage tank. The heat exchanger modifies the collector heat input to the storage tank and the level of temperature stratification.

- (ii) the thermal capacitance of the material structure of the storage tank is taken into account.
- (iii) the heat losses from the connecting pipework and the thermal capacitance of the pipework are modelled as part of the system thermal network simulation. The derivation of the heat transfer and energy storage processes within the pipework is outlined in Appendix 1.3.
- (iv) the heat energy generated by the operation of the circulation pump is significant in small domestic systems, and is incorporated into the system simulation. The heat input is estimated from the power rating of the particular pump.

The matrix representation and the numerical method chosen for the numerical solution of the simultaneous heat balance equations describing the collector unit is utilised for the storage tank and system pipework thermal simulation. The matrix representation is outlined in Appendix 1.3.

4.3 Computer Simulation

4.3.1 Description of computer program

The numerical solution of the heat balance equations describing the dynamic thermal behaviour of the storage tank and the system pipework, previously outlined, has been translated into a series of computer subprograms, written in Fortran. These subprograms have been incorporated into the solar collector performance and the solar radiation prediction routines to form an interactive computer simulation program. This program has the capability to model the dynamic thermal performance of various solar water heating systems under intermittent solar radiation and energy usage conditions. A flowchart representation of the subprogram structure of the program is given in Figure 4.3.

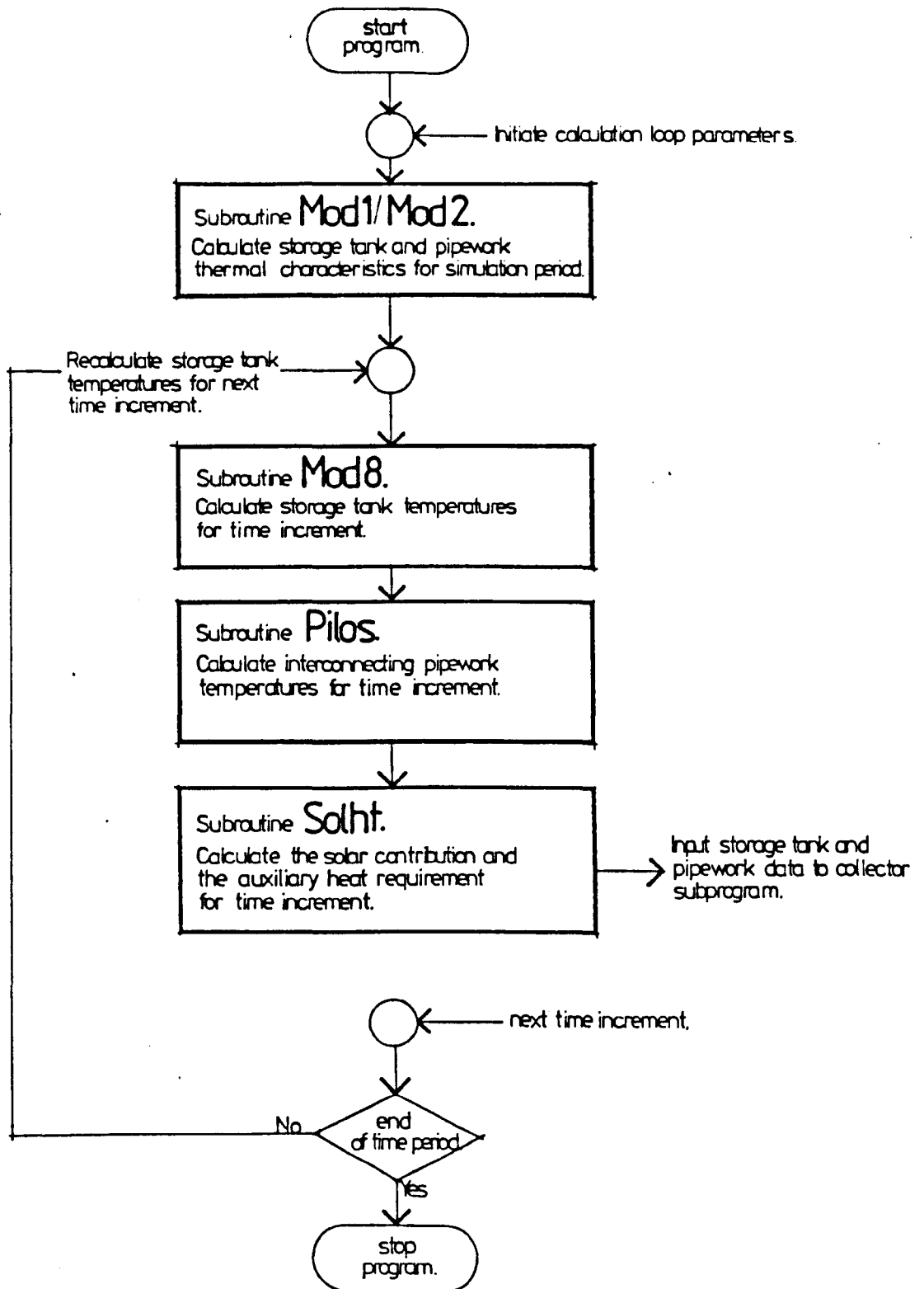


Figure 4.3 Flowchart representation of the storage tank and system pipework thermal prediction subprogram.

A brief description of each of the subprogram routines to perform the algorithmic functions in the prediction of the storage tank and system pipework thermal behaviour is outlined below. The computer program is fully listed in Appendix 2.1.

(i) Subroutine MOD 8

The function of the routine MOD 8, is to initialise the numerical method matrix, and iteratively solve by the Quartic Runge-Kutta method, the storage tank section temperatures after each time increment.

(ii) Subroutine PILOS

The function of the routine PILOS, is to initialise the numerical method matrix, and iteratively solve by the Quartic Runge-Kutta method, the system pipework temperatures after each time increment.

(iii) Subroutine SOLHT

The function of the routine SOLHT, is to calculate the heat supplied by the solar heating system and the auxiliary heat requirement to meet the specified load demand.

(iv) Subroutine MAINST

The function of the routine MAINST, is to calculate the cold water mains inlet temperature to the storage tank.

In addition, the existing program routines MOD 1, MOD 4, MOD 5 and PLOT 1, are expanded to incorporate the storage tank and the system pipework routines.

4.4. Experimental Investigation

4.4.1. Objectives of Experimental Investigation

The objective of the experimental investigation has been to validate the predicted dynamic storage tank behaviour under variable climatic conditions against actual results. This objective has been achieved by/

by the following experimental studies, utilising a purpose-built solar collector system test facility, to investigate the heat transfer and energy storage processes within the storage tank.

4.4.2. Apparatus and Experimental Procedure

A domestic scale solar water heating system, illustrated in Figure 2.5, has been designed for the indoor and outdoor system performance validation studies. The storage tank used is a 150 litre capacity insulated copper indirect tank connected to the collector array by 15mm uninsulated copper pipework. The procedure used in the indoor and outdoor experiments is fully outlined in section 2.4.3. The temperature, solar radiation and flowrate measurements were recorded at specified intervals by a Computer Automation data logging system. This system, by means of a purpose-written computer program, processes the analogue experimental readings into digital form, and subsequently prints these results. These results were analysed against the predicted values from the simulation program.

4.5. Presentation and Discussion of Results

The results from the indoor and outdoor system performance experiments are discussed and illustrated in section 4.5.1. In addition, the prediction results from the computer simulation are compared against the actual thermal behaviour of the storage tank.

4.5.1. Experimental Results and Prediction Validation

(i) Indoor experiments

In this section, the results of the indoor experiments carried out in the laboratory to investigate the collector system and the storage tank heat losses, under no insolation conditions are illustrated and discussed. The temperature stratification within the storage tank for one experiment representative of the heat loss studies is/

is illustrated in Figure 4.4. The temperature drop within the storage tank, over the experimental period, determines the rate of heat transfer from the storage tank. The heat energy stored within the water tank is primarily transferred by fluid flow to the collector array and by conduction and convection heat loss to the internal air. To facilitate the analysis of the temperature stratification within the storage tank, the results are plotted at 10 minute intervals.

The results predicted from the computer simulation studies are overlayed on the actual experimental observations, as shown in Figure 4.4. The predicted temperature stratification within the storage tank shows a good correlation with the measured values. As a result, this correlation validates the accuracy of the theoretical heat transfer and energy storage equations modelling the storage tank heat losses under steady-state, no insolation conditions.

(ii) Outdoor experiments

From the five experiments carried out on the outdoor collector system test facility, the results of two experiments, representative of the complete study are illustrated and discussed. The top, middle and bottom storage tank section temperatures, the mean collector fluid temperature and the incident solar radiation for these experiments are illustrated in Figures 4.5 and 4.6.

In the first experiment, illustrated in Figure 4.5, the storage tank and the collector system behaviour were monitored for 10 hours, at 1 minute intervals over a variety of solar radiation conditions. The results from the experiment indicate that the temperature stratification within the storage tank is divided into two sections, the top and bottom, with the middle section temperature/

Top middle and bottom storage tank temperatures
 Date of experiment 28 April 1980
 Experiment time interval
 1 minute.

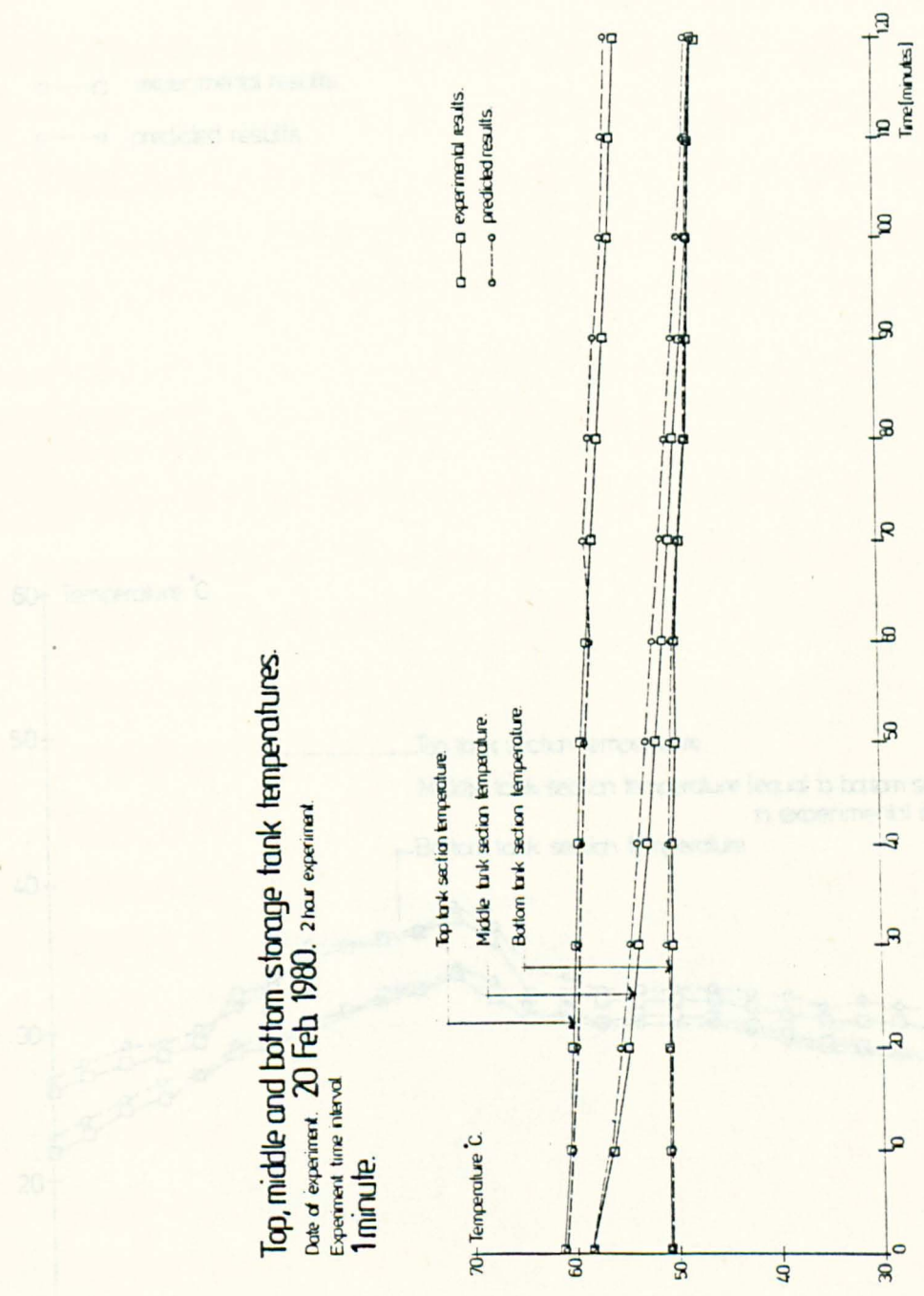


Figure 4.4 Actual vs Predicted storage tank section temperatures.

Top, middle and bottom storage tank temperatures.

Date of experiment. 28 April 1980. 10 hour experiment.

Experiment time interval.

1 minute.

□—□ experimental results.

○—○ predicted results.

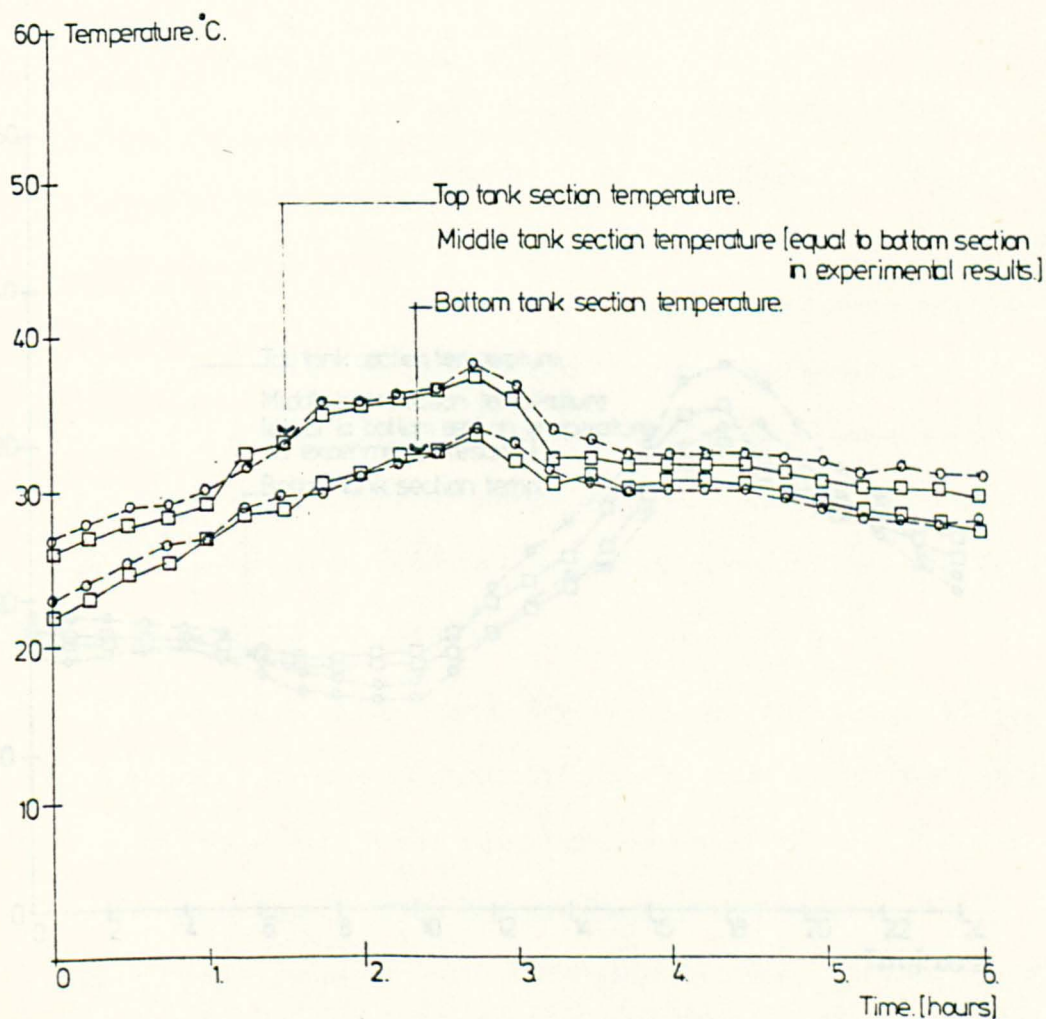


Figure 4.5 Actual vs Predicted storage tank section temperatures.

Top, middle and bottom storage tank temperatures.

Date of experiment. 29 April 1980. 1 day experiment.

Experiment time interval.

10 minutes.

□—□ experimental results.

○—○ predicted results.

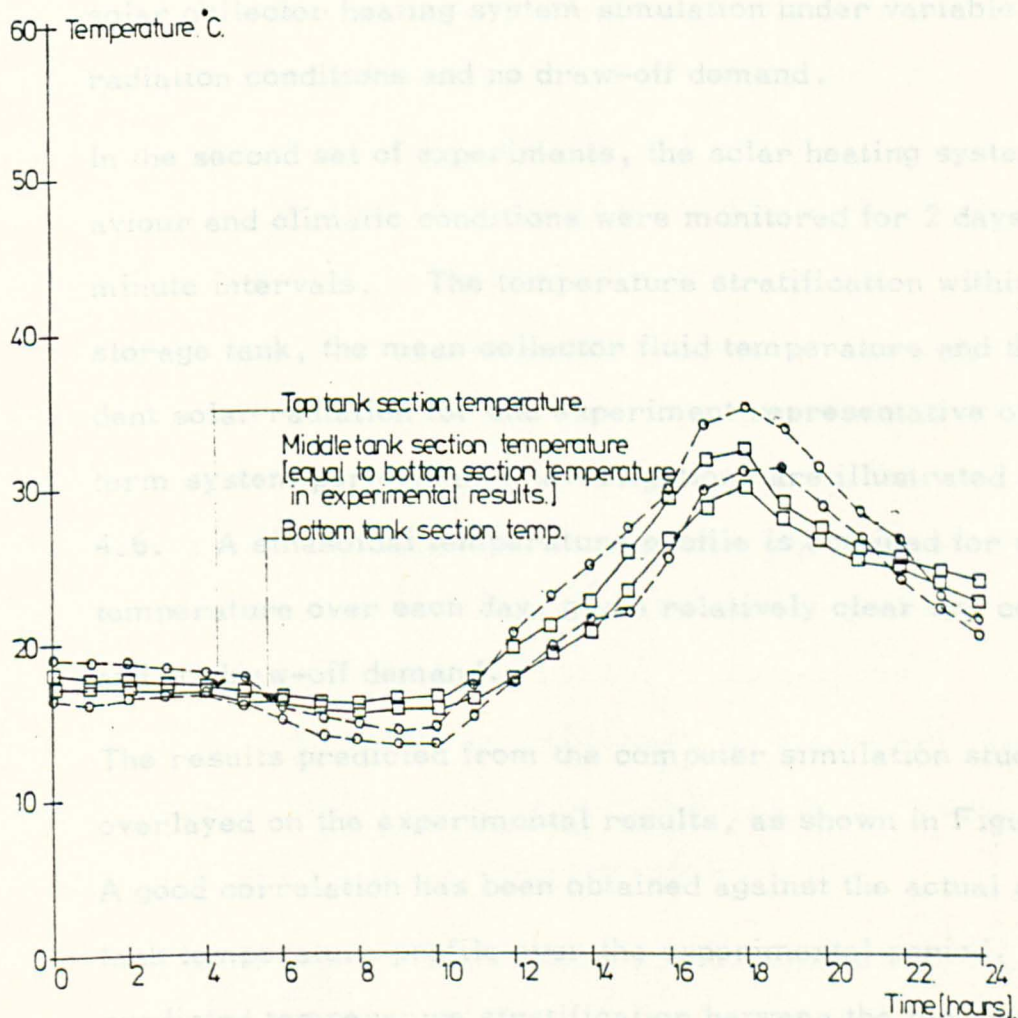


Figure 4.6 Actual vs Predicted storage tank section temperatures.

temperature being equal to the bottom section temperature.

The temperature stratification within the storage tank is small for the low temperatures involved.

The results predicted from the computer simulation studies are overlayed on the experimental results, as shown in Figure 4.5. A good correlation has been obtained against the actual storage tank temperature profile over the experimental period. For the temperature stratification, the predicted top and bottom section temperatures give good correlation to the actual measurements. The predicted middle tank section temperature is not equal to the bottom section temperature.

As a result, this correlation validates the general accuracy of the solar collector heating system simulation under variable solar radiation conditions and no draw-off demand.

In the second set of experiments, the solar heating system behaviour and climatic conditions were monitored for 2 days, at 10 minute intervals. The temperature stratification within the storage tank, the mean collector fluid temperature and the incident solar radiation for one experiment representative of the long term system performance investigation, are illustrated in Figure 4.6. A sinusoidal temperature profile is obtained for the tank temperature over each day, given relatively clear sky conditions and no draw-off demand.

The results predicted from the computer simulation studies are overlayed on the experimental results, as shown in Figure 4.6. A good correlation has been obtained against the actual storage tank temperature profile over the experimental period. The predicted temperature stratification between the top, middle and bottom sections is significantly greater than the actual results.

4.5.2. Summary of Results

The present indoor and outdoor solar heating system test rig experiments and the subsequent computer program validation studies can be summarised as follows.

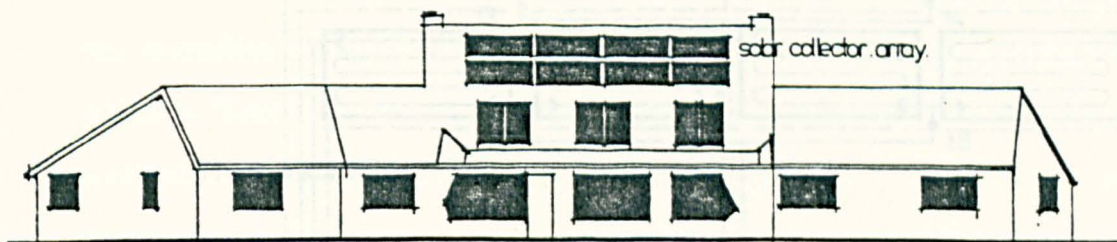
A good correlation has been obtained against the predicted and measured heat loss from the storage tank by fluid flow to the collector unit, and by conduction and convection to the internal air, under no insolation and no draw-off conditions. This correlation validates the general accuracy of the theoretical fluid flow, thermal capacitance and heat transfer equations modelling the storage tank dynamic thermal behaviour.

In the outdoor experiments, a good correlation has been obtained for the predicted storage tank temperature profile with the measured results over the short and long term experimental periods. In the prediction of the temperature stratification within the storage, three distinct levels of stratification are obtained against the two levels, observed at the top and bottom tank sections.

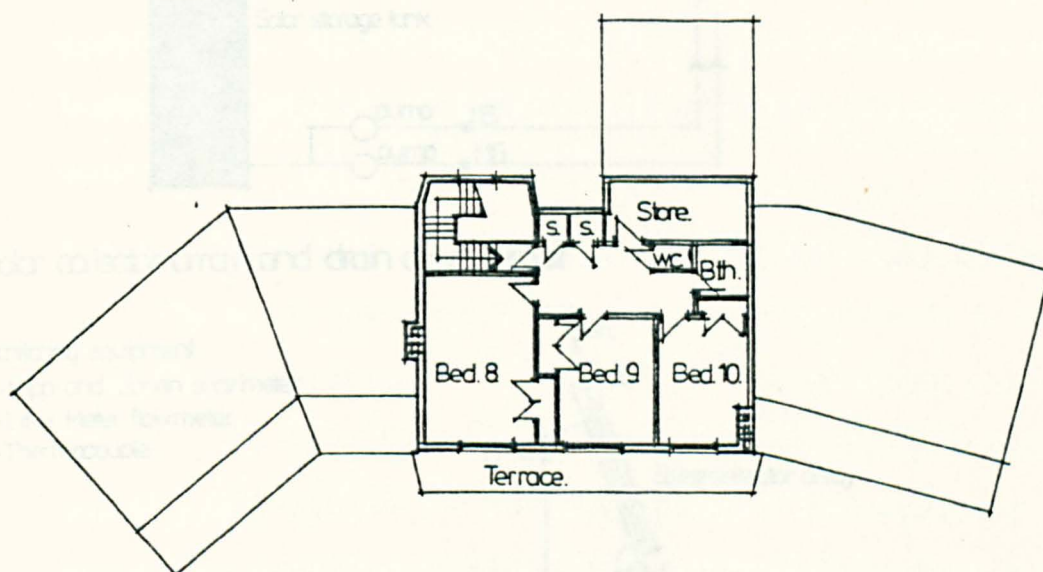
A good correlation is obtained for the temperature difference between the top and bottom tank sections. This discrepancy in the predicted temperature stratification can be explained by the low storage tank temperatures and temperature difference within the tank observed for the experimental period. At such low temperatures, below 35°C, the temperature stratification is limited to two sections. The simulation method requires further refinement to incorporate this feature into the model. As this point is not significant to the overall accuracy of prediction, this refinement has been neglected.

4.6. Monitoring of Solar Water Heating Installation in a 15 Person Hostel

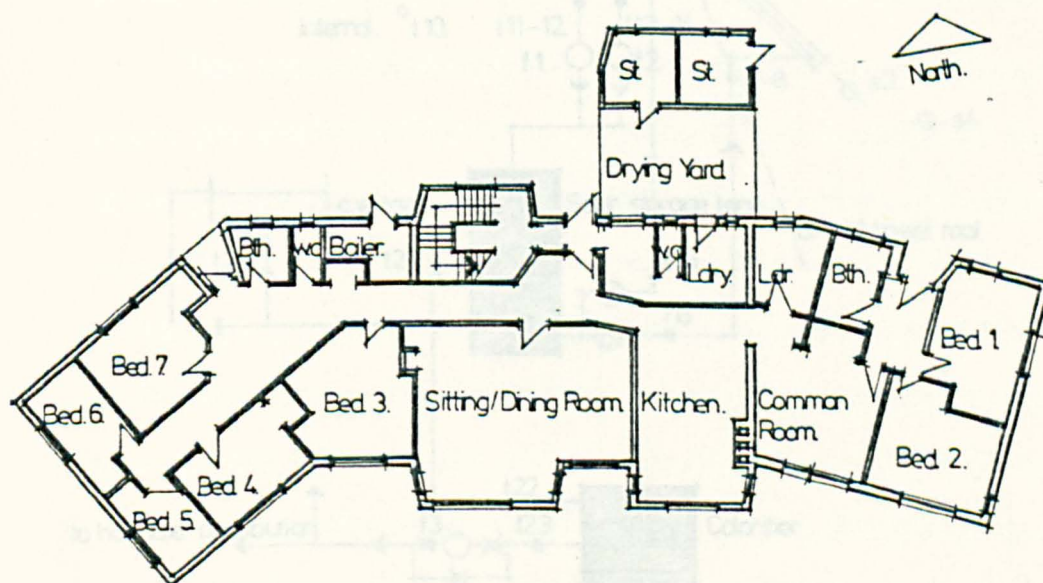
As no performance data on active solar heating system performance/



South Elevation.



First Floor Plan.

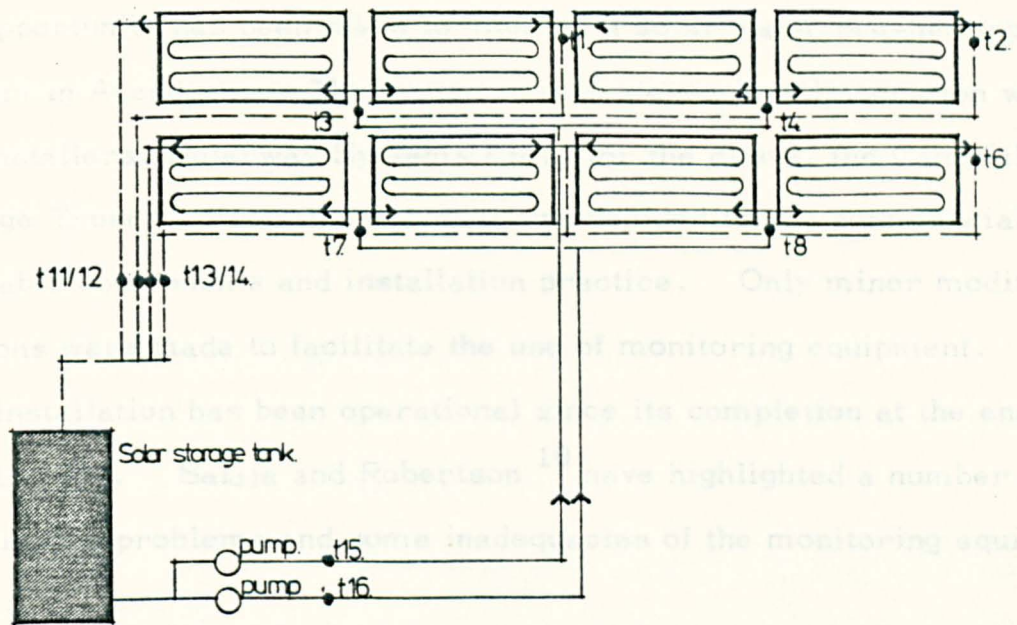


Ground Floor Plan.

0 2 4 6 8 10m
Scale: 1:250

Floor plans and elevation of low energy hostel

Figure 4.7 Plans and elevation of 15 Person Hostel,
Newton Dee Community, Aberdeen.



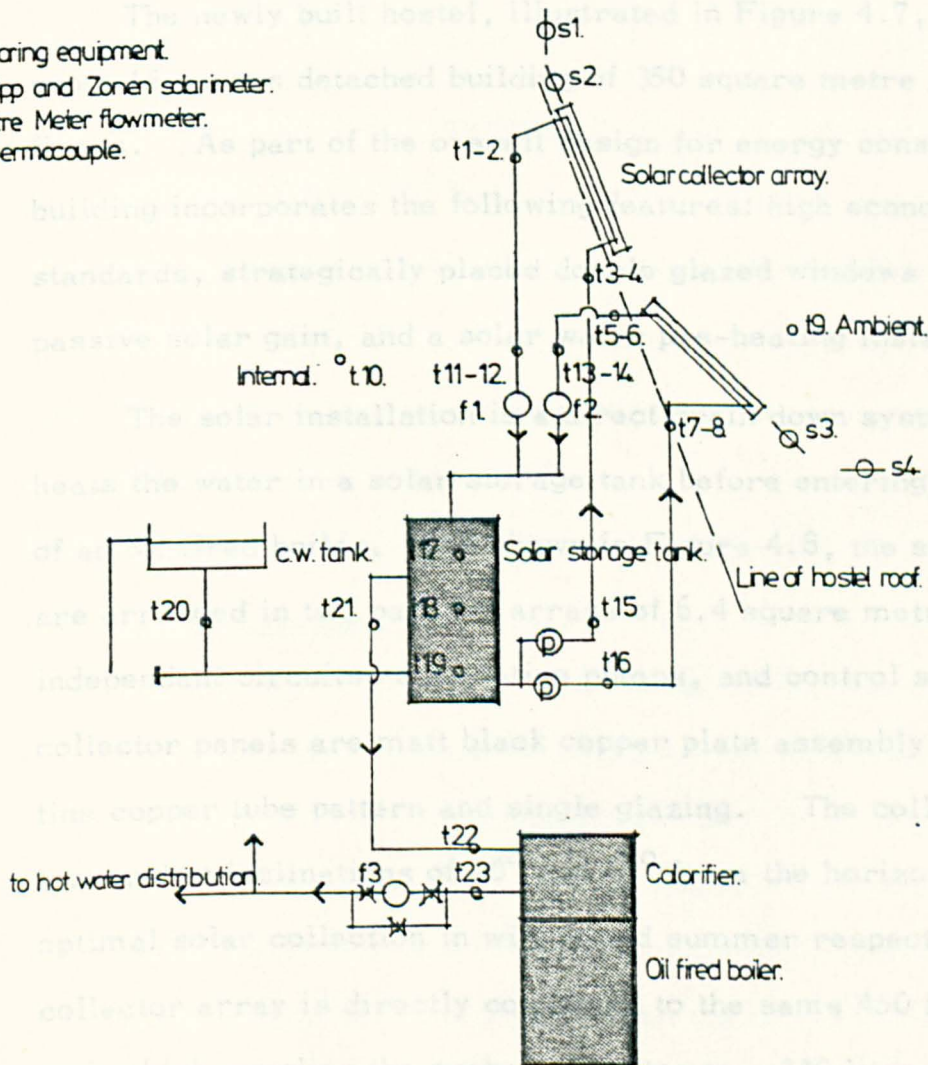
Solar collector array and drain down circuit.

Monitoring equipment.

s - Kipp and Zonen solarimeter.

f - Litre Meter flowmeter.

t - Thermocouple.



Solar water preheating system and monitoring instrumentation.

Figure 4.8 Schematic layout of solar water preheating system

performance was available for a high latitude location in this country, the opportunity has been taken to monitor a solar water pre-heating system in Aberdeen. The system was designed in collaboration with the installers, Solarway Systems Ltd., for the client, the Camphill Village Trust. From the outset it was decided to use commercially available components and installation practice. Only minor modifications were made to facilitate the use of monitoring equipment. The installation has been operational since its completion at the end of April, 1980. Saluja and Robertson¹⁰ have highlighted a number of installation problems and some inadequacies of the monitoring equipment.

4.6.1. Description of the Building and the Solar Installation

The newly built hostel, illustrated in Figure 4.7, is a ten bedroom 15 person detached building of 350 square metre area on two floors. As part of the overall design for energy conservation, the building incorporates the following features: high economic insulation standards, strategically placed double glazed windows to maximise passive solar gain, and a solar water pre-heating installation.

The solar installation is a direct drain down system which pre-heats the water in a solar storage tank before entering the calorifier of an oil fired boiler. As shown in Figure 4.8, the solar collectors are arranged in two parallel arrays of 6.4 square metres, each with independent circuits, circulating pumps, and control systems. The collector panels are matt black copper plate assembly with a serpentine copper tube pattern and single glazing. The collectors are roof mounted at inclinations of 70° and 45° from the horizontal for near optimal solar collection in winter and summer respectively. Each collector array is directly connected to the same 450 litre solar storage tank which supplies the preheated water to a 230 litre calorifier.

The flow of water through each panel array is governed by a differential/

differential temperature controller which operates the circulation pump when the controller temperature exceeds the tank temperature by a pre-set value of 3°C . The panels are drained automatically as soon as the pump stops. In addition to the differential controllers, the whole system is protected against freezing by incorporating a frostat in the system.

4.6.2. Description of the Monitoring System

The objective of the monitoring programme was to obtain detailed information on the following parameters:

- (i) The thermal performance of solar collectors at the two inclinations and the overall performance of the system under normal operating conditions.
- (ii) The solar contribution to the hot water energy requirement.
- (iii) The incident solar radiation on the horizontal, and at the two collector inclinations.
- (iv) The pattern of system drain down under normal operating and freezing conditions.
- (v) The temperature stratification within the solar tank under varied operating conditions.

Details of the monitoring equipment and techniques are as follows:

(a) Solar radiation

For the initial setting up of the monitoring system only one Kipp and Zonen solarimeter was used to measure the total horizontal radiation. For full scale monitoring, three Kipp and Zonen solarimeters have been used to measure the total incident radiation on the horizontal and the collector inclined surfaces. In addition, a shade ring has been installed on the horizontal solarimeter to measure the diffuse radiation level.

(b) Water flowrate

Three 'Litre Meter' electronic turbine flowmeters have been installed within the solar and auxiliary heating systems, positioned at each of the collector array circuits and the calorifier draw-off point. These meters electronically integrate the flowrate over a period of one minute, which is output in the form of a voltage signal to the recording instrument. The accuracy for these instruments is ± 0.05 litres/minute within the recommended range of flow for each meter.

In selecting the flowmeters for the solar circuits, no difficulty was encountered as the flowrate remains practically constant at the design value. The problem arises in measuring the draw-off flow rates at low values as the anticipated range could be large. This problem is further aggravated with the highly intermittent nature of the draw-off demand.

(c) Temperature

A network of premium grade calibrated copper constantan thermocouples have been positioned within the installation, as shown in Figure 4.8, to measure the temperatures at various locations, accurate to within $\pm 0.5^{\circ}\text{C}$.

(d) Data logging and analysis

A Solartron data logging unit, utilised in the collector test facility experiments, records the outputs in the form of analogue measurements and store the data in digital form on papertape. The data from the papertape is transferred onto a magnetic disc file and stored within the main computer for further processing. A purpose-written computer program MONITR, outlined in Appendix 2.3, is used to analyse, tabulate and graphically display the results of each monitored period. The output in terms of temperatures, /

temperatures, flowrates, insolation at collector inclinations, collector and system efficiencies and the solar contribution to the total energy requirements can be obtained in tabular or graphical form. The program output is illustrated in Figures 4.9 and 4.10. These results were finally analysed against the predicted values from the simulation program.

4.6.3. Presentation and Analysis of Monitored System Performance

The performance of the solar water heating system in the 15 person hostel has been continuously monitored since June, 1980. The measurements taken have been used to determine the feasibility of the solar water heating system from the following criteria:

- (i) The amount of solar energy available.
- (ii) The amount of solar energy collected by the solar panels.
- (iii) The level of the collected energy used by the occupants.
- (iv) The auxiliary energy required to supplement the solar water heating.

The amount of solar energy available and the percentage subsequently collected by the solar panel arrays are illustrated in Figure 4.11. The amount of solar energy collected over the period July to October, 1980, was 1165 kwh. Although the average collector efficiency over the period seems low at 43%, subsequent modifications to the system, described by Saluja and Robertson¹¹, in particular, the repositioning of the control sensors have increased the daily collector efficiency to 55%.

The level of the collected energy utilised and the amount of auxiliary heating required are illustrated in Figure 4.12. At this point, it must be stated that due to instrument failure of part of the flow monitoring equipment, only the most recent draw-off measurements have been used to gauge the overall performance. However, the results over/

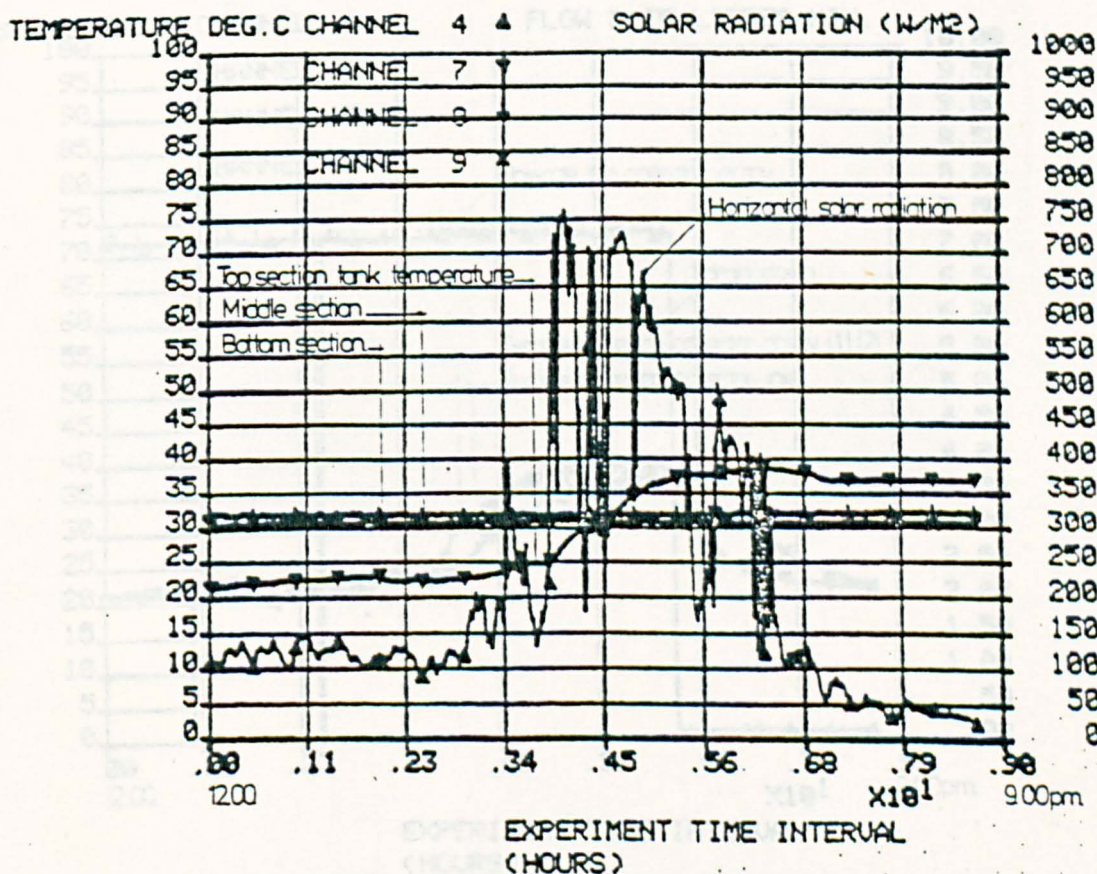
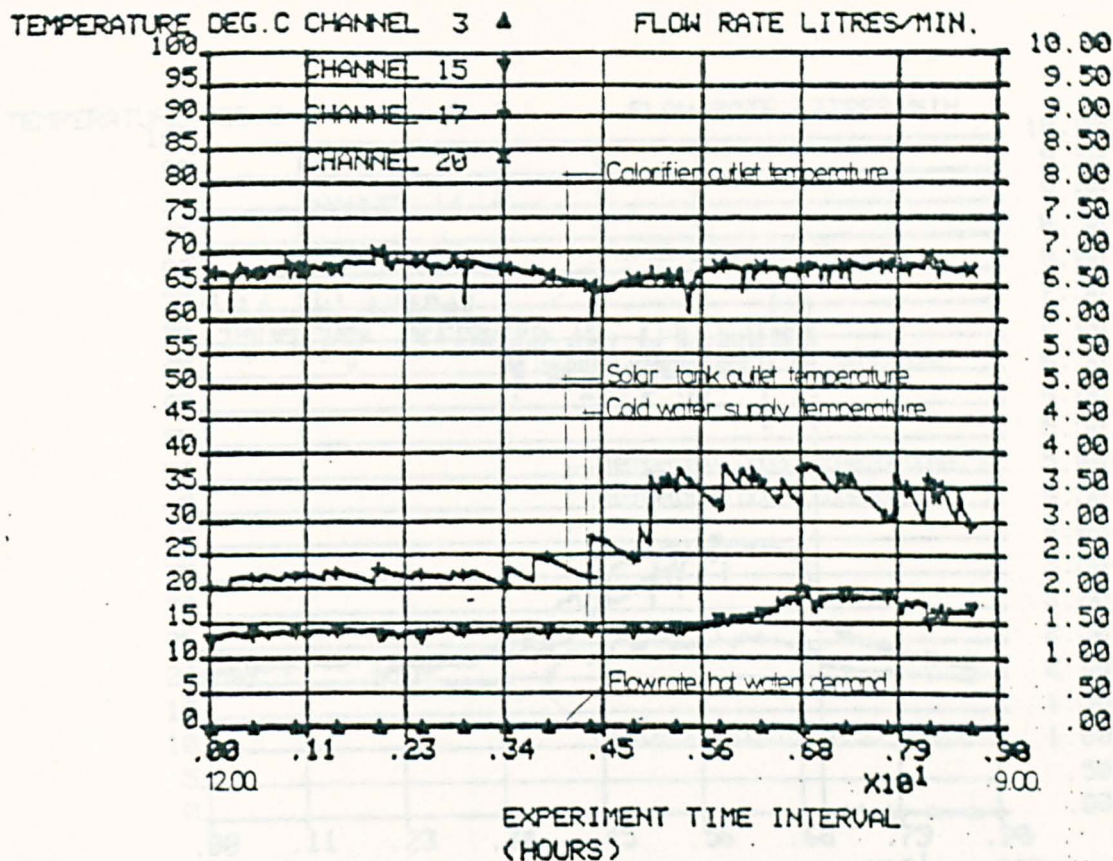


Figure 4.9 Graphical output from monitoring data analysis program MONITR.

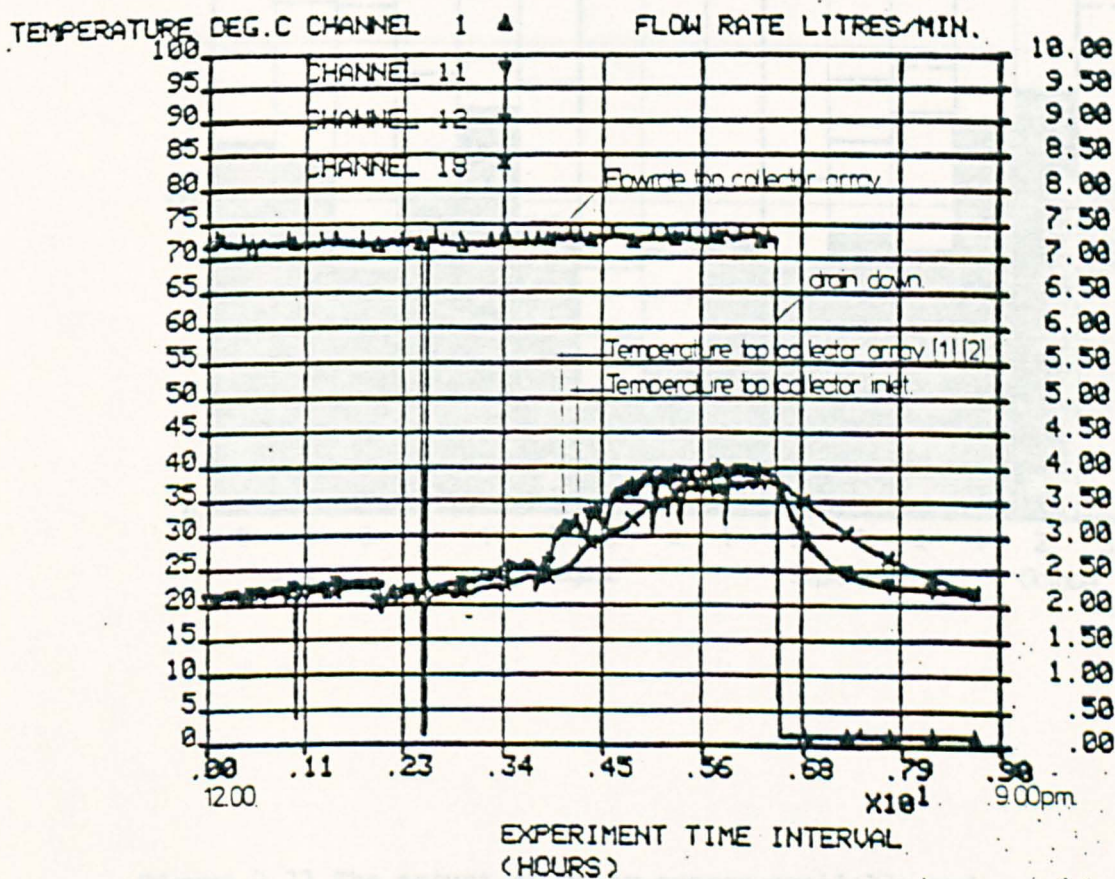
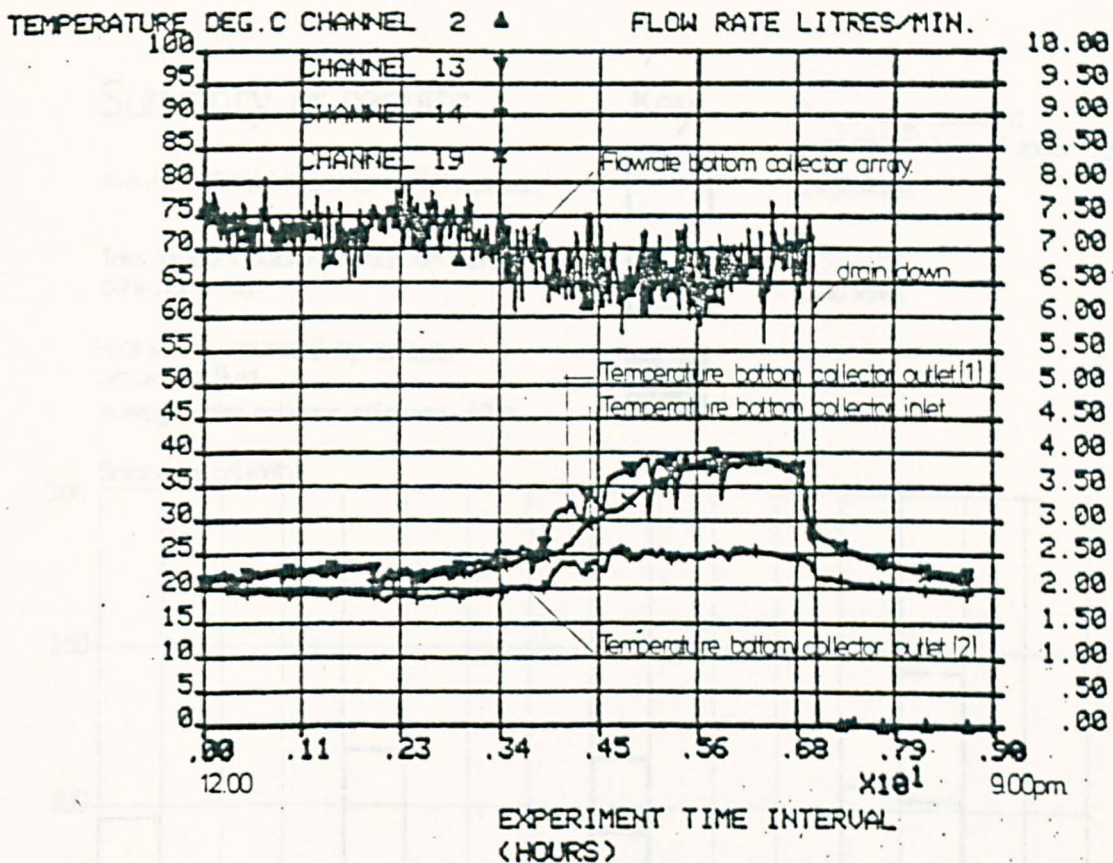


Figure 4.10 Graphical output from monitoring data analysis program MONITR.

Summary of results.

Available Total Horizontal Solar Radiation.

Total Incident Solar Radiation on inclined collector array.

Heat energy collected by collector circulating fluid.

Average solar collector efficiency. 43%.

Key.



Total energy collected over period July - October 1980.

2430 kWh.

2710 kWh.

1165 kWh.

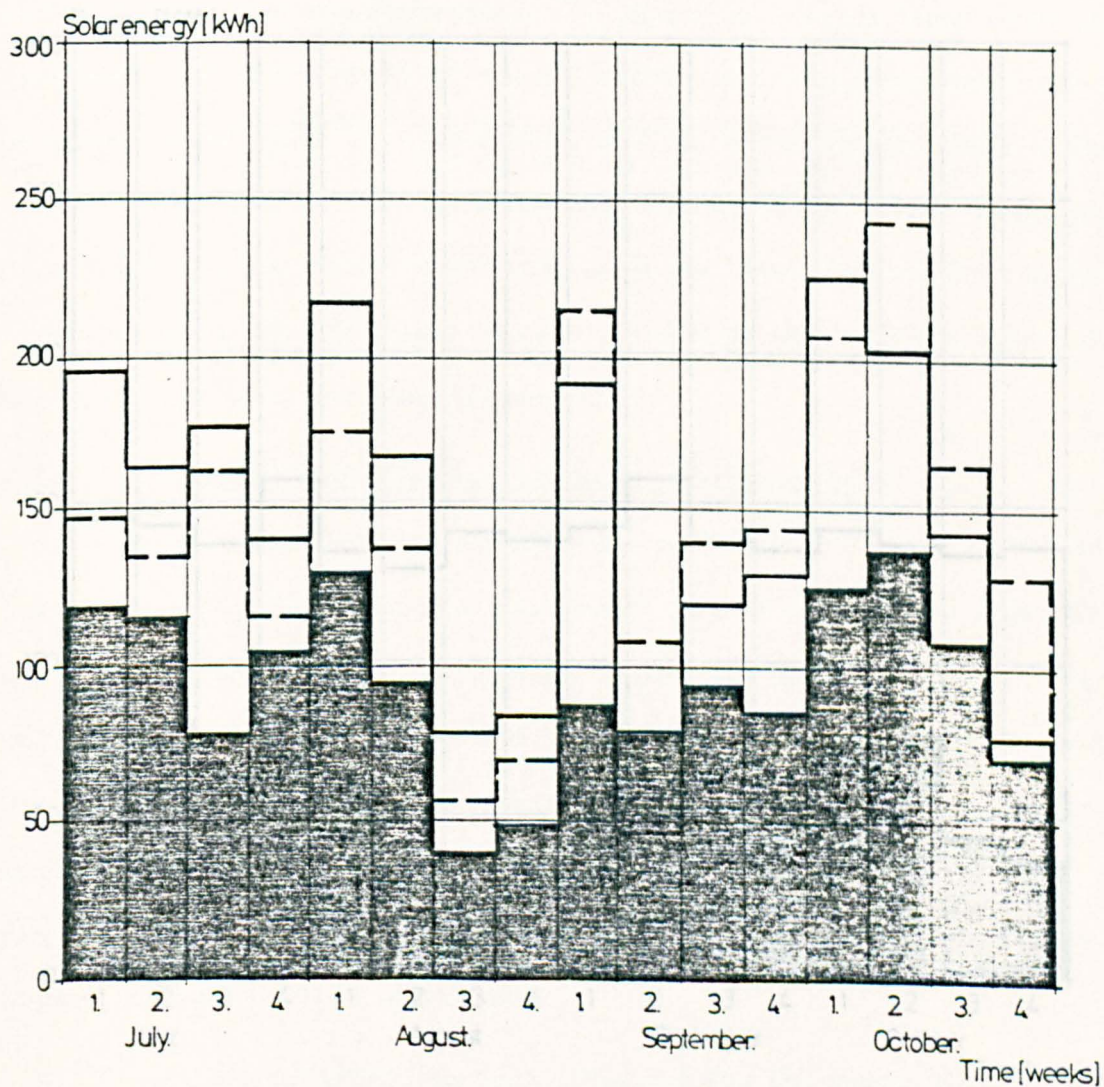


Figure 4.11 The amount of solar energy available and the energy collected by the solar panel array.

Summary of results.

Key.

Total hot water draw-off energy demand.



over period July-October 1980

2110 kWh

Total energy contribution by solar installation.
39% of hot water load.



825 kWh

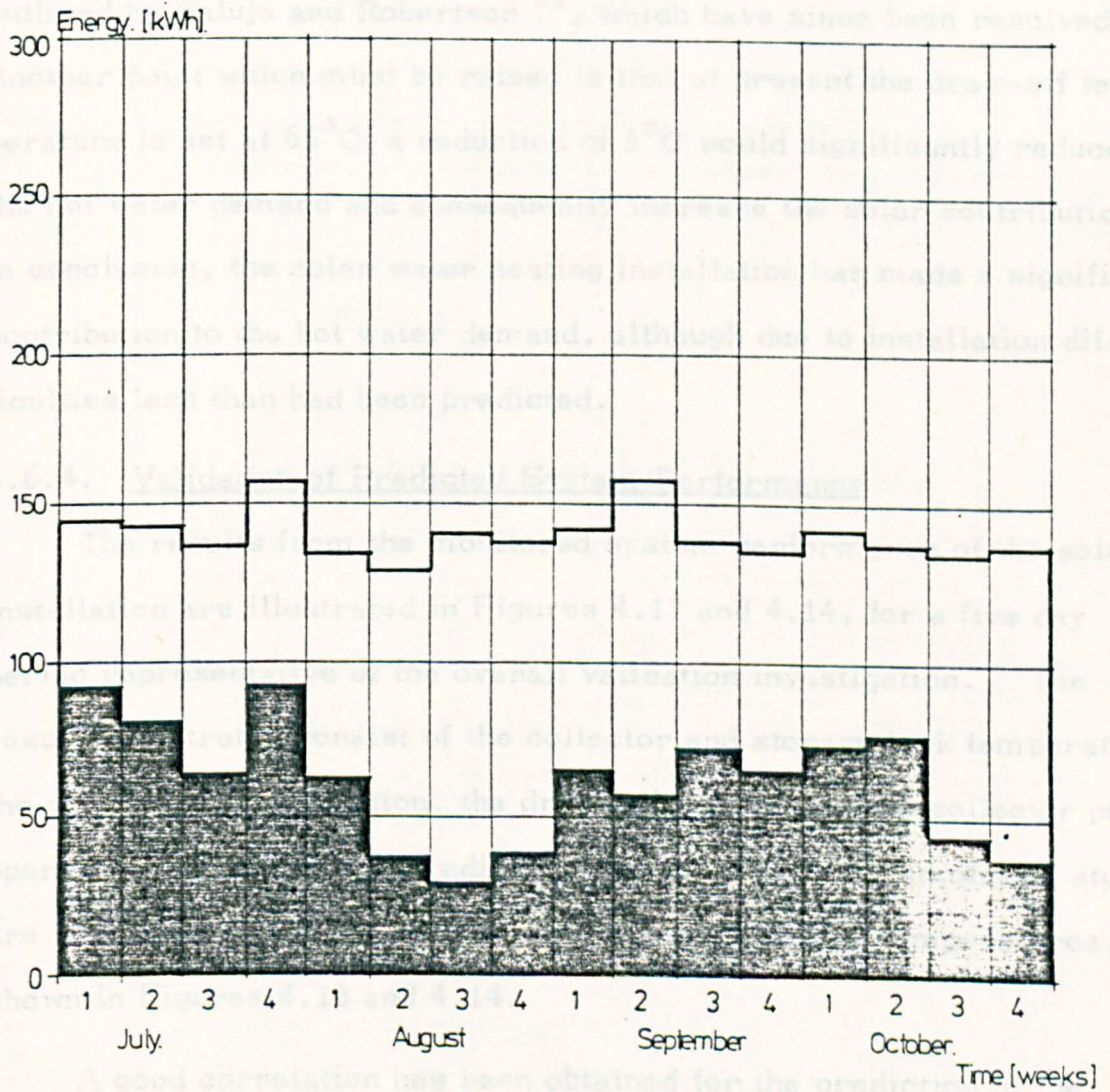


Figure 4.12 The solar system energy contribution and the hot water draw-off energy demand.

over the period have shown that the draw-off demand pattern and level tends to remain relatively constant. The draw-off demand of the hostel was approximately 2110 kwh over the period. The solar energy system contribution was 825 kwh or 39% of the required hot water demand.

These results illustrate a lower than expected solar contribution. This can be partially attributed to the earlier installation problems, outlined by Saluja and Robertson¹¹, which have since been resolved. Another point which must be raised is that at present the draw-off temperature is set at 65°C; a reduction of 5°C would significantly reduce the hot water demand and consequently increase the solar contribution. In conclusion, the solar water heating installation has made a significant contribution to the hot water demand, although due to installation difficulties less than had been predicted.

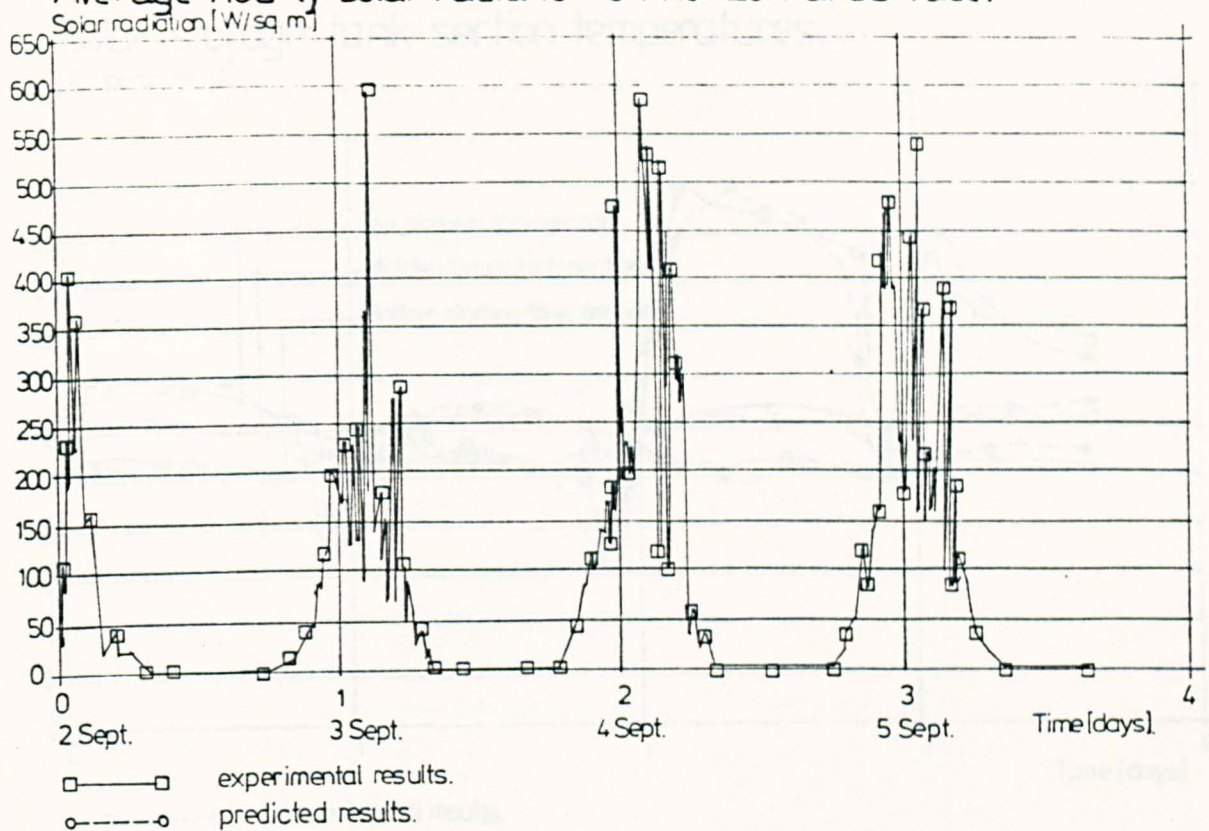
4.6.4. Validation of Predicted System Performance

The results from the monitored system performance of the solar installation are illustrated in Figures 4.13 and 4.14, for a five day period representative of the overall validation investigation. The results illustrated consist of the collector and storage tank temperatures, the incident solar radiation, the draw-off pattern and the collector pump operation. The results predicted from the computer simulation studies are overlayed on the actual collector and storage tank temperatures, as shown in Figures 4.13 and 4.14.

A good correlation has been obtained for the prediction of the overall daily solar contribution, collector efficiency and collector performance against monitored results, as illustrated in Figure 4.15. A prediction accuracy of within $\pm 10\%$ has been achieved.

The temperature stratification within the storage tank, for the higher operating temperatures involved, is distinctly divided into three sections./

Average hourly solar radiation on horizontal surface.



Top solar collector array outlet fluid temperature.

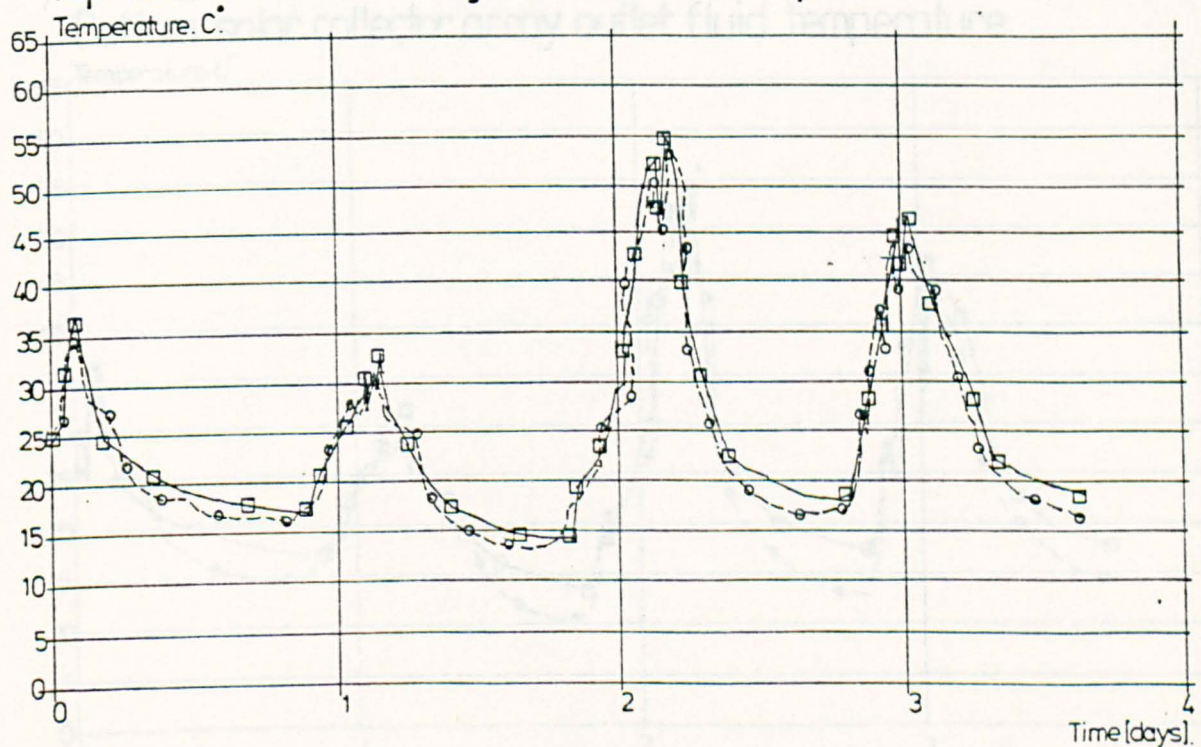
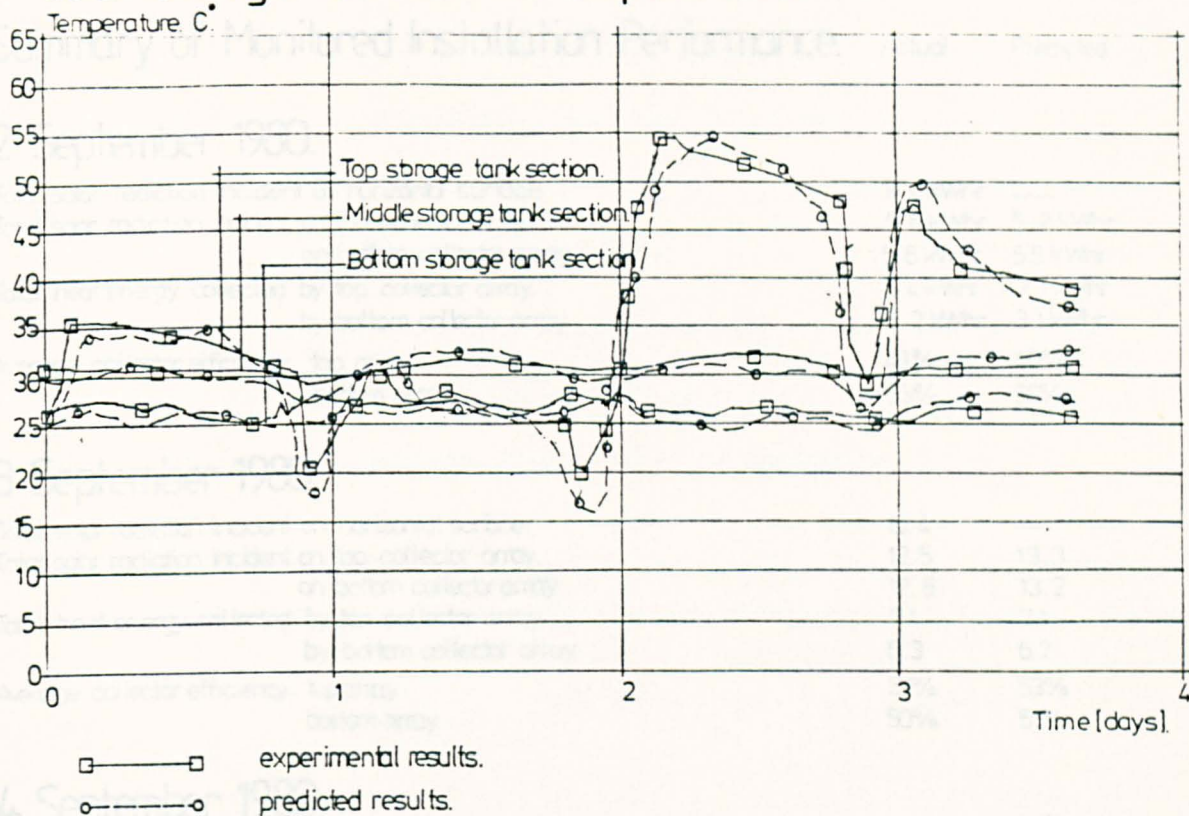


Figure 4.13 Actual vs Predicted solar collector array outlet fluid temperatures.

Solar storage tank section temperatures.



Bottom solar collector array outlet fluid temperature.

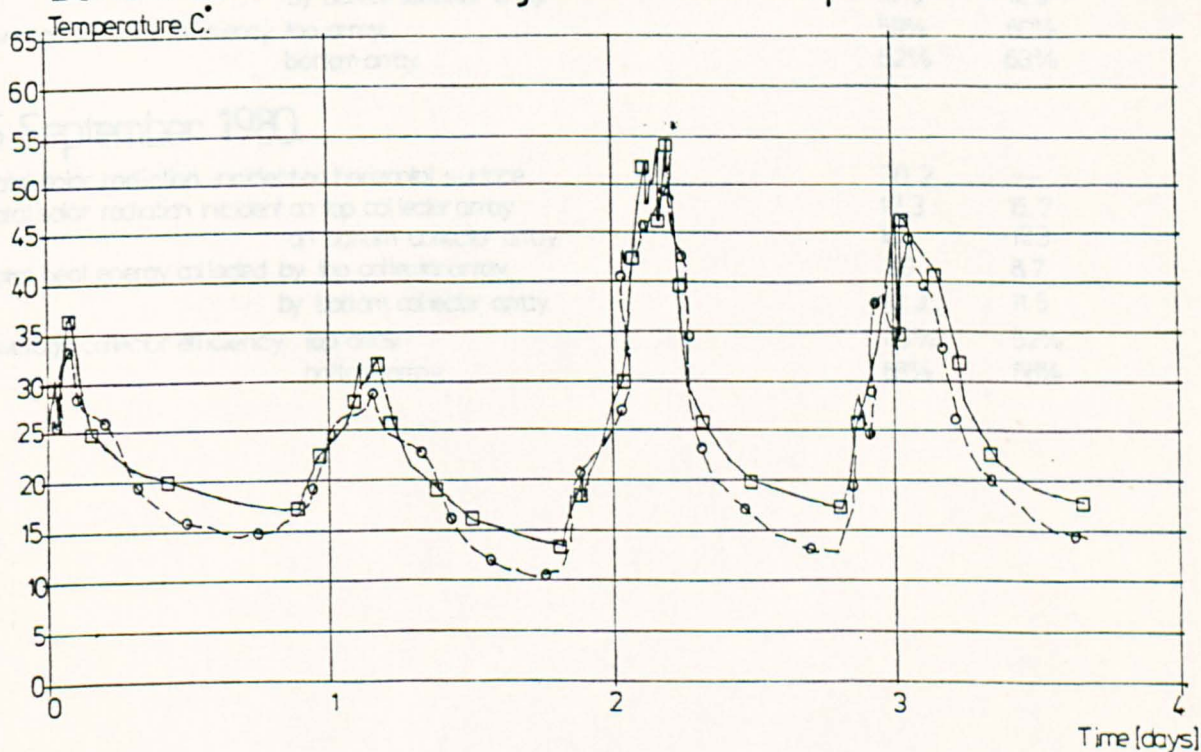


Figure 4.14 Actual vs Predicted solar collector array outlet fluid and storage tank section temperatures.

Summary of Monitored Installation Performance.

Actual Predicted

2 September 1980.

Total solar radiation incident on horizontal surface.	9.0 kWhr.	—
Total solar radiation incident on top collector array.	5.6 kWhr.	5.2 kWhr.
on bottom collector array.	5.8 kWhr.	5.5 kWhr.
Total heat energy collected by top collector array.	2.4 kWhr.	2.1 kWhr.
by bottom collector array.	3.2 kWhr.	3.1 kWhr.
Average collector efficiency top array.	43%	40%
bottom array.	55%	56%

3 September 1980.

Total solar radiation incident on horizontal surface.	19.4	—
Total solar radiation incident on top collector array.	12.5	13.3
on bottom collector array.	12.6	13.2
Total heat energy collected by top collector array.	7.4	7.1
by bottom collector array.	6.3	6.7
Average collector efficiency top array.	59%	53%
bottom array.	50%	51%

4 September 1980.

Total solar radiation incident on horizontal surface.	33.6	—
Total solar radiation incident on top collector array.	21.0	19.8
on bottom collector array.	21.9	20.4
Total heat energy collected by top collector array.	12.3	11.8
by bottom collector array.	13.5	12.9
Average collector efficiency top array.	59%	60%
bottom array.	62%	63%

5 September 1980.

Total solar radiation incident on horizontal surface.	30.2	—
Total solar radiation incident on top collector array.	17.3	16.7
on bottom collector array.	18.1	17.3
Total heat energy collected by top collector array.	7.9	8.7
by bottom collector array.	12.3	11.5
Average collector efficiency top array.	46%	52%
bottom array.	68%	66%

Figure 4.15 Actual vs Predicted daily solar contribution, collector array performance and efficiency.

This stratification pattern and the temperature profile closely follows the behaviour predicted by the computer model, as illustrated in Figure 4.14. A good correlation has been obtained against the overall storage tank temperature profile over the simulation period, under intermittent hot water draw-off conditions.

A good correlation for the predicted collector performance has been obtained against the monitored collector array inlet and outlet temperatures, under variable solar radiation conditions.

Section 4

References

1. Duffie, J.A. and Beckman, W.A., Solar Energy Thermal Processes, 1974. pp. 220-222.
2. Close, D.J., 'A design approach for solar processes'. Solar Energy, 1967. pp. 112-115.
3. Ibid., pp. 113-114.
4. Ibid., p. 114.
5. Ibid., pp. 115-117.
6. Gutierrez, G., Hincapie, F., Duffie, J.A. and Beckman, W.A., 'Simulation of forced circulation water heaters; effects of auxiliary energy supply, load type and storage capacity'. Solar Energy, 1974. pp. 289-291.
7. Courtney, R.G., 'A computer study of solar water heating'. Building and Environment, 1977. pp. 76-77.
8. Beckman, W.A., 'Duct and pipe losses in solar energy systems'. Solar Energy, 1978. pp. 531-532.
9. Brinkworth, B.J., 'British Standards for solar heating'. Proc. Conf. Solar Energy Codes of Practice and Test Procedures, 1980. pp. 99-111.
10. Saluja, G.S. and Robertson, P., 'Monitoring of solar water heating installation in a 15 person hostel'. Proc. Conf. Solar Energy in the 80's, 1980. pp. 124-130.
11. Ibid., pp. 128-130.

SECTION 5

DESIGN AND THERMAL PERFORMANCE OF INTEGRATED SOLAR COLLECTOR INSTALLATIONS IN BUILDINGS

5.1. The Influence of Restricted Built Environmental Conditions on the Performance of Solar Water Heating Installations

The previous investigation has modelled and studied the solar collector thermal performance under fluctuating climatic conditions. These variable solar radiation and cloud conditions are prevalent in the United Kingdom. In the modelling of the collector performance, the effect of the surrounding buildings and the building installation itself must be taken into consideration as an important factor in the modification of the prevalent climatic conditions. The effect on the collector performance is two fold.

Firstly, the density and the position of the surrounding buildings, determines the amount of sunlight available to the collector installation. In an inner city area, the amount of incident solar energy would be closely related to the level of overshadowing on the collector surface caused by the surrounding buildings.

In addition, the level of exposure to the prevailing weather is also directly related to the type of location, that is whether it is in open country or within a town. This factor indirectly influences the transmission of the solar radiation, by the level of pollution in the atmosphere, as illustrated by the difference between a country and an industrial location.

The second factor is the construction of the building to be fitted with a solar installation. The amount of roof area which is useful, that is suitable for solar collection is limited by the overshadowing of the roof, the angle of the roof, and the orientation of the building.

5.2. Theoretical Analysis - Dynamic Behaviour of Integrated Solar Installations in Restricted Built Environmental Conditions

5.2.1. Method of Analysis

In this section, the simulation model describing the effect of transient solar radiation and intermittent energy usage conditions on the/

the system performance, has been extended to take into account the effect of restricted built environmental conditions. These conditions can be described by the following parameters:

- (i) The overshadowing of the collector surface by surrounding buildings,
- (ii) The limitation of the usable roof area in existing buildings suitable for solar collection.

The objective of this study is to model and predict the effect of these conditions on the collector performance, as outlined by Saluja and Robertson¹. No previous work has been cited to quantify the influence of built environmental conditions on urban solar installations.

The method used to achieve this aim has been to amend and develop the solar radiation and the thermal prediction mathematical models to incorporate the above features. In addition, the effect of integrating the solar collector installation as part of the roof fabric has been investigated and modelled, as a possible technique to improve the system performance.

5.2.2. Overshadowing of Collector Installations

The method adopted to predict the period of shadowing on the collector surface has been to amend the existing building and window shadow prediction techniques as outlined by Souster² and Clarke³. This method involves the adaption of the shadowing effects on vertical surfaces to inclined collector surfaces.

The shadowing of the collector surface is a combination of a number of components which can be defined as:

- (i) The effect of dirt on the collector cover,
- (ii) The effect of the shading of the collector plate by the collector frame unit,
- (iii) The effect of the shadowing of the collector surface by surrounding buildings.

These factors can be outlined as follows:

(i) The effect of dirt on the collector cover

The effect of dirt on the collector cover and the subsequent reduction in the cover transmittance of solar radiation has been studied by Garg⁴; this effect is expressed as a reduction factor applied to the transmitted solar radiation.

$$F_d = (1 - fd) \quad (5.1)$$

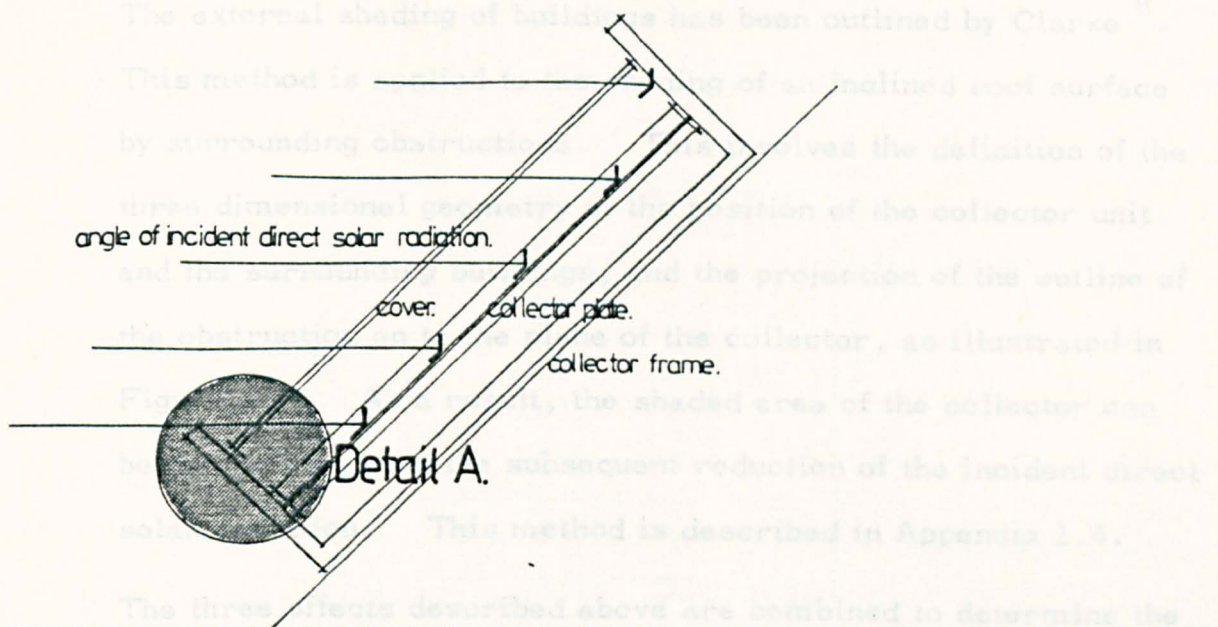
where fd has been taken by Garg⁵ and Duffie and Beckman⁶ to be 0.02. It can be assumed however that this constant fd , changes due to the geographical location of the solar installation. In this study, the constant is determined by the type of location; a dense urban location $fd = 0.04$, an open country location, $fd = 0.01$ ⁴.

(ii) The effect of the shading of the collector plate by the collector frame unit

The effect of the collector plate shading by the frame unit has been expressed by Hottel and Woertz⁷ as a reduction factor of 0.97 applied to the daily incident solar radiation.

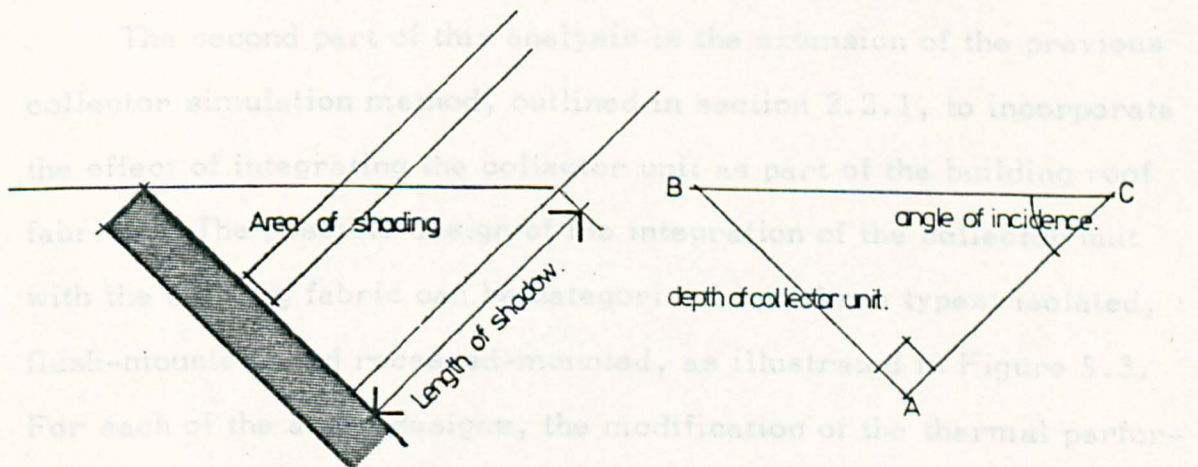
However, such a simplification is inaccurate for the detailed hourly simulation of shadow prediction. In this study, the area and the period of the shadow cast on the collector plate are calculated from the solar angle of incidence and the collector frame dimensions.

This method is described in Appendix 1.4 and illustrated in Figure 5.1. The effect on the collector thermal performance for the overshadowed collector surface area, is an obstruction of the direct incident solar radiation. Diffuse solar radiation is unaffected by the shadow cast.



Typical collector installation design.

5.2.3. Dynamic Thermal Behaviour of Integrated Solar Collector Installations



Detail A. length of shadow. $AC = AB \cdot \frac{\sin B}{\sin C}$

Figure 5.1 Prediction of the shading of the collector plate by the collector frame unit.

(iii) The effect of the shadowing of the collector surface by surrounding buildings

The external shading of buildings has been outlined by Clarke⁸.

This method is applied to the shading of an inclined roof surface by surrounding obstructions. This involves the definition of the three dimensional geometry of the position of the collector unit and the surrounding buildings, and the projection of the outline of the obstruction on to the plane of the collector, as illustrated in Figure 5.2. As a result, the shaded area of the collector can be determined, and the subsequent reduction of the incident direct solar radiation. This method is described in Appendix 1.4.

The three effects described above are combined to determine the total reduction in the incident solar radiation on the collector for each time increment.

5.2.3. Dynamic Thermal Behaviour of Integrated Solar Collector Installations

The second part of this analysis is the extension of the previous collector simulation method, outlined in section 2.2.1, to incorporate the effect of integrating the collector unit as part of the building roof fabric. The possible design of the integration of the collector unit with the building fabric can be categorised into three types: isolated, flush-mounted, and recessed-mounted, as illustrated in Figure 5.3. For each of the above designs, the modification of the thermal performance of the collector can be defined as the reduction of the edge and rear heat losses, and the upward forced convection heat losses due to wind. The modified heat loss equations for the integrated collector designs are described in Appendix 1.4.

As a result of the decreased heat losses due to the particular type of collector integration design applied, the overall collector performance is improved. The validity of the amended collector heat loss/

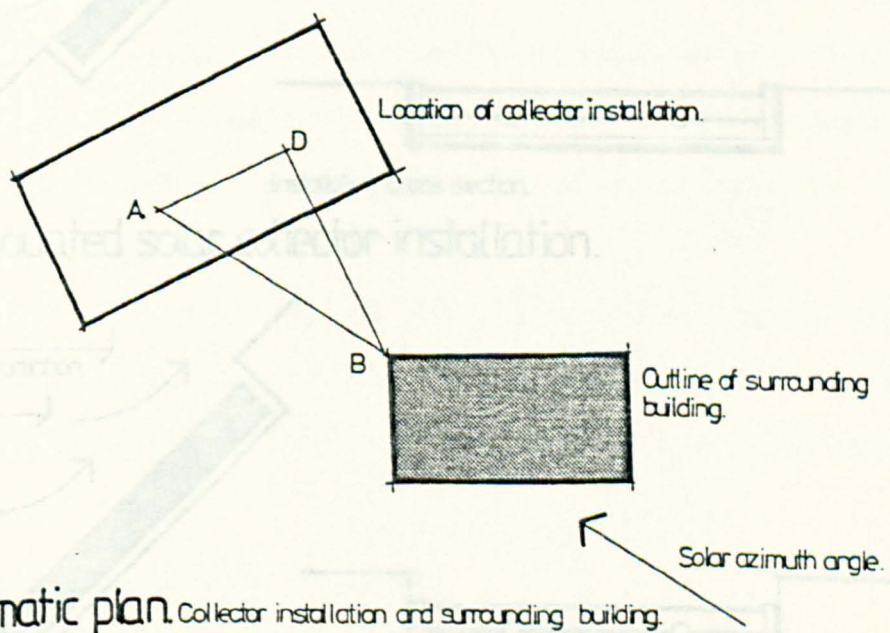
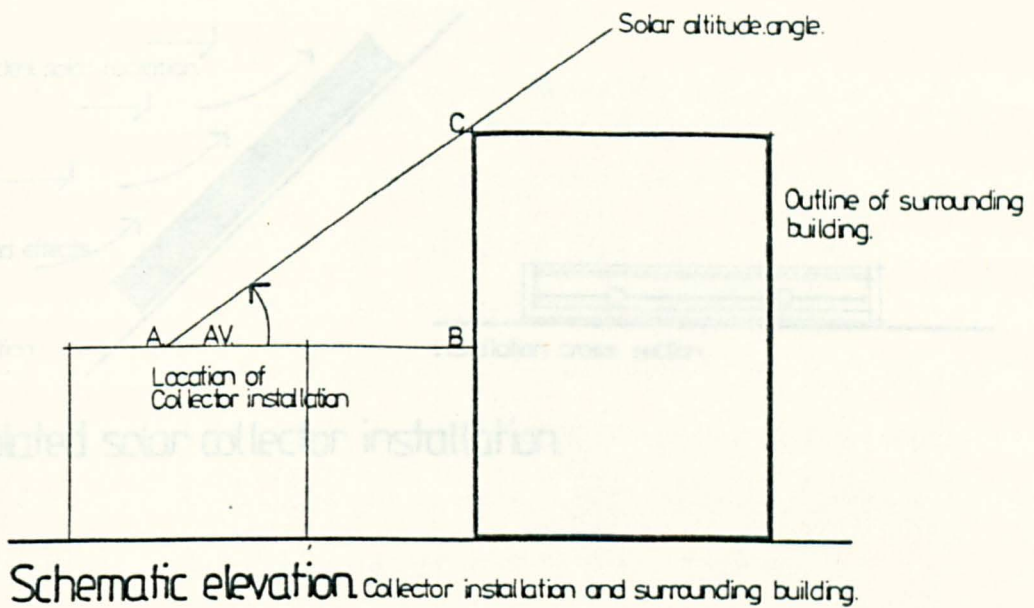
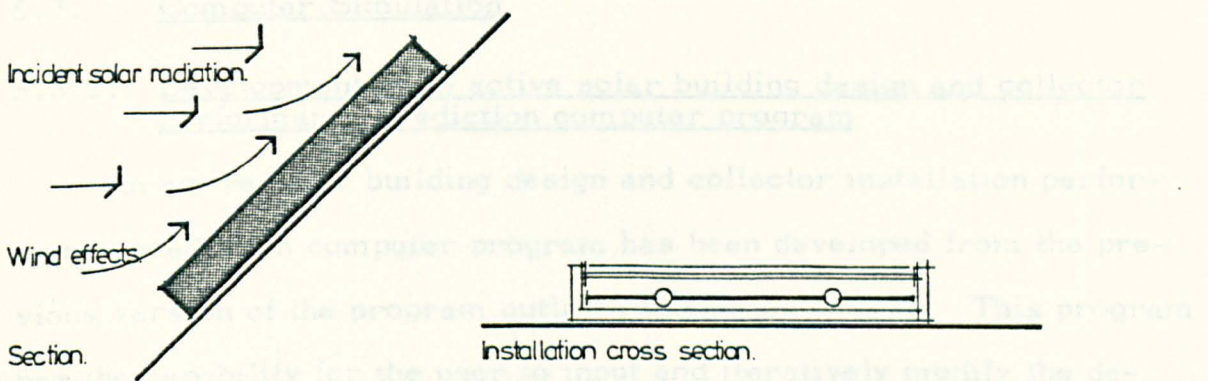
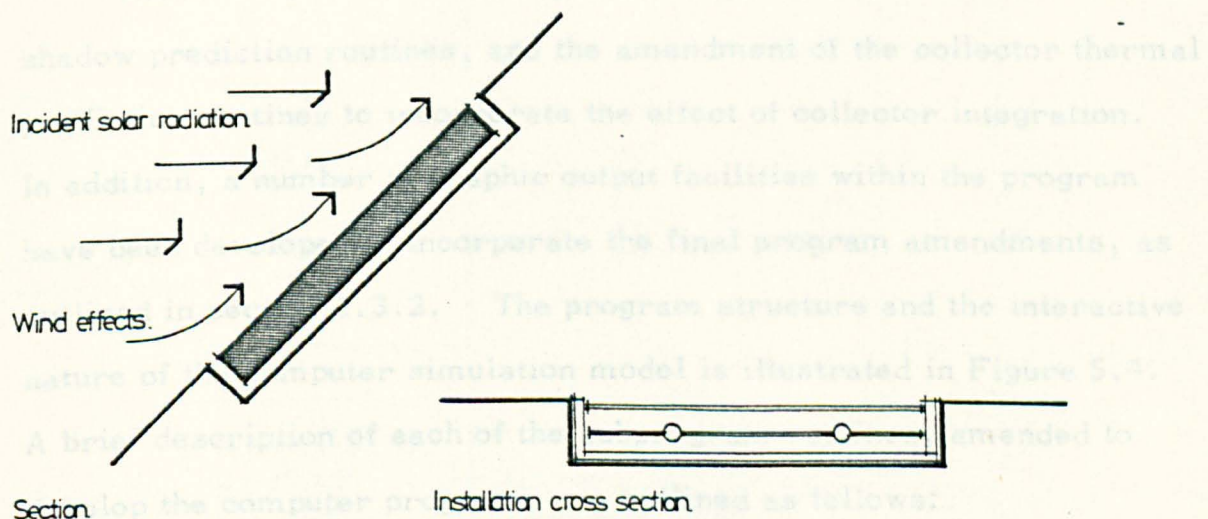


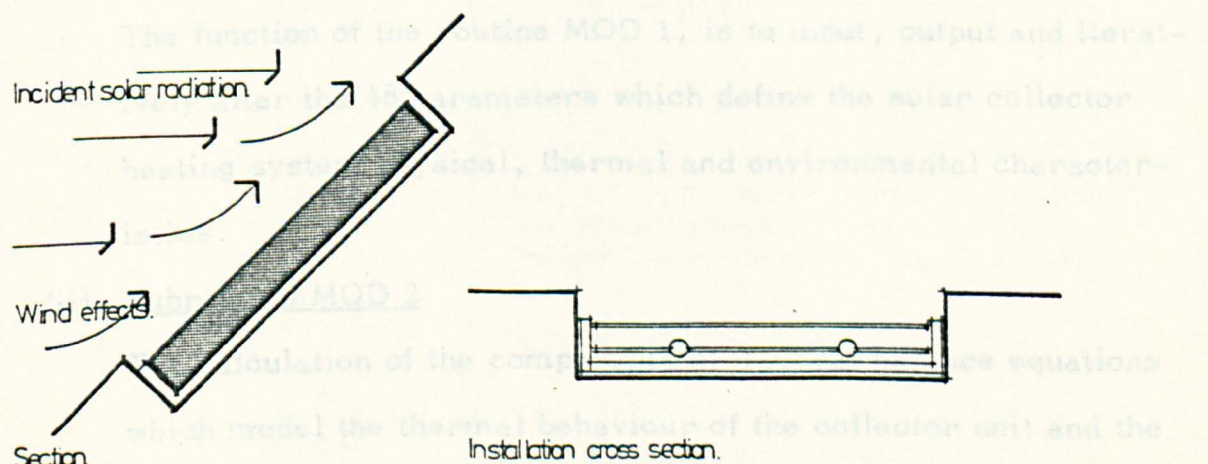
Figure 5.2 Prediction of the shading of the collector surface by surrounding buildings.



Isolated solar collector installation.



Flush mounted solar collector installation.



Recessed mounted solar collector installation.

Figure 5.3 Possible designs of integrated solar collector installations.

loss expressions, and the possible increase in the collector performance are experimentally studied in Section 5.4.

5.3. Computer Simulation

5.3.1. Development of an active solar building design and collector performance prediction computer program

An active solar building design and collector installation performance prediction computer program has been developed from the previous version of the program outlined in section 4.3.1. This program has the capability for the user to input and iteratively modify the design of the solar collector water heating system and the building form of the installation, and predict the resultant dynamic system performance under the prevalent environmental conditions.

The development of the program consisted of the insertion of the shadow prediction routines, and the amendment of the collector thermal prediction routines to incorporate the effect of collector integration. In addition, a number of graphic output facilities within the program have been developed to incorporate the final program amendments, as outlined in section 5.3.2. The program structure and the interactive nature of the computer simulation model is illustrated in Figure 5.4. A brief description of each of the subprogram routines, amended to develop the computer program, are outlined as follows:

(i) Subroutine MOD 1

The function of the routine MOD 1, is to input, output and iteratively alter the 48 parameters which define the solar collector heating system physical, thermal and environmental characteristics.

(ii) Subroutine MOD 2

The calculation of the components of the heat balance equations which model the thermal behaviour of the collector unit and the storage tank.

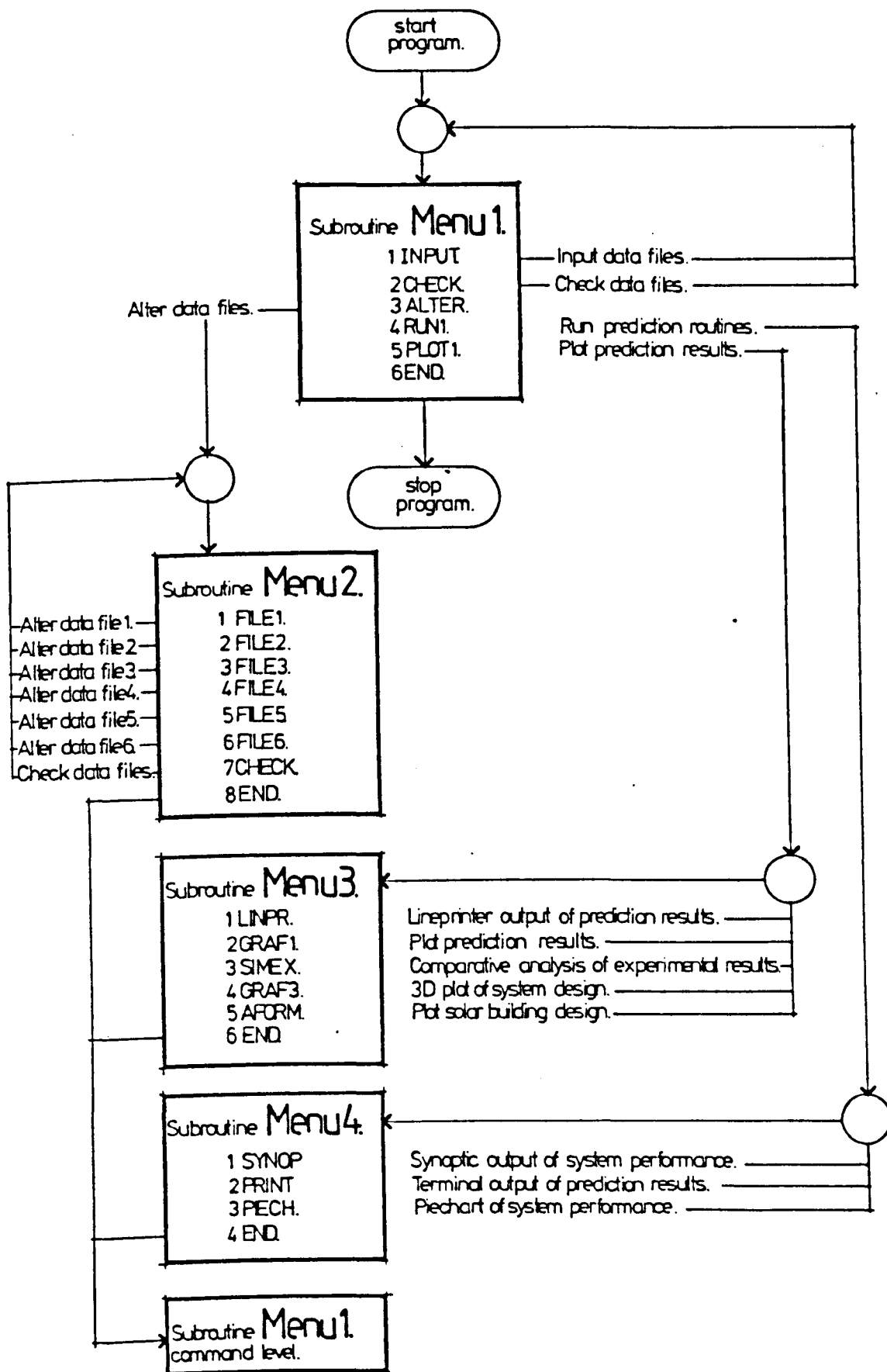


Figure 5.4 Flowchart representation of the computer program SOLAR 7.

(iii) Subroutine MOD 3

The solution of the heat balance equations for the collector unit by the Quartic Runge-Kutta numerical method.

(iv) Subroutine MOD 4

The function of the routine MOD 4, is to control the interrelated subprogram calculations for each time increment over the simulation period.

(v) Subroutine MOD 6

The output, in tabular form, of the predicted values of the system thermal network temperatures, the collector efficiency and the climatic parameters over the simulation period.

(vi) Subroutine MOD 8

The solution of the heat balance equations for the storage tank by the Quartic Runge-Kutta numerical method.

(vii) Subroutine PILOS

The solution of the heat balance equations for the connecting system pipework by the Quartic Runge-Kutta numerical method.

(viii) Subroutine SOLHT

The calculation of the energy supplied by the solar heating system and the auxiliary heat requirement for each time increment over the simulation period.

(ix) Subroutine SUNRAD

The calculation of the incident solar radiation, taking into account the effect of the cover dirt losses, the self-shading of the collector and the collector overshadowing by surrounding buildings.

(x) Subroutine MENU 1

The function of the routine MENU 1, is to control the operation of the program by presenting the user with the following options: input, check and alter the simulation data, run the prediction program and plot the results.

(xi) Subroutine MENU 2

The modification of the parameters of the solar heating system and environmental simulation.

(xii) Subroutine MENU 3

The function of the routine MENU 3, is to present the user with the following options of displaying the program prediction results: full tabular and graphical output, or diagram of system layout and installation design.

(xiii) Subroutine MENU 4

The presentation of the salient results of the system performance in the form of synoptic tabular or piechart output.

(xiv) Subroutine PLOT 1

The function of the routine PLOT 1, is to display in graph form the range of system network temperature results and the climatic conditions over the simulation period.

5.3.2. Outline of program operation

The program operation for a representative simulation study of the dynamic thermal performance of a solar water heating system can be outlined as follows.

1. Input data

The program requires the following information, tabulated in Figure 5.5, to initialise the physical and thermal parameters of the solar collector, storage tank, system layout and installation design. In addition, the climatic conditions for the simulation period and the geometry data of the installation and the surrounding buildings for the location is required.

This information is held in external files and can be modified within the program during operation. The information input to the program is automatically checked by the program or if required visually checked by the user to determine any data errors.

1.	XF-THICKNESS OF ABSORBER PLATE (M):	0.0010
2.	B1-TUBE CENTRE LINE SPACING (M):	0.1500
3.	B2-PROJECTED WIDTH-TUBE BOND (M):	0.0200
4.	D1-DIAMETER OF COLLECTOR TUBES (M):	0.0130
5.	C1-THERMAL CAPACITY OF TUBES(J/M3C):	3511.2000
6.	XT-THICKNESS OF TUBE MATERIAL (M):	0.0010
7.	UT-CONDUCTIVITY OF TUBES (W/M.C):	56.0000
8.	EP-EMISSIVITY OF ABSORBER PLATE:	0.9000
1.	C2-THERMAL CAPACITY OF PLATE(J/M3C):	3511.2000
2.	C3-THERMAL CAPACITY OF COVER(J/M3C):	2268.0000
3.	UA-CONDUCTIVITY-ABSORBER (W/M.C):	56.0000
4.	EG-EMISSIVITY OF GLASS COVER (E):	0.7000
5.	TGC-TRANSMITTANCE OF GLASS COVER:	0.8000
6.	ABS-ABSORPTIVITY COLLECTOR PLATE:	0.9500
7.	XG-THICKNESS OF GLASS COVER (M):	0.0040
8.	XR-THICKNESS OF REAR INSULATION (M):	0.1000
1.	KF-COLLECTOR PLATE CONSTRUCTION (M):	2.0000
2.	C4-THERMAL CAPACITY OF REAR(J/M3C):	20.2000
3.	CI-COLLECTOR-ROOF INTEGRATION(N):	0.0000
4.	UI-CONDUCTIVITY-INSULATION (W/M.C):	0.0800
5.	XF-THICKNESS OF FRAME UNIT (M) :	0.0020
6.	C5-THERMAL CAPACITY OF FRAME(J/M3C):	1792.0000
7.	NC-NUMBER OF COLLECTOR SEGMENTS:	1.0000
8.	UF-CONDUCTIVITY-FRAME UNIT (W/M.C):	180.0000
1.	NHR-LENGTH OF SIMULATION RUN (HR):	24.0000
2.	TLT-COLLECTOR UNIT TILT ANGLE(DEG):	45.0000
3.	FFR-COLLECTOR FLUID FLOW RATE(L/S):	0.0200
4.	XLC-COLLECTOR UNIT LENGTH (METRES):	1.5000
5.	XWC-COLLECTOR UNIT WIDTH (METRES):	0.9000
6.	XDC-COLLECTOR UNIT DEPTH (METRES):	0.2000
7.	NCU-NUMBER OF COLLECTOR UNITS (N):	2.0000
8.	DT-SIMULATION TIME INCREMENT (HR):	0.1000
1.	SLT-SITE LATITUDE (DEGREES, N+VE):	57.0000
2.	SLG-SITE LONGITUDE (DEGREES, W+VE):	0.0000
3.	YNO-SIMULATION YEAR NUMBER (EG1979):	1976.0000
4.	NMO-SIMULATION MONTH NUMBER (EG02):	7.0000
5.	DST-STARTING DATE OF SIMULATION:	1.0000
6.	NDY-LENGTH OF SIMULATION RUN (DAYS):	1.0000
7.	LIZ-LOCAL INTERNATIONAL ZONE TIME:	0.0000
8.	WZA-COLLECTOR UNIT ORIENTATION(DEG):	180.0000
1.	CTS-TEMPERATURE CONTROL SYSTEM (N):	1.0000
2.	SSV-VOLUME OF SOLAR STORAGE TANK(L):	150.0000
3.	DDT-DRAW-OFF DELIVERY TEMPERATURE:	55.0000
4.	SSD-DIAMETER OF SOLAR STORAGE TANK:	0.6000
5.	SIL-LEVEL OF SYSTEM INSULATION (M):	0.0500
6.	CPL-LENGTH OF CIRCULATION PIPE (M):	2.0000
7.	HEX-TYPE OF TANK HEAT EXCHANGER:	0.0000
8.	TAH-TYPE OF AUXILIARY HEATING FUEL:	0.0000

Figure 5.5 List of parameters required for input data to computer program SOLAR 7.

2. Execute prediction program

At this stage, the user has the option to execute the program and analyse the predicted performance in synoptic or detailed graphical and numerical form, as illustrated in Figures 5.6 - 5.9.

In most cases, a synoptic study of the initial thermal performance of the solar heating system is required before the user can assess any possible improvements and modifications to the installation design. However, the detailed graphical or numerical output of the system network temperatures can reveal particular dynamic defects in the system design, such as collector self shading, excessive collector overshadowing or user energy demands at critical times during the simulation period.

3. Analyse results and modify data

At this stage, the user can analyse the predicted results of the system performance during the program operation. As a consequence, the thermal and physical design of the collector installation can be modified by the alteration of the stored parameters held within the program. Steps 1 - 3 are repeated until a satisfactory performance or installation design is obtained.

The application of such a comprehensive program lies in the development of innovative solar collector system and installation designs to achieve optimum system performance under transient climatic and restricted site conditions.

5.4. Experimental Investigation

5.4.1. Objectives of Experimental Investigation

The objective of the experimental investigation has been to study the thermal behaviour of two designs of integrated solar collector installations: recessed and flush-mounted collector units. As a result, the predicted dynamic collector thermal performance under variable climatic/

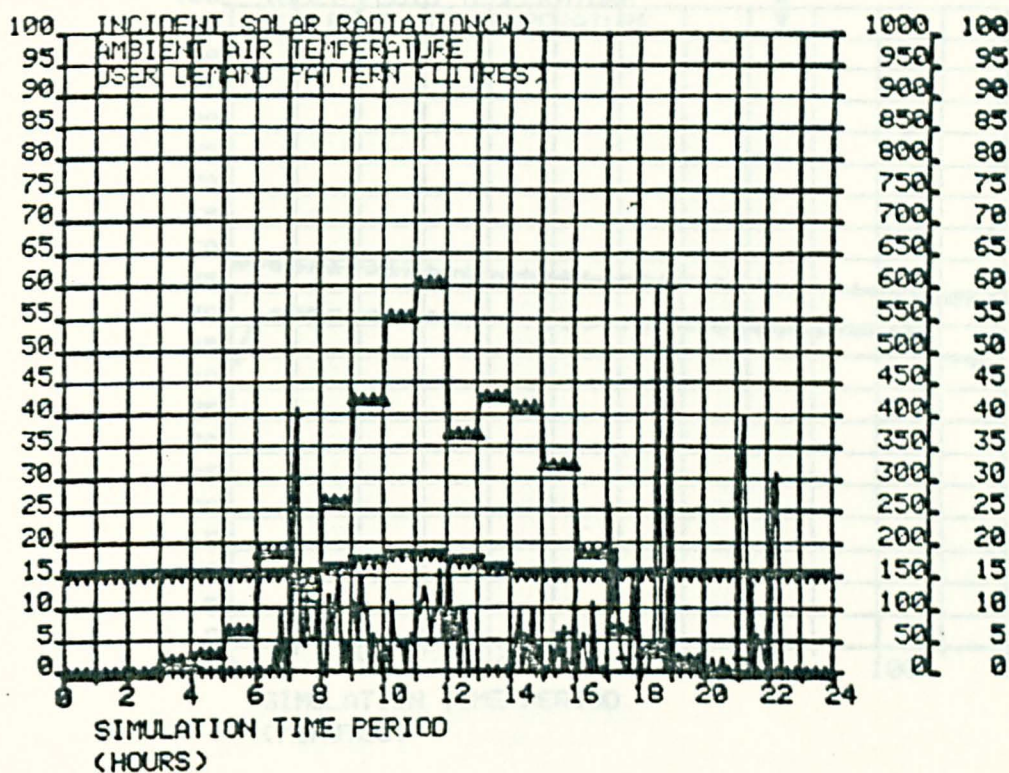


Figure 5.6 Simulation program output - Environmental parameters and collector efficiency.

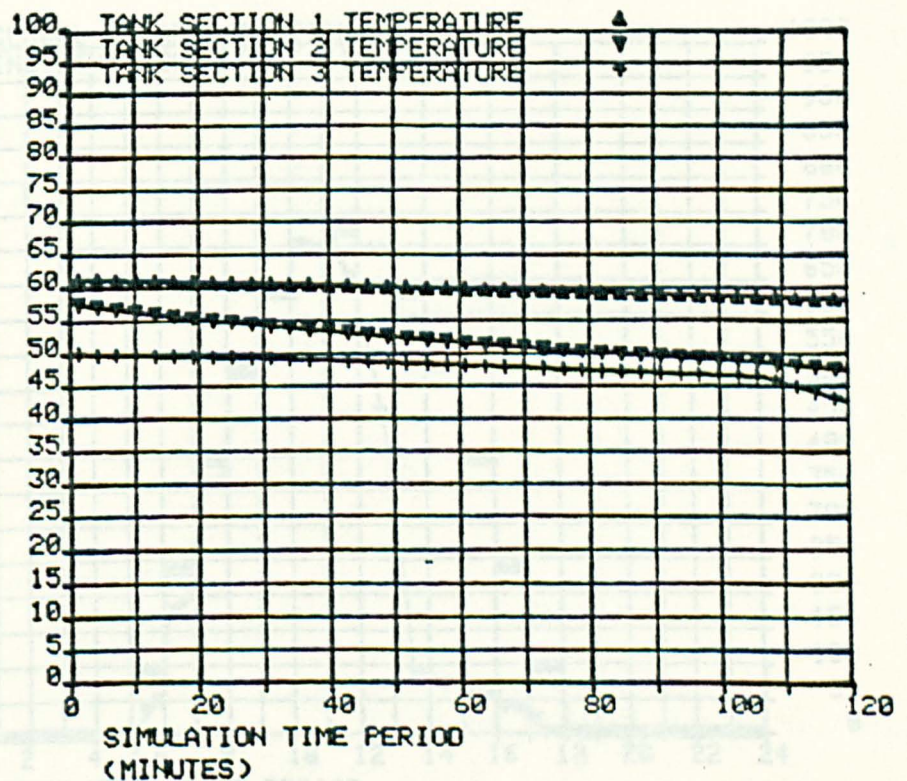
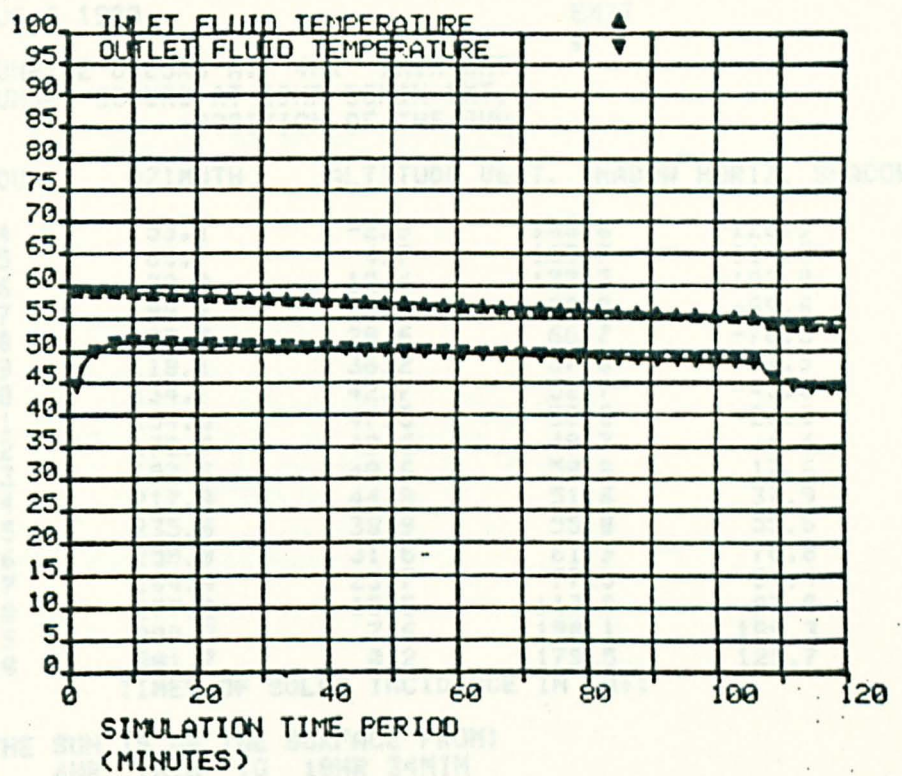


Figure 5.7 Simulation program output - Solar collector and storage tank temperatures.

AUG 6 1980

EXIT

SUNRISE OCCURS AT 4HR 1MIN GMT.

SUNSET OCCURS AT 19HR 58MIN GMT.

POSITION OF THE SUN

HOUR	AZIMUTH	ALTITUDE	VERT. SHADOW	HORIZ. SHADOW
4	53.1	-2.3	183.8	-126.9
5	65.7	4.7	168.7	-114.3
6	78.0	12.4	133.3	-102.0
7	90.4	20.5	88.9	-89.6
8	103.5	28.6	66.7	-76.5
9	118.1	36.2	57.3	-61.9
10	134.7	42.7	52.7	-45.3
11	154.0	47.5	50.5	-26.0
12	175.6	49.6	49.7	-4.4
13	197.6	48.6	50.0	17.6
14	217.9	44.8	51.6	37.9
15	235.6	38.9	55.0	55.6
16	250.8	31.6	61.9	78.8
17	264.4	23.7	77.5	84.4
18	277.0	15.5	113.8	97.0
19	289.3	7.6	158.1	109.3
20	301.7	0.2	179.5	121.7

TIMES OF SOLAR INCIDENCE IN GMT:

THE SUN IS ON THE SURFACE FROM:

1 4HR 1MIN TO 18HR 34MIN

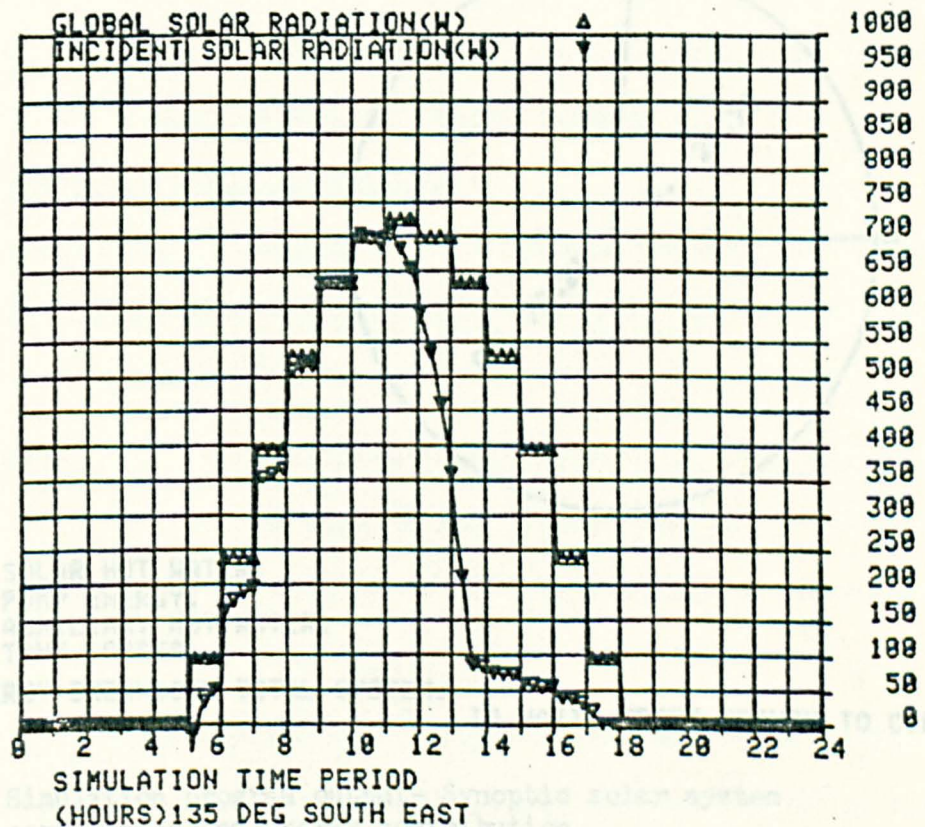


Figure 5.8 Simulation program output - Solar data.

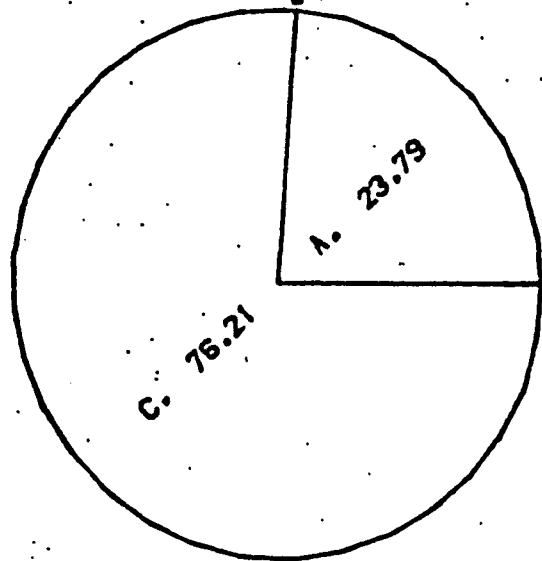
DO YOU WISH TO INITIALISE SOLAR SYSTEM TEMPERATURES ?, (0-NO, 1-YES)

0

SEPTEMBER 1 1980

SUNRISE OCCURS AT 5HR 3MIN. GMT
SUNSET OCCURS AT 18HR 55MIN. GMT

DAILY TOTAL RADIATION INCIDENT ON GLASS 8.4KWHR
DAILY TOTAL RADIATION INCIDENT ON COLLECTOR PANELS 7.7KWHR
DAILY TOTAL HEAT ENERGY COLLECTED 3.6KWHR
DAILY HEAT SUPPLIED BY SOLAR SYSTEM 3.1KWHR
DAILY AUXILIARY HEAT REQUIREMENT 11.7KWHR
DAILY RUNNING TIME OF PUMP 3HR 13MIN
DAILY AVERAGE COLLECTOR EFFICIENCY 47.0%
IO WAIT, PRESS RETURN TO CONTINUE



A. SOLAR HOT WATER.
B. PUMP ENERGY.
C. AUXILIARY HOT WATER.
D. TANK LOSSES.

ENERGY-BREAKDOWN TOTAL SYSTEM.

IO WAIT, PRESS RETURN TO CONTINUE

Figure 5.9 Simulation program output- Synoptic solar system performance and energy contribution.

climatic conditions can be verified.

5.4.2. Apparatus and Experimental Procedure

As outlined in section 2.4.3, a flat-plate solar collector water heating system outdoor test facility has been designed and constructed. This facility has been modified to incorporate the recessed and flush-mounting of the collector unit within a simulated building roof fabric. The basic outdoor test facility, described in section 2.4.3, has been unaltered to allow for the comparison of performance results. The two outdoor integrated collector facilities are outlined below.

(i) Recessed roof-mounted collector unit

The construction and performance of a recessed roof-mounted collector unit has been represented by the design of a timber roof structure and fabric to the existing outdoor collector test facility as illustrated in Figure 5.10. The roof structure has been constructed of a timber joist structure fixed to the existing mild steel collector angle frame and surfaced with a plywood skin to model the potential roof surface. The collector unit is recessed 50mm within the simulated roof structure.

(ii) Flush roof-mounted collector unit

The construction of the experimental roof structure was modified to obtain a flush-mounted integrated collector test facility, as illustrated in Figure 5.11.

The timber frame roof structure and the plywood skin were altered to lower the roof level to the plane of the collector cover. As with the recessed unit, the collector cover opening is sealed to the exposed climatic conditions.

As with previous experiments, the measurement of the integrated solar collector system temperature behaviour was monitored by a network of premium grade copper constantan thermocouples, positioned

Key.

t. position of thermocouples.
s. solarimeters.
w. wind speed recorder.

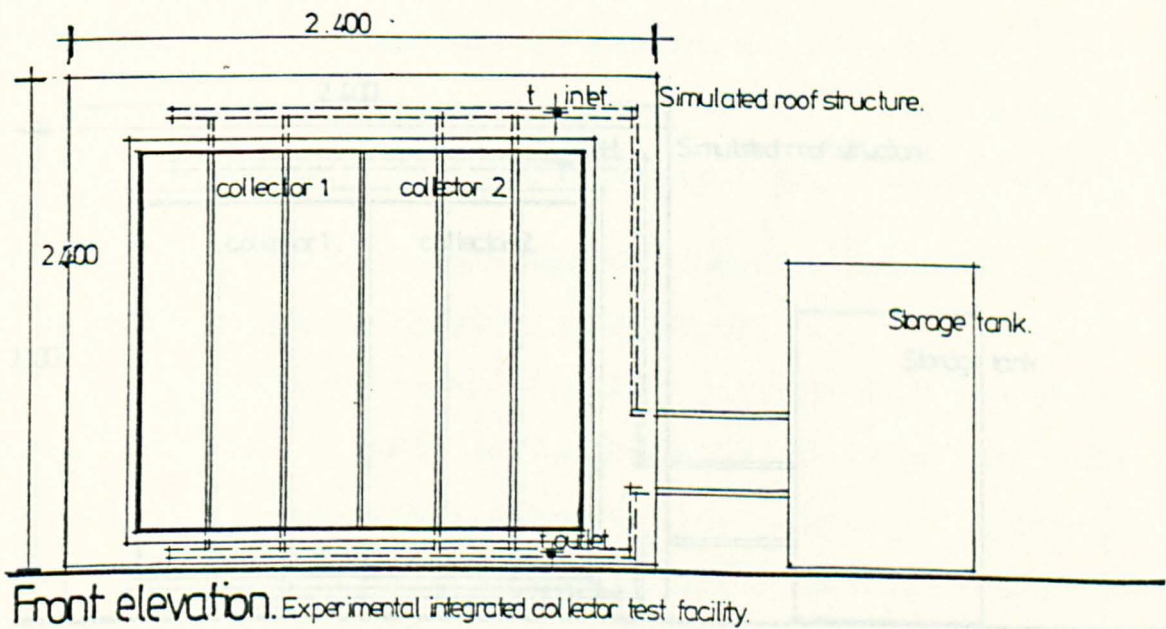
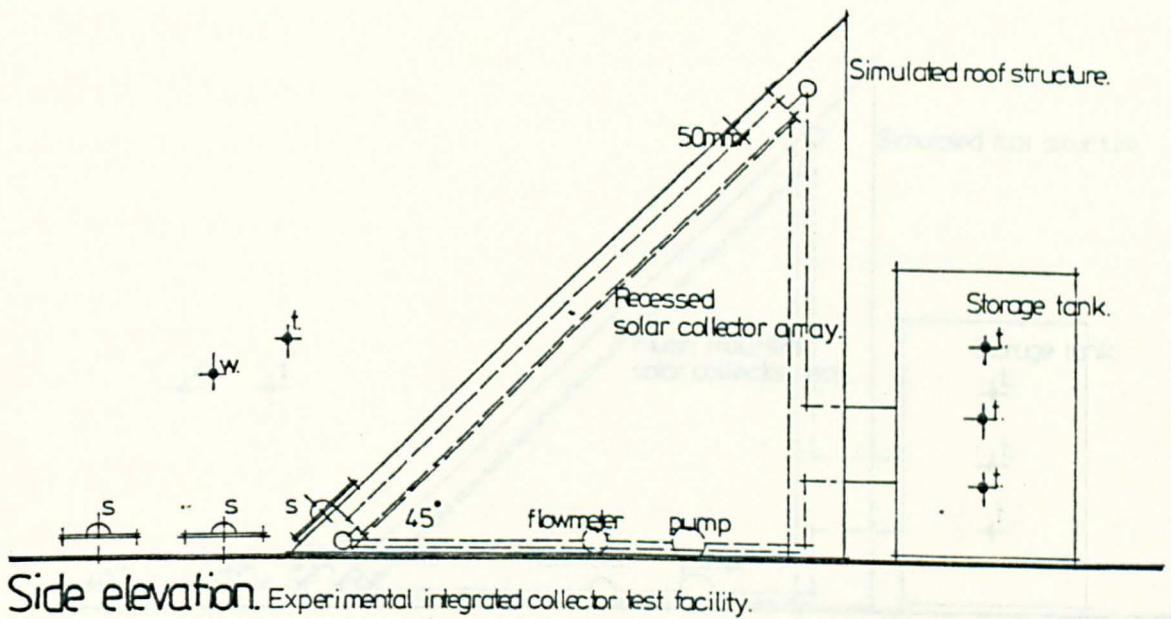


Figure 5.10 Recessed roof-mounted collector test facility.

Key.

- t. position of thermocouples.
- s. solarimeters.
- w. wind speed recorder.

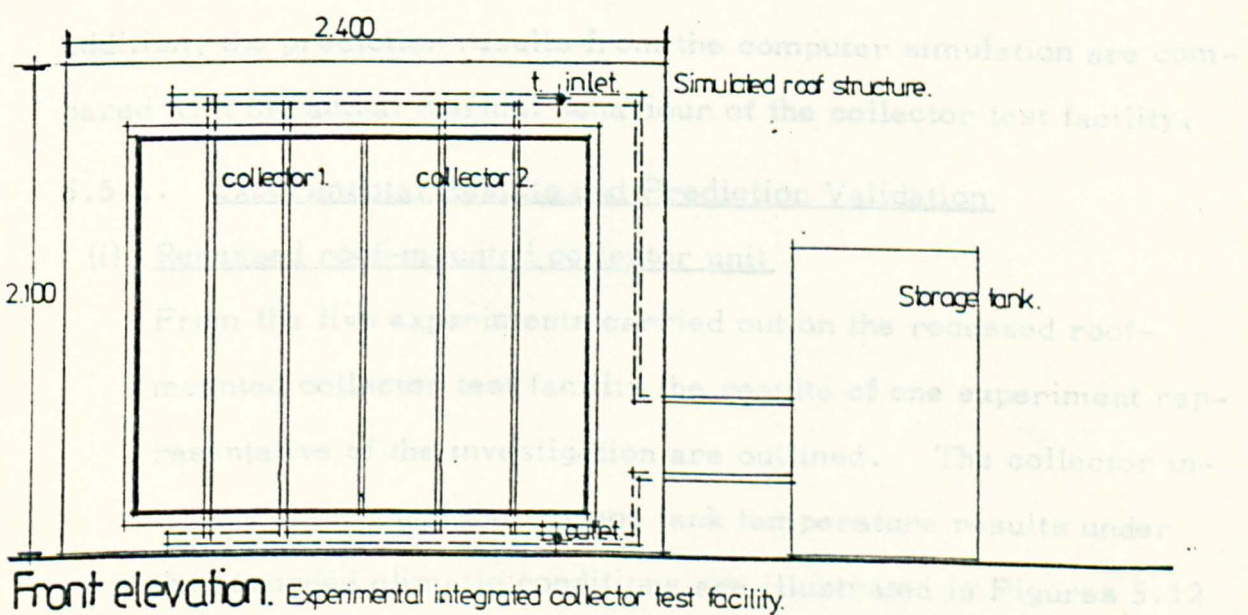
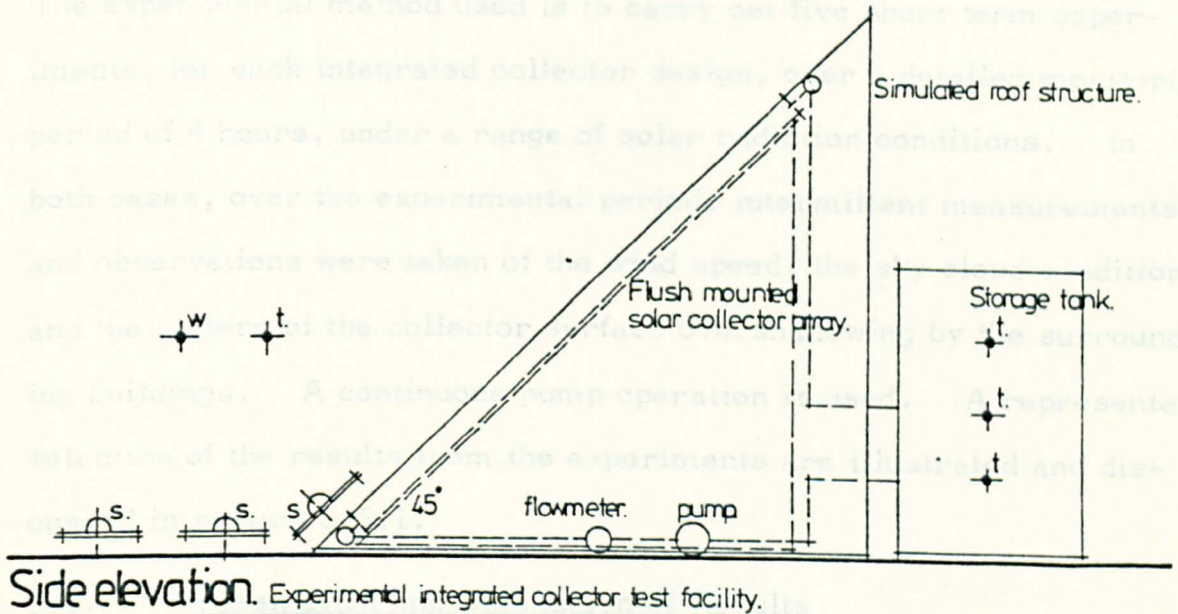


Figure 5.11 Flush roof-mounted collector test facility

as shown in Figure 5.10. This network presents a complete record of the temperature behaviour within the system components, accurate to within $\pm 0.5^{\circ}\text{C}$. Apart from the reallocation of the temperature probes, the previous experiment measurement apparatus was retained as outlined in section 2.4.3, and illustrated in Figure 5.10.

The procedure used to obtain the results from the recessed and the flush-mounted outdoor collector experiments is outlined as follows. The experimental method used is to carry out five short term experiments, for each integrated collector design, over a detailed monitoring period of 4 hours, under a range of solar radiation conditions. In both cases, over the experimental period, intermittent measurements and observations were taken of the wind speed, the sky cloud conditions and the pattern of the collector surface overshadowing by the surrounding buildings. A continuous pump operation is used. A representative selection of the results from the experiments are illustrated and discussed in section 5.5.1.

5.5. Presentation and Discussion of Results

The results from the recessed and the flush-mounted collector installations are discussed and illustrated in section 5.4.1. In addition, the prediction results from the computer simulation are compared with the actual thermal behaviour of the collector test facility.

5.5.1. Experimental Results and Prediction Validation

(i) Recessed roof-mounted collector unit

From the five experiments carried out on the recessed roof-mounted collector test facility the results of one experiment representative of the investigation are outlined. The collector inlet and outlet, and the storage tank temperature results under the recorded climatic conditions are illustrated in Figures 5.12 and 5.13. The collector installation thermal behaviour, the climatic/

Solar radiation on inclined collector plane.

Date of experiment. 27 October 1980. 4 hour experiment.

Experiment time interval.

1 minute.

□—□ experimental results.
○---○ predicted results.

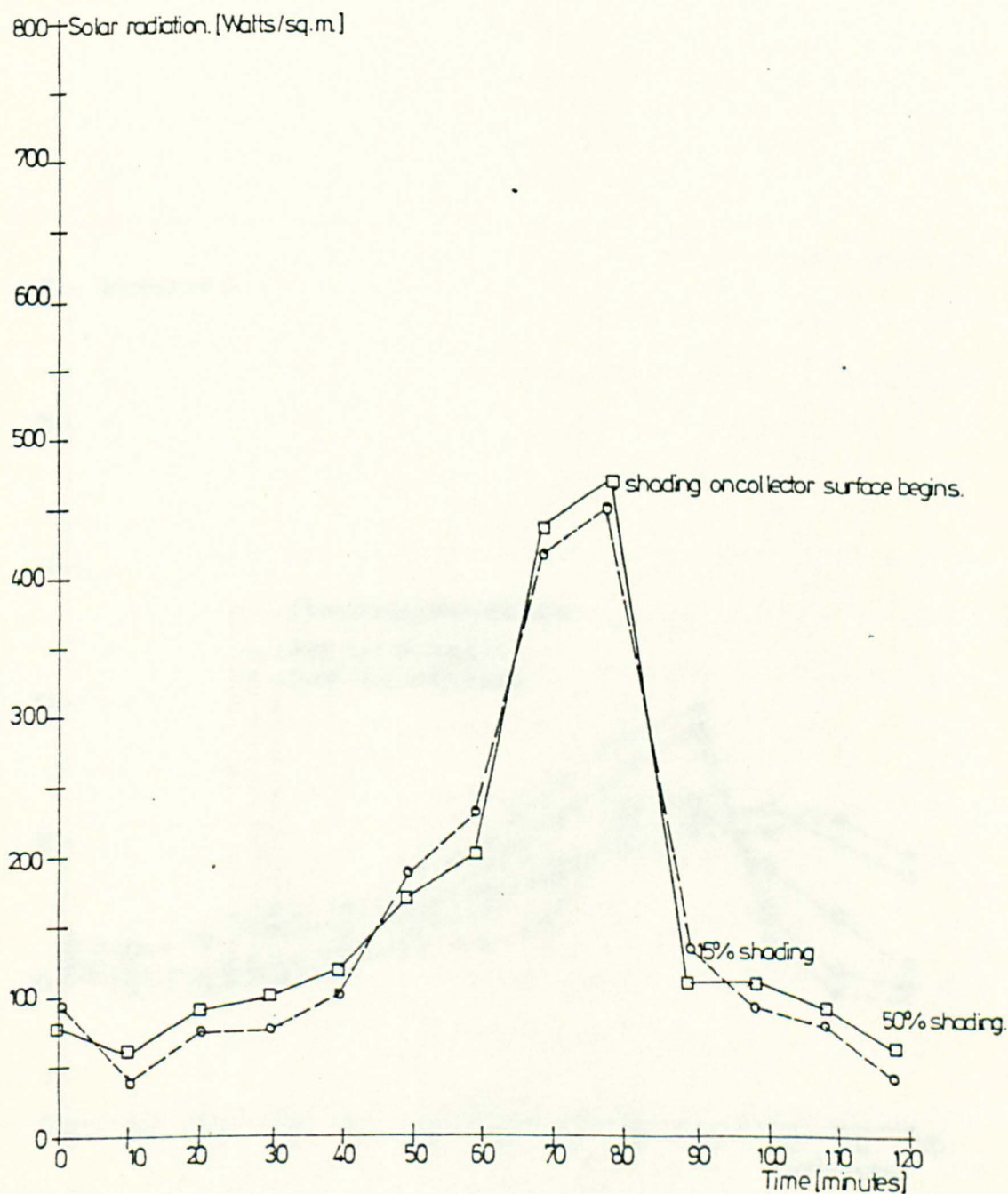


Figure 5.12 Actual vs Predicted solar radiation incident on inclined collector plane.

Mean storage tank and collector inlet and outlet fluid temperatures.

Date of experiment. 27 October 1980. 4 hour experiment.

Experiment time interval.

1 minute.

□—□ experimental results.

○---○ predicted results.

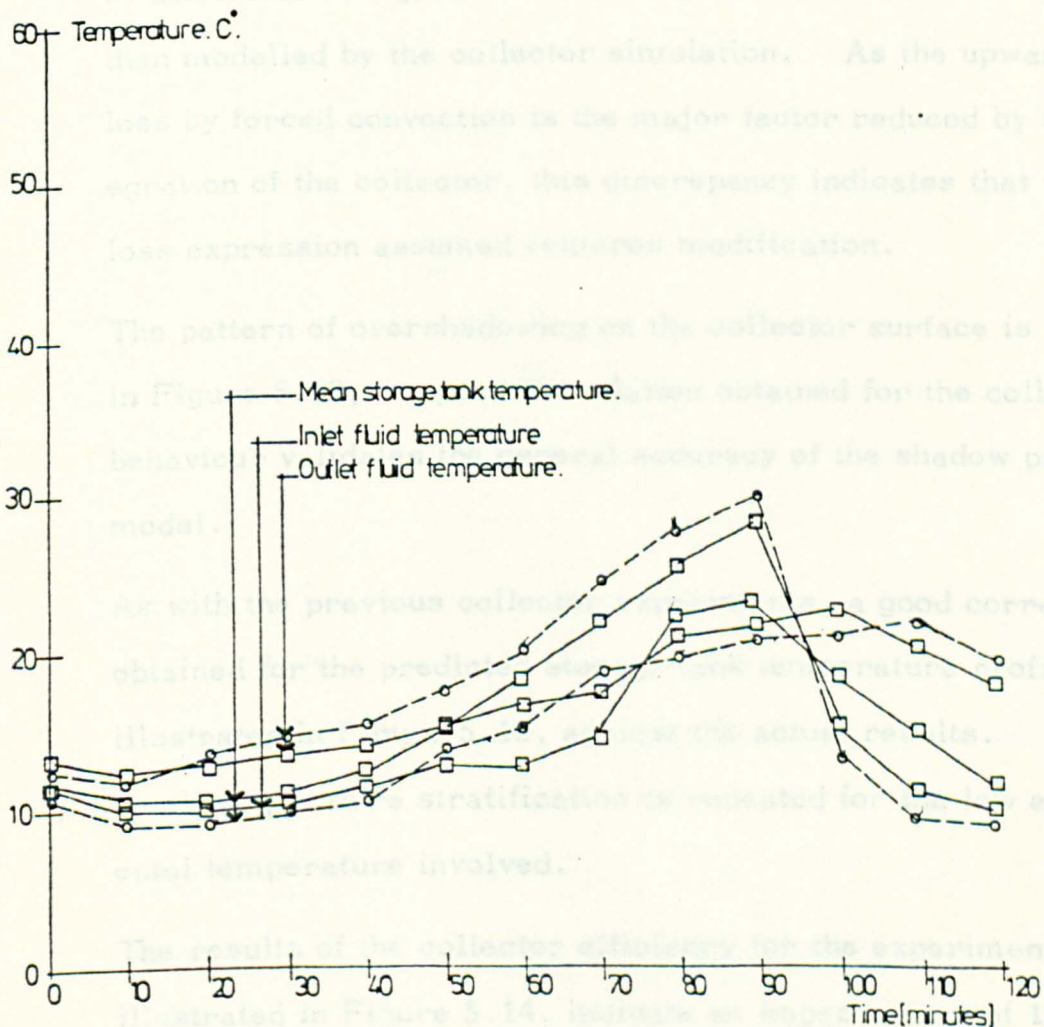


Figure 5.13 Actual vs Predicted mean storage tank and collector fluid temperatures.

climatic conditions and the collector overshadowing patterns were monitored for 4 hours, at 1 minute intervals. In addition, the collector efficiency has been plotted, from the results of the thermal performance, over the experimental period as illustrated in Figure 5.14.

The results predicted from the computer simulation studies are overlaid on the experimental results, as shown in Figures 5.12 - 5.14. A good correlation has been obtained for the predicted collector temperature rise against the actual results, over variable solar radiation conditions. The predicted temperature rise is slightly higher than gained experimentally, by 2 - 3°C. This factor, given the same collector physical parameters, may be attributed to a greater level of upward and rear heat losses than modelled by the collector simulation. As the upward heat loss by forced convection is the major factor reduced by the integration of the collector, this discrepancy indicates that the heat loss expression assumed requires modification.

The pattern of overshadowing on the collector surface is indicated in Figure 5.12, the good correlation obtained for the collector behaviour validates the general accuracy of the shadow prediction model.

As with the previous collector experiments, a good correlation is obtained for the predicted storage tank temperature profile, as illustrated in Figure 5.13, against the actual results. A two level temperature stratification is repeated for the low experimental temperature involved.

The results of the collector efficiency for the experimental period, illustrated in Figure 5.14, indicate an improvement of 15% in the overall performance of the recessed roof-mounted collector unit over/

Collector efficiency.

Date of experiment 27 October 1980. 4 hour experiment.
Experiment time interval.

1 minute.

- predicted results.
- experimental results.

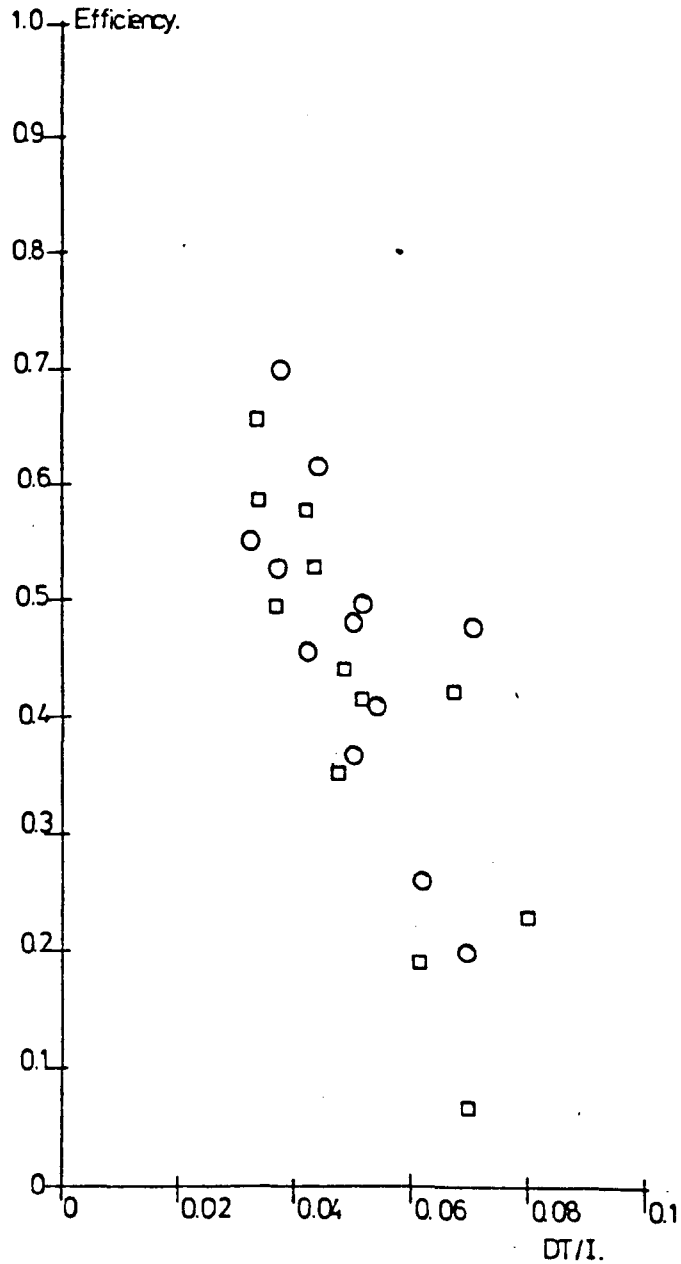


Figure 5.14 Actual vs Predicted collector efficiency.

over the performance of the isolated collector unit installation, illustrated in Figure 2.8.

(ii) Flush roof-mounted collector unit

As with the previous study, five experiments were carried out on the flush roof-mounted collector test facility. The results of one experiment, representative of the investigation is outlined. The collector unit inlet and outlet fluid temperatures, the storage tank temperatures and the recorded climatic conditions are illustrated in Figures 5.15 and 5.16. The collector efficiency has been calculated and plotted in Figure 5.17.

The results predicted from the computer simulation studies are overlayed on the experimental results, as shown in Figures 5.15 - 5.17. A good correlation has been obtained for the predicted collector fluid temperature rise against the actual experimental results, over variable solar radiation conditions, as illustrated in Figure 5.15. As with the results obtained from the recessed collector unit, the predicted temperature rise is higher than gained experimentally, in this case by 2°C .

The pattern of overshadowing on the collector surface is indicated in Figure 5.15. The general accuracy of the shadow prediction model is validated by the good correlation obtained with the actual collector thermal behaviour.

The correlation obtained from the previous storage tank temperature profile against actual experimental results is repeated for this investigation, as illustrated in Figure 5.16.

The results of the collector efficiency for the experimental period, illustrated in Figure 5.17, indicate an improvement of 10 - 15% in the overall performance of the flush-mounted collector unit against the previous isolated collector unit experimental results.

Solar radiation on inclined collector plane.

Date of experiment. 24 November 1980. 4 hour experiment.

Experiment time interval

1 minute.

□—□ experimental results
○---○ predicted results.

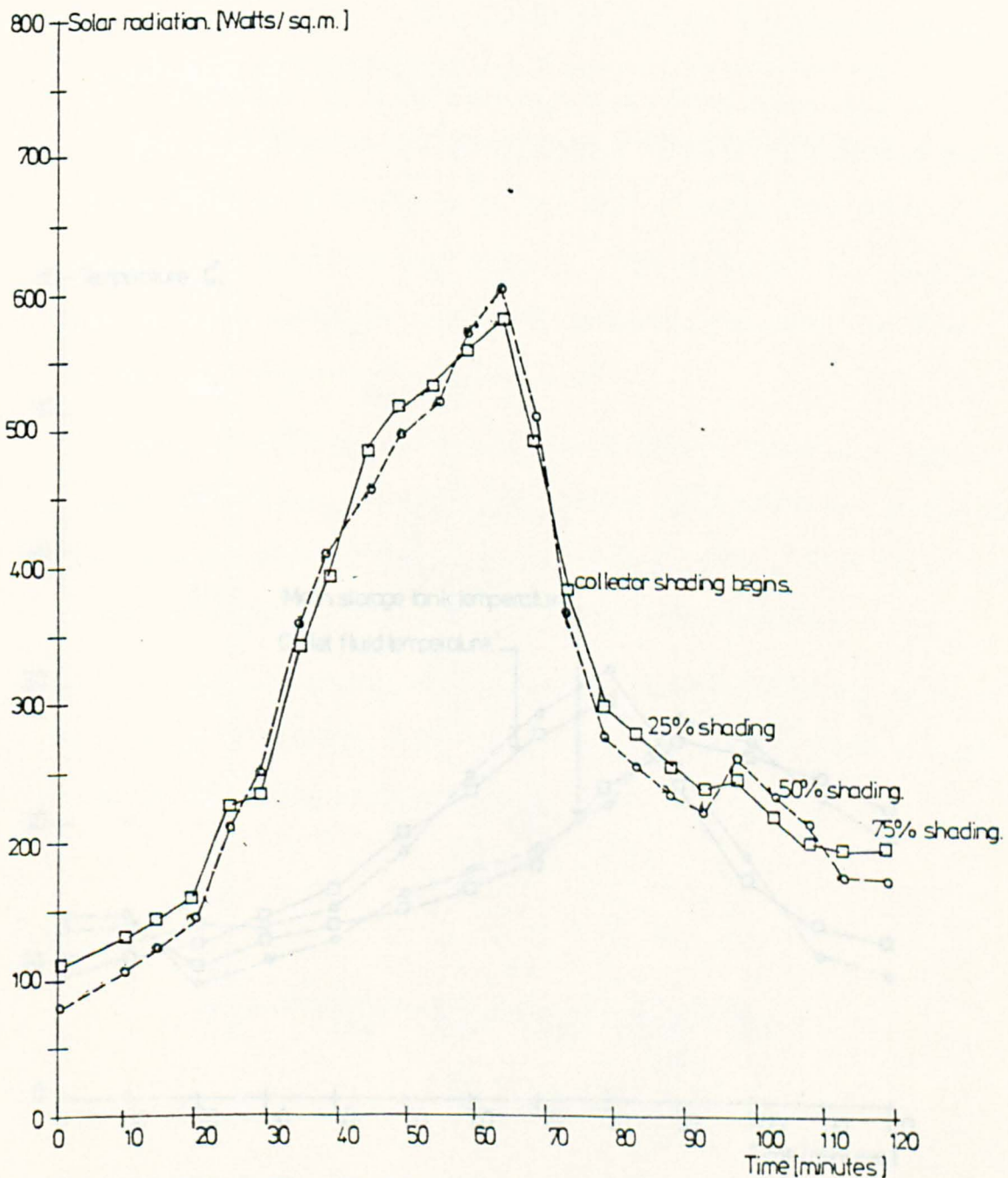


Figure 5.15 Actual vs Predicted solar radiation incident on inclined collector plane.

Mean storage tank and collector outlet fluid temperatures.

Date of experiment. 24 November 1980. 4 hour experiment.

Experiment time interval.

1 minute.

- experimental results.
- predicted results.

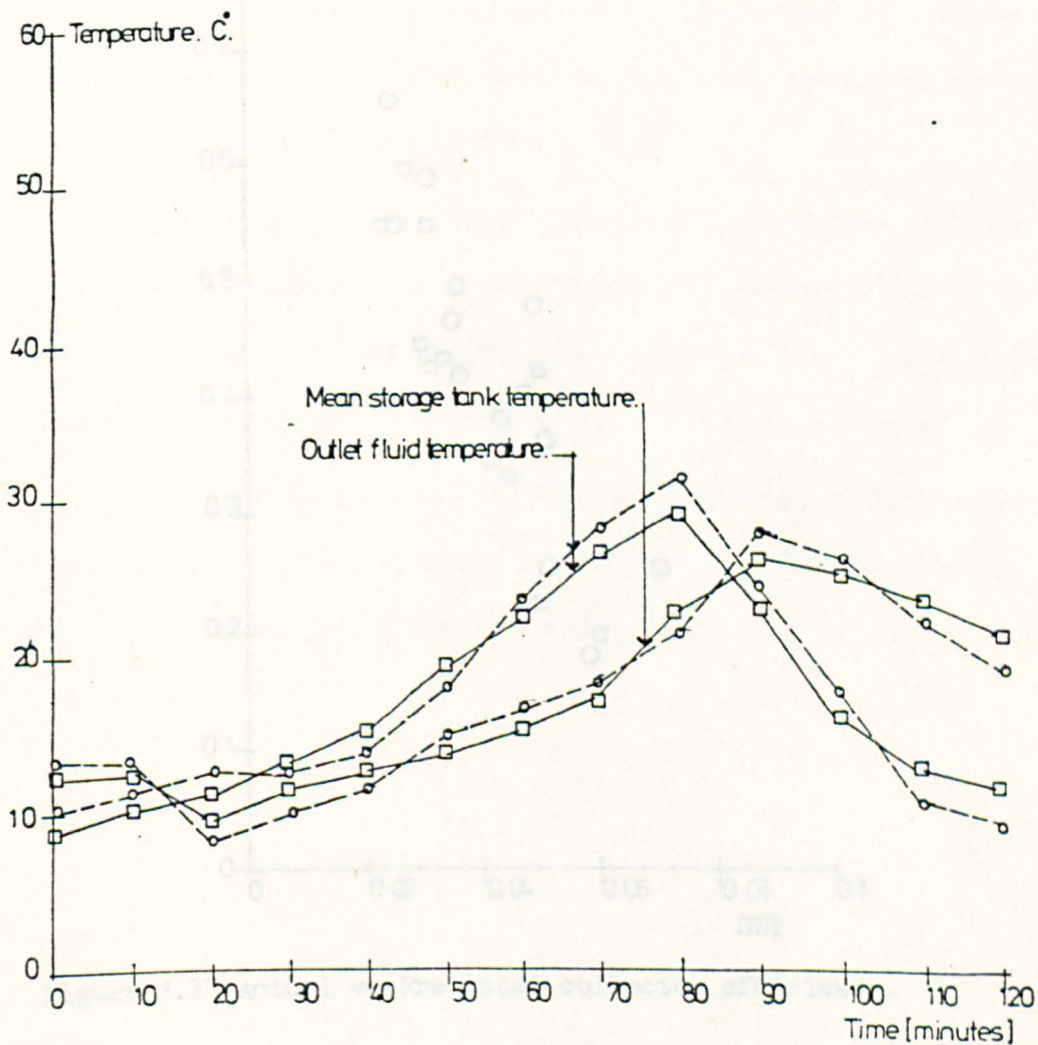


Figure 5.16 Actual vs Predicted mean storage tank and collector fluid temperatures.

Collector efficiency.

Date of experiment. 24 November 1980 4 hour experiment.

Experiment time interval.

1 minute.

□ experimental results.

○ predicted results.

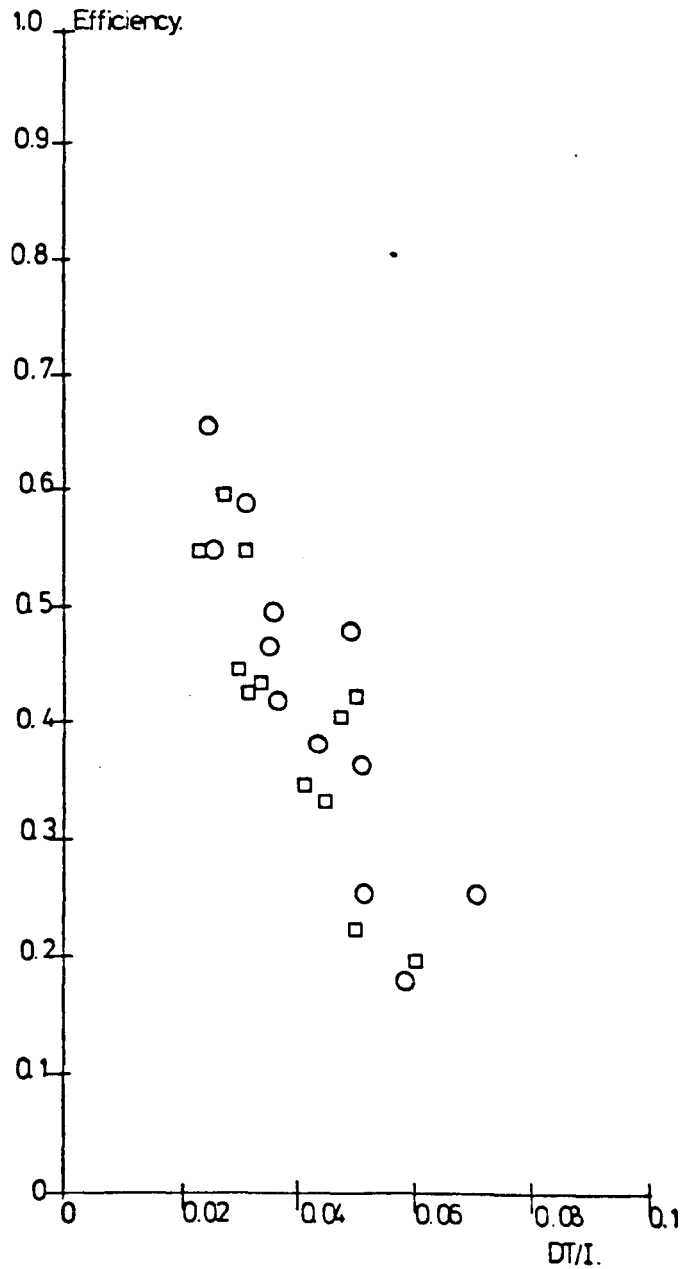


Figure 5.17 Actual vs Predicted collector efficiency.

5.5.2. Summary of Results

The results obtained from the integrated solar collector experiments and the subsequent computer program validation studies can be summarised as follows.

A good correlation has been obtained for the predicted temperature behaviour against the experimental results of the integrated collector unit and the storage tank. This correlation is obtained under variable solar radiation conditions and no hot water draw-off demand from the storage tank. The collector surface was overshadowed during a period of these experiments.

The experimental and the predicted results indicate that the collector efficiency is improved by 10 - 15% with the integration of the collector unit within the roof fabric. The collector efficiency of the three collector installation designs: isolated, recessed and flush-mounted are illustrated in Figure 5.18.

As a consequence, these results illustrate that under exposed climatic conditions, the integration of the solar collector within the roof, reduces the heat losses to the external air. This factor significantly increases the thermal efficiency of the collector.

The general accuracy of the simulation program has been validated, under fluctuating solar radiation and collector shading conditions, by the above series of experiments.

Collector efficiency. Isolated, Recessed and Flush mounted collector units.

- Isolated collector efficiency.
- Recessed collector efficiency.
- + Flush mounted collector efficiency.

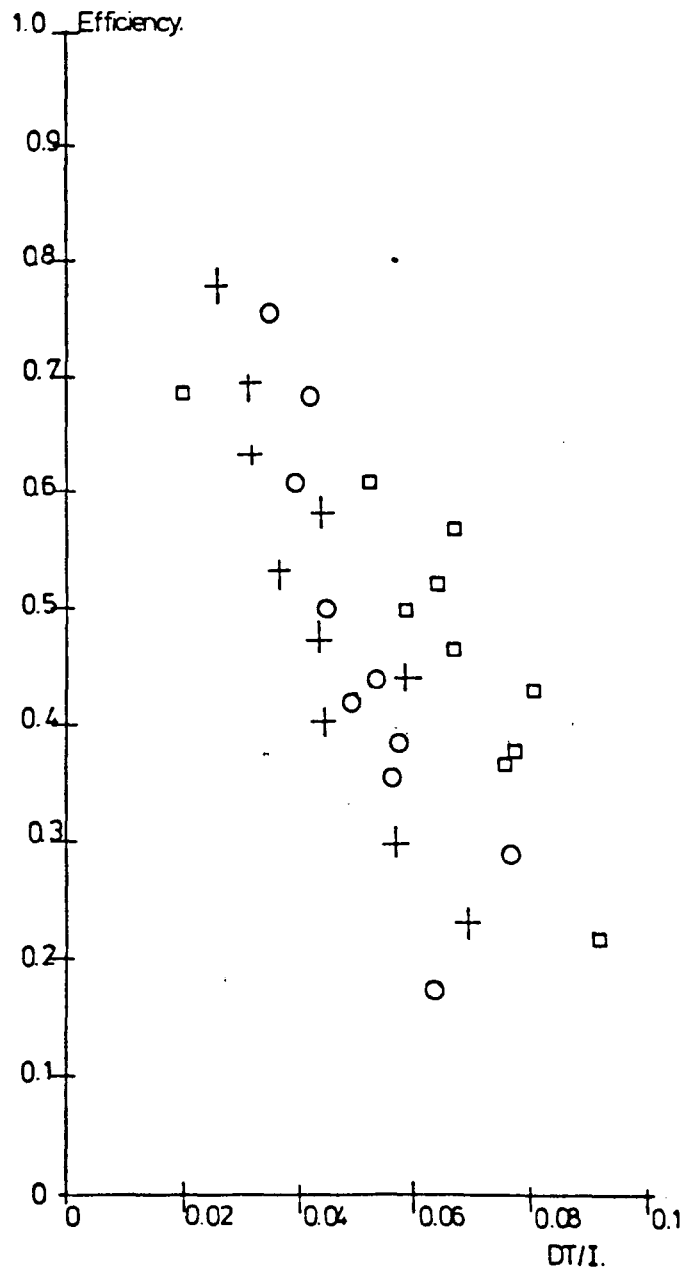


Figure 5.18 Actual collector efficiency - isolated, recessed and flush-mounted collector units.

Section 5

References

1. Saluja, G.S. and Robertson, P., 'Dynamic Thermal Simulation of solar water heating systems under transient climatic conditions'. Proc. ISES Solar World Forum, 1981.
2. Souster, C.G., 'Solar and Surface Geometry'. User Guide to Program SANG, 1977. pp. 1-5.
3. Clarke, J., 'External shading of buildings'. ABACUS Occasional Paper No. 49, 1976. pp. 3-8.
4. Garg, H.P., 'Effect of dirt on transparent covers in flat-plate solar energy collectors'. Solar Energy, 1974. pp. 299-300.
5. Ibid., p. 300.
6. Duffie, J.A. and Beckman, W.A., Solar Energy Thermal Processes. 1974. pp. 156-157.
7. Hottel, H.C. and Woertz, B.B., 'Performance of flat-plate solar heat collectors'. Solar Energy, 1942. p. 101.
8. Clarke, J., 'External shading of buildings'. ABACUS Occasional Paper No. 49, 1976. pp. 6-8.

SECTION 6

CONCLUSIONS AND SUGGESTIONS FOR FURTHER WORK

6.1. Conclusions

The conclusions obtained from the investigation into the dynamic thermal performance of various types of solar heating installations under transient climatic and restricted urban site conditions are summarised as follows.

6.1.1. Dynamic Thermal Simulation of Solar Collector Performance

At present, the thermal performance of the solar collector can be modelled by steady-state or simple dynamic prediction models. The accuracy of these models is limited by the variable nature of solar radiation conditions and the simple modelling of the energy storage processes within the collector unit.

From these previous models, a multi-node network technique has been developed to model the dynamic thermal performance of the solar collector under transient solar radiation conditions prevalent in this climate. The accuracy of the prediction obtained is dependant upon the length of the time increment for the available climatic data, and the complexity of the thermal network chosen. A good correlation has been obtained, within $\pm 5\%$ of actual collector performance, under variable solar radiation conditions.

6.1.2. Dynamic Simulation of Climatic Conditions

The incident solar radiation on an inclined collector surface can be however predicted under clear sky and overcast cloud conditions. At present, no method is available to predict the incident solar radiation under intermittent cloud conditions.

A simple hybrid solar prediction method, has been developed from previous work, to estimate the prevalent cloud conditions and calculate the direct and diffuse solar radiation components on inclined surfaces, from the available measured horizontal radiation data. A good/

good correlation has been obtained against experimental measurements taken under variable solar radiation and cloud conditions.

6.1.3. Dynamic Thermal Simulation of Solar System Performance

The prediction accuracy of present simulation models of solar water heating installations is limited by the variable nature of the solar radiation, system operation and energy usage conditions.

The network technique developed in the collector simulation has been applied to an existing storage tank model. In conjunction with a model of the connecting system pipework, a computer simulation program has been developed to model the dynamic thermal performance of the solar water heating system. A good correlation has been obtained against experimental system performance. At low experimental temperatures, a two level temperature stratification has been found, as compared with the theoretical three levels predicted. This discrepancy has no significant effect on the system performance.

The validation of the system model against the monitored performance of a commercial solar water heating system has achieved an average prediction accuracy of $\pm 10\%$, under fluctuating solar radiation, system operation and hot water draw-off conditions.

6.1.4. Dynamic Thermal Simulation of Integrated Solar Collector Installation Performance

The restricted site conditions in urban locations can significantly reduce the feasibility of solar installations in buildings. No method is currently available to determine the effect of such conditions on collector performance.

The experimental test facility and the computer simulation model have been developed to investigate the effect of collector overshadowing. These studies have demonstrated that shading of the collector surface can/

can significantly reduce the possible useful energy collection of a solar heating system. In addition, a good correlation has been obtained with actual shading profiles on the collector surface.

A possible method of improving the collector performance, by the integration of the collector unit within the roof fabric has been postulated. The results obtained from the experimental investigation of flush and recessed roof-mounted collector constructions have demonstrated an increase of 10 - 15% in the overall collector performance, as compared with an isolated collector unit. This significant increase in performance can be attributed to the reduction of the exposed collector surface area, and the subsequent decrease in the collector heat loss.

6.2. Suggestions for Further Work

6.2.1. Micro-computer applications

The present computer program is operated on expensive main-frame computer and graphic terminal facilities, unsuitable for large scale commercial application. This program could be translated, with minor modifications, into a computer language suitable for use on existing micro-computers. The effect of this modification would be the development of an inexpensive design tool for architects and engineers involved in the dynamic analysis of solar installation performance.

6.2.2. Passive solar building design applications

The present thermal network technique used could be applied to the investigation of the passive utilisation of solar energy in buildings. Such an investigation would involve the development of the present simulation method to incorporate the dynamic thermal processes within solar air collectors and various types of building construction.

APPENDIX 1

DERIVATION OF SOLAR COLLECTOR SYSTEM MODEL

Appendix 1.1.

Derivation of heat transfer and energy storage processes within the solar collector.

The two node capacitance technique, outlined in section 2.1.3, has been developed to form a multi-node simulation method. The collector unit is divided into a series of elemental sections. The internal heat transfer and energy storage processes within each section are modelled by nodes positioned at the collector cover and plate.

The equations describing the heat balance within each elemental section can be expressed as follows:

Heat balance within collector cover

$$\begin{aligned} \text{Energy stored within} &= \text{Solar radiation absorbed} + \text{Net heat gain} \\ \text{cover section} &\quad \text{by cover section} \quad \text{from collector} \\ &\quad \text{plate} \end{aligned}$$
$$C_1 \frac{dT_c}{dt} = S_1 + [h_1 \cdot (T_p - T_c) - h_2 \cdot (T_c - T_a)] \quad (A1.1)$$

Heat balance within collector plate

$$\begin{aligned} \text{Energy stored within} &= \text{Solar radiation absorbed} + \text{Upward heat loss} \\ \text{collector plate} &\quad \text{by collector plate section} \quad \text{from collector} \\ \text{section} &\quad \quad \quad \text{plate to cover} \\ &\quad \quad \quad - \text{Rear and edge heat losses} - \text{Heat transfer} \\ &\quad \quad \quad \text{from collector plate to} \quad \text{from plate to} \\ &\quad \quad \quad \text{external air} \quad \quad \text{circulating fluid} \end{aligned}$$

$$C_2 \frac{dT_p}{dt} = S_2 - h_1 \cdot (T_p - T_c) - U_R \cdot (T_p - T_a) - mC_{p_w} \cdot dT_w \quad (A1.2)$$

The heat transfer coefficients, h_1 , h_2 and U_R can be described as

- (i) the heat transfer from the collector plate to the cover by radiation and convection.

$$h_1 = \left[\sigma \cdot \frac{(T_p^4 - T_c^4)}{1/\epsilon_p + 1/\epsilon_c - 1} + h_c \cdot (T_p - T_c) \right] / (T_p - T_c) \quad (A1.3)$$

- (ii) the heat transfer from the collector cover to the external air by radiation and convection.

$$h_2 = \left[\sigma \cdot \epsilon_c \cdot (T_c^4 - T_a^4) + h_w \cdot (T_c - T_a) \right] / (T_c - T_a) \quad (A1.4)$$

- (iii) the rear and edge heat transfer from the collector plate by conduction to the perimeter of collector unit, and by radiation and conduction to the external air.

$$U_R = F_e \cdot (T_p - T_a) / \left(\frac{d_r}{k_r} + \frac{1}{h_r} \right) \quad (A1.5)$$

The derivation of the energy storage terms C_1 and C_2 within the heat balance equations can be outlined as follows:

- (i) the heat energy stored within the cover section.

The energy stored within the cover section can be assumed to be the product of the thermal capacitance of the cover times the change in the cover temperature over time, expressed in equation form as:

$$C_1 = \rho_c \cdot C_{p_c} \cdot A_s \cdot d_c \quad (A1.6)$$

- (ii) the heat energy stored within the collector plate section.

The energy stored within the collector plate section can be assumed to be the product of the net thermal capacitance of the collector plate section times the change in the mean plate temperature over time, expressed in equation form as:

C_2 = Sum of thermal capacitance of: collector fluid + collector tubes + collector plate + insulation + frame unit.

$$C_2 = [V_w \cdot \rho_w \cdot C_{p_w}] + [V_t \cdot \rho_t \cdot C_{p_t}] + [d_p \cdot A_s \cdot \rho_p \cdot C_{p_p}] + [(A_s + A_p) \cdot d_i \cdot \rho_i \cdot C_{p_i}] + [(A_s + A_p) \cdot d_u \cdot \rho_u \cdot C_{p_u}] \quad (A1.7)$$

The heat balance equations can be further developed by expressing the heat transfer and energy storage processes in terms of the fluid temperature rather than the plate temperature, by inserting the plate efficiency factor F' to obtain:

$$C_1 \cdot \frac{dT_c}{dt} = S_1 + \left[F' \cdot \sigma \cdot \frac{(T_w^4 - T_c^4)}{\frac{1}{\epsilon_p} + \frac{1}{\epsilon_c} - 1} + F' \cdot h_c \cdot (T_w - T_c) \right] - \left[\sigma \cdot \epsilon_c \cdot (T_c^4 - T_a^4) + h_w \cdot (T_c - T_a) \right] \quad (A1.8)$$

$$C_2 \cdot \frac{dT_w}{dt} = S_2 - \left[F' \cdot \sigma \cdot \frac{(T_w^4 - T_c^4)}{\frac{1}{\epsilon_p} + \frac{1}{\epsilon_c} - 1} + F' \cdot h_c \cdot (T_w - T_c) \right] - \left[F' \cdot F_e \cdot \frac{(T_w - T_a)}{\frac{k_r}{d_r} + \frac{1}{h_r}} \right] - m C_{p_w} \cdot dT_w \quad (A1.9)$$

The plate efficiency factor F' relates the actual heat transfer from the collector fluid to the heat transfer from the collector plate, which can be defined as:

$$F' = \frac{h_1}{\frac{1}{h_1} + R_p} \quad (A1.10)$$

similarly, in terms of U_R

$$F' = \frac{U_R}{\frac{1}{U_R} + R_p} \quad (A1.11)$$

where h_1 and U_R are the heat transfer coefficients from the plate to the cover and to the perimeter of the collector unit respectively.

R_p is the heat transfer resistance, from the plate to the tube fluid, for the particular collector plate construction under study.

$$\begin{aligned} \text{Heat transfer from the tube fluid to the plate} &= \text{Heat transfer through the plate} = \text{Heat transfer from the plate through the tube bond} \\ &+ \text{Heat transfer through tube wall} + \text{Heat transfer from tube wall into circulating fluid} \end{aligned}$$

$$R_p = r_p + r_b + r_t + (1/h_t) \quad (A1.12)$$

The heat balance equations (A1.8 and 1.9) can be factorised to a matrix notation to facilitate the numerical solution, and simplified to express the equations, the equations in terms of the new cover and fluid section temperatures T'_c and T'_w .

$$T'_c = T_c + a_{11} - a_{12} \cdot T_c + a_{13} \cdot T_w + a_{14} \cdot T_a \quad (A1.13)$$

$$T'_w = T_w + a_{21} - a_{22} \cdot T_c - a_{23} \cdot T_w + a_{24} \cdot T_a \quad (A1.14)$$

where the matrix notation used can be defined as:

$$a_{11} = \frac{\Delta t \cdot S_1}{C_1}$$

$$a_{21} = \frac{\Delta t \cdot S_2}{C_2}$$

$$a_{12} = \frac{\Delta t}{C_1} \cdot (F \cdot \sigma \cdot \frac{(T_w^2 + T_c^2)(T_w + T_c)}{\frac{1}{ep} + \frac{1}{ec} - 1} + F \cdot h_c) + \frac{\Delta t}{C_1} \cdot (\sigma \cdot ec \cdot (T_c^2 + T_a^2)(T_c + T_a) + h_w)$$

$$a_{22} = \frac{\Delta t}{C_2} \cdot (F \cdot \sigma \cdot \frac{(T_w^2 + T_c^2)(T_w + T_c)}{\frac{1}{ep} + \frac{1}{ec} - 1} + F \cdot h_c)$$

$$a_{23} = \frac{\Delta t}{C_2} \cdot (F \cdot \sigma \cdot \frac{(T_w^2 + T_c^2)(T_w + T_c)}{\frac{1}{ep} + \frac{1}{ec} - 1} + F \cdot h_c) + \frac{\Delta t}{C_2} \cdot \frac{(F \cdot F_e)}{\frac{d_r + 1}{\bar{k}_r} h_r} + \frac{\Delta t \cdot mCp_w}{C_2}$$

$$a_{14} = \frac{\Delta t}{C_1} \cdot (\sigma \cdot ec \cdot (T_c^2 + T_a^2)(T_c + T_a) + h_w)$$

$$a_{24} = \frac{\Delta t}{C_2} \cdot \frac{(F \cdot F_e)}{\frac{d_r + 1}{\bar{k}_r} h_r}$$

Appendix 1.2

Derivation of Solar Radiation Prediction Model

The previous techniques utilised to predict the incident solar radiation on an inclined plane under clear sky and overcast cloud conditions, outlined in section 3.1, have been incorporated to form a hybrid prediction method. This method is described below in equation form, for the calculation of the solar geometry, the incident solar radiation and the solar transmission. The amendments to the previous work and the present work involved are outlined in section 3.2.

(i) Solar geometry

The relative position of the sun and the earth with respect to the celestial sphere, illustrated in Figure 3.1, can be determined by the calculation of the solar azimuth and altitude angles which are expressed in equation form as:

$$\cos \delta = \sin \phi . \sin \delta + \cos \phi . \cos \delta . \cosh \quad (\text{A1.16})$$

$$\sin \alpha = \cos \delta . \sinh / \cos \delta \quad (\text{A1.17})$$

where ϕ is the latitude of the location and h is the hour angle calculated from solar noon. From the principles of spherical geometry, the solar declination δ , in the above equations can be expressed in terms of the longitude of the sun.

$$\sin \delta = \sin \epsilon . \sin \phi \quad (\text{A1.18})$$

where ϵ is the angle between the plane of the ecliptic and the plane of the celestial equator, illustrated in Figure 3.1, and defined as:

$$\epsilon = 23.442^\circ - (3.56^\circ \times 10^{-7}).t \quad (\text{A1.19})$$

The position of the sun on the celestial sphere is determined by the calculation of the longitude of the sun L , as defined as:

$$\begin{aligned} L = & 4.900968 + (3.67474 \times 10^{-7}).t \\ & + (0.033434 - 2.3 \times 10^{-9}.t). \sin g \\ & + 0.000349 \sin 2g + \theta \end{aligned} \quad (\text{A1.20})$$

where g is the mean anomaly of the earth, given by:

$$g = -0.031271 - (4.53963 \times 10^{-7}).t + \theta \quad (A1.21)$$

$$\text{where } \theta = 2\pi t/365.25 \quad (A1.22)$$

and t is the time taken as Greenwich Mean Time.

(ii) Solar radiation on inclined surfaces under actual sky conditions

The transformation of the horizontal total solar radiation under actual conditions to the total solar radiation incident on an inclined surface has been defined in section 3.1.1, as the following expression:

$$\begin{array}{lcl} \text{Total solar radiation} & = & \text{Direct solar} \\ \text{incident on an} & & \text{radiation} \\ \text{inclined surface} & & + \text{Sky diffuse} \\ & & \text{radiation} \\ & & + \text{ground re-} \\ & & \text{flected} \\ & & \text{diffuse} \\ & & \text{radiation} \end{array}$$

this expression is translated into equation form as:

$$I_c = (I_H - I_d).RD + I_d.Rd + I_H.Rs \quad (3.1)$$

In this study, the total horizontal solar radiation is taken to be measured for the specified simulation period. As a result, only the unknown relative quantities of the horizontal direct and sky diffuse solar radiation requires to be predicted for insertion into equation 3.1. The method utilised to determine these components consists of two stages. Firstly, the calculation of the possible horizontal direct and diffuse solar radiation under clear sky and overcast cloud conditions. Secondly, the actual cloud conditions and horizontal radiation components.

(a) The horizontal direct and diffuse solar radiation under clear sky and overcast cloud conditions

The diffuse solar radiation on a horizontal surface under clear sky conditions can be determined by the following expression:

$$I_{dh} = a' + b'\alpha \quad (A1.23)$$

where α is the altitude of the sun at the mid point of that particular period and a' and b' are constants derived by Page ²⁷ for the/

the particular location. For Aberdeen, the values taken for the constants a' and b' are 2 and 5.068 respectively.

As a consequence, the direct beam radiation can be calculated in a similar manner, using a linear relationship between the diffuse and direct horizontal solar radiation under clear sky conditions.

$$I_{bh} = (a_o - I_{dh})/a_1 \quad (A1.24)$$

where I_{bh} is the direct radiation on a horizontal surface and a_o and a_1 are constants derived by Page²⁷ for a particular solar altitude.

The total possible solar radiation on a horizontal surface under clear sky conditions I_{H_c} is subsequently calculated from the sum of the direct and diffuse components.

$$I_{H_c} = I_{bh} + I_{dh} \quad (A1.25)$$

The diffuse solar radiation on a horizontal surface under overcast cloud conditions can be determined by the following expression:

$$I'_{dh} = I_{dh} + 6.17CC \quad (A1.26)$$

where I'_{dh} is the possible diffuse radiation under overcast cloud conditions, and CC is the cloud cover ratio, derived by Kreider and Kreith²⁹.

CC = 0 indicates a clear sky and CC = 10 indicates an overcast cloud sky. As outlined in equation A1.26, the direct radiation component is negligible under overcast cloud conditions.

(b) The actual cloud conditions and horizontal radiation components

As a result of the estimation of the direct, diffuse and total horizontal radiation under clear sky and overcast cloud conditions, the actual cloud conditions and the horizontal radiation components can be determined.

The method developed is to present the clear sky and the overcast cloud conditions as the two parameters of the possible radiation component/

component levels. The difference between the two parameter conditions is described as a linear relationship in the absence of previous work. This relationship is illustrated in Figure 3.1. The actual cloud conditions and the consequent radiation components are determined at the point of intersection of the actual total horizontal and possible total horizontal solar radiation.

As a consequence, the estimated horizontal direct and diffuse solar radiation components, can be transformed to an inclined collector surface. The method involves the application of conversion factors to the horizontal direct, diffuse and total radiation components.

(i) Direct solar radiation on an inclined surface

The direct solar radiation incident on the collector surface can be calculated from the following expression:

$$I_{Dh} = I_D \cdot RD \quad (A1.27)$$

where I_{Dh} is the horizontal direct radiation, and RD is the conversion factor for the transformation of the direct beam radiation from the horizontal to the inclined surface, outlined in section 3.1.1, and expressed as:

$$RD = \frac{\cos(\phi - \beta) \cdot \cos\delta \cdot \cosh + \sin(\phi - \beta) \cdot \sin\delta}{\cos\phi \cdot \cos\delta \cdot \cosh + \sin\phi \cdot \sin\delta} \quad (3.2)$$

(b) Sky diffuse radiation on inclined surface

The diffuse solar radiation incident on the collector surface can be calculated from the following expression:

$$I_{dc} = I_d \cdot Rd \quad (A1.28)$$

where I_d is the horizontal sky diffuse radiation, and Rd is the conversion factor for the transformation of the diffuse radiation from the horizontal to the inclined surface, outlined in section 3.1.1, and expressed as:

$$Rd = (1 + \cos\beta)/2 \quad (3.3)$$

(c) Ground reflected diffuse radiation on inclined surface

The total horizontal radiation reflected from the ground onto the collector surface can be expressed as:

$$I_{dg} = I_H \cdot R_s \quad (A1.29)$$

where I_H is the total horizontal radiation and R_s is the conversion factor for radiation reflected from the ground surface onto the collector plane, outlined in section 3.1.1, and expressed as:

$$R_s = \rho_g \cdot (1 - \cos\beta)/2 \quad (3.4)$$

where ρ_g is the ground reflectance.

(iii) Solar radiation transmission through collector cover

For a single cover collector, the fraction of the incident direct solar radiation which is absorbed by the collector cover and the plate can be expressed by the following equations.

collector cover

$$S_{1D} = I_D \cdot \alpha_c \cdot (1 + \tau_c \cdot \rho_p / (1 - \rho_c \cdot \rho_p)) \quad (3.6)$$

collector plate

$$S_{2D} = I_D \cdot (\tau_c \cdot \alpha_p) / (1 - \rho_c \cdot \rho_p) \quad (3.7)$$

The radiation reflection and absorption losses are dependant upon the angle of incidence of the direct solar radiation and the transmittance of the cover material. The angle of incidence of the direct solar radiation on an inclined surface is calculated from the following expression:

$$\begin{aligned} \cos\theta = & \sin\delta \cdot \sin\phi \cdot \cos\beta - \sin\delta \cdot \cos\phi \cdot \sin\beta \cdot \cos\theta \\ & + \cos\delta \cdot \cos\phi \cdot \cos\beta \cdot \cosh + \cos\delta \cdot \sin\phi \cdot \sin\beta \cdot \cos\theta \cdot \cosh \\ & + \cos\delta \cdot \sin\beta \cdot \sin\theta \cdot \sinh \end{aligned} \quad (A1.30)$$

The transmission and absorption coefficients for direct radiation are dependant upon the solar angle of incidence θ , and are expressed for a glass cover material as follows:

transmittance of glass cover

$$\begin{aligned} \tau_c = & -0.00885 + 2.71235 \cdot \theta - 0.62062 \cdot \theta^2 \\ & - 7.07329 \cdot \theta^3 + 9.75995 \cdot \theta^4 - 3.89922 \cdot \theta^5 \end{aligned} \quad (A1.31)$$

absorption of glass cover

$$\alpha_c = 0.01154 + 0.77674.\theta - 3.94657.\theta^2 + 8.57881.\theta^3 - 8.38135.\theta^4 + 3.01188.\theta^5 \quad (A1.32)$$

As a result, the reflectance of the glass cover can be determined from the above expressions to obtain:

$$\rho_c = 1 - (\tau_c + \alpha_c) \quad (A1.33)$$

The transmission and absorption of diffuse radiation through the collector cover is treated separately with the coefficients constant for a particular material. In this case, the transmittance, and absorption coefficients, τ_c' and α_c' , for a glass cover are taken as 0.796 and 0.056 respectively.

The combined equation for the absorption of the incident direct and diffuse solar radiation on the collector cover and plate can be expressed as:

collector cover

$$S_1 = I_D.\alpha_c.(1 + \tau_c.\rho_p/(1 - \rho_c.\rho_p)) + (I_{dc} + I_{dg})\alpha_c' \quad (A1.34)$$

collector plate

$$S_2 = I_D.(\tau_c.\alpha_p)/(1 - \rho_c.\rho_p) + (I_{dc} + I_{dg}).(\tau_c'.\alpha_p)/(1 - \rho_p.\rho_c') \quad (A1.35)$$

Appendix 1.3

Derivation of heat transfer and energy storage processes within the solar water storage tank.

The multi-node thermal network technique, outlined in section 4.1.1, has been applied to form a three node model of a stratified water storage tank. The storage tank is divided into three sections: the top, middle and bottom sections. The heat transfer and energy processes within each section are modelled by a node positioned within the tank section fluid.

The equations describing the heat balance within each tank section can be expressed as follows:

Heat balance within the top tank section

Energy stored within top tank section = Net energy gain from solar collector - Heat loss from top tank section - Net heat loss taken away by usage demand

$$C_3 \cdot \frac{dT_1}{dt} = F_1 \cdot F_2 \cdot mCp_w \cdot (T_o - T_1) - U_s \cdot (T_1 - T'_a) - F_5 \cdot C_L \cdot (T_1 - T_2) \quad (A1.36)$$

Heat balance within the middle tank section

Energy stored within middle tank section = Net energy gain from solar collector - Heat loss from middle tank section - Net heat loss taken away by usage demand
+ Heat transfer from top tank section to middle tank section

$$C_4 \cdot \frac{dT_2}{dt} = F_1 \cdot F_3 \cdot mCp_w \cdot (T_o - T_2) - U_s \cdot (T_2 - T'_a) - F_5 \cdot C_L \cdot (T_2 - T_3) + F_1 \cdot F_2 \cdot mCp_w (T_1 - T_2) \quad (A1.37)$$

Heat balance within the bottom tank section

Energy stored within bottom tank section = Net energy gain from solar collector - Heat loss from bottom tank section - Net heat loss taken away by usage demand
+ Heat transfer from middle tank section to bottom tank section

$$C_5 \cdot \frac{dT_3}{dt} = F_1 \cdot F_4 \cdot mCp_w \cdot (T_o - T_3) - U_s \cdot (T_3 - T'_a) - F_5 \cdot C_L \cdot (T_3 - T_{mw}) + [F_1 \cdot F_3 \cdot mCp_w \cdot (T_2 - T_3) + F_1 \cdot F_2 \cdot mCp_w \cdot (T_2 - T_3)] \quad (A1.38)$$

The heat transfer coefficient, U_s can be described as:

- (i) The heat transfer from the storage tank fluid to the internal air by conduction.

$$U_s = \frac{1}{\frac{d_{st}}{k_{st}} + \frac{d_{ti}}{k_{ti}}} \quad (A1.39)$$

where T_{st} is the elemental storage tank section temperature.

The derivation of the energy storage terms C_3 , C_4 and C_5 within the heat balance equations can be outlined as follows:

- (ii) The heat energy stored within the storage tank section

The energy stored within the elemental storage tank section can be assumed to be the product of the net thermal capacitance of the tank section times the change in the mean tank section temperature over time, expressed in general equation form as:

$$C_{st} = (V_{st} \cdot \rho_w \cdot C_{p_w}) + (A_{st} \cdot d_{st} \cdot \rho_{st} \cdot C_{p_{st}}) + (A_{st} \cdot d_{si} \cdot \rho_{si} \cdot C_{p_{si}}) \quad (A1.40)$$

where C_{st} is the elemental storage tank section thermal capacitance.

The heat balance equations (A1.36-38) can be factorised to a matrix notation to facilitate the numerical solution, and simplified to express the equations in terms of the new storage tank section fluid temperatures, T'_1 , T'_2 and T'_3 .

$$T'_1 = T_1 + a_{11} \cdot T_o - a_{12} \cdot T_1 + a_{13} \cdot T_2 + a_{15} \cdot T'_a \quad (A1.41)$$

$$T'_2 = T_2 + a_{21} \cdot T_o + a_{22} \cdot T_1 - a_{23} \cdot T_2 + a_{25} \cdot T'_a \quad (A1.42)$$

$$T'_3 = T_3 + a_{31} \cdot T_o + a_{33} \cdot T_2 - a_{34} \cdot T_3 + a_{35} \cdot T'_a + a_{36} \cdot T_{mw} \quad (A1.43)$$

where the matrix notation used can be defined as:

$$a_{11} = \frac{\Delta t \cdot F_1 \cdot F_2 \cdot m C_{p_w}}{C_3} \quad a_{12} = \frac{\Delta t \cdot (F_1 \cdot F_2 \cdot m C_{p_w} + F_5 \cdot C_L + U_s)}{C_3}$$

$$a_{13} = \frac{\Delta t \cdot F_5 \cdot C_L}{C_3} \quad a_{15} = \frac{\Delta t \cdot U_s}{C_3}$$

$$a_{21} = \frac{\Delta t \cdot F_1 \cdot F_3 \cdot mC_{p_w}}{C_4} \quad a_{22} = \frac{\Delta t \cdot F_1 \cdot F_2 \cdot mC_{p_w}}{C_4}$$

$$a_{23} = \frac{\Delta t \cdot (F_1 \cdot F_2 \cdot mC_{p_w} + F_5 \cdot C_L + F_1 \cdot F_3 \cdot mC_{p_w} + U_s)}{C_4}$$

$$a_{25} = \frac{\Delta t \cdot U_s}{C_4} \quad a_{31} = \frac{\Delta t \cdot F_1 \cdot F_4 \cdot mC_{p_w}}{C_5} \quad a_{33} = \frac{\Delta t \cdot (F_1 \cdot F_2 \cdot mC_{p_w} + F_1 \cdot F_3 \cdot mC_{p_w})}{C_5}$$

$$a_{34} = \frac{\Delta t \cdot (F_1 \cdot F_2 \cdot mC_{p_w} + F_1 \cdot F_3 \cdot mC_{p_w} + F_1 \cdot F_4 \cdot mC_{p_w} + F_5 \cdot C_L + U_s)}{C_5}$$

$$a_{35} = \frac{\Delta t \cdot F_5 \cdot C_L}{C_5} \quad a_{36} = \frac{\Delta t \cdot U_s}{C_5}$$

The heat transfer and energy storage processes within the pipework sections between the collector array and the storage tank are modelled by a node positioned within the pipework section fluid. The equation describing the heat balance within the pipework section can be expressed as follows:

Heat balance within the pipework section

Energy stored within the pipework section = Net energy transfer from the storage to collector fluid - Heat loss from the pipework section

$$C_6 \cdot \frac{dT_{pw}}{dt} = F_1 \cdot mC_{p_w} \cdot (T_o - T_{pw}) - U_{pw} \cdot (T_{pw} - T_a) \quad (A1.44)$$

The heat transfer coefficient U_{pw} can be described as:

$$U_{pw} = \frac{1}{\frac{d_{pw}}{k_{pw}} + \frac{d_{pi}}{k_{pi}}} \quad (A1.45)$$

where k_{pw} and k_{pi} are the thermal conductivity of the pipework and the insulation respectively.

The derivation of the energy storage term C_6 within the heat balance equation can be outlined as follows:

C_6 = sum of thermal capacitance of: pipework fluid + pipework wall + pipework insulation

$$C_6 = (V_{pw} \cdot \rho_w \cdot C_{p_w}) + (A_{sp} \cdot d_{pw} \cdot \rho_{pw} \cdot C_{p_{pw}}) + (A_{sp} \cdot d_{pi} \cdot \rho_{pi} \cdot C_{p_{pi}}) \quad (A1.46)$$

where C_6 is the elemental pipework section thermal capacitance.

The heat balance equation A1.44 can be factorised to a matrix notation to facilitate the numerical solution, and simplified to express the equation in terms of the new pipework section fluid temperature

$$T_{pw}' = T_{pw} + a_{11} \cdot T_o - a_{12} \cdot T_{pw} + a_{13} \cdot T_a' \quad (A1.47)$$

where the matrix notation used can be defined as:

$$a_{11} = \frac{\Delta t \cdot F_1 \cdot mCp_w}{C_6} \quad a_{12} = \frac{\Delta t \cdot (F_1 \cdot mCp_w + U_{pw})}{C_6}$$

$$a_{13} = \frac{\Delta t \cdot U_{pw}}{C_6}$$

Appendix 1.4

Overshadowing of the Collector Installation

The method utilised to determine the overshadowing of the collector installation is an amendment of present building and window shadow prediction techniques. The calculation of the effect of the shading of the collector plate by the collector frame unit and by surrounding buildings is outlined as follows:

(i) Shading by the collector frame unit

The method utilised to calculate the shading area caused by the obstruction of the direct radiation by the collector unit frame is defined by the length of the shadow cast, which is expressed as:

$$\text{length of shadow (AC)} = \frac{AB \cdot \sin B}{\sin C} \quad (\text{A1.48})$$

where C is the solar angle of incidence and AB is the dimension of the collector unit. The shadow area is determined by multiplying the shadow length by the dimension perpendicular to the shadow line. This method is illustrated in Figure 5.1.

(ii) Overshadowing by surrounding buildings

The method utilised to determine whether the collector surface is self-shaded is illustrated in Figure 5.2, and outlined as follows.

The collector unit is orientated at an angle of A° and subject to incident solar radiation at a horizontal angle of AH where

$$AH = \text{azimuth angle} - 90^\circ \quad (\text{A1.49})$$

and the angle of orientation ANG, of the collector surface is expressed as:

$$ANG = A^\circ + 180^\circ \quad (\text{A1.50})$$

The conditions for self-shading of the collector surface are: if the angle ANG is less than $(360 - AH)$ or if the angle ANG is greater than $(180 - AH)$. Within these parameters no direct solar radiation is incident on the collector surface.

If the collector surface is not self-shaded, the next stage in the shadow prediction is the calculation of the overshadowing caused by the obstruction of the direct solar radiation by surrounding buildings. The method used is the geometric projection of the solar angle of incidence from the surface corners of surrounding buildings onto the collector. To facilitate the explanation of the method used, a simple example of a flat roof overshadowing is taken. The derivation of the solar projection equations and the shadow projection dimensions, illustrated in Figure 5.2, are expressed as follows.

$$\tan AV = \frac{CB}{AB} \therefore AB = \frac{CB}{\tan AV} \quad (A1.51)$$

where AV is the solar altitude angle

$$\cos(A+AH) = \frac{AD}{AB} \therefore AD = AB \cdot \cos(A+AH) \quad (A1.52)$$

$$\sin(A+AH) = \frac{DB}{AB} \therefore DB = AB \cdot \sin(A+AH) \quad (A1.53)$$

This technique is repeated for each corner of the surfaces of the surrounding buildings. As a result, the shape of the shaded area on the collector surface can be determined.

APPENDIX 2

DESCRIPTION OF COMPUTER PROGRAMS

Appendix 2.1.

SOLAR 7 - Solar Collector System Model

```

SUBROUTINE MOD1
DIMENSION TXT1(3,3),TXT2(3,3),TXT3(3,3),TXT4(3,3),
1 TXT5(3,3),TXT6(3,3),DAT1(6,3),DAT2(3),ST(4),TS1(12),
2 TS2(10),DAT3(10),SS(6),TS3(3),DAT4(2)
DOUBLE PRECISION FILE1
COMMON DAT1,DAT2,ST,TS1,TS2,DAT3,SS,TS3,DAT4
C***COLLECTOR UNIT PHYSICAL PARAMETERS***
DATA TXT1/39H 1. XP-THICKNESS OF ABSORBER PLATE (M):,
1 36H 2. B1-TUBE CENTRE LINE SPACING (M):,
2 37H 3. B2-PROJECTED WIDTH-TUBE BOND (M):,
3 39H 4. D1-DIAMETER OF COLLECTOR TUBES (M):,
4 40H 5. C1-THERMAL CAPACITY OF TUBES(J/M3C):,
5 38H 6. XT-THICKNESS OF TUBE MATERIAL (M):,
6 37H 7. UT-CONDUCTIVITY OF TUBES (W/M.C):,
7 36H 8. EP-EMISSIVITY OF ABSORBER PLATE:/
C***COLLECTOR UNIT PHYSICAL PARAMETERS***
DATA TXT2/40H 1. C2-THERMAL CAPACITY OF PLATE(J/M3C):,
1 40H 2. C3-THERMAL CAPACITY OF COVER(J/M3C):,
2 37H 3. UA-CONDUCTIVITY-ABSORBER (W/M.C):,
3 37H 4. EG-EMISSIVITY OF GLASS COVER (E):,
4 40H 5. UB-CONDUCTIVITY OF TUBE BOND(W/M.C):,
5 37H 6. ABS-ABSORPTIVITY COLLECTOR PLATE:,
6 36H 7. XG-THICKNESS OF GLASS COVER (M):,
7 40H 8. XR-THICKNESS OF REAR INSULATION (M):/
C***COLLECTOR UNIT PHYSICAL PARAMETERS***
DATA TXT3/40H 1. KF-COLLECTOR PLATE CONSTRUCTION (M):,
1 39H 2. C4-THERMAL CAPACITY OF REAR(J/M3C):,
2 40H 3. SP-COLLECTOR/GLASS COVER SPACING(M):,
3 39H 4. UI-CONDUCTIVITY-INSULATION (W/M.C):,
4 36H 5. XF-THICKNESS OF FRAME UNIT (M) :,
5 40H 6. C5-THERMAL CAPACITY OF FRAME(J/M3C):,
6 36H 7. NC-NUMBER OF COLLECTOR SEGMENTS:,
7 39H 8. UF-CONDUCTIVITY-FRAME UNIT (W/M.C):/
C***COLLECTOR UNIT PHYSICAL PARAMETERS***
DATA TXT4/38H 1. NHR-LENGTH OF SIMULATION RUN (HR):,
1 39H 2. TLT-COLLECTOR UNIT TILT ANGLE(DEG):,
2 39H 3. FFR-COLLECTOR FLUID FLOW RATE(L/S):,
3 39H 4. XLC-COLLECTOR UNIT LENGTH (METRES):,
4 38H 5. XWC-COLLECTOR UNIT WIDTH (METRES):,
5 38H 6. XDC-COLLECTOR UNIT DEPTH (METRES):,
6 38H 7. NCU-NUMBER OF COLLECTOR UNITS (N):,
7 39H 8. DT-SIMULATION TIME INCREMENT (MIN):/
C***COLLECTOR UNIT ENVIRONMENTAL PARAMETERS***
DATA TXT5/38H 1. SLT-SITE LATITUDE (DEGREES, N+VE):,
1 39H 2. SLG-SITE LONGITUDE (DEGREES, W+VE):,
2 40H 3. YNO-SIMULATION YEAR NUMBER (EG1979):,
3 39H 4. NMO-SIMULATION MONTH NUMBER (EG02):,
4 36H 5. DST-STARTING DATE OF SIMULATION:,
5 40H 6. NDY-LENGTH OF SIMULATION RUN (DAYS):,
6 38H 7. LIZ-LOCAL INTERNATIONAL ZONE TIME:,
7 40H 8. WZA-COLLECTOR UNIT ORIENTATION(DEG):/
C***STORAGE TANK UNIT PHYSICAL PARAMETERS***
DATA TXT6/39H 1. CTS-TEMPERATURE CONTROL SYSTEM (N):,
1 40H 2. SSV-VOLUME OF SOLAR STORAGE TANK(L):,
2 38H 3. DDT-DRAW-OFF DELIVERY TEMPERATURE:,
3 39H 4. SSD-DIAMETER OF SOLAR STORAGE TANK:,
4 39H 5. SIL-LEVEL OF SYSTEM INSULATION (M):,

```



```

5 39H 6. CPL-LENGTH OF CIRCULATION PIPE (M):,
6 37H 7. CI-COLLECTOR-ROOF INTEGRATION(N):,
7 39H 8. TAH-TYPE OF AUXILIARY HEATING FUEL:/
C***SPECIFY SOLAR COLLECTOR SYSTEM DATA FILENAME***
WRITE(5,1)
1  FORMAT(' TYPE IN THE SOLAR COLLECTOR SYSTEM DATA FILENAME')
E')
    READ(5,2) FILE1
2  FORMAT(A10)
C***TRANSFER DATA FROM SPECIFIED FILE***
OPEN(UNIT=1, DEVICE='DSK', FILE=FILE1)
REWIND 1
READ(1,5)((DAT1(I,J),J=1,8),I=1,6)
5  FORMAT(3F9.4)
CLOSE(UNIT=1, DEVICE='DSK', FILE=FILE1)
C***DATA INPUT SEQUENCE***
WRITE(5,10)
10  FORMAT('H DATA INPUT SEQUENCE-COLLECTOR PARAMETERS. '/')
C***WRITE PARAMETER DATA***
DO 100 K=1,6
  IF(K.EQ.4) CALL NEWPAG
  DO 100 J=1,8
    IF(K.EQ.1) WRITE(5,20)(TXT1(I,J),I=1,8), DAT1(K,J)
    IF(K.EQ.2) WRITE(5,20)(TXT2(I,J),I=1,8), DAT1(K,J)
    IF(K.EQ.3) WRITE(5,20)(TXT3(I,J),I=1,8), DAT1(K,J)
    IF(K.EQ.4) WRITE(5,20)(TXT4(I,J),I=1,8), DAT1(K,J)
    IF(K.EQ.5) WRITE(5,20)(TXT5(I,J),I=1,8), DAT1(K,J)
    IF(K.EQ.6) WRITE(5,20)(TXT6(I,J),I=1,8), DAT1(K,J)
20  FORMAT(8A5, F9.4)
100 CONTINUE
RETURN
C***DATA INPUT CHECK***
ENTRY CHECK1
CALL NEWPAG
DO 200 K=1,6
  IF(K.EQ.4) CALL WAIT1
  IF(K.EQ.4) CALL NEWPAG
  DO 200 J=1,8
    IF(K.EQ.1) WRITE(5,30)(TXT1(I,J),I=1,8), DAT1(K,J)
    IF(K.EQ.2) WRITE(5,30)(TXT2(I,J),I=1,8), DAT1(K,J)
    IF(K.EQ.3) WRITE(5,30)(TXT3(I,J),I=1,8), DAT1(K,J)
    IF(K.EQ.4) WRITE(5,30)(TXT4(I,J),I=1,8), DAT1(K,J)
    IF(K.EQ.5) WRITE(5,30)(TXT5(I,J),I=1,8), DAT1(K,J)
    IF(K.EQ.6) WRITE(5,30)(TXT6(I,J),I=1,8), DAT1(K,J)
30  FORMAT(8A5, F9.4)
200 CONTINUE
RETURN
C***ALTER PARAMETER DATA***
ENTRY ALTER1(N)
WRITE(5,40)
40  FORMAT('H HOW MANY PARAMETERS ARE TO BE CHANGED: '/')
READ(5,50) M
50  FORMAT(I)
DO 300 L=1,M
  WRITE(5,60)
60  FORMAT('H TYPE IN THE PARAMETER NUMBER AND ITS NEW
    1 VALUE: '/')
  READ(5,70) NP, PV

```



```

70      FORMAT(1,F)
      DAT1(J,NP)=PV
      IF(N.EQ.1)WRITE(5,80)(TXT1(1,NP),I=1,8),DAT1(J,NP)
      IF(N.EQ.2)WRITE(5,80)(TXT2(1,NP),I=1,8),DAT1(J,NP)
      IF(N.EQ.3)WRITE(5,80)(TXT3(1,NP),I=1,8),DAT1(J,NP)
      IF(N.EQ.4)WRITE(5,80)(TXT4(1,NP),I=1,8),DAT1(J,NP)
      IF(N.EQ.5)WRITE(5,80)(TXT5(1,NP),I=1,8),DAT1(J,NP)
      IF(N.EQ.6)WRITE(5,80)(TXT6(1,NP),I=1,8),DAT1(J,NP)
80      FORMAT(8A5,F9.4)
300     CONTINUE
      RETURN
      END

C
C*****
C***THE FUNCTION OF THE SUBROUTINE NUSELT IS TO CALCULATE*
C***THE THERMO PHYSICAL PROPERTIES OF THE HEAT TRANSFER***
C***FLUID. FROM THE TABULATED PHYSICAL DATA OF THE*****
C***FLUID FOR VARIOUS TEMPERATURES, STORED WITHIN THE*****
C***ROUTINE ARRAYS, THE PRANDLT, REYNOLD'S AND NUSSELT****
C***NUMBERS, CONDUCTIVITY, VISCOSITY AND DENSITY ARE*****
C***CALCULATED TO DETERMINE THE FLUID CONVECTIVE HEAT*****
C***TRANSFER COEFFICIENT, HC.*****
C
      SUBROUTINE NUSELT(TEMP,VELH,HC)
      DIMENSION DAT1(6,8),PR(6),CO(6),VI(7),DE(6),
      1 DAT2(8),ST(4),TS1(10),TS2(10),DAT3(10),SS(6),TS3(3),
      2 DAT4(2)
      COMMON DAT1,DAT2,ST,TS1,TS2,DAT3,SS,TS3,DAT4
      DATA PR/13.60,7.02,4.34,3.02,2.22,1.74/
C***THERMAL CONDUCTIVITY OF WATER***
      DATA CO/0.55,0.60,0.63,0.65,0.67,0.68/
C***FLUID VISCOSITY***
      DATA VI/17.90,9.80,6.82,4.71,3.47,2.67,2.30/
C***FLUID DENSITY***
      DATA DE/1002.28,1000.52,994.59,985.46,974.03,960.63/
      XLC=DAT1(4,4)
      DI=DAT1(1,4)
      FFR=DAT1(4,3)
      XLC=DAT1(4,4)
      XWC=DAT1(4,5)
      ACU=DAT1(4,7)
      KT=IFIX(TEMP)
      CA=XLC*XWC*ACU
      FLOW=DAT2(6)
      NFLOW=IFIX(FLOW)
      IF(NFLOW.EQ.0)GO TO 300
C***DETERMINE THERMOPHYSICAL PROPERTIES OF FLUID***
      IT1=-20
      IT2=0
      DO 100 I=1,6
      IT1=IT1+20
      IT2=IT2+20
      J=I
      IF(KT.GE.IT1.AND.KT.LT.IT2)GO TO 200
100     CONTINUE
200     PRILT=PR(J)
      CONDY=CO(J)

```



```

      VISCY=VI(J)*2.0221
      UW=VI(J+1)*0.0201
      DENSY=DE(J)
C***CALCULATE REYNOLDS NUMBER***
      R=D1/2.0
      A=3.14*R*R
      P=2.0*3.14*R
      VEL=VELH/3600.0
C***HYDRAULIC DIAMETER***
      HD=(4.0*A)/P
      RE=(DENSY*HD*VEL)/VISCY
C***CALCULATE NUSSELT NUMBER***
      C=((D1/XLC)**0.33)*((VISCY/UW)**0.14)
      FNU=1.86*(RE**0.33)*(PRDLT**0.33)*C
C***HEAT TRANSFER COEFFICIENT OF FLUID***
      HC=(FNU*CONDY)/HD
      GO TO 400
300    HC=20.0
400    RETURN
      END
C
C      FUNCTION CPRO(TEMP)
      DIMENSION DE(6),CA(6)
C***FLUID DENSITY***
      DATA DE/1002.28,1000.52,994.59,985.46,974.03,960.63/
C***SPECIFIC HEAT CAPACITY OF FLUID***
      DATA CA/4.22,3*4.18,4.20,4.22/
      KT=IFIX(TEMP)
C***DETERMINE THERMOPHYSICAL PROPERTIES OF FLUID***
      IT1=-20
      IT2=0
      DO 100 I=1,6
      IT1=IT1+20
      IT2=IT2+20
      J=I
      IF(KT.GE.IT1.AND.KT.LT.IT2)GO TO 200
100    CONTINUE
200    DENSY=DE(J)
      CAPCY=CA(J)
      CPRO=DENSY*CAPCY*1000.0
      RETURN
      END
C
C      SUBROUTINE MOD2(FR)
      DIMENSION DAT1(6,8),DAT2(8),ST(4),TS1(10),TS2(10),
      1 DAT3(10),SS(6),TS3(3),DAT4(2)
      COMMON DAT1,DAT2,ST,TS1,TS2,DAT3,SS,TS3,DAT4
C
C
C
C      REAL MIDS
C***INITIALISE COLLECTOR AND SYSTEM PHYSICAL PARAMETERS***
      XP=DAT1(1,1)
      B1=DAT1(1,2)

```

```

B2=DAT1(1,3)
D1=DAT1(1,4)
C1=DAT1(1,5)*1000.0
XT=DAT1(1,6)
UT=DAT1(1,7)
EP=DAT1(1,8)

C
C2=DAT1(2,1)*1000.0
C3=DAT1(2,2)*1000.0
UA=DAT1(2,3)
EG=DAT1(2,4)
UBT=DAT1(2,5)
ABS=DAT1(2,6)
XG=DAT1(2,7)
XR=DAT1(2,8)

C
KF=IFIX(DAT1(3,1))
C4=DAT1(3,2)*1000.0
SPACP=DAT1(3,3)
UI=DAT1(3,4)
XF=DAT1(3,5)
C5=DAT1(3,6)*1000.0
NC=IFIX(DAT1(3,7))
UF=DAT1(3,8)

C
TLT=DAT1(4,2)
FFR=DAT1(4,3)
XLC=DAT1(4,4)
XWC=DAT1(4,5)
XDC=DAT1(4,6)
ACU=DAT1(4,7)
DT=1.0/DAT1(4,8)

C
ITC=IFIX(DAT1(6,1))
SSV=DAT1(6,2)/1000.0
HDR=DAT1(6,3)
SSD=DAT1(6,4)
SIL=DAT1(6,5)
CPL=DAT1(6,6)
CC=DAT1(6,7)

C***CALCULATE STORAGE TANK SEGMENT AREA***
PI=3.141593
RTANK=SSD/2.0
ATOP=PI*RTANK*RTANK
SSH=SSV/ATOP
TOPS=ATOP+2.0*PI*RTANK*((SSH/3.0)+RTANK)
MIDS=2.0*PI*RTANK*((SSH/3.0)+RTANK)
BOTS=TOPS

C***COLLECTOR SEGMENT AREA***
CS=DAT1(3,7)
ACA=XLC*XWC*ACU

C***FLUID MASS FLOWRATE***
VOL=(FFR*ACA*3600.0)/1000.0
CA=(XLC*XWC*ACU)/CS

C***COLLECTOR SEGMENT PERIMETER AREA***
PA=2.0*XDC*(XLC/CS)+2.0*XDC*(XWC/CS)

C***THERMAL CAPACITY OF SEGMENT COMPONENTS***

```



```

CI=XF*CA*C4
CP=CA*XP*C2
TR=D1/2.0
TRO=(D1+0.002)/2.0
CT=(ABS(XWC/B1))*(XLC/CS)*ACU*C1*PI*((TRO*TRO)-(TR*TR))
CF=(CA+PA)*XF*C5
CG=CA*XC*C3
C***CALCULATE CONNECTING PIPEWORK AREA AND CAPACITANCE***
APIPE=2.0*PI*0.007*(CPL+0.007)
CPIPE=CPL*C1*PI*((0.008*0.008)-(0.007*0.007))
C***CALCULATE REAR HEAT LOSS COEFFICIENT***
IC=IFIX(CC)
IF(IC.EQ.0)HB=23.0
IF(IC.EQ.1)HB=14.0
IF(IC.EQ.2)HB=9.5
C***CALCULATE COLLECTOR COMPONENT THERMAL RESISTANCES***
RT=XT/UT
BC=(UBT*B2)/0.001
RB=1.0/BC
RI=XR/UI
RFR=XF/UF
FE=0.6
C***EMISSIVITY FACTOR***
E=(1.0/EP)+(1.0/EG)-1.0
C***VOLUME OF FLUID WITHIN SEGMENT***
NT=IFIX((XWC/B1))
TN=FLOAT(NT)
VOLW=TN*(XLC/CS)*PI*TR*TR*ACU
C***VOLUME OF FLUID WITHIN COLLECTOR CIRCUIT***
VOLC1=((TN*XLC*PI*TR*TR)+(XWC*2.0*PI*TR*TR))*ACU
C***VOLUME OF FLUID WITHIN CONNECTING PIPEWORK***
VOLC2=(CPL+SSH)*PI*0.007*0.007
C***VOLUME OF FLUID WITHIN SOLAR CIRCUIT***
VOLC=VOLC1+VOLC2
C***FLOW REVOLUTIONS THROUGH COLLECTOR PER HOUR***
SPL=((TN*XLC)+2.0*XWC)*ACU+CPL+SSH
C***AVERAGE FLOW VELOCITY THROUGH COLLECTOR PER HOUR***
VEL=(VOL/VOLC)*SPL
C***FLOW REVOLUTIONS AROUND SOLAR CIRCUIT PER HOUR***
FF=VOL/VOLC
FR=FLOAT(IFIX(FF))
C***CALCULATE THE CORRECTED REAR HEAT LOSS COEFFICIENT***
RB1=RI+RFR
RB2=1.0/HB
FD1=0.93*((XR/XLC)+(XR/XWC))
FD2=0.175*(XR/XLC)*(XR/XWC)
UB=1.0/((RB1+RB2)*(1.0+FD1+FD2))
C***THERMAL CAPACITANCE OF SEGMENT 1***
DAT2(1)=CG
C
    RETURN
C
    ENTRY MOD2BC(VL DOV,HRAD)
C***CALCULATION ROUTINE OF VARIABLES***
T1=ST(1)
T2=ST(2)
TA=ST(4)

```



```

TOUT=SS(1)
T3=SS(2)
T4=SS(3)
T5=SS(4)
TE=SS(5)
C***CALCULATE THE FORCED CONVECTION LOSS COEFFICIENT***
HW=5.8+4.1*VM
C***CALCULATE THE UPWARD HEAT LOSS COEFFICIENT***
T1K=T1+273.0
T2K=T2+273.0
TAK=TA+273.0
SBC=5.669E-8
T1KT=(T1K*T1K+TAK*TAK)*(T1K+TAK)
T2KT=(T2K*T2K+T1K*T1K)*(T2K+T1K)
U1=(SBC*T1KT*CA)+HW*CA
CALL MOD5(HP)
RAD=(SBC*T2KT)/E
C***CALCULATE THERMAL CAPACITANCE OF SEGMENT 2 ***
IF(KF.EQ.1.OR.KF.EQ.2)GO TO 100
IF(KF.EQ.3)GO TO 200
C***COLLECTOR TUBES ABOVE OR BELOW PLATE***
100 CALL NUSELT(T2,VEL,HC)
CW=VOLW*CPRO(T2)
RF=(1.0/(HP+RAD+UB))*XLC*(FE*(B1-B2)+B2)
R1=1.0/RF
R2=1.0/(RF+RB+RT+(1.0/HC))
R3=HC
R4=1.0/((1.0/HC)+RT)
R5=1.0/(RF+R1)
R6=1.0/(RF+R1+RFR)
TCS2=CW+CP*(R1/R2)+CT*(R3/R4)+C1*(R5/R2)
1 +CF*(R6/R2)
DAT2(2)=TCS2
GO TO 300
C***COLLECTOR TUBES INTEGRAL WITH PLATE ***
200 CALL NUSELT(T2,VEL,HC)
CW=VOLW*CPRO(T2)
RF=(1.0/(HP+RAD+UB))*XLC*(FE*(B1-B2)+B2)
R1=1.0/RF
R2=1.0/(RF+RB+RT+(1.0/HC))
R3=HC
R4=1.0/((1.0/HC)+RT)
R5=1.0/(RF+R1)
R6=1.0/(RF+R1+RFR)
TCS2=CW+CP*(R1/R2)+CT*(R3/R4)+C1*(R5/R2)
1 +CF*(R6/R2)
DAT2(2)=TCS2
300 CONTINUE
C***CALCULATE UPWARD HEAT TRANSFER RATE FROM SEGMENT 1 ***
DAT2(3)=U1*3600.0
C***UPWARD HEAT TRANSFER RATE FROM SEGMENT 2 ***
U2=HP*(R1/R2)*CA+RAD*(R1/R2)*CA
DAT2(4)=U2*3600.0
C***DOWNWARD HEAT TRANSFER RATE FROM SEGMENT 2***
DAT2(5)=UB*(R1/R2)*CA*3600.0
C***CALCULATE THE THERMAL CAPACITANCE OF CONNECTING PIPEWORK***
CPIPE1=(CPL*PI*0.007*0.007*CPRO(T3))*FR+CPIPE*(R3/R4)

```



```

CPIPE2=(CPL*PI*0.007*0.007*CPR0(T5))*FR+CPIPE*(R3/R4)
DAT4(1)=CPIPE*(R3/R4)+VOLC2*CPR0(T5)
DAT4(1)=CPIPE1
C***CALCULATE THE THERMAL CAPACITANCE OF STORAGE TANK SEGMENTS**
CTANK1=(SSV/3.0)*CPR0(T3)+TOPS*XT*C1*(R3/R4)
CTANK2=(SSV/3.0)*CPR0(T4)+MIDS*XT*C1*(R3/R4)
CTANK3=(SSV/3.0)*CPR0(T5)+BOTS*XT*C1*(R3/R4)
DAT3(1)=CTANK1
DAT3(2)=CTANK2
DAT3(3)=CTANK3
C***DETERMINE PUMP AND STORAGE TANK CONTROL FUNCTIONS***
C***OPTION 0 INDOOR TEST RIG HEAT LOSS EXPERIMENT***
IF(ITC.EQ.0)GO TO 310
GO TO 320
C***CONSTANT PUMP FLOW ON***
310 F1=1.0
C***COLLECTOR FLOW/STORAGE TANK FUNCTION***
F2=0.0
F3=0.75
F4=0.0
GO TO 330
C***OPTION 1 DIFFERENTIAL TEMPERATURE CONTROL***
320 F1=0.0
IF(ITC.EQ.1.AND.TOUT.GE.(T5+1.0))F1=1.0
IF(HRAD.LT.10.0)F1=0.0
C***OPTION 2 SET TEMPERATURE CONTROL***
C***TEMPERATURE SETTING : 20 DEG.C.***
IF(ITC.EQ.2.AND.TOUT.GE.20.0)F1=1.0
C***OPTION 3 OUTDOOR TEST RIG EXPERIMENTS***
IF(ITC.EQ.3)F1=1.0
C***STORAGE TANK FUNCTIONS***
F2=0.0
IF(TOUT.GE.T3)F2=1.0
F3=0.0
IF(TOUT.GE.T4.AND.TOUT.LT.T3)F3=1.0
F4=0.0
IF(TOUT.GE.T5.AND.TOUT.LT.T4)F4=1.0
330 CONTINUE
C***CALCULATE THE HEAT TRANSFER FROM THE STORAGE TANK***
IF(IFIX(100.0*SIL).EQ.0)GO TO 350
RS1=(XT/UT)+(SIL/0.033)
GO TO 375
350 RS1=XT/UT
375 U4A4=(1.0/RS1)*TOPS
U5A5=(1.0/RS1)*MIDS
U6A6=(1.0/RS1)*BOTS
DAT3(4)=U4A4*3600.0
DAT3(5)=U5A5*3600.0
DAT3(6)=U6A6*3600.0
U7A7=(1.0/((XT/UT)+0.1))*APIPE
DAT4(2)=U7A7*3600.0
C***THERMAL CAPACITANCE OF COLLECTOR FLUID MASS FLOW***
CWF=VOL*CPR0(T2)
C***ENERGY CONVECTED OUT OF SEGMENT***
FR1=2.0*CWF
FRT=CWF
DAT2(6)=FR1*F1

```



```

    DAT3(7)=F1*F2*FRT
    DAT3(9)=F1*F3*FRT
    DAT3(10)=F1*F4*FRT
C***CALCULATE HEAT ENERGY DELIVERED TO LOAD***
    VDOV=DOV/1000.0
    SOLG=CPR0(T3)*VDOV
    IF(VDOV.GT.(SSV/3.0).AND.VDOV.LE.(SSV/1.5))SOLG=
    1 CPR0(T3)*(SSV/3.0)+CPR0(T4)*(VDOV-(SSV/3.0))
    IF(VDOV.GT.(SSV/1.5).AND.VDOV.LE.SSV)SOLG=CPR0(T3)*
    1 (SSV/3.0)+CPR0(T4)*(SSV/3.0)+CPR0(T5)*(VDOV-(SSV/1.5))
    IF(VDOV.GT.SSV)SOLG=CPR0(T3)*(SSV/3.0)+CPR0(T4)*(SSV/3.0
    1 +CPR0(T5)*(SSV/3.0)
    DAT3(8)=SOLG
    RETURN

```

C

```

    ENTRY MOD2D(S1,S2)
C***CALCULATE FIN AND COLLECTOR EFFICIENCY FACTORS***
    HL=(B1-B2)/2.0
    BC=(UBT*B2)/0.001
    UT=1.0/((1.0/(U1/CA))+(1.0/(U2/CA)))
    UL=UT+(1.0/UB)
    UL1=UL
    A=SQRT(UL/(UA*XP))
C***FIN EFFICIENCY FACTOR***
    FE=(TANH(A*HL))/(A*HL)
C***DETERMINE COLLECTOR CONSTRUCTION***
    IF(KF.EQ.1)GO TO 400
    IF(KF.EQ.2)GO TO 500
    IF(KF.EQ.3)GO TO 600
C***COLLECTOR TUBES BELOW PLATE***
400    CE1=(B1*UL)/(3.14*D1*HC)
        CE2=(B1*UL)/BC
        CE3=B1/(B2+2.0*HL*FE)
        CE=1.0/(CE1+CE2+CE3)
        GO TO 700
C***COLLECTOR TUBES ABOVE PLATE***
500    CE1=(B1*UL)/(3.14*D1*HC)
        CE2=(D1-2.0*XT)/B1
        CE3=(B1*UL)/BC
        CE4=B1/(2.0*HL*FE)
        CE5=1.0/(CE2+(1.0/(CE3+CE4)))
        CE=1.0/(CE1+CE5)
        GO TO 700
C***COLLECTOR TUBES INTEGRAL WITH PLATE***
600    CE1=(B1*UL)/(3.14*D1*HC)
        CE2=B1/(B2+2.0*HL*FE)
        CE=1.0/(CE1+CE2)
700    CONTINUE
C***CALCULATE RADIANT HEAT ENERGY ABSORBED BY SEGMENTS***
C***CALCULATE THE INCIDENT SOLAR RADIATION ABSORBED BY THE
C***COLLECTOR COVER SEGMENT***
    DAT2(8)=S1*CA*3600.0
C***CALCULATE THE INCIDENT SOLAR RADIATION ABSORBED BY THE
C***COLLECTOR PLATE UNIT SEGMENT***
    DAT2(7)=S2*CA*3600.0
    RETURN
END

```



```

C
C
SUBROUTINE MOD3(DT,N)
  DIMENSION DAT1(6,8),DAT2(3),CM(2,4),TS1(10),TS2(10),
  1 CT(2),ST(4),F(2),DAT3(10),SS(6),TS3(3),DAT4(2)
  COMMON DAT1,DAT2,ST,TS1,TS2,DAT3,SS,TS3,DAT4
C***INITIALISE MATRIX CALCULATION COMPONENTS***
  J1=N
  ST(1)=TS1(J1)
  ST(2)=TS2(J1)
  W1=DAT2(1)
  W2=DAT2(2)
C
  A1=DAT2(3)
  A2=DAT2(4)
  A3=DAT2(5)
C
  B1=DAT2(6)
  B2=DAT2(7)
  B3=DAT2(8)
C***INITIALISE THE FIRST ROW OF THE CALCULATION MATRIX***
  C1=DT/(W1)
  CM(1,1)=-C1*(A1+A2)
  CM(1,2)=C1*A2
  CM(1,3)=0.0
  CM(1,4)=C1*A1
C***INITIALISE THE SECOND ROW OF THE CALCULATION MATRIX***
  C2=DT/(W2)
  CM(2,1)=C2*A2
  CM(2,2)=-C2*(A2+A3+B1)
  CM(2,3)=C2*B1
  CM(2,4)=C2*A3
C
C***INITIALISE THE MATRIX ADDITION FUNCTIONS***
  F(1)=C1*B3
  F(2)=C2*B2
C
C***START QUARTIC RUNGE-KUTTA METHOD CALCULATION***
  IROW=0
100  IROW=IROW+1
     DO 300 I=1,2
       II=I
       SUM=0.0
       W=1.0/FLOAT(2**((II-1)))
       DO 200 K=1,4
200   SUM=SUM+CM(IROW,K)*ST(K)
       Y=SUM+F(IROW)
C***PREDICTED VALUE OF SEGMENT TEMPERATURE***
       QK1=W*Y
       QK2=W*(Y+(QK1/2.0))
       QK3=W*(Y+(QK2/2.0))
       QK4=W*(Y+QK3)
       CT(IROW)=ST(IROW)+(QK1+(2.0*QK2)+(2.0*QK3)+QK4)/6.0
300   ST(IROW)=CT(IROW)
       IF(IROW.EQ.2)GO TO 400
       GO TO 100
400   TS1(J1)=ST(1)

```

```

TS2(J1)=ST(2)
RETURN
END

```

C
C

```

SUBROUTINE MOD4
DIMENSION ST(4), SUN1(7,24,60), TAMB(7,24,60),
1 WIND(7,24,60), DAT1(6,8), DAT2(8), TS1(10), TS2(10),
2 ICHAR(10), USER(7,24,60), DAT3(10), DAT4(2),
3 SS(6), TS3(3), NDAY(12), DX(3,500), DY(15,500),
4 XPLOT(500), YPLOT(500), KPLOTT(15)
COMMON DAT1, DAT2, ST, TS1, TS2, DAT3, SS, TS3, DAT4
DOUBLE PRECISION FILE2, FILE3, FILE4, FILES, S

```

C

```

DATA NDAY/0,31,59,90,120,151,181,212,243,273,304,334/

```

C

C

```

C***INITIALISE COUNTING LOOP PARAMETERS***

```

```

TINV=DAT1(4,8)
DT1=TINV/60.0
NDY=IFIX(DAT1(5,6))
NDST=IFIX(DAT1(5,5))
NDT=IFIX(60.0/TINV)
NC=IFIX(DAT1(3,7))
CS=DAT1(3,7)
NHOUR=IFIX(DAT1(4,1))
ITC=IFIX(DAT1(6,1))

```

```

C***SET CLIMATE DATA ARRAYS TO ZERO***

```

```

DO 1 K1=1,7
DO 1 K2=1,24
DO 1 K3=1,60
SUN1(K1,K2,K3)=0.0
TAMB(K1,K2,K3)=0.0
WIND(K1,K2,K3)=0.0
USER(K1,K2,K3)=0.0

```

1

```

CONTINUE

```

```

C***INITIALISE SYSTEM PARAMETERS***

```

```

WRITE(5,2000)

```

```

2000 FORMAT('H DO YOU WISH TO INITIALISE SOLAR SYSTEM
1 TEMPERATURES ?, (0-NO, 1-YES) '/')

```

```

READ(5,2010)NANS

```

2010

```

FORMAT(1)

```

```

IF(NANS.EQ.0)GO TO 2060

```

```

WRITE(5,2020)

```

2020

```

FORMAT('H TYPE IN STORAGE TANK TEMPERATURES (3): '/')

```

```

READ(5,2030)T3,T4,T5

```

2030

```

FORMAT(3F)

```

```

WRITE(5,2040)

```

2040

```

FORMAT('H TYPE IN COVER AND COLLECTOR TEMPERATURES: '/')

```

```

READ(5,2050)T1,T2

```

2050

```

FORMAT(2F)

```

```

TS3(1)=T3

```

```

TS3(2)=T4

```

```

TS3(3)=T5

```

```

ST(1)=T1

```

```

ST(2)=T2

```

```

SS(1)=15.0

```



```

50      SS(2)=T3
100     SS(3)=T4
        SS(4)=T5
        GO TO 2070
2060    DO 2 J=1,3
        TS3(J)=15.0
2       CONTINUE
        ST(1)=15.0
        ST(2)=15.0
        SS(1)=15.0
        SS(2)=20.0
        SS(3)=20.0
        SS(4)=20.0
        SS(5)=20.0
2070    TS3(1)=SS(2)
        TS3(2)=SS(3)
        TS3(3)=SS(4)
        DO 3 K=1,NC
        TS1(K)=ST(1)
        TS2(K)=ST(2)
3       CONTINUE
        RETURN
        ENTRY INPUT1
        CALL NEWPAG
        WRITE(5,5)
5       FORMAT(' TYPE IN THE SOLAR RADIATION DATA FILENAME: '/')
        READ(5,10)FILE2
10      FORMAT(A10)
        RETURN
        ENTRY INPUT2
        WRITE(5,15)
15      FORMAT(' TYPE IN THE AMBIENT TEMPERATURE DATA FILENAME: '

        READ(5,20)FILE3
20      FORMAT(A10)
        RETURN
        ENTRY INPUT3
        WRITE(5,25)
25      FORMAT(' TYPE IN THE WIND PATTERN DATA FILENAME: '/')
        READ(5,30)FILE4
30      FORMAT(A10)
        RETURN
        ENTRY INPUT4
        WRITE(5,35)
35      FORMAT(' TYPE IN THE USER DEMAND PATTERN DATA
        1 FILENAME: '/')
        READ(5,40)FILE5
40      FORMAT(A10)
        CALL WAIT1
        RETURN
        ENTRY ALTER2
C***TRANSFER SOLAR RADIATION DATA FROM FILE2***
        OPEN(UNIT=1,DEVICE='DSK',FILE=FILE2)
        REWIND 1
        DO 100 K1=1,NDY
        DO 100 K2=1,NHOUR
        DO 100 K3=1,NDT
        READ(1,50)SUN1(K1,K2,K3)

```

```

50      FORMAT(20F)
100     CONTINUE
        CLOSE(UNIT=1, DEVICE='DSK', FILE=FILE2)
        RETURN
        ENTRY ALTER3
C***TRANSFER AMBIENT TEMPERATURE DATA FROM FILE3***
        OPEN(UNIT=1, DEVICE='DSK', FILE=FILE3)
        REWIND 1
        DO 150 K1=1,NDY
        DO 150 K2=1,NHOUR
        DO 150 K3=1,NDT
        READ(1,60)TAMB(K1,K2,K3)
60      FORMAT(20F)
150     CONTINUE
        CLOSE(UNIT=1, DEVICE='DSK', FILE=FILE3)
        RETURN
        ENTRY ALTER4
C***TRANSFER WIND PATTERN DATA FROM FILE4***
        OPEN(UNIT=1, DEVICE='DSK', FILE=FILE4)
        REWIND 1
        DO 200 K1=1,NDY
        DO 200 K2=1,NHOUR
        DO 200 K3=1,NDT
        READ(1,70)WIND(K1,K2,K3)
70      FORMAT(20F)
200     CONTINUE
        CLOSE(UNIT=1, DEVICE='DSK', FILE=FILE4)
        RETURN
        ENTRY ALTER5
C***TRANSFER USER DEMAND PATTERN DATA FROM FILE5***
        OPEN(UNIT=1, DEVICE='DSK', FILE=FILE5)
        REWIND 1
        DO 250 K1=1,NDY
        DO 250 K2=1,NHOUR
        DO 250 K3=1,NDT
        READ(1,80)USER(K1,K2,K3)
80      FORMAT(20F)
250     CONTINUE
        CLOSE(UNIT=1, DEVICE='DSK', FILE=FILE5)
        RETURN
C
C
C
C***INITIATE CALCULATION LOOP***
        ENTRY MOD4B(FR,NPV)
        MONTH=IFIX(DAT1(5,4))
        NF=IFIX((FR*DT1)+0.5)
        NDT1=NDT
        N1=0; NP=0
        DO 275 I=1,12
        N1=N1+1
        IF(MONTH.EQ.N1)GO TO 277
275     CONTINUE
277     DAY=FLOAT(NDY+NDAY(N1))-1.0
        VM=1.0
        DOV=0.0
        DT=1.0/FR

```



```

IDAY1=IFIX(DAT1(5,5))
NDY=IFIX(DAT1(5,6))
IDAY2=IDAY1+NDY-1
MDAY=IDAY1-1
HRAD=0.0
CALL MOD2BC(V4,DOV,HRAD)
KOUNT1=0
IF(NPV.EQ.200)CALL MOD6
TL=0.0
SHW=0.0
AHW=0.0
DO 302 IDAY=IDAY1,IDAY2
NPUMP=0
SOLGD=0.0
AUXGD=0.0
SOLGH=0.0
AUXGH=0.0
B1=DAT1(1,2)
TR=(DAT1(1,4))/2.0
XLC=DAT1(4,4)
XWC=DAT1(4,5)
ACU=DAT1(4,7)
PI=3.142
NT=IFIX((XWC/B1))
TN=FLOAT(NT)
VOLW=TN*XLC*PI*TR*TR*ACU

```

C

```

TOTCOL=0.0
COLHT=0.0
TRAD1=0.0
TRAD2=0.0
DAY=DAY+1
NYDAY=IFIX(DAY)
MDAY=MDAY+1
CALL MAINST(NYDAY,TCW)
SS(5)=TCW
CALL SUNRS(DAY,SUNR,SUNS)
NHR1=IFIX(SUNR)
NHR2=IFIX(SUNS)
NHR3=IFIX(SUNS+0.5)
MIN1=IFIX(60.0*(SUNR-FLOAT(NHR1)))
MIN2=IFIX(60.0*(SUNS-FLOAT(NHR2)))
THR=FLOAT(NDY*24)
NPL0T=(NDY*24)*NDT
IF(NPV.EQ.100.OR.NPV.EQ.200)CALL PRINT1(NPV,MDAY,NHR1,
1 NHR2,MIN1,MIN2)
DO 301 NHR=1,11HOUR
HR=FLOAT(NHR)
IF(NHR.LT.NHR1.OR.NHR.GT.NHR3)GO TO 230
IF(NHR.LT.NHR1.OR.NHR.GT.NHR3)DT=DT1
IF(NHR.GE.NHR1.AND.NHR.LE.NHR3)GO TO 232
DT=DT1
NF=1
GO TO 235
232 DT=1.0/FR
DT2=1.0/(FR*CS)
NF=IFIX((FR*DT1)+0.5)

```

230

232

CONTINUE

DO 301 NDT=1, NDT1

K1=1DAY

K2=1HR

K3=1NDT

ST(4)=TAMB(K1, K2, K3)

SS(6)=ST(4)

S0=SUN1(K1, K2, K3)

VM=WIND(K1, K2, K3)

DOV=USER(K1, K2, K3)

MIN=(1FIX(TINV))*NDT

CALL SUNPOS(DAY, HR, MIN, AZI, DECL, HANG, ALT)

CALL SHADE1(AZI, ALT, NSHAD1)

KOUNT1=KOUNT2

HRAD=S0*1000.0

CALL SUNRAD(HRAD, ALT, NSHAD1, DECL, HANG, S1, S2)

NSHAD1=0

CALL MOD2D(S1, S2)

SRAD1=(S1+S2)*DT1

SRAD2=S2*DT1

TRAD2=TRAD2+SRAD2

TRAD1=TRAD1+SRAD1

DO 300 K4=1, NF

PTE1P=TS3(3)

CALL PILOS(DT, PTEMP, OUTLT)

ST(3)=OUTLT

FLIN=OUTLT

COLHT=0.0

DO 290 K5=1, NC

K=K5

CALL MOD2BC(VM, DOV, HRAD)

CALL MOD3(DT, K)

ST(3)=ST(2)-ST(3)+ST(2)

290

CONTINUE

PTEMP=ST(3)

CALL PILOS(DT, PTEMP, OUTLT)

SS(1)=OUTLT

CALL MOD8(DT)

PUMP=DAT2(6)*(CS/2.0)

FLOW=VOLW*CPR0(ST(2))

IF(1FIX(PUMP).EQ.0) FLOW=0.0

IF(OUTLT.LT.FLIN.OR.HRAD.LT.5.0) FLOW=0.0

COLHT=COLHT+(OUTLT-FLIN)*FLOW

IF(1FIX(PUMP).GT.0) NPUMP=NPUMP+1

TOTCOL=TOTCOL+COLHT

CALL SOLHT(DOV, SOLG, AUXG)

SOLGD=SOLGD+SOLG*DT

AUXGD=AUXGD+AUXG*DT

300

CONTINUE

TL1=(DAT3(4)*(SS(2)-SS(6)))*DT1

TL2=(DAT3(5)*(SS(3)-SS(6)))*DT1

TL3=(DAT3(6)*(SS(4)-SS(6)))*DT1

TL=TL+(TL1+TL2+TL3)/1000.0

NP=NP+1

TAV2=(FLIN+OUTLT)/2.0

CA=XLC*XWC*ACU

FR1=DAT2(6)


```

IF(S2.NE.0.0)DTI1=(TAV2-ST(4))/S2
IF(S2.NE.0.0)EFCY1=(FR1*(OUTLT-TAV2))/(S2*3600.0*CA)
IF(DTI1.LT.0.0.OR.DTI1.GT.0.1)DTI1=0.0
IF(EFCY1.LT.0.0.OR.EFCY1.GT.100.0)EFCY1=0.0
EFCY1=EFCY1*100.0
IF(NPV.NE.200)GO TO 901
S3=S1+S2
IF(NHR.GE.NHR1.AND.NHR.LE.NHR3)CALL PRINT2(S3,K2,K3,
1 FLIN,OUTLT)
IF(ITC.EQ.0)CALL PRINT2(S2,K2,K3,FLIN,OUTLT)
GO TO 902
901 DY(1,NP)=HRAD
DY(2,NP)=SRAD1/DTI1
DY(3,NP)=ST(4)
DY(4,NP)=VM
DY(5,NP)=DOV
DY(6,NP)=ST(1)
DY(7,NP)=(FLIN+SS(1))/2.0
DY(8,NP)=FLIN
DY(9,NP)=SS(1)
DY(10,NP)=EFCY1
DY(11,NP)=SS(2)
DY(12,NP)=SS(3)
DY(13,NP)=SS(4)
DY(14,NP)=(SS(2)+SS(3)+SS(4))/3.0
DY(15,NP)=EFCY2
EX(1,NP)=FLOAT(NP)
EX(2,NP)=DTI1
EX(3,NP)=DTI2
902 CONTINUE
301 CONTINUE
DT=1.0/FR
NPL0T=NP
PTIME=FLOAT(NPUMP)*DT
NPHR=IFIX(PTIME)
NPMIN=IFIX((PTIME-FLOAT(NPHR))*60.0)
IF(NPV.EQ.100.OR.NPV.EQ.200)CALL PRINT3(SOLGD,AUXGD,
1 NPHR,NPMIN,TRAD1,TRAD2,TOTCOL)
302 CONTINUE
POWER=50.0
SHW=SHW+SOLGD
NPE=(NPHR*3600)+(NPMIN*60)
PE=(FLOAT(NPE)*POWER)/1000.0
AHW=AHW+AUXGD
IF(NPV.EQ.300)CALL PIECHT(SHW,PE,AHW,TL)
RETURN

C
C
C
ENTRY PLOT1
C***INITIALISE NUMBER AND NAME OF PARAMETERS TO BE PLOTTED***
305 WRITE(5,310)
310 FORMAT('H SPECIFY NUMBER OF PARAMETERS TO BE PLOTTED'/)
READ(5,315)NCP1
315 FORMAT(I)
IF(NCP1.GT.15)WRITE(5,320)
GO TO 325

```

```

320  FORMAT('H ERROR!! AVAILABLE NUMBER OF PARAMETERS = 15')
    GO TO 305
325  DO 340 J1=1,NCPI
      WRITE(5,330)
330  FORMAT('H PARAMETER NUMBER : ')
      READ(5,335)KPL0T1(J1)
335  FORMAT(I)
340  CONTINUE
C***CLEAR DRAWING AREA***
      CALL PICCLE
      XSP=20.0; YSP=130.0
      NLAY=0
C***DETERMINE PLOT TIME INTERVAL AND PERIOD***
      IF(NDY.LE.2)GO TO 345
      IF(NDY.GT.2.AND.NDY.LE.14)GO TO 350
      IF(NDY.GT.14.AND.NDY.LE.140)GO TO 355
345  FACT=DT1
      IF(NHOUR.LT.24)FACT=1.0
      NINTX=NDY*24
      IF(NHOUR.LT.24)NINTX=(60*NHOUR)/10
      XBEG=0.0
      XEND=FLOAT(NDY*24)
      IF(NHOUR.LT.24)XEND=FLOAT(60*NHOUR)
      NTEXT=1
      IF(NHOUR.LT.24)NTEXT=0
      GO TO 365
350  FACT=DT1/24.0
      NINTX=NDY
      XBEG=FLOAT(IDAY1)
      XEND=FLOAT(IDAY2)
      NTEXT=2
      GO TO 365
355  FACT=DT1/(24.0*7.0)
      NINTX=(NDY)/7
      XBEG=0.0
      XEND=FLOAT(NINTX+1)
      NTEXT=3
      GO TO 365
365  J2=0; NDEV1=0
1000 J2=J2+1
      J3=KPL0T1(J2)
      IF(NDEV1.NE.0)GO TO 367
      J5=1
      IF(J3.EQ.10)GO TO 1005
      IF(J3.EQ.15)GO TO 1010
      GO TO 1015
1005 J5=2
      XBEG=0.0
      NINTX=10
      XEND=0.1
      NTEXT=4
      GO TO 1015
1010 J5=3
      XBEG=0.0
      NINTX=10
      XEND=0.1
      NTEXT=5

```



```

1015 DO 366 J4=1, NPL0T
366 XPL0T(J4)=LY(J5,J4)*FACT
C***INITIALISE Y-AXIS VALUES***
367 IF(J3.EQ.3.OR.J3.GE.6)NDEV='T'
      IF(J3.EQ.4)NDEV='V'
      IF(J3.EQ.5)NDEV='F'
      IF(J3.EQ.1.OR.J3.EQ.2)NDEV='S'
      IF(J3.EQ.10.OR.J3.EQ.15)NDEV='E'
      DO 370 J6=1,NPL0T
370 YPL0T(J6)=DY(J3,J6)
      YEND=100.0
      IF(J3.EQ.1.OR.J3.EQ.2)YEND=1000.0
      IF(J3.EQ.4)YEND=20.0
      IF(J3.EQ.5)YEND=100.0
      IF(NDEV1.EQ.NDEV)GO TO 375
      XPOS=15.0
      IF(J3.EQ.1.OR.J3.EQ.2)XPOS=135.0
      IF(J3.EQ.4.OR.J3.EQ.5)XPOS=155.0
      CALL AXIPOS(1,15.0,30.0,120.0,1)
      CALL AXIPOS(1,XPOS,30.0,100.0,2)
      CALL AXISCA(3,NINTX,XBEG,XEND,1)
      CALL AXISCA(3,20.0,0.0,YEND,2)
      CALL AXIDRA(1,1,1)
      IF(J3.NE.3.AND.J3.LT.6)CALL AXIDRA(1,1,2)
      IF(J3.EQ.3.OR.J3.GE.6)CALL AXIDRA(-1,-1,2)
      CALL GRID(3,0,0)
375 NDEV1=NDEV
      IF(J3.EQ.10.OR.J3.EQ.15)GO TO 380
      CALL GRASYM(XPL0T,YPL0T,NPL0T,J2,2)
      CALL GRAPOL(XPL0T,YPL0T,NPL0T)
      GO TO 385
380 CALL GRASYM(XPL0T,YPL0T,NPL0T,J2,0)
C***OUTPUT GRAPH***
C***INITIALISE VARIABLE TO BE PLOTTED***
C***Y-AXIS NOTATION***
385 NPV=J3
      IF(NPV.EQ.1)GO TO 400
      IF(NPV.EQ.2)GO TO 401
      IF(NPV.EQ.3)GO TO 402
      IF(NPV.EQ.4)GO TO 403
      IF(NPV.EQ.5)GO TO 404
      IF(NPV.EQ.6)GO TO 405
      IF(NPV.EQ.7)GO TO 406
      IF(NPV.EQ.8)GO TO 407
      IF(NPV.EQ.9)GO TO 408
      IF(NPV.EQ.10)GO TO 409
      IF(NPV.EQ.11)GO TO 410
      IF(NPV.EQ.12)GO TO 411
      IF(NPV.EQ.13)GO TO 412
      IF(NPV.EQ.14)GO TO 413
      IF(NPV.EQ.15)GO TO 414
      GO TO 500
C***GLOBAL SOLAR RADIATION***
400 CALL MOVTO2(XSP,YSP)
      CALL CHAHOL(27HGLOBAL SOLAR RADIATION(W)*.)
      GO TO 500
C***INCIDENT SOLAR RADIATION***

```



```

401      CALL MOVTO2(XSP,YSP)
        CALL CHAHOL(29HINCIDENT SOLAR RADIATION(W)*.)
        GO TO 500
C***AMBIENT AIR TEMPERATURE***
402      CALL MOVTO2(XSP,YSP)
        CALL CHAHOL(25HAMBIENT AIR TEMPERATURE*.)
        GO TO 500
C***WIND VELOCITY***
403      CALL MOVTO2(XSP,YSP)
        CALL CHAHOL(21HWIND VELOCITY (M/S)*.)
        GO TO 500
C***USER DEMAND PATTERN***
404      CALL MOVTO2(XSP,YSP)
        CALL CHAHOL(30HUSER DEMAND PATTERN (LITRES)*.)
        GO TO 500
C***COVER TEMPERATURE***
405      CALL MOVTO2(XSP,YSP)
        CALL CHAHOL(20HCOVER TEMPERATURE *.)
        GO TO 500
C***MEAN FLUID TEMPERATURE***
406      CALL MOVTO2(XSP,YSP)
        CALL CHAHOL(25HMEAN FLUID TEMPERATURE *.)
        GO TO 500
C***OUTLET FLUID TEMPERATURE***
408      CALL MOVTO2(XSP,YSP)
        CALL CHAHOL(26HOUTLET FLUID TEMPERATURE*.)
        GO TO 500
C***INLET FLUID TEMPERATURE***
407      CALL MOVTO2(XSP,YSP)
        CALL CHAHOL(25HINLET FLUID TEMPERATURE*.)
        GO TO 500
- C***COLLECTOR EFFICIENCY***
409      CALL MOVTO2(XSP,YSP)
        CALL CHAHOL(22HCOLLECTOR EFFICIENCY*.)
        GO TO 500
C***TANK SECTION 1 TEMPERATURE***
410      CALL MOVTO2(XSP,YSP)
        CALL CHAHOL(28HTANK SECTION 1 TEMPERATURE*.)
        GO TO 500
C***TANK SECTION 2 TEMPERATURE***
411      CALL MOVTO2(XSP,YSP)
        CALL CHAHOL(28HTANK SECTION 2 TEMPERATURE*.)
        GO TO 500
C***TANK SECTION 3 TEMPERATURE***
412      CALL MOVTO2(XSP,YSP)
        CALL CHAHOL(28HTANK SECTION 3 TEMPERATURE*.)
        GO TO 500
C***MEAN STORAGE TANK TEMPERATURE***
413      CALL MOVTO2(XSP,YSP)
        CALL CHAHOL(31HMEAN STORAGE TANK TEMPERATURE*.)
        GO TO 500
C***SOLAR SYSTEM EFFICIENCY***
414      CALL MOVTO2(XSP,YSP)
        CALL CHAHOL(25HSOLAR SYSTEM EFFICIENCY*.)
500      CONTINUE
        CALL MOVTO2(100.0,YSP+2.0)
        CALL SYMBOL(J2)

```



```

      NDAY=NDAY+1
      YSP=130.0-(FLOAT(NDAY*4))
      IF(J2.NE.NCP1)GO TO 1000
C***X-AXIS TEXT***
      CALL MOVT02(20.0,20.0)
      CALL CHAHOL(24HSIMULATION TIME PERIOD*.)
      CALL MOVT02(20.0,15.0)
      IF(J3.EQ.10.OR.J3.EQ.15)GO TO 510
      IF(NTEXT.EQ.0)CALL CHAHOL(11H(MINUTES)*.)
      IF(NTEXT.EQ.1)CALL CHAHOL(9H(HOURS)*.)
      IF(NTEXT.EQ.2)CALL CHAHOL(8H(DAYS)*.)
      IF(NTEXT.EQ.3)CALL CHAHOL(9H(WEEKS)*.)
      IF(NTEXT.EQ.4)CALL CHAHOL(22H DT/1 (DEGC.SQ.M.)/W*.)
      GO TO 520
510   CALL CHAHOL(8H(DT/1)*.)
520   READ(5,530)WAIT
530   FORMAT(A1)
      RETURN
      END
C
C
      SUBROUTINE MOD6
      DIMENSION DAT1(6,8),DAT2(8),ST(4),TXT1(9,7),TXT2(9,7),
     1 TS1(10),TS2(10),DAT3(10),SS(6),TS3(3),NMON(12),DAT4(2)
      COMMON DAT1,DAT2,ST,TS1,TS2,DAT3,SS,TS3,DAT4
      DOUBLE PRECISION NMON
      DATA NMON/'JANUARY','FEBRUARY','MARCH','APRIL','MAY',
     1 'JUNE','JULY','AUGUST','SEPTEMBER','OCTOBER',
     2 'NOVEMBER','DECEMBER'/
C***TEXT DATA FOR TAELE HEADING***
      DATA TXT1/44H HR-TIME OF SIMULATION PROGRAM
     1 (ACTUAL TIME),
     2 43H DT-CALCULATION PROGRAM TIME INCREMENT (HR),
     3 44H TG-COLLECTOR GLASS COVER TEMPERATURE (DEGC),
     4 43H TM-MEAN COLLECTOR FLUID TEMPERATURE (DEGC),
     5 44H T1-COLLECTOR INLET FLUID TEMPERATURE (DEGC),
     6 45H T2-COLLECTOR OUTLET FLUID TEMPERATURE (DEGC),
     7 41H T3-TOP STORAGE TANK SECTION TEMPERATURE /
C
      DATA TXT2/43H T4-MIDDLE STORAGE TANK SECTION
     1 TEMPERATURE,
     2 43H T5-BOTTOM STORAGE TANK SECTION TEMPERATURE,
     3 42H TS-AVERAGE SOLAR STORAGE TANK TEMPERATURE,
     4 44H TA-ENVIRONMENT AMBIENT AIR TEMPERATURE (DEGC),
     5 45H S2-INCIDENT SOLAR RADIATION-COLLECTOR (W/M2),
     6 44H EFCY-INSTANTANEOUS COLLECTOR EFFICIENCY (E),
     7 42H DTI-TEMPERATURE/INCIDENT ENERGY (C/W.M2)/
C
      WRITE(5,10)
10    FORMAT('H SOLAR COLLECTOR AND STORAGE SYSTEM
     1 TEMPERATURE PROFILE. '/')
C***WRITE TEXT***
      DO 100 K=1,2
      DO 100 J=1,7
      IF(K.EQ.1)WRITE(5,20)(TXT1(I,J),I=1,9)
      IF(K.EQ.2)WRITE(5,20)(TXT2(I,J),I=1,9)
20    FORMAT(9A5)

```



```

102  CONTINUE
      CALL NEWLIN
      RETURN
      ENTRY PRINT1(NPV, NDATE, NHR1, NHR2, MIN1, MIN2)
      MONTH=IFIX(DAT1(5,4))
      NYEAR=IFIX(DAT1(5,3))
      ITC=IFIX(DAT1(6,1))
      IF(ITC.EQ.0)GO TO 55
      WRITE(5,30)NMON(MONTH),NDATE,NYEAR
30    FORMAT(2X,A10,1X,I2,1X,I4,/)
      WRITE(5,40)NHR1,MIN1
40    FORMAT('H SUNRISE OCCURS AT ',I2,'HR ',I2,'MIN. GMT')
      WRITE(5,50)NHR2,MIN2
50    FORMAT('H SUNSET OCCURS AT ',I2,'HR ',I2,'MIN. GMT')
55    IF(NPV.EQ.200)WRITE(5,60)
60    FORMAT('H HR',2X,'DT',5X,'TG'3X,'T1',3X,'T2',
           1 3X,'T3',3X,'T4',3X,'T5',3X,'TA',5X,'S2',4X,
           2 'EFCY',3X,'DTI'/)
      RETURN
      ENTRY PRINT2(S2,NHR,NDT,TIN,TOUT)
C***INITIALISE TABLE PARAMETERS***
      TA=ST(4)
      T3=SS(2)
      T4=SS(3)
      T5=SS(4)
      CS=DAT1(3,7)
      NC=IFIX(CS)
      XLC=DAT1(4,4)
      XWC=DAT1(4,5)
      ACU=DAT1(4,7)
      ITC=IFIX(DAT1(6,1))
C***COLLECTOR AREA***
      CA=XLC*XWC*ACU
C***AVERAGE COLLECTOR FLUID TEMPERATURE***
      TAV2=(TIN+TOUT)/2.0
C***THEORETICAL INSTANTANEOUS COLLECTOR EFFICIENCY***
      DT=DAT1(4,8)
      FR1=DAT2(6)
      F=FR1*100.0
      IF(IFIX(F).EQ.0)GO TO 65
      IF(ITC.EQ.0)GO TO 65
      EFCY=(FR1*(TOUT-TAV2))/(S2*3600.0*CA)
C***CHANGE IN COLLECTOR TEMPERATURE/INSOLATION***
      DTI=(TAV2-TA)/S2
      GO TO 67
65    EFCY=0.0
      DTI=0.0
C***AVERAGE STORAGE TANK FLUID TEMPERATURE***
67    TAV4=(T3+T4+T5)/3.0
C***WRITE TEMPERATURE DATA***
      WRITE(5,70)NHR,NDT,TIN,TA,S2
70    FORMAT(2(2X,I2),10X,F4.1,21X,F4.1,3X,F5.1)
C***WRITE COLLECTOR SEGMENT TEMPERATURES***
      N=0
      200  N=N+1
      WRITE(5,80)TS1(N),TS2(N)
80    FORMAT(13X,F4.1,6X,F4.1)

```

```

      IF(N.LT.NC)GO TO 200
C***WRITE STORAGE TANK SEGMENT TEMPERATURES***
      WRITE(5,90)T3,T4,T5,EFCY,DTI
90    FORMAT(28X,F4.1,1X,F4.1,1X,F4.1,14X,F4.1,3X,F4.2,/)
      RETURN
      ENTRY PRINT3(SOLGDY,AUXGDY,NPHR,NPMIN,TRAD1,TRAD2,
1    TOTCOL)
      XLC=DAT1(4,4)
      XWC=DAT1(4,5)
      ACU=DAT1(4,7)
C***COLLECTOR AREA***
      CA=XLC*XWC*ACU
      TRAD1=TRAD1*CA/1000.0
      TRAD2=TRAD2*CA/1000.0
      TOTCOL=TOTCOL/3.6E6
      EFCY1=(TOTCOL/TRAD2)*100.0
      SOLGDY=SOLGDY/3.6E6
      AUXGDY=AUXGDY/3.6E6
      WRITE(5,101)TRAD1
101   FORMAT('H DAILY TOTAL RADIATION INCIDENT ON GLASS',F7.1,
1    'KWHR')
      WRITE(5,110)TRAD2
110   FORMAT('H DAILY TOTAL RADIATION INCIDENT ON
1    COLLECTOR PAVELS',F7.1,'KWHR')
      WRITE(5,120)TOTCOL
120   FORMAT('H DAILY TOTAL HEAT ENERGY COLLECTED',F7.1,'KWHR')
      WRITE(5,130)SOLGDY
130   FORMAT('H DAILY HEAT SUPPLIED BY SOLAR SYSTEM',F7.1,'KWH')
      WRITE(5,140)AUXGDY
140   FORMAT('H DAILY AUXILIARY HEAT REQUIREMENT',F7.1,'KWHR')
      WRITE(5,150)NPHR,NPMIN
150   FORMAT('H DAILY RUNNING TIME OF PUMP',1X,12,'HR',
1    1X,12,'MIN')
      WRITE(5,160)EFCY1
160   FORMAT('H DAILY AVERAGE COLLECTOR EFFICIENCY',F5.1,'%')
C
C
      RETURN
      END
C
C
      SUBROUTINE MOD5(HP)
      DIMENSION DAT1(6,8),DAT2(8),ST(4),TS1(10),
1    TS2(10),DAT3(10),SS(6),TS3(3),DAT4(2)
      COMMON DAT1,DAT2,ST,TS1,TS2,DAT3,SS,TS3,DAT4
C
C***SUBPROGRAM TO CALCULATE THE NATURAL CONVECTION BETWEEN
C***PARALLEL FLAT PLATES (DATA TAKEN FROM TABOR, 1958)
C***INITIALISE THE SUBPROGRAM PARAMETERS***
C***SPACP- THE PLATE SPACING IN CENTIMETRES***
      SPACP=DAT1(3,3)*10.0
C***NTLT- THE COLLECTOR TILT IN DEGREES***
      NTLT=IFIX(DAT1(4,2))
      T1=ST(1)
      T2=ST(2)
C***DETERMINE THE TEMPERATURE DIFFERENCE BETWEEN THE PLATE

```



```

DTMP=ABS(T2-T1)
KTMP=IFIX(DTMP)
C***CALCULATE THE HEAT TRANSFER COEFFICIENT, HP***
C***HORIZONTAL PLANE HEAT FLOW UPWARDS***
      IF(NTLT.GE.0.AND.NTLT.LE.30)HP=(1.613*1.91)/(SPACP**0.15

C***30-60 DEG. PLANE HEAT FLOW UPWARDS***
      IF(NTLT.GT.30.AND.NTLT.LE.60)HP=(1.14*2.04)/(SPACP**0.07

C***60-VERTICAL PLANE***
      IF(NTLT.GT.60)HP=(0.82*2.12)/(SPACP**0.019)
C***APPLY CORRECTION FACTOR FOR TEMPERATURES***
C***OTHER THAN 10 DEG.C.***
      IF(KTMP.GT.10)GO TO 100
      GO TO 200
100    HP=HP*(1.0-0.0013*(DTMP-10.0))
200    RETURN
      END

```

C
C
C
C

```

      SUBROUTINE MENU1
      DIMENSION MODUL1(56)
C***MENU1*****
C***1INPUT*****
C***2CHECK*****
C***3ALTER*****
C***4RUN*****
C***5PLOT1*****
C***6END*****
      DATA MODUL1/32,32,77,69,78,85,49,32,
        1 32,49,73,73,80,85,84,32,
        2 32,50,67,72,69,67,75,32,
        3 32,51,65,76,84,69,82,32,
        4 32,52,82,85,73,32,32,32,
        5 32,53,80,76,79,84,49,32,
        6 32,54,69,73,68,32,32,32/
C***CALL CHAR SIZE***
100    CALL CSIZE(KHORSZ,KVERSZ)
C***GO TO MENU POSITION***
      CALL NEWPAG
      CALL MOVREL(0,-600)
C***OUTPUT MODUL1 CHARS***
      K=0
      DO 200 J=1,7
      CALL NEMLIN
      DO 200 I=1,8
      K=K+1
      CALL ANCHO(MODUL1(K))
200    CONTINUE
C***DRAW BOX AROUND MENU***
      CALL MOVREL(-660,0)
      CALL DRWREL(0,2*KVERSZ)
      CALL DRWREL(-2*KHORSZ,0)
      CALL DRWREL(0,-2*KVERSZ)
      CALL DRWREL(2*KHORSZ,0)
C***CURSOR COMMAND MODE***

```

```

CALL BELL
CALL NEWPAG
CALL AINMODE
C***IDENTIFY ICHAR CONDITION***
  IF(ICHAR.EQ.49)GO TO 300
  IF(ICHAR.EQ.50)GO TO 400
  IF(ICHAR.EQ.51)GO TO 500
  IF(ICHAR.EQ.52)GO TO 600
  IF(ICHAR.EQ.53)GO TO 800
  IF(ICHAR.EQ.54)GO TO 700
C***INITIALISE SYSTEM OF NODAL TEMPERATURE VALUES***
C***FOR THE GRAPH PLOTTING ROUTINES*****
800  CALL MOD4
    CALL ALTER2
    CALL ALTER3
    CALL ALTER4
    CALL ALTER5
    CALL MOD2(FR)
    NPV=500
    CALL MOD4B(FR,NPV)
    CALL MENU3
C***END OF DATA SAVE FACILITIES***
  GO TO 100
C***DATA INPUT SEQUENCE***
300  CALL MOD1
    CALL MOD4
    CALL INPUT1
    CALL ALTER2
    CALL INPUT2
    CALL ALTER3
    CALL INPUT3
    CALL ALTER4
    CALL INPUT4
    CALL ALTER5
    GO TO 100
C***DATA INPUT CHECK***
400  CALL CHECK1
    CALL WAIT1
    GO TO 100
C***ALTER DESIGN PARAMETERS***
500  CALL MENU2
    GO TO 100
C***RUN CALCULATION PROGRAM***
600  CALL MENU9(NPV)
    IF(NPV.EQ.999)GO TO 100
    CALL MOD4
    CALL ALTER2
    CALL ALTER3
    CALL ALTER4
    CALL ALTER5
    CALL MOD2(FR)
    CALL MOD4B(FR,NPV)
    CALL WAIT1
    GO TO 100
700  RETURN
    END

```

C


```

SUBROUTINE MENU2
DIMENSION MODUL2(72)
DATA MODUL2/32,32,77,69,73,85,50,32,
1 32,49,70,73,76,69,49,32,
2 32,50,70,73,76,69,50,32,
3 32,51,70,73,76,69,51,32,
4 32,52,70,73,76,69,52,32,
5 32,53,70,73,76,69,53,32,
6 32,54,70,73,76,69,54,32,
7 32,55,67,76,73,77,65,32,
8 32,56,69,78,68,32,32,32/

C***CALL CHAR SIZE***
100 CALL CSIZE(KHORSZ,KVERSZ)
C***GO TO MENU POSITION***
CALL NEWPAG
CALL MOVREL(0,-534)
C***OUTPUT MODUL2 CHARS***
K=0
DO 200 J=1,9
CALL NEWLIN
DO 200 I=1,8
K=K+1
CALL ANCHO(MODUL2(K))
200 CONTINUE
C***DRAW BOX AROUND MENU***
CALL MOVREL(-390,0)
CALL DRWREL(0,3*KVERSZ)
CALL DRWREL(-2*KHORSZ,0)
CALL DRWREL(0,-3*KVERSZ)
CALL DRWREL(2*KHORSZ,0)
C***CURSOR COMMAND MODE***
CALL DCUPSR(ICHAR,IX,IY)
CALL BELL
CALL NEWPAG
C***IDENTIFY ICHAR CONDITION***
IF(ICHAR.EQ.55)GO TO 400
IF(ICHAR.GE.56)GO TO 500
IF(ICHAR.GE.49.AND.ICHAR.LE.54)GO TO 300
C***ALTER FILE PARAMETER DATA***
300 N=ICHAR-48
CALL ALTER1(N)
GO TO 100
400 CONTINUE
GO TO 100
500 RETURN
END
SUBROUTINE MENU3
DIMENSION MODUL3(56)
DOUBLE PRECISION A

C***MENU3*****
C***1LINPR*****
C***2GRAF1*****
C***3SIMEX*****
C***4GRAF3*****
C***5AFOR1*****
C***6END*****
DATA MODUL3/32,32,77,69,73,85,51,32,

```

```

1 32,49,76,73,73,80,82,32,
2 32,50,71,82,65,70,49,32,
3 32,51,83,73,77,69,83,32,
4 32,52,71,82,65,70,51,32,
5 32,53,65,70,79,82,77,32,
6 32,54,32,69,73,63,32,32/

C***CALL CHAR SIZE***
100 CALL CSIZE(KHORSZ,KVERSZ)
C***GO TO MENU POSITION***
CALL NEWPAG
CALL MOVREL(0,-600)
C***OUTPUT MODUL3 CHARS***
K=0
DO 200 J=1,7
CALL NEWLIN
DO 200 I=1,8
K=K+1
CALL ANCHO(MODUL3(K))
200 CONTINUE
C***DRAW BOX AROUND MENU***
CALL MOVREL(-660,0)
CALL DRWREL(0,2*KVERSZ)
CALL DRWREL(-2*KHORSZ,0)
CALL DRWREL(0,-2*KVERSZ)
CALL DRWREL(2*KHORSZ,0)
C***CURSOR COMMAND MODE***
CALL DCURSR(ICAR,IX,IY)
CALL BELL
CALL NEWPAG
C***IDENTIFY ICAR CONDITION***
IF(ICAR.EQ.49)GO TO 300
IF(ICAR.EQ.50)GO TO 400
IF(ICAR.EQ.51)GO TO 500
IF(ICAR.EQ.52)GO TO 600
IF(ICAR.EQ.53)GO TO 700
IF(ICAR.EQ.54)GO TO 800
C***DISK STORE DATA AND PRINT***
300 WRITE(5,10)
10 FORMAT('H TYPE DATA FILE-NAME: ')
READ(5,20)A
20 FORMAT(A10)
CALL MOD4
CALL ALTER2
CALL ALTER3
CALL ALTER4
CALL ALTER5
OPEN(UNIT=5,DEVICE='DSK',FILE=A)
CALL CHECK1
CALL MOD2(FR)
NPV=200
CALL MOD4B(FR,NPV)
CLOSE(UNIT=5,DEVICE='DSK',FILE=A)
GO TO 100
C***PLOT ENVIRONMENT AND SYSTEM NODAL TEMPERATURE***
C***NETWORK VALUES*****
C***TABULATE LIST OF POSSIBLE PARAMETERS AVAILABLE*****
400 WRITE(5,410)

```



```

410  FORMAT('H LIST OF POSSIBLE SYSTEM PARAMETERS AVAILABLE')
    WRITE(5,420)
420  FORMAT('H1.-GLOBAL SOLAR RADIATION'/' 2.-INCIDENT
1 SOLAR RADIATION'/' 3.-AMBIENT AIR TEMPERATURE'/'
2 ' 4.-WIND VELOCITY'/' 5.-USER DEMAND PATTERN'/'
3 ' 6.-COVER TEMPERATURE'/' 7.-MEAN COLLECTOR
4 TEMPERATURE'/' 8.-INLET COLLECTOR TEMPERATURE'/'
5 ' 9.-OUTLET COLLECTOR TEMPERATURE'/' 10.-
6 COLLECTOR EFFICIENCY'/' 11.-TOP STORAGE TANK
7 TEMPERATURE'/' 12.-MIDDLE STORAGE TANK TEMPERATURE'/'
8 ' 13.-BOTTOM STORAGE TANK TEMPERATURE'/' 14.-MEAN
9 STORAGE TANK TEMPERATURE'/' 15.-SYSTEM EFFICIENCY')
    CALL PLOT1
    GO TO 100
C***PLOT COLLECTOR TEMPERATURE VALUES***
500  CONTINUE
    GO TO 100
C***PLOT STORAGE TANK TEMPERATURE VALUES***
600  CONTINUE
    GO TO 100
C***PLOT ARCHITECTURAL FORM OF SOLUTION***
700  CONTINUE
    GO TO 100
C***RETURN TO MENU1 LEVEL***
800  CONTINUE
    RETURN
    END

```

C
C

```

SUBROUTINE HOUR(DAY,HR,H)
DIMENSION DAT1(6,3),DAT2(8),ST(4),TS1(10),TS2(10),
1 DAT3(10),SS(6),TS3(3),DAT4(2)
REAL LAT,MIN,LONG
COMMON DAT1,DAT2,ST,TS1,TS2,DAT3,SS,TS3,DAT4
LAT=DAT1(5,1)
LONG=DAT1(5,2)
YEAR=DAT1(5,3)
MIN=0.0
SEC=0.0
RAD=0.017453293
DELYR=YEAR-1980.0
LEAP=IFIX(DELYR/4.0)
T=HR+(MIN+SEC/60.0)/60.0
TIME=DELYR*365.0+LEAP+DAY-1.0+(T/24.0)
TIME=TIME-1.0
THETA=(360.0*(TIME/365.25))*RAD
G=-0.031271-4.53963E-7*TIME+THETA
EL=4.900963+3.67474E-7*TIME+(0.033434-2.3E-9*TIME)
1 *SIN(G)*0.000349*SIN(2.0*G)+THETA
EPS=0.40914-6.2149E-9*TIME
SEL=SIN(EL)
DECL=ASIN(SEL*SIN(EPS))
PHI=LAT*RAD
RS1=SIN(-1.4544E-2)-SIN(PHI)*SIN(DECL)
RS2=COS(PHI)*COS(DECL)
H=((1.0/15.0)*ACOS(RS1/RS2))/RAD
RETURN

```


END

SUBROUTINE SUNRS(DAY, SUNR, SUNS)

HR=6.0

CALL HOUR(DAY, HR, H)

SUNR=12.0-H

HR=18.0

CALL HOUR(DAY, HR, H)

SUNS=12.0+H

RETURN

END

SUBROUTINE SUNPOS(DAY, HR, MIN, AZI, DECL, HANG, ALT)

DIMENSION DAT1(6,8), DAT2(8), ST(4), TS1(10), TS2(10),

1 DAT3(10), SS(6), TS3(3), DAT4(2)

REAL LAT, LONG

COMMON DAT1, DAT2, ST, TS1, TS2, DAT3, SS, TS3, DAT4

LAT=DAT1(5,1)

LONG=DAT1(5,2)

YEAR=DAT1(5,3)

ZONE=DAT1(5,7)

SEC=0.0

TWOPI=6.2831853

RAD=0.017453293

XMIN=FLOAT(MIN)

T=HR+(XMIN+SEC/60.0)/60.0

IF(T.GT.12.0)T1=(T-12.0)*(-1.0)

IF(T.LE.12.0)T1=ABS(T-12.0)

DELYR=YEAR-1980.0

LEAP=IFIX(DELYR/4.0)

TIME=DELYR*365.0+LEAP+DAY-1.0+(T/24.0)

IF((IFIX(DELYR)).EQ.LEAP*4)TIME=TIME-1.0

IF((DELYR.LT.0.0).AND.(DELYR.NE.LEAP*4))TIME=TIME-1.0

THETA=360.0*(TIME/365.25)*RAD

G=-0.031271-4.53963E-7*TIME+THETA

EL=4.900968+3.6747E-7*TIME+(0.033434-2.3E-9*TIME)

1 *SIN(G)+0.000349*SIN(2.0*G)+THETA

EPS=0.409140-6.2149E-9*TIME

SEL=SIN(EL)

A1=SEL*COS(EPS)

A2=COS(EL)

RA=ATAN2(A1,A2)

IF(IFIX(RA).LE.0)RA=RA+TWOPI

DECL=ASIN(SEL*SIN(EPS))/RAD

ST1=1.759335+TWOPI*(TIME/365.25-DELYR)+3.694E-7*TIME

IF(ST1.GE.TWOPI)ST1=ST1-TWOPI

S=ST1-LONG*RAD+1.0027379*(T+ZONE)*15.0*RAD

H=RA-S

HANG=H/RAD

DECLR=DECL*RAD

PHI=LAT*RAD

ALT=ASIN(SIN(PHI)*SIN(DECLR)+COS(PHI)*COS(DECLR)*COS(H))

AZI=ASIN(COS(DECLR)*SIN(H)/COS(ALT))/RAD

IF(SIN(ALT).GE.SIN(DECL)/SIN(PHI))GO TO 10

IF(AZI.LT.0.0)AZI=AZI+360.0

AZI=180.0-AZI

```

10  AZI=180.-AZI
    ALT=ALT/RAD
    RETURN
    END

C
C
SUBROUTINE SUNRAD(S0,ALT,NSHAD,DECL,HANG,S1,S2)
DIMENSION DAT1(6,8),DAT2(8),ST(4),TS1(10),TS2(10),
1  DAT3(10),SS(6),TS3(3),HBD(13)
COMMON DAT1,DAT2,ST,TS1,TS2,DAT3,SS,TS3
REAL LAT,LATR
DATA HBD/0.0,28.0,43.0,54.0,63.0,71.0,77.0,83.0,88.0,
1  93.0,99.0,101.0,105.0/
ABS=DAT1(2,6)
TILT=DAT1(4,2)
WZA=DAT1(5,8)
LAT=DAT1(5,1)
C***DETERMINE THE INTENSITY OF THE HORIZONTAL BACKGROUND DIFFUSE
C***RADIATION*****
    IF(ALT.LE.2.5)GO TO 600
    ALT1=-7.5
    ALT2=-2.5
    ICOUNT=0
    DO 100 I=1,13
    ALT1=ALT1+5.0
    ALT2=ALT2+5.0
    ICOUNT=ICOUNT+1
    IF(ALT.GE.ALT1.AND.ALT.LT.ALT2)GO TO 200
100  CONTINUE
200  HBDR=HBD(ICOUNT)
    IF(HBDR.GT.S0)HBDR=S0
C***CHANGE CALCULATION PARAMETERS ANGLES INTO RADIANS***
    RAD=0.01745
    LATR=LAT*RAD
    ALTR=ALT*RAD
    WZA=(WZA-180.0)*(-1.0)
    AZIR=WZA*RAD
    TILTR=TILT*RAD
    HANGR=HANG*RAD
    DECLR=DECL*RAD
C***CALCULATE THE ANGLE OF INCIDENCE OF THE BEAM RADIATION***
    C1=SIN(DECLR)
    C2=COS(DECLR)
    C3=SIN(LATR)
    C4=COS(LATR)
    C5=SIN(TILTR)
    C6=COS(TILTR)
    C7=SIN(AZIR)
    C8=COS(AZIR)
    C9=SIN(HANGR)
    C10=COS(HANGR)
    COSA=C1*C3*C6
    COSB=C1*C4*C5*C3
    COSC=C2*C4*C6*C10
    COSD=C2*C3*C5*C3*C10
    COSE=C2*C5*C7*C9
    COSI=COSA-COSB+COSC+COSD+COSE

```



```

C***CALCULATE THE BEAM RADIATION***
COSDT=COS(LATR-TILTR)*C2*C10+SIN(LATR-TILTR)*C1
COSDZ=C4*C2*C10+C3*C1
RBEAM=ABS(COSDT/COSDZ)
CC=0.0
HBDR=0.78+1.07*ALT+6.17*CC
DIRS=(S0-HBDR)*RBEAM
C***CALCULATE THE SKY DIFFUSE RADIATION***
CC=1.0
HBDR2=0.78+1.07*ALT+6.17*CC
DIFF1A=HBDR2*((1.0+COS(TILTR))/2.0)
DIFF1=HBDR*((1.0+COS(TILTR))/2.0)
C***CALCULATE THE REFLECTED GROUND RADIATION***
R0=0.2
DIFF2=S0*((1.0-COS(TILTR))*R0)/2.0
C***CALCULATE THE INCIDENT RADIATION ABSORBED BY THE COLLECTOR
COS2I=COSI*COSI
COS3I=COS2I*COSI
COS4I=COS3I*COSI
COS5I=COS4I*COSI
C***TRANSMISSION COEFFICIENT FOR DIRECT RADIATION***
TDIR=-0.00385+2.71235*COSI-0.62062*COS2I
1-7.07329*COS3I+9.75995*COS4I-3.89922*COS5I
C***ABSORPTION COEFFICIENT FOR DIRECT RADIATION***
ADIR=0.01154+0.77674*COSI-3.94657*COS2I
1+8.57331*COS3I-3.38135*COS4I+3.01188*COS5I
C***REFLECTION COEFFICIENT FOR DIRECT RADIATION***
RDIR=1.0-TDIR-ADIR
C***TRANSMISSION AND ABSORPTION COEFFS. FOR DIFFUSE RADIATION
TDIF=0.796;ADIF=0.056
C***REFLECTION COEFFICIENT FOR DIFFUSE RADIATION***
RDIF=1.0-TDIF-ADIF
C***ABSORPTION COEFFICIENT FOR COLLECTOR SURFACE***
C***1-MATT BLACK SURFACE***
IF(ABS.EQ.1.0)CALL ABSORB(COSI,ACOL)
C***2-SELECTIVE SURFACE***
IF(ABS.EQ.2.0)ACOL=0.96
C***REFLECTION COEFFICIENT FOR COLLECTOR SURFACE***
RCOL=1.0-ACOL
ABTR1=TDIR*ACOL/(1.0-(1.0-ACOL)*RDIR)
ABTR2=TDIF*ACOL/(1.0-(1.0-ACOL)*RDIF)
IF(NSHAD.NE.0)GO TO 500
400 S1=ADIF*(DIFF1+DIFF2)+(ADIR)*DIRS
S2=ABTR2*(DIFF1+DIFF2)+ABTR1*DIRS
GO TO 700
500 S1=ADIF*(DIFF1+DIFF2)
S2=ABTR2*(DIFF1+DIFF2)
GO TO 700
600 S1=0.0
S2=0.0
700 RETURN
END
C
C
SUBROUTINE SHADE1(AZI,ALT,NSHAD1)
DIMENSION DAT1(6,3),DAT2(8),ST(4),TS1(10),TS2(10),
1 DAT3(10),SS(6),TS3(3),DAT4(2)

```

```

COMMON DAT1,DAT2,ST,TS1,TS2,DAT3,SS,TS3,DAT4
TILT=DAT1(4,2)
WAZI=DAT1(5,8)
RAD=2.017453293
ALTR=ALT*RAD
HSA=AZI-WAZI
TILT=180.0-TILT
IF(HSA.GT.180.0)HSA=HSA-360.0
TANAR=SIN(ALTR)/COS(ALTR)
VSA=ATAN(TANAR/COS(HSA*RAD))
VSA=VSA/RAD
IF(HSA.GT.90.0.OR.HSA.LT.-90.0)VSA=VSA+180.0
NSHAD1=0
IF(HSA.GT.90.0.OR.HSA.LT.-90.0)NSHAD1=1
IF(VSA.LE.TILT)NSHAD1=0
IF(VSA.GT.TILT)NSHAD1=1
GO TO 600
RETURN
END

```

600

C

```

SUBROUTINE MAINST(DAY,TCW)
C***SUBROUTINE TO CALCULATE THE COLD WATER INLET TEMPERATURE
C***TO THE SOLAR STORAGE TANK WHICH IS ASSUMED TO VARY OVER
C***THE YEAR AS GIVEN BELOW, FROM BRINKWORTH*****
PI=3.14159265
DAY=DAY+11.25
TCW=9.0-3.0*COS((2.0*PI/365.0)*DAY)
RETURN
END

```

C

```

SUBROUTINE MODS(DT)
DIMENSION DAT1(6,8),DAT2(8),DAT3(10),CM(3,6),TS1(10),
1 TS2(10),TS3(3),ST(4),SS(6),CT(3),DAT4(2)
COMMON DAT1,DAT2,ST,TS1,TS2,DAT3,SS,TS3,DAT4
C***INITIALISE MATRIX CALCULATION COMPONENTS***
SS(2)=TS3(1)
SS(3)=TS3(2)
SS(4)=TS3(3)

```

C

```

W3=DAT3(1)
W4=DAT3(2)
W5=DAT3(3)

```

C

```

A4=DAT3(4)
A5=DAT3(5)
A6=DAT3(6)

```

C

```

B4=DAT3(7)
B5=DAT3(8)
B6=DAT3(9)
B7=DAT3(10)

```

```

C***INITIALISE THE FIRST ROW OF THE CALCULATION MATRIX***
C3=DT/(W3)
CM(1,1)=C3*B4
CM(1,2)=-C3*(B4+B5+A4)
CM(1,3)=C3*B5
CM(1,4)=2.0

```



```

      CM(1,5)=0.0
      CM(1,6)=C3*A4
C***INITIALISE THE SECOND ROW OF THE CALCULATION MATRIX***
      C4=DT/W4
      CM(2,1)=C4*B6
      CM(2,2)=C4*B4
      CM(2,3)=-C4*(B4+B5+B6+A5)
      CM(2,4)=0.0
      CM(2,5)=0.0
      CM(2,6)=C4*A5
C***INITIALISE THE THIRD ROW OF THE CALCULATION MATRIX***
      C5=DT/(W5)
      CM(3,1)=C5*B7
      CM(3,2)=0.0
      CM(3,3)=C5*(B4+B6)
      CM(3,4)=-C5*(B4+B5+B7+A6)
      CM(3,5)=C5*B5
      CM(3,6)=C5*A6
C***START QUARTIC RUNGE-KUTTA METHOD CALCULATION***
      IROW=0
100    IROW=IROW+1
      DO 300 I=1,2
        I1=I
        SUM=0.0
        W=1.0/FLOAT(2**((I1-1)))
        DO 200 K=1,6
200    SUM=SUM+CM(IROW,K)*SS(K)
        Y=SUM
C***PREDICTED VALUE OF SEGMENT TEMPERATURE***
        QK1=W*Y
        QK2=W*(Y+(QK1/2.0))
        QK3=W*(Y+(QK2/2.0))
        QK4=W*(Y+QK3)
        CT(IROW)=SS(IROW+1)+(QK1+(2.0*QK2)+(2.0*QK3)+QK4)/6.0
300    SS(IROW+1)=CT(IROW)
        IF(IROW.EQ.3)GO TO 400
        GO TO 100
400    TS3(1)=SS(2)
        TS3(2)=SS(3)
        TS3(3)=SS(4)
        RETURN
      END
C
C
C
      SUBROUTINE MENU9(NPV)
      DIMENSION MODUL9(56)
C***MENU9*****
C***1SYNOP*****
C***2PRINT*****
C***3PIECH*****
C***4BARCH*****
C***5END*****
      DATA MODUL9/32,32,77,69,73,85,57,32,
1 32,49,83,89,73,79,80,32,
2 32,50,80,82,73,78,84,32,
3 32,51,80,73,69,67,72,32,

```


4 32, 52, 66, 65, 32, 67, 72, 32,
 5 32, 53, 69, 78, 63, 3*32,
 6 3*32/

C***CALL CHAR SIZE***

100 CALL CSIZE(ICHORSZ, KVERSZ)

C***GO TO MENU POSITION***

CALL NEWPAG

CALL MOVREL(0, -600)

C***OUTPUT MODUL9 CHARS***

K=0

DO 200 J=1, 7

CALL NEWLIN

DO 200 I=1, 8

K=K+1

CALL ANCHO(MODUL9(K))

200 CONTINUE

C***DRAW BOX AROUND MENU***

CALL MOVREL(-660, 0)

CALL DRWREL(0, 2*KVERSZ)

CALL DRWREL(-2*KHORSZ, 0)

CALL DRWREL(0, -2*KVERSZ)

CALL DRWREL(2*KHORSZ, 0)

C***CURSOR COMMAND MODE***

CALL DCURS(ICHAR, IX, IY)

CALL BELL

CALL NEWPAG

CALL A'MODE

C***IDENTIFY ICHAR CONDITION***

IF(ICHAR.EQ.49)GO TO 300

IF(ICHAR.EQ.50)GO TO 400

IF(ICHAR.EQ.51)GO TO 500

IF(ICHAR.EQ.52)GO TO 600

IF(ICHAR.EQ.53)GO TO 700

C***PRINT SYNOPTIC OUTPUT OF RESULTS***

300 NPV=100

GO TO 800

C***PRINT FULL OUTPUT OF RESULTS***

400 NPV=200

GO TO 800

C***DRAW PIECHART OF SYNOPTIC OUTPUT OF RESULTS***

500 NPV=300

GO TO 800

C***DRAW BARCHART OF SYNOPTIC OUTPUT OF RESULTS***

600 NPV=400

GO TO 800

C***RETURN TO MENU1 COMMAND LEVEL***

700 NPV=999

300 RETURN

END

C

C

C

SUBROUTINE SOLHT(DOV, SOLG, AUKG)

DIMENSION DAT1(6, 3), DAT2(8), ST(4), TS1(10), TS2(10),

1 DAT3(10), SS(6), TS3(3), DAT4(2)

COMMON DAT1, DAT2, ST, TS1, TS2, DAT3, SS, TS3, DAT4

C***INITIALISE STORAGE TANK TEMPERATURES***


```

DDT=DAT1(6,3)
SSV=DAT1(6,2)/1000.2
T3=SS(2)
T4=SS(3)
T5=SS(4)
TCW=SS(5)
C***CALCULATE THE VOLUME OF WATER DRAWN OFF***
VOL=DOV/1000.0
C***CALCULATE THE HEAT SUPPLIED BY THE SOLAR SYSTEM***
C***CALCULATE THE AUXILIARY HEAT REQUIREMENT*****
IF(VOL.EQ.0.0)GO TO 100
IF(VOL.LE.(SSV/3.0))GO TO 200
IF(VOL.GT.(SSV/3.0).AND.VOL.LE.(SSV/1.5))GO TO 300
IF(VOL.GT.(SSV/1.5).AND.VOL.LE.SSV)GO TO 400
IF(VOL.GT.SSV)GO TO 500
100 SOLG=0.0; AUXG=0.0
GO TO 600
200 SOLG=CPRO(T3)*VOL*(T3-TCW)
AUXG=(CPRO(TCW)*(DDT-TCW)*VOL)-SOLG
GO TO 600
300 SOLG=CPRO(T3)*(SSV/3.0)*(T3-TCW)+CPRO(T4)
1*(VOL-(SSV/3.0))*(T4-TCW)
AUXG=(CPRO(TCW)*(DDT-TCW)*VOL)-SOLG
GO TO 600
400 SOLG=CPRO(T3)*(SSV/3.0)*(T3-TCW)+CPRO(T4)
1*(SSV/3.0)*(T4-TCW)+CPRO(T5)*(VOL-(SSV/1.5))
2*(T5-TCW)
AUXG=(CPRO(TCW)*(DDT-TCW)*VOL)-SOLG
GO TO 600
500 SOLG=CPRO(T3)*(SSV/3.0)*(T3-TCW)+CPRO(T4)*
1(SSV/3.0)*(T4-TCW)+CPRO(T5)*(SSV/3.0)*(T5-TCW)
AUXG=(CPRO(TCW)*(DDT-TCW)*VOL)-SOLG
600 RETURN
END

C
SUBROUTINE WAIT1
TYPE 10
10 FORMAT('H IO WAIT, PRESS RETURN TO CONTINUE')
ACCEPT 20, A
20 FORMAT(F)
RETURN
END

C
C
SUBROUTINE PIECHT(SHW,PE,AHW,TL)
DIMENSION ENERGY(4),LABEL1(4),LABEL2(7)
C***PIECHART LABEL***
DATA LABEL1/3H A.,3H B.,3H C.,3H D./
C***INITIALISE PIECHART VALUES***
CALL PICCLE
ENERGY(1)=SHW
ENERGY(2)=PE
ENERGY(3)=AHW
ENERGY(4)=TL
C***DEFINE PIECHART FRAME***
CALL PIEPAP(40.0,110.0,80.0)
C***DRAW ANNOTATED PIECHART***

```

```

CALL PIECH(ENERGY,LABEL1,4,1,3,1)
C***INITIALISE PIECHART HEADING AND TITLES***
LABEL2(1)=5HA. SO
LABEL2(2)=5HLAR H
LABEL2(3)=5HOT WA
LABEL2(4)=5HTER.
CALL MOVT02(10.0,30.0)
CALL CHAARR(LABEL2,4,5)
LABEL2(1)=5HB. PU
LABEL2(2)=5HMP EN
LABEL2(3)=5HERGY.
CALL MOVT02(10.0,26.0)
CALL CHAARR(LABEL2,3,5)
LABEL2(1)=5HC. AU
LABEL2(2)=5HXILIA
LABEL2(3)=5HRY HO
LABEL2(4)=5HT WAT
LABEL2(5)=5HER.
CALL MOVT02(10.0,22.0)
CALL CHAARR(LABEL2,5,5)
LABEL2(1)=5HD. TA
LABEL2(2)=5HNK LO
LABEL2(3)=5HSSSES.
CALL MOVT02(10.0,18.0)
CALL CHAARR(LABEL2,3,5)
LABEL2(1)=5HENERG
LABEL2(2)=5HY BRE
LABEL2(3)=5HAKDOW
LABEL2(4)=5HN TOT
LABEL2(5)=5HAL SY
LABEL2(6)=5HSTEM.
CALL MOVT02(10.0,12.0)
CALL CHAARR(LABEL2,6,5)
CALL MOVT02(10.0,6.0)
RETURN
END

C
SUBROUTINE PILOS(DT,PTEMP,OUTLT)
DIMENSION DAT1(6,8),DAT2(8),CM(1,2),TS1(10),TS2(10),
1 CT(1),ST(4),DAT3(10),SS(6),TS3(3),DAT4(2),TS4(2)
COMMON DAT1,DAT2,ST,TS1,TS2,DAT3,SS,TS3,DAT4
C***INITIALISE MATRIX CALCULATION COMPONENTS***
TS4(1)=PTEMP
TS4(2)=ST(4)
W6=DAT4(1)
A7=DAT4(2)
C***INITIALISE THE ROW OF THE CALCULATION MATRIX***
C6=DT/W6
CM(1,1)=C6*A7
CM(1,2)=-C6*A7
C***START QUARTIC RUNGE-KUTTA METHOD CALCULATION***
IROW=1
DO 300 I=1,2
I1=I
SUM=0.0
W=1.0/FLOAT(2**((I1-1)))
DO 200 K=1,2

```



```

200 SU1=SU1+CK(IROW,K)*TS4(K)
   Y=SU1
C***PREDICTED VALUE OF SEGMENT TEMPERATURE***
   QK1=W*Y
   QK2=W*(Y+(QK1/2.0))
   QK3=W*(Y+(QK2/2.0))
   QK4=W*(Y+QK3)
   CT(IROW)=TS4(IROW)-(QK1+(2.0*QK2)+(2.0*QK3)+QK4)/6.0
300 TS4(IROW)=CT(IROW)
   OUTLT=TS4(IROW)
   RETURN
END

C
C
SUBROUTINE ABSORB(COSI,ACOL)
  DIMENSION ABSC(9)
  DATA ABSC/3*0.96,0.95,0.93,0.91,0.88,0.81,0.66/
C***SUBPROGRAM TO CALCULATE THE ANGULAR VARIATION OF*****
C***ABSORPTANCE OF MATT BLACK PAINT. ADAPTED FROM LOF***
C***AND TYBOUT (1972). *****
  ANGI=ACOS(COSI)
  IANG=IFIX(ANGI)
  INC1=0; INC2=0
  KOUNT=0
100 INC2=INC2+10
  KOUNT=KOUNT+1
  IF(IANG.GE.INC1.AND.IANG.LT.INC2)GO TO 200
  INC1=INC2
  GO TO 100
200 ACOL=ABSC(KOUNT)
  RETURN
END

C
C
C
C***EXECUTIVE PROGRAM***
C
C
  DIMENSION DAT1(6,8),DAT2(8),ST(4),TS1(10),TS2(10),
  1 DAT3(10),SS(6),TS3(3),DAT4(2)
  COMMON DAT1,DAT2,ST,TS1,TS2,DAT3,SS,TS3,DAT4
C***INITIALISE MENU COMMAND PROGRAM***
  CALL INITT(120)
C***DEFINE TYPE OF OUTPUT DEVICE REQUIRED***
  CALL T4010
  CALL DEVSPE(1200)
  CALL MENU1
  CALL DEVEND
  CALL FINITT(0,730)
  END

```

Appendix 2.2.

STAPEL - Analysis of Experimental Results

The function of the computer program STAPEL is to analyse the papertape data output from the series of solar collector experiments. The subprogram structure and the operation of the program is illustrated in flowchart form in Figure A2.1. The program is fully listed.

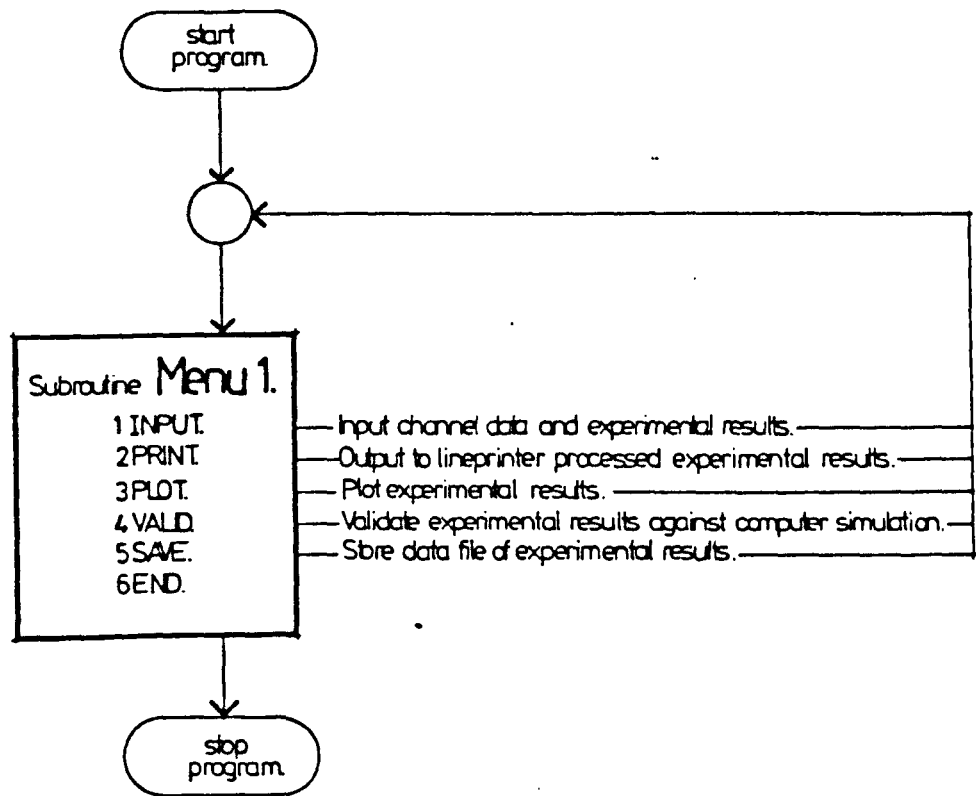


Figure A2.1 Flowchart representation of the analysis program STAPEL.


```

SUBROUTINE INPUT(NC, IT, KEND)
DIMENSION EXP(50, 1200), SPEC(50), KDATA(50), KRANGE(50),
1 NCHAN(50), DUM(50)
DOUBLE PRECISION FILE2, FILE
COMMON SPEC, EXP, FILE

C
C***SPECIFY FILENAME OF EXPERIMENT DATA RESULTS***
WRITE(5, 10)
10  FORMAT('H TYPE IN THE PARTICULAR EXPERIMENT DATA
1  FILENAME TO BE STUDIED'//)
READ(5, 20) FILE2
20  FORMAT(A10)
FILE=FILE2
WRITE(5, 30)
30  FORMAT('H TYPE IN THE NUMBER OF CHANNELS TO BE
1  INVESTIGATED'//)
READ(5, 40) NC
40  FORMAT(I)
WRITE(5, 50)
50  FORMAT('H SPECIFY THE TYPE OF CHANNEL DEVICES USED: '//
1  '(1-FILE INPUT, 2-TERMINAL INPUT)'//)
READ(5, 60) KDU
60  FORMAT(I)
IF(KDU.EQ.1) CALL CHAN1(NC)
IF(KDU.EQ.2) CALL CHAN2(NC)
WRITE(5, 70)
70  FORMAT('H TYPE IN EXPERIMENT TIME INTERVAL (MINS) : '//)
READ(5, 80) IT
80  FORMAT(I)
C***TRANSFER DATA FROM SPECIFIED FILE***
OPEN(UNIT=1, DEVICE='DSK', FILE=FILE2)
REWIND 1
K2=0
100  K2=K2+1
READ(1, 90, END=300, ERR=400) NTIME
90  FORMAT(I)
101  READ(1, 110, END=300, ERR=500) (NCHAN(I), DUM(I), KDATA(I),
1  KRANGE(I), I=1, NC)
110  FORMAT(5(I3, A1, I4, I1, 2X))
DO 200 J=1, NC
K1=J
IDATA=KDATA(K1)
IRANGE=KRANGE(K1)
IF(SPEC(K1).EQ.'T') CALL CALIB1(K2, IDATA, IRANGE, RDATA)
IF(SPEC(K1).EQ.'S') CALL CALIB2(K2, IDATA, IRANGE, RDATA)
IF(SPEC(K1).EQ.'F') CALL CALIB3(IDATA, IRANGE, RDATA)
EXP(K1, K2)=RDATA
200  CONTINUE
GO TO 100
300  ENDFILE 1
KEND=K2-1
CLOSE(UNIT=1, DEVICE='DSK', FILE=FILE2)
GO TO 700
400  WRITE(5, 410) FILE2
410  FORMAT('H ERROR FOUND IN READING CHANNEL TIME FROM
1  DISK FILE', A10, //)
WRITE(5, 420) NTIME

```



```

420     FORMAT('H NTIME = ', I5)
      WRITE(5, 430)
430     FORMAT('H TYPE C TO CONTINUE, OR A TO ABORT RUN'//)
      READ(5, 440) ANS1
440     FORMAT(A1)
      IF(ANS1.EQ.'C') GO TO 101
      IF(ANS1.EQ.'A') GO TO 300
      GO TO 700
500     WRITE(5, 510) FILE2
510     FORMAT('H ERROR FOUND IN READING CHANNEL DATA FROM
      1 DISK FILE', A10, //)
      WRITE(5, 520) NCHAN, DUM, KDATA(1), K RANGE(1)
520     FORMAT('H NCHAN = ', I3, //, 'DUM = ', A1, //, 'KDATA = ',
      1 I4, //, 'K RANGE = ', I1, //)
      WRITE(5, 525) K2
525     FORMAT('H NUMBER OF DATA = ', I)
      WRITE(5, 530)
530     FORMAT('H TYPE C TO CONTINUE, OR A TO ABORT RUN'//)
      READ(5, 540) ANS2
540     FORMAT(A1)
      IF(ANS2.EQ.'C') GO TO 101
      IF(ANS2.EQ.'A') GO TO 300
      GO TO 700
700     RETURN
      END

C
C
C
C
      SUBROUTINE CHAN1(NC)
      DIMENSION EXP(50, 1200), SPEC(50)
      DOUBLE PRECISION FILE1, FILE
      COMMON SPEC, EXP, FILE
C***SPECIFY FILENAME OF CHANNEL MEASUREMENT DEVICES***
      WRITE(5, 10)
10     FORMAT('H TYPE IN THE PARTICULAR CHANNEL MEASUREMENT
      1 DEVICES FILENAME', //, ' FOR THE EXPERIMENT'//)
      READ(5, 20) FILE1
20     FORMAT(A10)
C***TRANSFER DATA FROM SPECIFIED FILE***
      OPEN(UNIT=1, DEVICE='DSK', FILE=FILE1)
      REWIND 1
      READ(1, 30) (SPEC(I), I=1, NC)
30     FORMAT(A1)
      CLOSE(UNIT=1, DEVICE='DSK', FILE=FILE1)
      RETURN
      END

C
C
C
      SUBROUTINE CHAN2(NC)
      DIMENSION EXP(50, 1200), SPEC(50)
      DOUBLE PRECISION FILE1, FILE
      COMMON SPEC, EXP, FILE
C***IDENTIFY MEASUREMENT DEVICE FOR EACH CHANNEL***
      K=0
      WRITE(5, 10)

```

```

10  FORMAT('H IDENTIFY MEASUREMENT DEVICE FOR EACH
    1 CHANNEL '/' T-THERMOCOUPLE '/' F-FLOWMETER '/'
    2 ' S-SOLARIMETER '/')
    DO 100 I=1,NC
    K=K+1
    WRITE(5,20)K
20  FORMAT('H CHANNEL :',I)
    READ(5,30)SPEC(K)
30  FORMAT(A1)
100  CONTINUE
C***OPTION TO TRANSFER ARRAY DATA TO FILE***
    WRITE(5,40)
40  FORMAT('H DO YOU WISH TO SAVE CHANNEL SPECIFICATIONS
    1 ! '/' 0-NO, 1-YES '/')
    READ(5,50)NAME
50  FORMAT(I)
    IF(NAME.EQ.0)GO TO 200
C***SPECIFY FILENAME OF CHANNEL MEASUREMENT DEVICES***
    WRITE(5,60)
60  FORMAT('H TYPE IN THE PARTICULAR CHANNEL MEASUREMENT
    1 DEVICES FILENAME FOR THE EXPERIMENT '/')
    READ(5,70)FILE1
70  FORMAT(A10)
C***TRANSFER DATA FROM ARRAY TO SPECIFIED FILE***
    OPEN(UNIT=5, DEVICE='DSK', FILE=FILE1)
    REWIND 1
    WRITE(5,80)(SPEC(I),I=1,NC)
80  FORMAT(A1)
    CLOSE(UNIT=5, DEVICE='DSK', FILE=FILE1)
200  RETURN
    END
C
C
C
    SUBROUTINE MENU1
    DIMENSION MODUL1(56)
C***STAPEL***
C***1INPUT***
C***2PRINT***
C***3PLOT ***
C***4VALID***
C***5SAVE ***
C***6END ***
    DATA MODUL1/32,83,84,65,80,69,76,32,
    1 32,49,73,78,80,85,84,32,
    2 32,50,80,82,73,78,84,32,
    3 32,51,80,76,79,84,32,32,
    4 32,52,86,65,76,73,68,32,
    5 32,53,83,65,86,69,32,32,
    6 32,54,69,78,68,3*32/
C***CALL CHARACTER SIZE***
100  CALL CSIZE(KHORSZ,KVERSZ)
C***GO TO MENU POSITION***
    CALL NEWPAG
    CALL MOVREL(0,-600)
C***OUTPUT MODUL1 CHARACTERS***
    K=0

```



```

12      DO 200 J=1,7
        CALL NEWLIN
        DO 200 I=1,8
        K=K+1
        CALL ANCHO(MODULI(K))
200     CONTINUE
C***CURSOR COMMAND MODE***
        CALL DCURSR(ICHAR,IX,IY)
        CALL BELL
        CALL NEWPAG
        CALL ANMODE
C***IDENTIFY ICHAR CONDITION***
        IF(ICHAR.EQ.49)GO TO 300
        IF(ICHAR.EQ.50)GO TO 400
        IF(ICHAR.EQ.51)GO TO 500
        IF(ICHAR.EQ.52)GO TO 600
        IF(ICHAR.EQ.53)GO TO 700
        IF(ICHAR.EQ.54)GO TO 800
        IF(ICHAR.LT.49.OR.ICHAR.GT.54)GO TO 100
C***INPUT CHANNEL DEVICE DATA AND EXPERIMENT RESULTS***
300     CALL INPUT(NCHAN,ITIME,KOUNT)
        GO TO 100
C***PRINT CHANNEL DEVICE DATA AND EXPERIMENT RESULTS***
C***OUTPUT IS TO LINEPRINTER***
400     CALL PRINT(NCHAN,ITIME,KOUNT)
        GO TO 100
C***PLOT EXPERIMENT RESULTS***
C***OUTPUT IS T4010*****
500     CALL PLOT(NCHAN,ITIME,KOUNT)
        GO TO 100
C***VALIDATE EXPERIMENT RESULTS AGAINST COMPUTER SIMULATION***
600     CALL VALID(NCHAN,ITIME,KOUNT)
        GO TO 100
C***SAVE FILE OF EXPERIMENT RESULTS***
700     CALL SAVEI(NCHAN,ITIME,KOUNT)
        GO TO 100
C***END OF PROGRAM***
800     RETURN
        END
C
        SUBROUTINE CALIB(KTIME,IDATA,IRANGE,TEMP)
        DIMENSION EXP(50,1200),SPEC(50)
        DOUBLE PRECISION FILE
        COMMON SPEC,EXP,FILE
C***THIS SUBPROGRAM CALIBRATES AND CONVERTS THE CHANNEL
C***VOLTAGE INTO DEGREES CENTIGRADE*****
C***CHANNEL VOLTAGE***
        RVOLT=FLOAT(IDATA)
C***DETERMINE PARTICULAR RANGE FOR CHANNEL***
C***CONVERT MICROVOLTS TO DEGREES CENTIGRADE*****
        IF(IRANGE.EQ.3)TEMP=(RVOLT/10.0)
        IF(IRANGE.EQ.4)TEMP=(RVOLT/(10.0))
        IF(RVOLT.GT.1000.0.AND. IRANGE.EQ.4)TEMP=(RVOLT/100.0)
        IF(IRANGE.NE.3.AND. IRANGE.NE.4)GO TO 100
        GO TO 200
100     CALL BELL
        WRITE(5,10)

```



```

10  FORMAT('H CALIBRATION ERROR!! THERMOCOUPLE VOLTAGE
    1 OUT OF RANGE!!')
    WRITE(5,300)KTIME
300  FORMAT('H DATA = ',1)
200  RETURN
    END

C
C
    SUBROUTINE CALIB2(KTIME,IVOLT,IRANGE,SOLRAD)
    DIMENSION EXP(50,1200),SPEC(50)
    DOUBLE PRECISION FILE
    COMMON SPEC,EXP,FILE

C***THIS SUBPROGRAM CALIBRATES AND CONVERTS THE CHANNEL VOLTAGE
C***INTO WATTS PER SQUARE METRE, FOR THE PARTICULAR KIPP AND
C***ZONEN SOLARIMETER UTILISED*****
C***CHANNEL VOLTAGE***
    RVOLT=FLOAT(IVOLT)
C***DETERMINE PARTICULAR RANGE FOR CHANNEL***
C***CONVERT MILLIVOLTS TO MILLIWATTS/SQUARE CENTIMETRE***
    IF(IRANGE.EQ.3)SVOLT=(RVOLT/(0.121*100.0))
    IF(IRANGE.EQ.4)SVOLT=(RVOLT/(0.121*4.0*100.0))
    IF(IRANGE.NE.3.AND.IRANGE.NE.4)GO TO 100
    GO TO 200
100  CALL BELL
    WRITE(5,10)
10  FORMAT('H CALIBRATION ERROR!! SOLARIMETER VOLTAGE
    1 OUT OF RANGE!!')
    WRITE(5,150)KTIME
150  FORMAT('H ERROR DATA = ',1)
    GO TO 300
C***CONVERT MILLIWATTS/SQUARE CENTIMETRE TO WATTS/SQUARE METRE**
200  SOLRAD=SVOLT*10.0
300  RETURN
    END

C
C
C
    SUBROUTINE CALIB3(IDATA,IRANGE,FLOW)
    DIMENSION EXP(50,1200),SPEC(50)
    DOUBLE PRECISION FILE
    COMMON SPEC,EXP,FILE

C***THIS SUBPROGRAM CALIBRATES AND CONVERTS THE CHANNEL
C***VOLTAGE INTO LITRES/MINUTE*****
C***CHANNEL VOLTAGE***
    RVOLT=FLOAT(IDATA)
C***DETERMINE PARTICULAR RANGE FOR CHANNEL***
C***CONVERT MILLIVOLTS TO LITRES/MINUTE*****
    IF(IRANGE.EQ.3)FLOW=(RVOLT/1000.0)
    IF(IRANGE.EQ.4)FLOW=(RVOLT/(100.0*4.0))
    IF(IRANGE.NE.3.AND.IRANGE.NE.4)GO TO 100
    GO TO 200
100  CALL BELL
    WRITE(5,10)
10  FORMAT('H CALIBRATION ERROR!! FLOWMETER VOLTAGE
    1 OUT OF RANGE!!')
    CALL BELL
200  RETURN

```



```

      END
C
C
C
SUBROUTINE PRINT(NCHAN, ITIME, KOUNT)
  DIMENSION EXP(50, 1200), SPEC(50), NRANGE(10)
  DOUBLE PRECISION FILE
  COMMON SPEC, EXP, FILE
C***HEADER TITLE***
  WRITE(5, 10)
10  FORMAT(' SOLAR ENERGY TEST FACILITIES', //,
20  1 ' SOLAR EXPERIMENT TEST RIG DATA TAPE PROCESSING
30  2 FACILITIES', //, ' INDOOR EXPERIMENTS-<STAPEL1>', //,
40  3 ' WRITTEN BY P. ROBERTSON, 1980.' //)
  WRITE(5, 20) FILE
20  FORMAT(' INDOOR TEST EXPERIMENT', IX, A10, //
30  1 ' CHANNEL SPECIFICATIONS:', //, ' T - CU/CON
40  2 THERMOCOUPLES <DEG.C.>', //, ' F - FLOWMETERS
50  3 <LITRE/MIN>', //, ' S - KIPP & ZONEV SOLARIMETERS
60  4 <WATTS/SQ.M.>' //)
C***TABLE HEADER***
  K1=1 ; NEND=10
100  WRITE(5, 30)
30  FORMAT(' CHANNEL NUMBER :')
  N=0
  DO 200 K2=K1, NEND
  N=N+1
200  NRANGE(N)=K2-1
  WRITE(5, 40) (NRANGE(I), I=1, N)
40  FORMAT(10(3X, I3))
  WRITE(5, 50) (SPEC(I), I=K1, NEND)
50  FORMAT(' CHANNEL DEVICE :', //, (10(5X, A1)))
  WRITE(5, 60) ITIME
60  FORMAT(' CHANNEL SCAN INTERVAL :', I3, ' MINUTES' //)
C***TABULATE VALUES***
  DO 300 K3=1, KOUNT
  WRITE(5, 70) K3, (EXP(NC, K3), NC=K1, NEND)
70  FORMAT(14, IX, (10(F5.1, IX)))
300  CONTINUE
C***TEST FOR END OF RANGE***
  IF(NCHAN.GE.(K1+10).AND.NCHAN.LE.(NEND+10))GO TO 400
  IF(NCHAN.GT.(NEND+10))GO TO 500
  GO TO 600
400  NADD=NCHAN-(K1+10)
  K1=K1+10
  NEND=K1+NADD
  IF(NADD.EQ.0)NEND=K1
  GO TO 100
500  K1=K1+10
  NEND=NEND+10
  GO TO 100
600  RETURN
  END
C
C
C
SUBROUTINE PLOT(NCHAN, ITIME, KOUNT)

```



```

        DIMENSION EXP(50,1200),SPEC(50),DX(1200),DY(1200),
        1 KPL0T(20),ICHAR(10)
        DOUBLE PRECISION FILE
        COMMON SPEC,EXP,FILE
C***INITIALISE NUMBER AND NAME OF CHANNELS TO BE PLOTTED***
100     WRITE(5,10)
10      FORMAT('H SPECIFY NUMBER OF CHANNELS TO BE PLOTTED'/)
        READ(5,20)NCP
20      FORMAT(1)
        IF(NCP.GT.NCHAN)WRITE(5,30)NCHAN
        IF(NCP.LE.NCHAN)GO TO 200
30      FORMAT('H ERROR!! AVAILABLE CHANNELS EQUALS :',12,
        1 /, 'PLEASE RETYPE VALUE'/)
        GO TO 100
200     DO 300 J1=1,NCP
        WRITE(5,40)
40      FORMAT('H CHANNEL NUMBER: ')
        READ(5,50)KPL0T(J1)
50      FORMAT(1)
300     CONTINUE
C
C***CLEAR DRAWING AREA***
        CALL PICCLE
C***DETERMINE PLOT TIME INTERVAL AND PERIOD***
        IF(itime.EQ.1)GO TO 310
        IF(itime.EQ.10)GO TO 320
        IF(itime.EQ.30)GO TO 330
        IF(itime.EQ.60)GO TO 340
C***SCAN INTERVAL : 1 MINUTE***
310     IF(KOUNT.LE.180)FACT=1.0
        IF(KOUNT.GT.180.AND.KOUNT.LE.1440)FACT=1.0/60.0
        IF(KOUNT.GT.1440)FACT=1.0/(60.0*24.0)
        GO TO 350
C***SCAN INTERVAL 10 MINUTES***
320     IF(KOUNT.LE.18)FACT=10.0
        IF(KOUNT.GT.18.AND.KOUNT.LE.144)FACT=1.0/6.0
        IF(KOUNT.GT.144)FACT=1.0/(6.0*24.0)
        GO TO 350
C***SCAN INTERVAL 30 MINUTES***
330     IF(KOUNT.GT.6.AND.KOUNT.LE.48)FACT=0.5
        IF(KOUNT.GT.48)FACT=1.0/48.0
        GO TO 350
C***SCAN INTERVAL 60 MINUTES***
340     FACT=1.0
        IF(KOUNT.GT.24)FACT=1.0/24.0
350     CONTINUE
C***INITIALISE X-AXIS VALUES***
        DO 400 J2=1,KOUNT
400     DX(J2)=(FLOAT(J2))*FACT
        J3=0
        IF(itime.GE.60)NHR=(itime/60)*KOUNT
        IF(itime.LT.60)NHR=((itime*KOUNT)/60)
        IF(NHR.LT.3)GO TO 410
        IF(NHR.GE.3.AND.NHR.LE.24)GO TO 420
        IF(NHR.GT.24)GO TO 430
410     NTEXT=1
        NIT=KOUNT/10

```

```

XEND=FLOAT(KOUNT*ITIME)
GO TO 450
420 NTEXT=2
NIT=NHR
XEND=FLOAT(NHR)+1.0
GO TO 450
430 NTEXT=3
NIT=NHR/24
XEND=FLOAT((NHR+12)/24)
450 CONTINUE
CDEV1=0.0
KVAL1=0; KVAL2=0
KVAL3=0
500 J3=J3+1
J4=KPLOT(J3)
CDEV=SPEC(J4)
IF(CDEV.EQ.'T')YEND=100.0
IF(CDEV.EQ.'F')YEND=10.0
IF(CDEV.EQ.'S')YEND=1000.0
IF(CDEV.EQ.'T')KVAL1=1
IF(CDEV.EQ.'F')KVAL2=1
IF(CDEV.EQ.'S')KVAL3=1
C***BEGIN GRAPH PLOT ROUTINE***
C***INITIALISE GRAPH PLOT VARIABLES***
550 CONTINUE
DO 600 J5=1,KOUNT
600 DY(J5)=EXP(J4,J5)
IF(CDEV1.EQ.0.0)GO TO 650
IF(CDEV1.EQ.CDEV)GO TO 700
650 CALL AXIPOS(1,30.0,30.0,120.0,1)
IF(CDEV.EQ.'T')CALL AXIPOS(1,30.0,30.0,100.0,2)
IF(CDEV.EQ.'F')CALL AXIPOS(1,150.0,30.0,100.0,2)
IF(CDEV.EQ.'S')CALL AXIPOS(1,150.0,30.0,100.0,2)
CALL AXISCA(3,NIT,0.0,XEND,1)
CALL AXISCA(3,20.0,0.0,YEND,2)
CALL AXIDRA(1,1,1)
IF(CDEV.EQ.'T')CALL AXIDRA(-1,-1,2)
IF(CDEV.EQ.'F')CALL AXIDRA(1,1,2)
IF(CDEV.EQ.'S')CALL AXIDRA(1,1,2)
CALL GRID(3,0,0)
700 CALL GRASYM(DX,DY,KOUNT,J3,2)
CALL GRAPOL(DX,DY,KOUNT)
CDEV1=CDEV
YSP=140.0-(7.0*(FLOAT(J3)))
CALL MOVT02(45.0,YSP)
CALL CHAHOL(12HCHANNEL *.)
CALL MOVT02(65.0,YSP)
CALL CHAINT(KPLOT(J3),2)
YSM=YSP+2.0
CALL MOVT02(75.0,YSM)
CALL SYMBOL(J3)
IF(J3.NE.NCP)GO TO 500
C***X-AXIS TEXT***
CALL MOVT02(75.0,15.0)
CALL CHAHOL(26H( EXPERIMENT TIME INTERVAL*.)
CALL MOVT02(75.0,10.0)
IF(NTEXT.EQ.1)CALL CHAHOL(11H(MINUTES)*.)

```



```

      IF(NTXT.EQ.2)CALL CHAHOL(9H(HOURS)*.)
      IF(NTXT.EQ.3)CALL CHAHOL(8H(DAYS)*.)
      IF(KVAL1.EQ.1)GO TO 750
      GO TO 800
750   CALL MOVTO2(0.0,133.0)
      CALL CHAHOL(20HTEMPERATURE DEG.C *.)
800   IF(KVAL2.EQ.1)GO TO 850
      GO TO 900
850   CALL MOVTO2(95.0,133.0)
      CALL CHAHOL(23HFLOW RATE LITRES/MIN.*.)
900   IF(KVAL3.EQ.1)GO TO 950
      GO TO 1000
950   CALL MOVTO2(92.0,133.0)
      CALL CHAHOL(24HSOLAR RADIATION (W/M2)*.)
1000  READ(5,60)WAIT
60    FORMAT(A1)
      RETURN
      END

C
C
C
      SUBROUTINE SAVE1(NCHAN,ITIME,KOUNT)
      DIMENSION EXP(50,1200),SPEC(50)
      DOUBLE PRECISION FILE,FILE3
      COMMON SPEC,EXP,FILE
C***OPTION TO TRANSFER PROCESSED EXPERIMENT DATA TO FILE***
      WRITE(5,10)
10    FORMAT('H DO YOU WISH TO SAVE PROCESSED EXPERIMENT
      1 DATA ?','/, 'H0-NO, 1-YES'/)
      READ(5,20)NUMB
20    FORMAT(I)
      IF(NUMB.EQ.0)GO TO 100
C***SPECIFY FILENAME OF EXPERIMENT DATA***
      WRITE(5,30)
30    FORMAT('H TYPE IN THE FILENAME FOR THE EXPERIMENT'/)
      READ(5,40)FILE3
40    FORMAT(A10)
C***TRANSFER DATA FROM ARRAY TO SPECIFIED FILE***
      OPEN(UNIT=5,DEVICE='DSK',FILE=FILE3)
      REWIND 1
      CALL PRINT(NCHAN,ITIME,KOUNT)
      CLOSE(UNIT=5,DEVICE='DSK',FILE=FILE3,DISPOSE='PRINT')
100   RETURN
      END

C
C
C
C
      SUBROUTINE VALID(NCHAN,ITIME,KOUNT)
      DIMENSION EXP(50,1200),SPEC(50)
      DOUBLE PRECISION FILE,FILE4
      COMMON SPEC,EXP,FILE
C***OPTION TO TRANSFER EXPERIMENT DATA ARRAY TO FILE***
100   WRITE(5,10)
10    FORMAT('H DO YOU WISH TO SAVE EXPERIMENT DATA ON
      1 DISK FILE ?','/, 'H 0-NO, 1-YES'/)
      READ(5,20)NANS

```

```

20  FORMAT(1)
   IF(NANS.EQ.0)GO TO 300
C***SPECIFY THE DATA CHANNEL NUMBER TO BE UTILISED IN VALIDATION
   WRITE(5,25)
25  FORMAT('H TYPE IN THE PARTICULAR DATA CHANNEL REQUIRED')
   READ(5,27)NVAD
27  FORMAT(1)
C***SPECIFY FILENAME OF EXPERIMENT DATA***
   WRITE(5,30)
30  FORMAT('H TYPE IN THE PARTICULAR EXPERIMENT DATA
      1 FILENAME: '/')
   READ(5,40)FILE4
40  FORMAT(A10)
C***TRANSFER DATA FROM ARRAY TO SPECIFIED FILE***
   OPEN(UNIT=5, DEVICE='DSK', FILE=FILE4)
   REWIND 1
   J1=NVAD
   J2=0
   DO 1000 K1=1,KOUNT
     J2=J2+1
     WRITE(5,60,ERR=200)EXP(J1,J2)
60  FORMAT(20F)
1000 CONTINUE
     CLOSE(UNIT=5, DEVICE='DSK', FILE=FILE4)
     GO TO 300
200  WRITE(5,70)FILE4
70  FORMAT('H ERROR IN READING ARRAY TO DISK FILE',A10)
     GO TO 100
300  RETURN
     END

C
C
C
C***EXECUTIVE PROGRAM***
   CALL INITT(120)
   CALL T4010
   CALL DEVSPE(1200)
   CALL MENU1
   CALL DEVEND
   CALL FINITT(0,780)
   END

```


Appendix 2.3.

MONITR - Analysis of Monitored Installation Results

The function of the computer program MONITR, based on the previous analysis program STAPEL, is to analyse the papertape data output from the data logger facility monitoring the performance of a commercial solar water heating installation. The sub-program is illustrated in flowchart form in Figure A2.2. The program is fully listed.

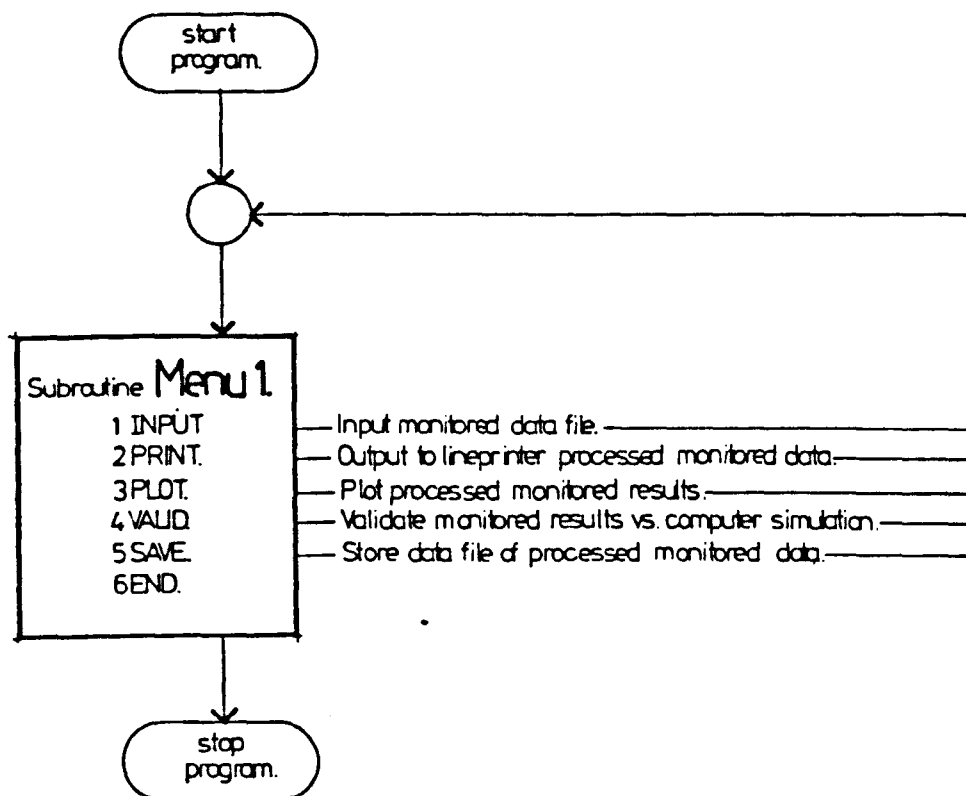


Figure A2.2 Flowchart representation of the analysis program MONITR.

```

SUBROUTINE INPUT( IC, IT, IEND)
DIMENSION EXP(50,1200),SPEC(50),IDATA(50),KDATA(50),
1 NCHAN(50),DUM(50)
DOUBLE PRECISION FILE2, FILE
COMMON SPEC, EXP, FILE
C***SPECIFY FILENAME OF EXPERIMENT DATA RESULTS***
WRITE(5,10)
10  FORMAT('H TYPE IN THE PARTICULAR EXPERIMENT DATA
1  FILENAME TO BE STUDIED')
READ(5,20)FILE2
20  FORMAT(A10)
FILE=FILE2
WRITE(5,30)
30  FORMAT('H TYPE IN THE NUMBER OF CHANNELS TO BE
1  INVESTIGATED')
READ(5,40)NC
40  FORMAT(I)
WRITE(5,50)
50  FORMAT('H SPECIFY THE TYPE OF CHANNEL DEVICES USED: '
1  '(1-FILE INPUT, 2-TERMINAL INPUT)')
READ(5,60)KDU
60  FORMAT(I)
IF(KDU.EQ.1)CALL CHAN1(NC)
IF(KDU.EQ.2)CALL CHAN2(NC)
WRITE(5,70)
70  FORMAT('H TYPE IN EXPERIMENT TIME INTERVAL (MINS) : ')
READ(5,80)IT
80  FORMAT(I)
C***TRANSFER DATA FROM SPECIFIED FILE***
OPEN(UNIT=1, DEVICE='DSK', FILE=FILE2)
REWIND 1
K2=0
100  K2=K2+1
READ(1,90,END=300,ERR=400)NTIME
90  FORMAT(I)
101  READ(1,110,END=300,ERR=500)(NCHAN(I),DUM(I),KDATA(I),
1  KDATA(I),I=1,NC)
110  FORMAT(5(I3,A1,I4,I1,2X))
DO 200 J=1,NC
K1=J
IDATA=KDATA(K1)
IRANGE=KDATA(K1)
IF(SPEC(K1).EQ.'T')CALL CALIB1(K2,IDATA,IRANGE,RDATA)
IF(SPEC(K1).EQ.'S')CALL CALIB2(K2,IDATA,IRANGE,RDATA)
IF(SPEC(K1).EQ.'F')CALL CALIB3(IDATA,IRANGE,RDATA)
EXP(K1,K2)=RDATA
200  CONTINUE
GO TO 100
300  ENDFILE 1
KEND=K2-1
CLOSE(UNIT=1, DEVICE='DSK', FILE=FILE2)
GO TO 700
400  WRITE(5,410)FILE2
410  FORMAT('H ERROR FOUND IN READING CHANNEL TIME FROM
1  DISK FILE',A10,/)
WRITE(5,420)NTIME
420  FORMAT('H NTIME =',I5)

```



```

WRITE(5,430)
430  FORMAT('H TYPE C TO CONTINUE OR A TO ABORT RUN')
READ(5,440)ANS1
440  FORMAT(A1)
      IF(ANS1.EQ.'C')GO TO 101
      IF(ANS1.EQ.'A')GO TO 302
      GO TO 700
500  WRITE(5,510)FILL2
510  FORMAT('H ERROR FOUND IN READING CHANNEL DATA FROM
      1 DISK FILE',A10,/)
      WRITE(5,520)NCHAN,DUM,KDATA(1),K RANGE(1)
520  FORMAT('HCHAN =',I3,/, 'DUM =',A1,/, 'KDATA =',
      1 I4,/, 'K RANGE =',I1,/)
      WRITE(5,525)K2
525  FORMAT('H NUMBER OF DATA = ',I)
      WRITE(5,530)
530  FORMAT('H TYPE C TO CONTINUE OR A TO ABORT RUN')
READ(5,540)ANS2
540  FORMAT(A1)
      IF(ANS2.EQ.'C')GO TO 101
      IF(ANS2.EQ.'A')GO TO 302
      GO TO 700
700  RETURN
      END

C
C
C
C
      SUBROUTINE CHAN1(NC)
      DIMENSION EXP(50,1200),SPEC(50)
      DOUBLE PRECISION FILE1,FILE
      COMMON SPEC,EXP,FILE
C***SPECIFY FILENAME OF CHANNEL MEASUREMENT DEVICES***
      WRITE(5,10)
10   FORMAT('H TYPE IN THE PARTICULAR CHANNEL MEASUREMENT
      1 DEVICES FILENAME',/, ' FOR THE EXPERIMENT')
      READ(5,20)FILE1
20   FORMAT(A10)
C***TRANSFER DATA FROM SPECIFIED FILE***
      OPEN(UNIT=1,DEVICE='DSK',FILE=FILE1)
      REWIND 1
      READ(1,30)(SPEC(I),I=1,NC)
30   FORMAT(A1)
      CLOSE(UNIT=1,DEVICE='DSK',FILE=FILE1)
      RETURN
      END

C
C
C
      SUBROUTINE CHAN2(NC)
      DIMENSION EXP(50,1200),SPEC(50)
      DOUBLE PRECISION FILE1,FILE
      COMMON SPEC,EXP,FILE
C***IDENTIFY MEASUREMENT DEVICE FOR EACH CHANNEL***
      K=0
      WRITE(5,10)
10   FORMAT('H IDENTIFY MEASUREMENT DEVICE FOR EACH

```

```

1 CHANNEL '/' T-THERMOCOUPLE '/' F-FLOWMETER '/'
2 ' S-SOLARIMETER '/'
DO 100 I=1,NC
K=K+1
WRITE(5,20)K
20  FORMAT('H CHANNEL :',I)
    READ(5,30)SPEC(K)
30  FORMAT(A1)
100  CONTINUE
C***OPTION TO TRANSFER ARRAY DATA TO FILE***
    WRITE(5,40)
40  FORMAT('H DO YOU WISH TO SAVE CHANNEL SPECIFICATIONS
1 ! '/' 0-NO, 1-YES '/')
    READ(5,50)NAME
50  FORMAT(I)
    IF(NAME.EQ.0)GO TO 200
C***SPECIFY FILENAME OF CHANNEL MEASUREMENT DEVICES***
    WRITE(5,60)
60  FORMAT('H TYPE IN THE PARTICULAR CHANNEL MEASUREMENT
1 DEVICES FILENAME FOR THE EXPERIMENT '/')
    READ(5,70)FILE1
70  FORMAT(A10)
C***TRANSFER DATA FROM ARRAY TO SPECIFIED FILE***
    OPEN(UNIT=5,DEVICE='DSK',FILE=FILE1)
    REWIND 1
    WRITE(5,80)(SPEC(I),I=1,NC)
80  FORMAT(A1)
    CLOSE(UNIT=5,DEVICE='DSK',FILE=FILE1)
200  RETURN
    END

C
C
C
      SUBROUTINE MENU1
      DIMENSION MODUL1(56)
C***STAPEL***
C***1INPUT***
C***2PRINT***
C***3PLOT ***
C***4VALID***
C***5SAVE ***
C***6END ***
      DATA MODUL1/32,33,34,65,30,69,76,32,
1 32,49,73,78,30,85,34,32,
2 32,50,80,32,73,78,34,32,
3 32,51,30,76,79,34,32,32,
4 32,52,36,65,76,73,63,32,
5 32,53,33,65,86,69,32,32,
6 32,54,69,78,63,3*32/
C***CALL CHARACTER SIZE***
100  CALL CSIZE(KHORSZ,KVERSZ)
C***GO TO MENU POSITION***
    CALL NEWPAG
    CALL MOVREL(0,-600)
C***OUTPUT MODUL1 CHARACTERS***
    K=0
    DO 200 J=1,7

```



```

      CALL NEWLIN
      DO 200 I=1,3
      K=K+1
      CALL ANCHO(MODUL(K))
200   CONTINUE
C***DRAW BOX AROUND MENU***
      CALL MOVREL(-660,0)
      CALL DRWREL(0,2*KVERSZ)
      CALL DRWREL(-2*KHORSZ,0)
      CALL DRWREL(0,-2*KVERSZ)
      CALL DRWREL(2*KHORSZ,0)
C***CURSOR COMMAND MODE***
      CALL DCURSR(ICAR,IX,IY)
      CALL BELL
      CALL NEWPAGE
      CALL ANMODE
C***IDENTIFY ICAR CONDITION***
      IF(ICAR.EQ.49)GO TO 300
      IF(ICAR.EQ.50)GO TO 400
      IF(ICAR.EQ.51)GO TO 500
      IF(ICAR.EQ.52)GO TO 600
      IF(ICAR.EQ.53)GO TO 700
      IF(ICAR.EQ.54)GO TO 800
      IF(ICAR.LT.49.OR.ICAR.GT.54)GO TO 100
C***INPUT CHANNEL DEVICE DATA AND EXPERIMENT RESULTS***
300   CALL INPUT(NCHAN,ITIME,KOUNT)
      GO TO 100
C***PRINT CHANNEL DEVICE DATA AND EXPERIMENT RESULTS***
C***OUTPUT IS TO LINEPRINTER***
400   CALL PRINT(NCHAN,ITIME,KOUNT)
      GO TO 100
C***PLOT EXPERIMENT RESULTS***
C***OUTPUT IS T4010*****
500   CALL PLOT(NCHAN,ITIME,KOUNT)
      GO TO 100
C***VALIDATE EXPERIMENT RESULTS AGAINST COMPUTER SIMULATION***
600   CALL VALID(NCHAN,ITIME,KOUNT)
      GO TO 100
C***SAVE FILE OF EXPERIMENT RESULTS***
700   CALL SAVE(NCHAN,ITIME,KOUNT)
      GO TO 100
C***END OF PROGRAM***
800   RETURN
      END
C
      SUBROUTINE CALIB(KTIME,IDATA,IRANGE,TEMP)
      DIMENSION EXP(50,1200),SPEC(50)
      DOUBLE PRECISION FILE
      COMMON SPEC,EXP,FILE
C***THIS SUBPROGRAM CALIBRATES AND CONVERTS THE CHANNEL
C***VOLTAGE INTO DEGREES CENTIGRADE*****
C***CHANNEL VOLTAGE***
      RVOLT=FLOAT(IDATA)
C***DETERMINE PARTICULAR RANGE FOR CHANNEL***
C***CONVERT MICROVOLTS TO DEGREES CENTIGRADE*****
      IF(IRANGE.EQ.3)TEMP=(RVOLT/10.0)
      IF(IRANGE.EQ.4)TEMP=(RVOLT/(12.0))

```



```

      IF(RVOLT.CT.1000.0)TRIP=RVOLT/100.0
      IF(IRANGE.NE.3.AND.IRANGE.NE.4)GO TO 100
      GO TO 200
100   CALL BELL
      WRITE(5,10)
10    FORMAT('H CALIBRATION ERROR!! THERMOCOUPLE VOLTAGE
      1 OUT OF RANGE!!')
      WRITE(5,300)KTIME
300   FORMAT('H DATA = ',1)
200   RETURN
      END

C
C
      SUBROUTINE CALIB2(KTIME,IVOLT,IRANGE,SOLRAD)
      DIMENSION EXP(50,1200),SPEC(50)
      DOUBLE PRECISION FILE
      COMMON SPEC,EXP,FILE
C***THIS SUBPROGRAM CALIBRATES AND CONVERTS THE CHANNEL VOLTAGE
C***INTO WATTS PER SQUARE METRE, FOR THE PARTICULAR KIPP AND
C***ZONEN SOLARIMETER UTILISED*****
C***CHANNEL VOLTAGE***
      RVOLT=FLOAT(IVOLT)
C***DETERMINE PARTICULAR RANGE FOR CHANNEL***
C***CONVERT MILLIVOLTS TO MILLIWATTS/SQUARE CENTIMETRE***
      IF(IRANGE.EQ.3)SVOLT=(RVOLT/(0.121*100.0))
      IF(IRANGE.EQ.4)SVOLT=(RVOLT/(0.121*4.0*100.0))
      IF(IRANGE.NE.3.AND.IRANGE.NE.4)GO TO 100
      GO TO 200
100   CALL BELL
      WRITE(5,10)
10    FORMAT('H CALIBRATION ERROR!! SOLARIMETER VOLTAGE
      1 OUT OF RANGE!!')
      WRITE(5,150)KTIME
150   FORMAT('H ERROR DATA = ',1)
      GO TO 300
C***CONVERT MILLIWATTS/SQUARE CENTIMETRE TO WATTS/SQUARE METRE**
200   SOLRAD=SVOLT*10.0
300   RETURN
      END

C
C
C
      SUBROUTINE CALIB3(IDATA,IRANGE,FLOW)
      DIMENSION EXP(50,1200),SPEC(50)
      DOUBLE PRECISION FILE
      COMMON SPEC,EXP,FILE
C***THIS SUBPROGRAM CALIBRATES AND CONVERTS THE CHANNEL
C***VOLTAGE INTO LITRES/MINUTE*****
C***CHANNEL VOLTAGE***
      RVOLT=FLOAT(IDATA)
C***DETERMINE PARTICULAR RANGE FOR CHANNEL***
C***CONVERT MILLIVOLTS TO LITRES/MINUTE*****
      IF(IRANGE.EQ.3)FLOW=(RVOLT/1000.0)
      IF(IRANGE.EQ.4)FLOW=(RVOLT/(100.0*4.0))
      IF(IRANGE.NE.3.AND.IRANGE.NE.4)GO TO 100
      GO TO 200
100   CALL BELL

```



```

WRITE(5,10)
10  FORMAT('H CALIBRATION ERROR!! FLOWMETER VOLTAGE
      1 OUT OF RANGE!!')
      CALL BELL
200  RETURN
      END
C
C
C
      SUBROUTINE PRINT(NCHAI,ITIME,KOUNT)
      DIMENSION EXP(50,1200),SPEC(50),NRANGE(10)
      DOUBLE PRECISION FILE
      COMMON SPEC,EXP,FILE
C***HEADER TITLE***
      WRITE(5,10)
10  FORMAT(' SOLAR ENRGY TEST FACILITIES',/,
      1 ' SOLAR EXPERIMENT TEST RIG DATA TAPE PROCESSING
      2 FACILITIES',/, ' INDOOR EXPERIMENTS-<STAPEL1>'
[SYSTEM GOING DOWN AT 23-APR-31 09:00:00]
/,
      3 ' WRITTEN BY P. ROBERTSON, 1930.'//)
      WRITE(5,20)FILE
20  FORMAT(' INDOOR TEST EXPERIMENT',IX,A10,/,
      1 ' CHANNEL SPECIFICATIONS:',/, ' T - CU/CON
      2 THERMOCOUPLES <DEG.C.>',/, ' F - FLOWMETERS
      3 <LITRE/MIN>',/, ' S - KIPP & ZONEV SOLARIMETERS
      4 <WATTS/SQ.M.>'//)
C***TABLE HEADER***
      K1=1 ; NEND=10
100  WRITE(5,30)
30  FORMAT(' CHANNEL NUMBER :')
      N=0
      DO 200 K2=K1,NEND
      N=N+1
200  NRANGE(N)=K2-1
      WRITE(5,40)(NRANGE(I),I=1,N)
40  FORMAT(10(3X,13))
      WRITE(5,50)(SPEC(I),I=K1,NEND)
50  FORMAT(' CHANNEL DEVICE:',/, (10(5X,A1)))
      WRITE(5,60)ITIME
60  FORMAT(' CHANNEL SCAN INTERVAL:',13,'MINUTES')
C***TABULATE VALUES***
      DO 300 K3=1,KOUNT
      WRITE(5,70)K3,(EXP(NC,K3),NC=K1,NEND)
70  FORMAT(14,IX,(10(F5.1,1X)))
300  CONTINUE
C***TEST FOR END OF RANGE***
C***END OF MONITORED DATA PERIOD***
      IF(NCHAI.GE.(K1+10).AND.NCHAI.LE.(NEND+10))GO TO 400
      IF(NCHAI.GT.(NEND+10))GO TO 500
      GO TO 600
400  NADD=NCHAI-(K1+10)
      K1=K1+10
      NEND=K1+NADD
      IF(NADD.EQ.0)NEND=K1
      GO TO 100
500  K1=K1+10
      NEND=NEND+10
      GO TO 100

```

```

622      RETURN
      END

C
C
C
SUBROUTINE PLOT(NCHAN,ITIME,KOUNT)
  DIMENSION EXP(50,1200),SPEC(50),EX(1200),DY(1200),
  1 KPLOT(20),ICHAR(10)
  DOUBLE PRECISION FILE
  COMMON SPEC,EXP,FILE
  C***INITIALISE NUMBER AND NAME OF CHANNELS TO BE PLOTTED***
100      WRITE(5,10)
10      FORMAT('H SPECIFY NUMBER OF CHANNELS TO BE PLOTTED'/)
      READ(5,20)NCP
20      FORMAT(I)
      IF(NCP.GT.NCHAN)WRITE(5,30)NCHAN
      IF(NCP.LE.NCHAN)GO TO 200
30      FORMAT('H ERROR!! AVAILABLE CHANNELS EQUALS :',I2,
  1 '/', 'PLEASE RETYPE VALUE'/)
      GO TO 100
200      DO 300 J1=1,NCP
      WRITE(5,40)
40      FORMAT('H CHANNEL NUMBER:')
      READ(5,50)KPLOT(J1)
50      FORMAT(I)
300      CONTINUE
C
C***CLEAR DRAWING AREA***
      CALL PICCLE
C***DETERMINE PLOT TIME INTERVAL AND PERIOD***
      IF(ITIME.EQ.1)GO TO 310
      IF(ITIME.EQ.10)GO TO 320
      IF(ITIME.EQ.30)GO TO 330
      IF(ITIME.EQ.60)GO TO 340
C***SCAN INTERVAL : 1 MINUTE***
310      IF(KOUNT.LE.180)FACT=1.0
      IF(KOUNT.GT.180.AND.KOUNT.LE.1440)FACT=1.0/60.0
      IF(KOUNT.GT.1440)FACT=1.0/(60.0*24.0)
      GO TO 350
C***SCAN INTERVAL 10 MINUTES***
320      IF(KOUNT.LE.18)FACT=10.0
      IF(KOUNT.GT.18.AND.KOUNT.LE.144)FACT=1.0/6.0
      IF(KOUNT.GT.144)FACT=1.0/(6.0*24.0)
      GO TO 350
C***SCAN INTERVAL 30 MINUTES***
330      IF(KOUNT.GT.6.AND.KOUNT.LE.48)FACT=0.5
      IF(KOUNT.GT.48)FACT=1.0/48.0
      GO TO 350
C***SCAN INTERVAL 60 MINUTES***
340      FACT=1.0
      IF(KOUNT.GT.24)FACT=1.0/24.0
350      CONTINUE
C***INITIALISE X-AXIS VALUES***
      DO 400 J2=1,KOUNT
400      EX(J2)=(FLOAT(J2))*FACT
      J3=0
      IF(ITIME.GE.60).NHR=(ITIME/60)*KOUNT

```



```

      IF(itime.lt.60).hr=((itime*kount)/60)
      IF(nhr.lt.3)GO TO 410
      IF(nhr.ge.3.and.nhr.le.24)GO TO 420
      IF(nhr.gt.24)GO TO 430
410   NTEXT=1
      NIT=kount/10
      XEND=FLOAT(kount*itime)
      GO TO 450
420   NTEXT=2
      NIT=nhr
      XEND=FLOAT(nhr)+1.0
      GO TO 450
430   NTEXT=3
      NIT=nhr/24
      XEND=FLOAT((nhr+12)/24)
450   CONTINUE
      CDEV1=0.0
      KVAL1=0; KVAL2=0
      KVAL3=0
500   J3=J3+1
      J4=kplot(J3)
      CDEV=SPEC(J4)
      IF(CDEV.EQ.'T')YEND=100.0
      IF(CDEV.EQ.'F')YEND=10.0
      IF(CDEV.EQ.'S')YEND=1000.0
      IF(CDEV.EQ.'T')KVAL1=1
      IF(CDEV.EQ.'F')KVAL2=1
      IF(CDEV.EQ.'S')KVAL3=1
C***BEGIN GRAPH PLOT ROUTINE***
C***INITIALISE GRAPH PLOT VARIABLES***
550   CONTINUE
      DO 600 J5=1,kount
600   DY(J5)=EXP(J4,J5)
      IF(CDEV1.EQ.0.0)GO TO 650
      IF(CDEV1.EQ.CDEV)GO TO 700
650   CALL AXIP0S(1,30.0,30.0,120.0,1)
      IF(CDEV.EQ.'T')CALL AXIP0S(1,30.0,30.0,100.0,2)
      IF(CDEV.EQ.'F')CALL AXIP0S(1,150.0,30.0,100.0,2)
      IF(CDEV.EQ.'S')CALL AXIP0S(1,150.0,30.0,100.0,2)
      CALL AXISCA(3,NIT,0.0,XEND,1)
      CALL AXISCA(3,20.0,0.0,YEND,2)
      CALL AXIDRA(1,1,1)
      IF(CDEV.EQ.'T')CALL AXIDRA(-1,-1,2)
      IF(CDEV.EQ.'F')CALL AXIDRA(1,1,2)
      IF(CDEV.EQ.'S')CALL AXIDRA(1,1,2)
      CALL GRID(3,0,0)
700   CALL GRASYM(DX,DY,kount,J3,23)
      CALL GRAPOL(DX,DY,kount)
      CDEV1=CDEV
      YSP=140.0-(7.0*(FLOAT(J3)))
      CALL MOVTO2(45.0,YSP)
      CALL CHAHOL(10CHANNEL *.)
      CALL MOVTO2(65.0,YSP)
      CALL CHAINT(kplot(J3),2)
      YSM=YSP+2.0
      CALL MOVTO2(75.0,YSM)
      CALL SYMBOL(J3)

```



```

      IF(J3.NE.NCP)GO TO 502
C***X-AXIS TEXT***
      CALL MOVT02(75.0,15.0)
      CALL CHAHOL(26H(EXPERIMENT TIME INTERVAL*.)
      CALL MOVT02(75.0,10.0)
      IF(NTEXT.EQ.1)CALL CHAHOL(11H(MINUTES)*.)
      IF(NTEXT.EQ.2)CALL CHAHOL(9H(HOURS)*.)
      IF(NTEXT.EQ.3)CALL CHAHOL(8H(DAYS)*.)
      IF(KVAL1.EQ.1)GO TO 750
      GO TO 800
750   CALL MOVT02(0.0,133.0)
      CALL CHAHOL(20H(TEMPERATURE DEG.C *.)
800   IF(KVAL2.EQ.1)GO TO 850
      GO TO 900
850   CALL MOVT02(95.0,133.0)
      CALL CHAHOL(23H(FLOW RATE LITRES/MIN.*.)
900   IF(KVAL3.EQ.1)GO TO 950
      GO TO 1000
950   CALL MOVT02(92.0,133.0)
      CALL CHAHOL(24H(SOLAR RADIATION (W/M2)*.)
1000  READ(5,60)WAIT
60    FORMAT(A1)
      RETURN
      END

C
C
C
      SUBROUTINE SAVE1(NCHAN,ITIME,KOUNT)
      DIMENSION EXP(50,1200),SPEC(50)
      DOUBLE PRECISION FILE,FILE3
      COMMON SPEC,EXP,FILE
C***OPTION TO TRANSFER PROCESSED EXPERIMENT DATA TO FILE***
      WRITE(5,10)
10    FORMAT('H DO YOU WISH TO SAVE PROCESSED EXPERIMENT
      1 DATA ?','/, 'H0-NO, 1-YES'/)
      READ(5,20)NUMB
20    FORMAT(I)
      IF(NUMB.EQ.0)GO TO 100
C***SPECIFY FILENAME OF EXPERIMENT DATA***
      WRITE(5,30)
30    FORMAT('H TYPE IN THE FILENAME FOR THE EXPERIMENT'/)
      READ(5,40)FILE3
40    FORMAT(A10)
C***TRANSFER DATA FROM ARRAY TO SPECIFIED FILE***
      OPEN(UNIT=5,DEVICE='DSK',FILE=FILE3)
      REWIND 1
      CALL PRINT(NCHAN,ITIME,KOUNT)
      CLOSE(UNIT=5,DEVICE='DSK',FILE=FILE3,DISPOSE='PRINT')
100   RETURN
      END

C
C
C
C
      SUBROUTINE VALID(NCHAN,ITIME,KOUNT)
      DIMENSION EXP(50,1200),SPEC(50)
      DOUBLE PRECISION FILE,FILE4

```

```

COMMON SPEC, EXP, FILE
C***OPTION TO ANALYSE CAMPBELL SOLAR HOSTEL DATA***
WRITE(5,10)
10  FORMAT('H TYPE IN DATE, HOUR, AND STARTING MINUTE OF
      1 MONITORING: '/')
      READ(5,20) DAY, HR, TMIN
20  FORMAT(3F)
      K=0
101  TRAD1=0.0; TRAD2=0.0
      COLHT1=0.0; COLHT2=0.0
      TOTRD1=0.0; TOTRD2=0.0
      TOTCL1=0.0; TOTCL2=0.0
      EFCY1=0.0; EFCY2=0.0
      TOTRD=0.0; TOTCOL=0.0
      HORZ=0.0
      99  K=K+1
          CALL SUNPOS(DAY, HR, TMIN, DECL, HANG, ALT)
          TMIN=TMIN+1.0*(FLOAT(1TIME))
          IF(TMIN.EQ.60.0) HR=HR+1.0
          IF(TMIN.EQ.60.0) TMIN=0.0
          S0=EXP(4,K)*FLOAT(1TIME)*60.0
          HORZ=HORZ+S0
          CALL SUNRD1(S0, ALT, DECL, HANG, S1)
          CALL SUNRD2(S0, ALT, DECL, HANG, S2)
          CA=6.5
          SRAD1=S1
          SPAD2=S2
          TRAD1=TRAD1+SRAD1
          TRAD2=TRAD2+SPAD2
          KFL01=IFIX(EXP(1,K)); KFL02=IFIX(EXP(2,K))
          IF(KFL01.EQ.0) EXP(1,K)=0.0
          IF(KFL02.EQ.0) EXP(2,K)=0.0
          CAPCY=CPR0(EXP(20,K))*FLOAT(1TIME)
          FLOW1=EXP(1,K)*CAPCY/1000.0
          FLOW2=EXP(2,K)*CAPCY/1000.0
          OUTLT1=EXP(12,K); FLIN1=EXP(20,K)
          OUTLT2=(EXP(13,K)+EXP(14,K))/2.0; FLIN2=EXP(13,K)
          COLHT1=COLHT1+(OUTLT1-FLIN1)*FLOW1
          COLHT2=COLHT2+(OUTLT2-FLIN2)*FLOW2
          IF(IFIX(HR).EQ.24) GO TO 100
          GO TO 99
100  THORZ=(HORZ*CA*2.0)/3.6E6
      TOTRD1=(TRAD1*CA)/3.6E6
      TOTRD2=(TRAD2*CA)/3.6E6
      TOTRD=TOTRD1+TOTRD2
      TOTCL1=COLHT1/3.6E6
      TOTCL2=COLHT2/3.6E6
      TOTCOL=TOTCL1+TOTCL2
      EFCY1=(TOTCL1/TOTRD1)*100.0
      EFCY2=(TOTCL2/TOTRD2)*100.0
      WRITE(5,25) THORZ
25  FORMAT('H TOTAL RADIATION INCIDENT ON HORIZONTAL', F7.1,
      1 'KWHR')
      WRITE(5,30) TOTRD1
30  FORMAT('H TOTAL RADIATION INCIDENT ON TOP COLLECTOR
      1 ARRAY', F7.1, 'KWHR')
      WRITE(5,40) TOTRD2

```



```

40  FORMAT('H TOTAL RADIATION INCIDENT ON BOTTOM COLLECTOR
    1 ARRAY',F7.1,'KWHR')
    WRITE(5,50)TOTCL1
50  FORMAT('H TOTAL HEAT ENERGY COLLECTED BY TOP
    1 COLLECTOR ARRAY',F7.1,'KWHR')
    WRITE(5,60)TOTCL2
60  FORMAT('H TOTAL HEAT ENERGY COLLECTED BY BOTTOM
    1 COLLECTOR ARRAY',F7.1,'KWHR')
    WRITE(5,70)EFCY1
70  FORMAT('H AVERAGE COLLECTOR EFFICIENCY (TOP):',
    1 F5.1,'%')
    WRITE(5,80)EFCY2
80  FORMAT('H AVERAGE COLLECTOR EFFICIENCY (BOTTOM):',
    1 F5.1,'%')
    DAY=DAY+1.0
    HR=0.0
    IF(K-GE.KOUNT)GO TO 90
    GO TO 101
90  READ(5,200)A
200  FORMAT(F)
    RETURN
    END

```

```

C      FUNCTION CPRO(TEMP)
        DIMENSION DE(6),CA(6)
C***FLUID DENSITY***
        DATA DE/1002.23,1002.52,994.59,985.46,974.03,960.63/
C***SPECIFIC HEAT CAPACITY OF FLUID***
        DATA CA/4.22,3*4.18,4.20,4.22/
        KT=IFIX(TEMP)
C***DETERMINE THERMOPHYSICAL PROPERTIES OF FLUID***
        IT1=-20
        IT2=0
        DO 100 I=1,6
            IT1=IT1+20
            IT2=IT2+20
            J=I
            IF(KT-GE.IT1.AND.KT-LT.IT2)GO TO 200
100    CONTINUE
200    DENSY=DE(J)
        CAPCY=CA(J)
        CPRO=DENSY*CAPCY*1000.0
        RETURN
    END

```

```

C
C      SUBROUTINE SUNPOS(DAY,HR,TMIN,DECL,HANG,ALT)
        DIMENSION EXP(50,1200),SPEC(50)
        DOUBLE PRECISION FILE
        COMMON SPEC,EXP,FILE
        REAL LAT, LONG
        LAT=57.3
        LONG=2.0
        YEAR=1980.0
        ZONE=-1.0
        SEC=0.0
        TWOPI=6.2831853

```

```

RAD=2.017453293
T=HR+(TIME/60.0)
DELYR=YEAR-1980.0
LEAP=IFIX(DELYR/4.0)
TIME=DELYR*365.0+LEAP+DAY-1.0+(T/24.0)
IF((IFIX(DELYR)).EQ.LEAP*4)TIME=TIME-1.0
IF((DELYR.LT.0.0).AND.(DELYR.NE.LEAP*4))TIME=TIME-1.0
THETA=360.0*(TIME/365.25)*RAD
G=-0.031271-4.53963E-7*TIME+THETA
EL=4.900968+3.6747E-7*TIME+(0.033434-2.3E-9*TIME)
1 *SIN(G)+0.000349*SIN(2.0*G)+THETA
EPS=0.409140-6.2149E-9*TIME
SEL=SIN(EL)
A1=SEL*COS(EPS)
A2=COS(EL)
RA=ATAN2(A1,A2)
IF(IFIX(RA).LE.0)RA=RA+TWOPI
DECL=ASIN(SEL*SIN(EPS))/RAD
ST1=1.759335+TWOPI*(TIME/365.25-DELYR)+3.694E-7*TIME
IF(ST1.GE.TWOPI)ST1=ST1-TWOPI
S=ST1-LONG*RAD+1.0027379*(T+ZONE)*15.0*RAD
H=RA-S
HANG=H/RAD
DECLR=DECL*RAD
PHI=LAT*RAD
ALT=ASIN(SIN(PHI)*SIN(DECLR)+COS(PHI)*COS(DECLR)*COS(H))
AZI=ASIN(COS(DECLR)*SIN(H)/COS(ALT))/RAD
IF(SIN(ALT).GE.SIN(DECL)/SIN(PHI))GO TO 10
IF(AZI.LT.0.0)AZI=AZI+360.0
10 AZI=180.0-AZI
ALT=ALT/RAD
RETURN
END

```

C

C

```

SUBROUTINE SUNRDI(S0,ALT,DECL,HANG,S1)
DIMENSION EXP(50,1200),SPEC(50),HBD(13)
DOUBLE PRECISION FILE
COMMON SPEC,EXP,FILE
REAL LAT,LATR

```

```

DATA HBD/0.0,28.0,43.0,54.0,63.0,71.0,77.0,83.0,88.0,
1 93.0,99.0,101.0,105.0/

```

```

RAD=0.017453293
ACOL=0.95
TILT=70.0

```

C***DETERMINE THE INTENSITY OF THE HORIZONTAL BACKGROUND DIFFUSE
C***RADIATION*****

```

ALT1=-7.5
ALT2=-2.5
ICOUNT=0

```

```

DO 100 I=1,13
ALT1=ALT1+5.0
ALT2=ALT2+5.0

```

```

ICOUNT=ICOUNT+1
IF(ALT.GE.ALT1.AND.ALT.LT.ALT2)GO TO 200
100 CONTINUE

```

100


```

202 HBDR=HBD(ICOUNT)
C***CHANGE CALCULATION PARAMETERS ANGLES INTO RADIAN***
RAD=2.01745
LAT=57.2
WZA=190.0
LATR=LAT*RAD
ALTR=ALT*RAD
WZA=(WZA-180.0)*(-1.0)
AZIR=WZA*RAD
TILTR=TILT*RAD
HANGR=HANG*RAD
DECLR=DECL*RAD
C***CALCULATE THE ANGLE OF INCIDENCE OF THE BEAM RADIATION***
C1=SIN(DECLR)
C2=COS(DECLR)
C3=SIN(LATR)
C4=COS(LATR)
C5=SIN(TILTR)
C6=COS(TILTR)
C7=SIN(AZIR)
C8=COS(AZIR)
C9=SIN(HANGR)
C10=COS(HANGR)
COSA=C1*C3*C6
COSB=C1*C4*C5*C8
COSC=C2*C4*C6*C10
COSD=C2*C3*C5*C8*C10
COSE=C2*C5*C7*C9
COSI=COSA-COSB+COSC+COSD+COSE
C***CALCULATE THE BEAM RADIATION***
COSDT=COS(LATR-TILTR)*C2*C10+SIN(LATR-TILTR)*C1
COSDZ=C4*C2*C10+C3*C1
RBEAM=ABS(COSDT/COSDZ)
CC=0.0
HBDR=0.78+1.07*ALT+6.17*CC
DIRS=(S0-HBDR)*RBEAM
C***CALCULATE THE SKY DIFFUSE RADIATION***
CC=1.0
HBDR2=0.78+1.07*ALT+6.17*CC
DIFF1A=HBDR2*((1.0+COS(TILTR))/2.0)
DIFF1=HBDR*((1.0+COS(TILTR))/2.0)
C***CALCULATE THE REFLECTED GROUND RADIATION***
R0=0.2
DIFF2=S0*((1.0-COS(TILTR))*R0)/2.0
C***CALCULATE THE INCIDENT RADIATION ABSORBED BY THE COLLECTOR
COS2I=COSI*COSI
COS3I=COS2I*COSI
COS4I=COS3I*COSI
COS5I=COS4I*COSI
C***TRANSMISSION COEFFICIENT FOR DIRECT RADIATION***
TDIR=-0.00885+2.71235*COSI-0.62062*COS2I
1-7.07329*COS3I+9.75995*COS4I-3.89922*COS5I
C***ABSORPTION COEFFICIENT FOR DIRECT RADIATION***
ADIR=0.01154+0.77674*COSI-3.94657*COS2I
1+8.57881*COS3I-8.38135*COS4I+3.01138*COS5I
C***REFLECTION COEFFICIENT FOR DIRECT RADIATION***
RDIR=1.0-TDIR-ADIR

```


C***TRANSMISSION AND ABSORPTION COEFFS. FOR DIFFUSE RADIATION

TDIF=0.796;ADIF=0.056

C***REFLECTION COEFFICIENT FOR DIFFUSE RADIATION***

RDIF=1.0-TDIF-ADIF

C***REFLECTION COEFFICIENT FOR COLLECTOR SURFACE***

RCOL=1.0-ACOL

ABTR1=TDIF*ACOL/(1.0-(1.0-ACOL)*RDIR)

ABTR2=TDIF*ACOL/(1.0-(1.0-ACOL)*RDIF)

S1=ABTR2*(DIFF1+DIFF2)+ABTR1*DIRS

RETURN

END

C

C

SUBROUTINE SUNRD2(S0,ALT,DECL,HANG,S2)

DIMENSION EXP(50,1200),SPEC(50),HBD(13)

DOUBLE PRECISION FILE

COMMON SPEC,EXP,FILE

REAL LAT,LATR

DATA HBD/0.0,23.0,43.0,54.0,63.0,71.0,77.0,83.0,88.0,

1 93.0,99.0,101.0,105.0/

RAD=0.017453293

ACOL=0.95

TILT=45.0

C***DETERMINE THE INTENSITY OF THE HORIZONTAL BACKGROUND DIFFUSE

C***RADIATION*****

ALT1=-7.5

ALT2=-2.5

ICOUNT=0

DO 100 I=1,13

ALT1=ALT1+5.0

ALT2=ALT2+5.0

ICOUNT=ICOUNT+1

IF(ALT.GE.ALT1.AND.ALT.LT.ALT2)GO TO 200

100 CONTINUE

200 HBDR=HBD(ICOUNT)

WZA=190.0

IF(HBDR.GT.S0)HBDR=S0

C***CHANGE CALCULATION PARAMETERS ANGLES INTO RADIAN***

LAT=57.2

LATR=LAT*RAD

ALTR=ALT*RAD

WZA=(WZA-180.0)*(-1.0)

AZIR=WZA*RAD

TILTR=TILT*RAD

HANGR=HANG*RAD

DECLR=DECL*RAD

C***CALCULATE THE ANGLE OF INCIDENCE OF THE BEAM RADIATION***

C1=SIN(DECLR)

C2=COS(DECLR)

C3=SIN(LATR)

C4=COS(LATR)

C5=SIN(TILTR)

C6=COS(TILTR)

C7=SIN(AZIR)

C8=COS(AZIR)

C9=SIN(HANGR)

C10=COS(HANGR)

```

      COSA=C1*C3*C6
      COSB=C1*C4*C5*C3
      COSC=C2*C4*C6*C10
      COSD=C2*C3*C5*C3*C10
      COSE=C2*C5*C7*C9
      COSI=COSA-COSE+COSC+COSD+COSE
C***CALCULATE THE BEAM RADIATION***
      COSDT=COS(LATR-TILTR)*C2*C10+SIN(LATR-TILTR)*C1
      COSDZ=C4*C2*C10+C3*C1
      RBEAM=ABS(COSDT/COSDZ)
      CC=0.0
      HBDR=0.73+1.07*ALT+6.17*CC
      DIRS=(S0-HBDR)*RBEAM
C***CALCULATE THE SKY DIFFUSE RADIATION***
      CC=1.0
      HBDR2=0.73+1.07*ALT+6.17*CC
      DIFF1A=HBDR2*((1.0+COS(TILTR))/2.0)
      DIFF1=HBDR*((1.0+COS(TILTR))/2.0)
C***CALCULATE THE REFLECTED GROUND RADIATION***
      R0=0.2
      DIFF2=S0*((1.0-COS(TILTR))*R0)/2.0
C***CALCULATE THE INCIDENT RADIATION ABSORBED BY THE COLLECTOR
      COS2I=COSI*COSI
      COS3I=COS2I*COSI
      COS4I=COS3I*COSI
      COS5I=COS4I*COSI
C***TRANSMISSION COEFFICIENT FOR DIRECT RADIATION***
      TDIR=-0.00885+2.71235*COSI-0.62062*COS2I
      1-7.07329*COS3I+9.75995*COS4I-3.89922*COS5I
C***ABSORPTION COEFFICIENT FOR DIRECT RADIATION***
      ADIR=0.01154+0.77674*COSI-3.94657*COS2I
      1+3.57881*COS3I-3.38135*COS4I+3.01188*COS5I
C***REFLECTION COEFFICIENT FOR DIRECT RADIATION***
      RDIR=1.0-TDIR-ADIR
C***TRANSMISSION AND ABSORPTION COEFFS. FOR DIFFUSE RADIATN
      TDIF=0.796;ADIF=0.056
C***REFLECTION COEFFICIENT FOR DIFFUSE RADIATION***
      RDIF=1.0-TDIF-ADIF
C***REFLECTION COEFFICIENT FOR COLLECTOR SURFACE***
      RCOL=1.0-ACOL
      ABTR1=TDIR*ACOL/(1.0-(1.0-ACOL)*RDIR)
      ABTR2=TDIF*ACOL/(1.0-(1.0-ACOL)*RDIF)
      S2=ABTR2*(DIFF1+DIFF2)+ABTR1*DIRS
      RETURN
      END
C
C***EXECUTIVE PROGRAM***
      CALL INITT(120)
      CALL T4010
      CALL DEVSPEC(1200)
      CALL MENU1
      CALL DEVEND
      CALL FINITT(0.730)
      END

```

BIBLIOGRAPHY

BIBLIOGRAPHY

- Beckman, W.A., "Duct and pipe losses in solar energy systems". Solar Energy, vol. 21, 1978. pp. 531-532.
- Bliss, R.W., "The derivations of several plate efficiency factors useful in the design of flat-plate solar heat collectors". Solar Energy, vol. 3, 1959. pp. 55-64.
- Brinkworth, B.J., "British Standards for solar heating". Proc. Conf. Solar Energy Codes of Practice and Test Procedures, UK - ISES, London, 1980. pp. 99-111.
- Clarke, J., "ESP - Package for appraisal of environmental systems performance". ABACUS Occasional Paper 48, 1976.
- Clarke, J., "External shading of buildings". ABACUS Occasional Paper 49, 1976.
- Close, D.J., "A design approach for solar processes". Solar Energy, vol. 11, 1967. pp. 112-122.
- Courtney, R.G., "A computer study of solar water heating". Building and Environment, vol. 12, 1977. pp. 73-80.
- Duffie, J.A. and Beckman, W.A., Solar Energy Thermal Processes. New York, John Wiley, 1974.
- Garg, H.P., "Effect of dirt on transparent covers in flat-plate solar energy collectors". Solar Energy, vol. 15, 1974. pp. 299-302.
- Gutierrez, G., Hincapie, F., Duffie, J.A., and Beckman, W.A., "Simulation of forced circulation water heaters; effects of auxiliary energy supply, load type and storage capacity". Solar Energy, vol. 15, 1974. pp. 287-298.
- Holman, J.P., Heat Transfer. 4th ed. London, McGraw-Hill, 1976.
- Hottel, H.C. and Woertz, B.B. "Performance of flat-plate solar heat collectors". Trans. ASME, vol. 64, 1942. pp. 91-103.
- Klein, S.A., "Transient considerations of flat-plate collectors". Trans. ASME, vol. 6A, 1974. pp. 109-113.
- Kreider, J.F. and Kreith, F., Solar Heating and Cooling. New York, McGraw-Hill, 1977.
- Liu, B.Y.H. and Jordan, R.C., "The inter-relationship and characteristic distribution of direct, diffuse and total solar radiation". Solar Energy, vol. 4, 1960. pp. 1-9.
- Liu, B.Y.H. and Jordan, R.C., "Daily insolation on surfaces tilted toward the equator". ASHRAE Journal, 1961. pp. 53-59.
- Liu, B.Y.H. and Jordan, R.C., "The long-term average performance of flat-plate solar-energy collectors". Solar Energy, vol. 7, 1963. pp. 53-74.
- McAdams, W.C., Heat Transmission. 3rd ed. New York, McGraw-Hill, 1954.

- Moon, P., "Proposed standard solar radiation curves for engineering use". J. Franklin Inst., vol. 230, 1940. pp. 582-617.
- Page, J.K., "Geographical variations in the climatic factors influencing solar building design". Proc. Conf. Solar Building Technology, UNESCO/NELP, London, 1977. pp. 1-23.
- Parmelee, G.V., "Irradiation of vertical and horizontal surfaces by diffuse solar radiation from cloudless skies". Heating, Piping and Air Conditioning, 1954. pp. 129-135.
- Saluja, G.S. and Robertson, P., "Monitoring of solar water heating installation in a 15 person hostel". Proc. Conf. Solar Energy in the 80's, UK - ISES, Birmingham, 1980. pp. 124-130.
- Saluja, G.S. and Robertson, P., "Dynamic thermal simulation of solar water heating systems under transient climatic conditions". accepted for presentation at Bi-annual International Solar Energy Society Congress, Brighton, 1981.
- Souster, C.G., "Solar and Surface Geometry". User guide to program SANG, Internal Report, Dept., of Building Science, University of Sheffield, 1977.
- Stark, P.A., Introduction to Numerical Methods, 2nd ed. Toronto, Collier-Macmillan, 1970.
- Sussock, H., "Graphics facilities for computer-aided architectural design". ABACUS Occasional Paper 25, 1973.
- Tabor, H., "Radiation, convection and conduction coefficients in solar collectors". BH. Res. Council Israel, 1958. pp. 155-167.
- Unsworth, M.H. and Monteith, J.L., "Aerosol and solar radiation in Britain". Quart. J.R. Met. Soc., vol. 98, 1972. pp. 778-797.
- Varma, H.K., "A model to calculate solar radiation absorbed by absorber surface of a flat plate solar collector". Proc. Conf. Solar Building Technology, UNESCO/NELP, London, 1977. pp. 711-715.
- Walraven, R., "Calculating the position of the sun". Solar Energy, vol. 20, 1978. pp. 393-397.
- Whillier, A., "Plastic covers for solar collectors". Solar Energy, vol. 7, 1963. pp. 148-151.
- Whillier, A., "Design factors influencing solar collector performance". Low Temperature Engineering Application of Solar Energy, ASHRAE, New York, 1967. pp. 27-40.
- Wijeyesundera, N.E., "Comparison of transient heat transfer models for flat-plate collectors". Solar Energy, vol. 21, 1978. pp. 517-521.
- "Astronomical Papers presented for the user of the use of the American Ephemeris and Nautical Almanac". vol. 6, 1898.
- "Explanatory Supplement to the Astronomical Ephemeris and the American Ephemeris and Nautical Almanac". H.M.S.O., London, 1961.

Details of postgraduate courses of study

1. Computer Studies, at the School of Mathematics, Robert Gordon's Institute of Technology, Aberdeen. Undergraduate course.
Attendance: full academic year, 1977-78, 2hours/week.
2. Mechanics and Thermodynamics of Fluids, at the School of Mechanical Engineering, Robert Gordon's Institute of Technology, Aberdeen. Undergraduate course.
Attendance: second and third terms, session 1977-78, 2 hours/week.
3. Experimental Techniques in Fluid Mechanics and Heat Transfer, Simon Engineering Laboratories, University of Manchester, Manchester. Postgraduate course.
Attendance: 18-22nd September 1978.